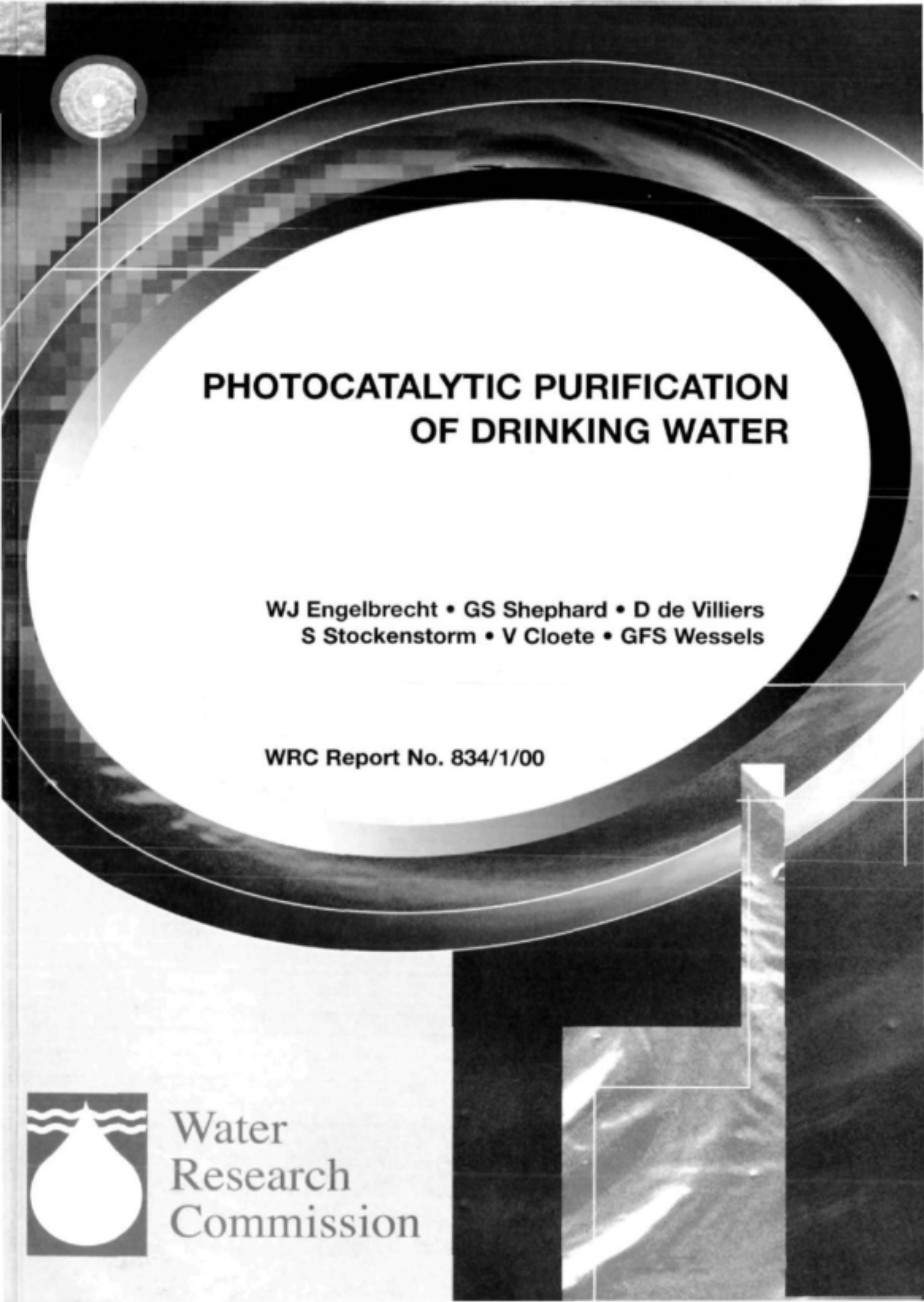

PHOTOCATALYTIC PURIFICATION OF DRINKING WATER

WJ Engelbrecht • GS Shephard • D de Villiers
S Stockenstorm • V Cloete • GFS Wessels

WRC Report No. 834/1/00

Water
Research
Commission

PHOTOCATALYTIC PURIFICATION OF DRINKING WATER

Final Report to the Water Research Commission

by

Willem J Engelbrecht[1], Gordon S Shephard[2], David de Villiers[1], Sonja Stockenström[2], Valeska Cloete[1] and Gawie FS Wessels[1]

Department of Chemistry, University of Stellenbosch, Stellenbosch 7600, South Africa
Programme on Mycotoxins and Experimental Carcinogenesis (PROMEC), Medical Research Council, PO Box 19070, Tygerberg 7505, South Africa

Project leaders : (1) Prof. WJ Engelbrecht
(2) Dr. GS Shephard

WRC Report No : 834/1/00

ISBN No : 1 86845 698 6

EXECUTIVE SUMMARY

Background and Motivation of Project

Raw surface and groundwater can contain a wide range of materials that are detrimental to human health. These material can be classified as:

1. Natural organic materials (NOM), which represent a complex variety of organic molecules characteristic of the vegetation in a catchment area.
2. A variety of material resulting from the excreta of humans and animals.
3. Breakdown products of algae (not necessarily toxic) causing a bad odour and taste, specifically geosmin and 2-methyl-isoborneol (2-MIB).
4. Microcystin toxins produced by the blue-green algae that present a serious health hazard to humans and animals.
5. A variety of organic molecules of industrial and agricultural origin that can produce adverse health effects.
6. A wide range of micro-organisms causing human disorders.
7. Inorganic species.

The traditional flocculation/coagulation process has proved not to be completely efficient in removing all the combinations of material that can occur in raw water. These combinations can vary on an hourly basis, which complicates the flocculation/coagulation procedure even further.

Various other processes are under investigation elsewhere e.g. ozonation, treatment by hydrogen peroxide, ultraviolet irradiation treatment, microfiltration, TiO_2 photocatalysis etc. Some of these techniques have found application especially in urban areas. Application of these techniques in isolated rural communities however, poses a serious problem.

This WRC sponsored project was undertaken to assess the effectiveness of TiO_2 photocatalysis for the oxidative removal of some of the above mentioned groups of compounds(1, 4 and 5) from raw water. The project comprised two phases: an initial screening phase (August 1995 to December 1997) and a follow-up phase (January 1998 to June 2000). Experimental research was jointly conducted by the Department of Chemistry (University of Stellenbosch) and the Programme on Mycotoxins and Experimental Carcinogenesis (PROMEC) at the Medical Research Council (based in Tygerberg).

Project Objectives

The objectives of this research programme were to:

- Develop and establish the optimum performance characteristics of a novel design of photocatalytic reactors for purification of raw drinking water containing humic acids, clay colloids and other organic pollutants.
- Evaluate and establish the optimum performance characteristics of photocatalytic reactor designs for the decomposition of microcystins in various raw water samples.
- Establish optimal growth conditions for the microcystins by toxic cultures of cyanobacteria.
- Isolate and purify known and novel microcystin variants from freeze-dried culture material.
- Apply pure microcystin variants to the photocatalytic reactor(s), using the optimised conditions determined under the second objective.
- Identify the decomposition products derived from individual pure microcystin variants.

Summary of Results

The oxidation efficiencies of three types of falling film photocatalytic reactors were investigated and optimised using statistical procedures. Three modes of operation namely recirculation , single pass and sequential single pass were investigated. Slurry phase, immobilised bed (IMM) and combined slurry immobilised-bed (SLIMM) configurations for application of the photocatalyst and different construction materials were also investigated.

To assess the oxidation efficiencies of these reactors, three compounds or mixture of compounds representing different classes of water pollutants were investigated.

First order rate constants for the removal of pollutants, percentage degradation and first order rate constant in terms of number of passes were used as response functions in the optimisation procedures.

Depending on the type of reactor, various statistical approaches for optimisation have been employed. Generally system parameters e.g. catalyst suspension loading, volumetric flow rate, horizontal irradiation distance, initial concentration of pollutant, reaction volume, water matrix, pH, purge gas, flow rate of purge gas and number of UV-C lamps were investigated at assigned levels.

The main results of these investigations can be summarised by:

1. An existing model of a falling film photocatalytic reactor (Reactor 1) based on TiO_2 catalyst (Degussa P-25), operating as a slurry phase system, has been tested and optimised for the destruction of:

   (i) *para*-chlorophenol as representative of industrial pollutants

   (ii) the microcystin toxins YA, YR, LR and RR

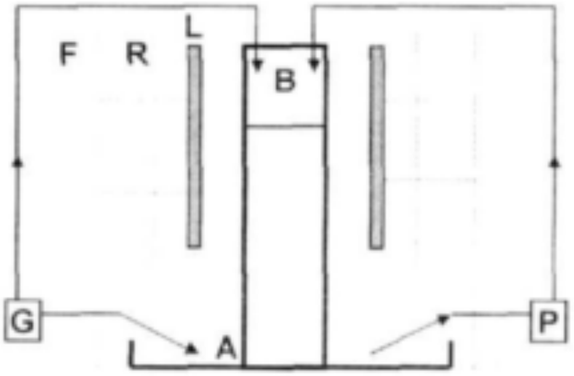

A: Glass cylinder B: Cup F: Frame R: Reflector L: Germicidal lamps
G: Gas purge P: peristaltic pump

Figure I.a: Schematic of Reactor 1

This was the first ever demonstration of TiO_2 photocatalytic removal of microcystin toxins (Stockenström *et al.*, 1996).

3 Due to the difficulty of separating the TiO_2 particles from purified water, Reactor 1 was not considered as a suitable system for upscaling.

4. A novel design of a falling film photocatalytic reactor based on TiO_2 catalyst (Degussa P-25) immobilised on a fibre glass sheet and driven by commercially available lamps (Reactor 2A), has been developed :

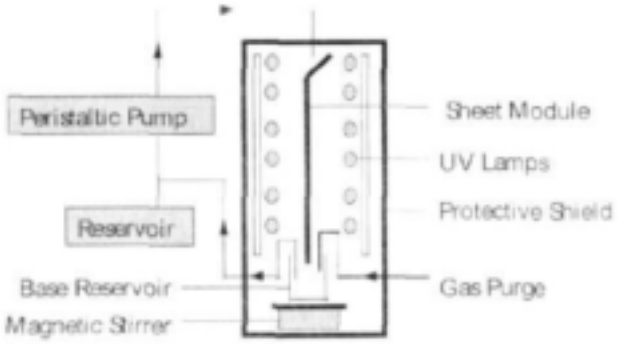

Figure I.b: Schematic of Reactor 2A

5. Two types of fibre glass sheets were evaluated and the reactor has been operated on an immobilised (IMM) and combined slurry phase and immobilised (SLIMM) configuration. This reactor has been tested and optimised in the recirculation and flow through modes of operation for the removal of *para*-chlorophenol (p-CP) as representative of industrial pollutants.The following curves were generated.

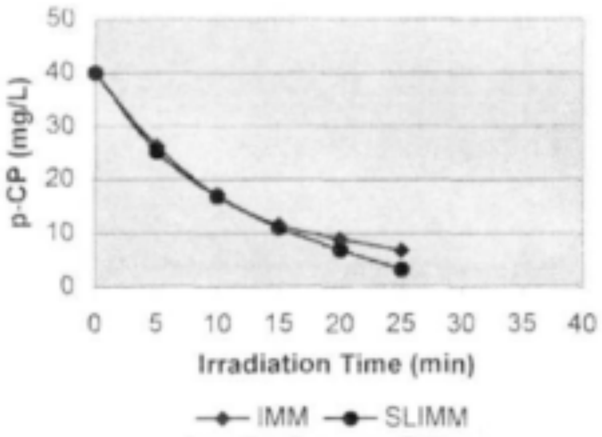

Figure I.c: p-CP concentration as a function of irradiation time and reactor configuration (IMM and SLIMM) in recirculation mode and using Fibre Glass Type 1 as sheet module

The results presented in Figure I.c show that additional suspended catalyst (1 g/L) did not enhance p-CP oxidation. Therefore an immobilised configuration is preferred.

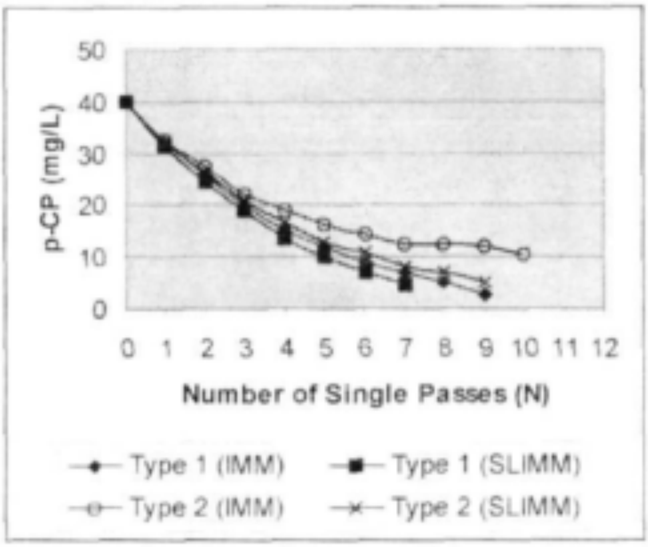

Figure I.d: p-CP concentration as a function of sheet module, reactor configuration and single pass number (N) - where each N equals 4.1 seconds of UV irradiation

The curves in Figures I.c and I.d were converted to rate constants ($10^2 k_{obs}$) and are summarised in Table I.a

Table I.a: Summary of kinetic analysis for p-CP oxidation as a function of sheet module, reactor configuration and single pass number (N)

	Fibre Glass Type 1 (reinforced sheet)		Fibre Glass Type 2 (non-reinforced tissue sheet)	
Kinetic Response Function	IMM Reactor	SLIMM Reactor	IMM Reactor	SLIMM Reactor
10^2 k_{obs} (N)* (pass^{-1})	27.9	30.3	13.2	22.9
Half-life (passes)	2.5	2.3	5.3	3.0
10^2 k_{obs} (t)** (sec^{-1})	6.73	7.37	3.19	5.64
Half-life (sec)	10.3	9.4	21.7	12.3
10^2 k_{obs} (t) (min^{-1})	403.8	442.4	191.4	338.1
Half-life (min)	0.17	0.15	0.36	0.21
R^2	0.99	0.99	0.96	0.99

k_{obs} (N)* = **Observed first order rate constant as a function of single pass number (N)**
(each single pass is equivalent to a UV contact time of 4.1 sec)
k_{obs} (t)** = **Observed first order rate constant as a function of irradiation time (in sec or min)**

The results for the two types of fibre glass sheets and IMM and SLIMM configurations are compared by means of the following bar graph.

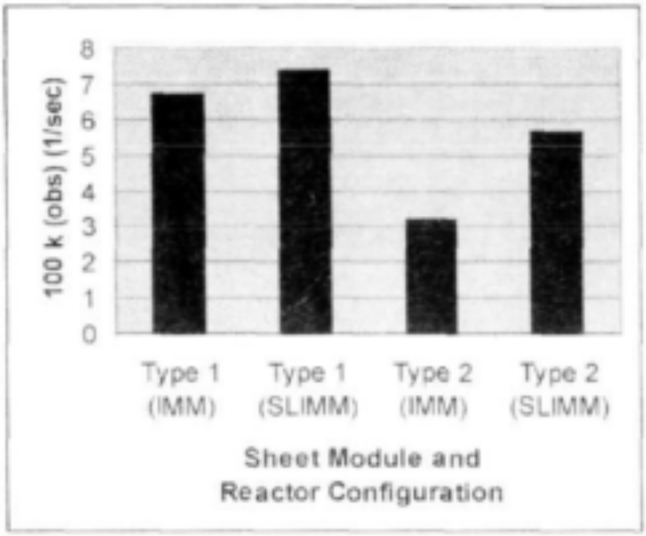

Figure I.e First order rate constants for photocatalytic oxidation of para-chlorophenol as a *function of sheet module and reactor configuration*

The fibre glass sheet Type 1 was better for immobilising TiO_2 for photocatalysis.

6. The reactor has also been evaluated for the destruction of the microcystin toxins YA, YR, LR and RR

The following tables give representative examples of the results.

Table I.b: Concentrations of microcystins as functions of single pass number (N)

Single Pass Number (N).	Microcystins (ug/L)		
	YA	YR	LR
0	21	71	49
1	17	57	18
2	NA	47	14
3	9	30	10
4	ND	20	ND
5		19	
6		16	
7		15	
8		ND	
9			
10			
10^2 k(N) (pass^{-1})	28.75	24.23	50.19

Table I.c: Concentration of microcystins as functions of cumulative time of irradiation

Cumulative Time of Irradiation (sec)	Microcystins (ug/L)		
	YA	YR	LR
0.00	21	71	49
4.05	17	57	18
8.10	NA	47	14
12.15	9	30	10
16.20	ND	20	ND
20.25		19	
24.30		16	
28.35		15	
32.40		ND	
36.45			
40.50			
10^2 k (sec^{-1})	7.10	5.98	12.40
Half-life (sec)	9.8	11.6	5.6
R^2	0.99	0.95	0.90

NA = Not analysed ; ND = Not detected

7. According to Bolton's formula for "Electrical Energy per Order" (EE/O) (Bolton *et al.*, 1996), data obtained from Reactor 2A operating in single pass mode, predicted :

- The cost for the reduction of 40 mg/L p-chlorophenol (in distilled water) to 4 mg/L (one order of magnitude reduction), as 11 cent / m^3
- The cost for the destruction of the microcystins in natural lake water as 26 cent / m^3

These are running costs and were calculated on a unit cost of 11.8 cent / kWh in Stellenbosch (May 2000). Administration and labour costs and replacement cost of lamps were ignored.

8. It has been proved that Reactor 2A can break down NOM in highly coloured water (TOC: 41.6 mg C / L), thereby reducing the total organic carbon (TOC)

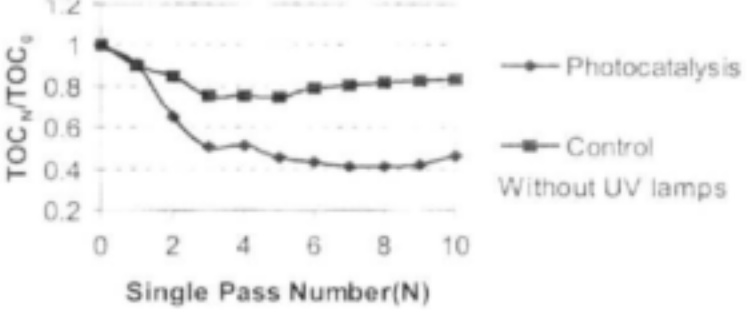

Figure I.f: The photocatalytic oxidation of NOM in terms of normalised TOC by Reactor 2 A

- The cost for the reduction of NOM by one order of magnitude was calculated as 53 cent / m^3.

This however was regarded as too expensive. The situation can be remedied by using this reactor system in series with a conventional coagulation / flocculation plant. Those pollutants e.g. fulvic acids as part of NOM and industrial pollutants passing through the first plant will be destroyed in the reactor, thereby reducing e.g. the disinfectant by-products on chlorination.

9. It was established that NOM adsorbs reasonably strongly on glass fibre with immobilised TiO_2 .

10. The contact time on Reactor 2A was regarded as too short (4.1 ± 0.1 sec).Increasing the contact time should increase the rate of removal and result in a reduction of treatment cost. Efforts to increase the contact time by variations in the configuration of the glass fibre sheet, did not substantially improve the contact time.

11. It was realised however that reactor 2A operating in the IMM configuration and in the recirculation mode should be an excellent system to obtain relative rate constants for the photocatalytic destruction of pollutants in various water matrixes.

12. In order to further improve the contact time of Reactor 2A the glass fibre sheet has been replaced by a fibrous activated carbon (FAC) sheet. This reactor (Reactor 2B) with various percentages of immobilised TiO_2 , has been investigated for the removal of:

    (i) p-chlorophenol as representative of industrial pollutants

    (ii) The microcystin toxins LR and RR

    The following curves were generated.

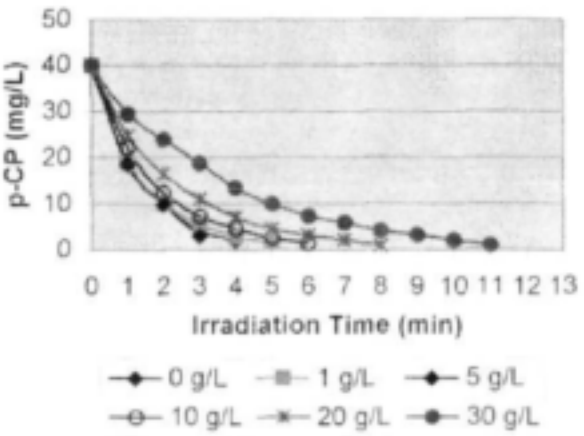

Figure I.g: p-CP concentration as a function of UV irradiation time and catalyst impregnation loading (expressed as catalyst suspension loading used for FAC impregnation)

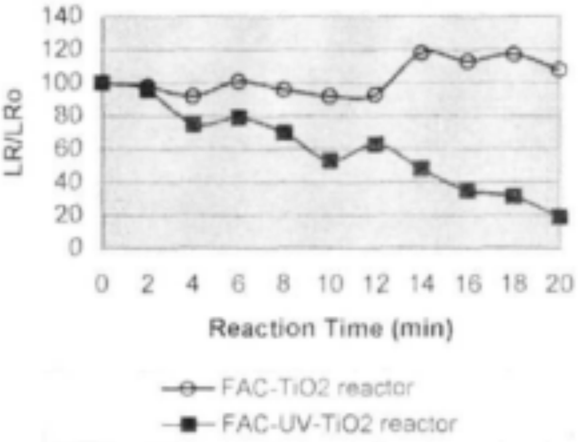

Figure I.h: Microcystin LR removal as a function of time in FAC-TiO_2 and FAC-UV-TiO_2 (photocatalytic) reactors. (Concentrations normalised)

The high rate of removal of p-chlorophenol must be attributed to strong adsorption on the FAC sheet.

The microcystin toxins being larger molecules do not adsorb strongly on the FAC sheet, therefore the removal of these species must be attributed to the photocatalytic oxidation effect.

13. Efforts to achieve a balance between adsorption and the photocatalysis of p-chlorophenol, by using intermittent TiO_2 covered and uncovered sections of the FAC sheet, were not successful. Adsorption remained the predominant factor.

14. Objectives 3 to 6 were not achieved; due to the difficulty in obtaining authentic samples to produce cultures without contamination.

15. The problem of obtaining the microcystin toxins for experiments on photocatalytic breakdown, was circumvented by using extracts of the appropriate toxins from lake water, when the relevant algal blooms occurred.

CONCLUSIONS

1. Reactor 2A - being a very rugged model and easy to operate - must be retained and used to obtain relative rate constants for the destruction of pollutants in various water matrices.

   These rate constants can be converted to absolute rate constants for a particular type of commercial reactor operating with the same water matrix, once the absolute rate constant for a standard compound e.g. *para* -chlorophenol has been determined on the commercial reactor.

   The rate constants can eventually be used to predict the performance of commercial reactors for various pollutants and various raw water matrixes.

   A more sensitive analytical technique e.g. capillary electrophoresis should be employed.

2. A falling film photocatalytic reactor based on TiO_2 immobilised on a glass fibre sheet (Reactor 2A) can remove p-chlorophenol, microcystin toxins and NOM from raw water of a low alkalinity.

   Although this reactor system is based on lower cost construction material and can be scaled up, the contact time is too short, thereby placing a restriction on the volume of raw water and the level of contamination that can be treated.

   This reactor system, however, due to its small size and utilisation of lower cost components for construction, can find application in households, clinics and hospitals in urban areas where flocculated water or water with a low TOC could be purified.

   Since the reactor requires UV lamps as radiation source, it is not suited for isolated rural communities.

3. In a falling film photocatalytic reactor based on TiO_2 immobilised on a FAC sheet, adsorption of the pollutants on the FAC is too strong and competes with the photocatalytic destruction process. This type of reactor is not recommended for water treatment. Other configurations employing FAC are however recommended.

4. A substantial body of knowledge has been developed with regard to the coating behaviour of fibre glass sheets and FAC sheets with Degussa P25 TiO_2 catalyst and the photocatalytic behaviour.

5. Based on the predicted treatment cost for photocatalytic purification of polluted water with germicidal lamps and TiO_2 , the development of photocatalytic reactors should continue, especially for large reactors employing solar radiation.

RECOMMENDATIONS

Recommendations for short term application

1. The application of UV lamp-driven falling film photocatalytic reactors based on fibre glass sheets (Reactor 2A), should be further investigated for the small scale final purification of flocculated water and raw water with a low total organic carbon content.

2. The disinfection and potential for bacterial regrowth in water treated by Reactor 2A for the purposes described under 1 should be investigated.

3. Lamp-driven falling film photocatalytic reactors based on fibre glass and/or FAC sheets should be evaluated for the purification of polluted air in buildings and removal of volatile organic compounds (VOCs), SO_2 and NO_x from emissions of factories. The body of knowledge generated in this project must be applied in such investigations.

Recommendations for long term application

1. In order to increase the contact time of UV photocatalytic oxidation, a modular type of reactor based on horizontal flow and TiO_2 catalyst immobilised on glass fibre rods should be investigated.

   The modules must be configured to operate on solar radiation in daytime, while the number of modules must be sufficient to remove pollutants to the required level.

   This reactor must be operated in series with a conventional coagulation/flocculation plant when raw water of a high TOC must be treated.

2. A modular reactor with a similar construction as under 1, but with TiO_2 catalyst immobilised on FAC should be investigated.

   This reactor must be placed parallel to the reactor under 1 and would be engaged during night-time operations. Enough modules must be included to remove all pollutants through adsorption.

   During daytime water will be circulated in a closed loop through this reactor to clean the FAC modules by photocatalysis and restore its adsorptive properties.

Proposed configurations

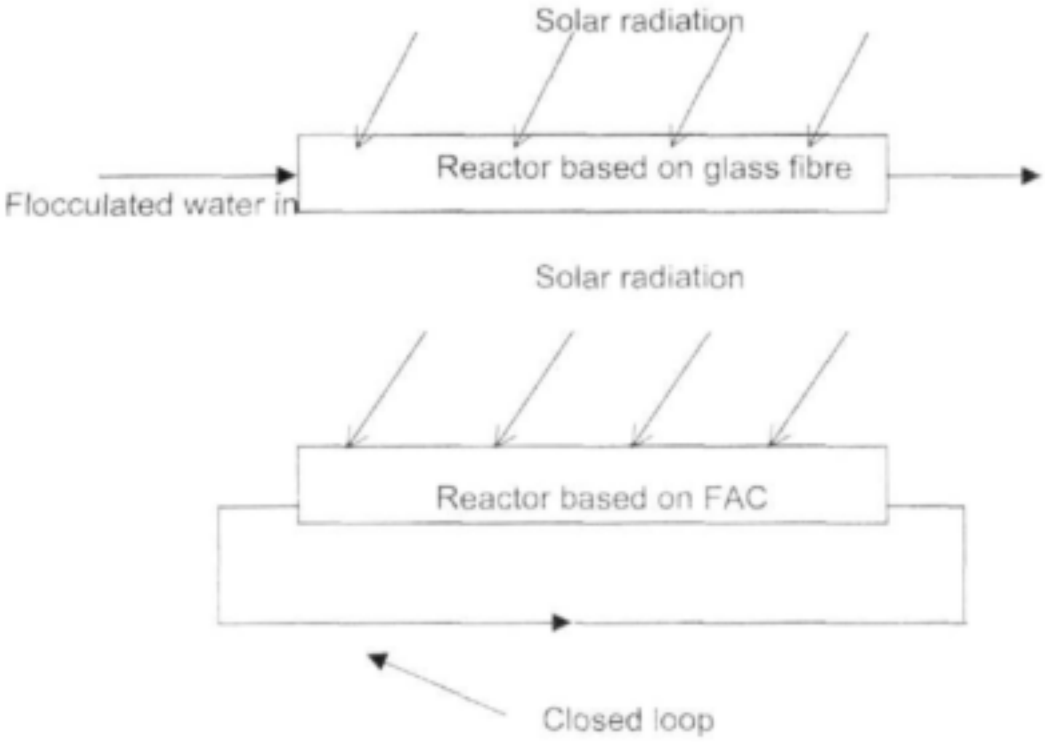

Day time operation

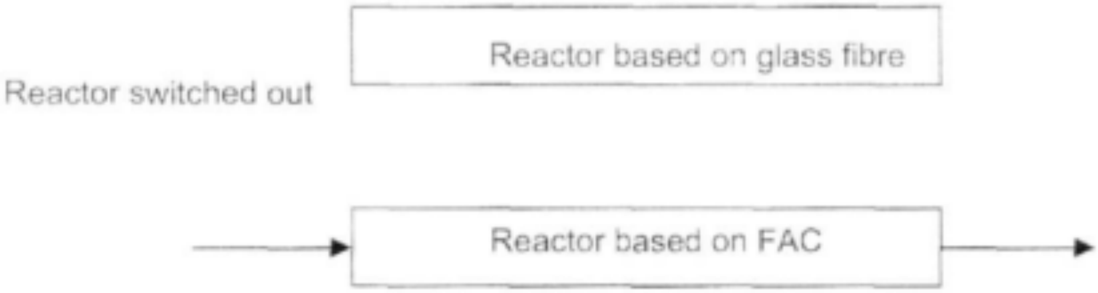

Night-time operation

FAC exhibits very strong adsorptive properties and by including a sufficient number of modules, this reactor will adsorb all the pollutants coming through from a conventional flocculation/coagulation plant during night-time operations.

When the solar intensity is high enough after sunrise, operations will be switched back to the glass fibre reactor. A conventional pump in a closed loop then circulates water – a reversed flow direction is recommended – through the FAC based reactor under solar radiation. This can continue – for the entire day if necessary – till the FAC is cleaned by photocatalysis.

Individual modules of the FAC based reactor can periodically be removed and subjected to steamstripping to restore adsorptive properties.

The capital and operating cost of this dual reactor system should be much reduced in comparison with a system where lamps are used for night-time operation.

This reactor system should also be applicable for the continuous wastewater treatment of industrial plants.

3. Small batch operating reactor systems based on solar radiation and TiO_2 immobilised on fibre glass should be developed for use by isolated rural communities.

4. Due to the interdisciplinary nature of the proposed investigations, a project team consisting of chemists, chemical engineers, microbiologists, specialists in microcystin toxins and community health specialists, should be established.

5. International co-operation should be established in order to develop better photocatalysts and better techniques for immobilising these catalysts.

6. A programme should be launched to determine the relative rate constants for the destruction of pollutants of various origin using Reactor 2A.

ACKNOWLEDGEMENTS

The research in this report emanated from a project funded by the Water Research Commission and entitled :

"PHOTOCATALYTIC PURIFICATION OF DRINKING WATER"

The Steering Committee responsible for this project consisted of the following persons:

Dr IM Msibi	Water Research Commission (Chairman)
Dr G Offringa	Water Research Commission
Prof CA Buckley	University of Natal
Mr M Pryor	Umgeni Water
Prof JU Grobbelaar	University of the Free State
Prof J Haarhoff	Rand Afrikaans University
Mr SA Pieterse	Cape Town Metropolitan Council
Mr DP Theron	Overberg Water
Mr O Hempel	Water Research Commission (Committee Secretary)

The financing of the project by the Water Research Commission and the contribution of the members of the Steering Committee is gratefully acknowledged.

This project was only possible with the co-operation of several individuals and institutions. The authors therefore wish to record their sincere thanks to the following persons:

Mr M Pryor	Umgeni Water
Dr M Van der Merwe	University of Stellenbosch
Dr N Barnardt	Enviro Services cc
Dr G Offringa	Water Research Commission
Mr SA Pieterse	Cape Town Metropolitan Council
Prof JU Grobbelaar	University of the Free State
Mr M Pieper	Freudenberg Nonwovens Pty Ltd
Mr L Van Niekerk	University of Stellenbosch
Mr E Ward	University of Stellenbosch
Mr DN Steenkamp	University of Stellenbosch
Mr D Gibbs	Rondevlei Nature Reserve

TABLE OF CONTENTS

CHAPTER 1 : INTRODUCTION AND OBJECTIVES

CHAPTER 2 : LITERATURE REVIEW

CHAPTER 3 : MATERIALS AND METHODS

CHAPTER 4 : EVALUATION OF REACTOR 1

CHAPTER 5 : EVALUATION OF REACTOR 2A

CHAPTER 6 : EVALUATION OF REACTOR 2B

CHAPTER 7 : SUMMARY OF RESULTS, CONCLUSIONS AND RECOMMENDATIONS

LIST OF SYMBOLS AND ABBREVIATIONS

Abbreviations:

ANOVA	Analysis of Variance
AOTs	Advanced Oxidation Technologies
BDOC	Biodegradable Organic Carbon
CCD	Central Composite Design
CIL	Catalyst Impregnation Loading
COD	Chemical Oxygen Demand
CSL	Catalyst Suspension Loading
CSTR	Continuously Stirred Tank Reactor
DBPs	Disinfection By-Products
DCAA	Dynamic Contact Angle Analyser
DRS	Diffuse Reflectance Spectrometry
EDAX	*Energy Dispersive Analysis of X-rays*
EE/O	Electrical Energy per Order
FAC	Fibrous Activated Carbon
HID	Horizontal Irradiation Distance
HPLC	High-Performance Liquid Chromatography
IMM	Immobilised-Bed Reactor
NA	Not Analysed
ND	Not Detected
NOM	Natural Organic Matter
PCO	Photocatalytic Oxidation
p-CP	*para*-chlorophenol
PROMEC	Programme on Mycotoxins and Experimental Carcinogenesis
PZC	*Point of Zero Charge*
RSD	Relative Standard Deviation
RSM	Response Surface Methodology
SEM	Scanning Electron Microscopy
SD	Standard Deviation
SLIMM	Combined Slurry-Immobilised Bed Reactor
THMs	Trihalomethanes
TOC	*Total Organic Carbon*
WRC	Water Research Commission

Symbols:

k_A	adsorption rate constant (in min^{-1})
k_{obs}	observed first order rate constant (in min^{-1} or sec^{-1})
k_P	rate constant for photocatalytic oxidation (in min^{-1})
k_T	rate constant for total removal (in min^{-1})
n	number of intermittent TiO_2 segments on FAC sheet
N	number of single passes
κ	illuminated specific surface area (in m^2/m^3)

CHAPTER 1 : INTRODUCTION AND OBJECTIVES

1.1 INTRODUCTION

Photocatalytic oxidation (PCO) as a means for treating polluted water has enjoyed extensive global interest in recent years (Mills and Le Hunte, 1997; Fox and Dulay, 1993; Fujishima *et al.*, 1999; Linsebigler *et al.*, 1995; Hoffmann *et al.*, 1995; Mills *et al.*, 1993). The method revolves around the heterogeneous catalytic activation of a semiconductor by UV irradiation of a suitable wavelength depending on the band gap energy of the semiconductor. Hydroxyl radicals and other highly reactive oxidant species are produced by the activation process. The oxidant species possess high diffusion rates in water media which facilitate oxidative degradation of various dissolved organic compounds (mostly recalcitrant) to carbon dioxide, water and inorganic ions (or mineral acids). Anatase TiO_2 has been the popular choice as semiconductor photocatalyst due to its non-toxicity, high activity, low-cost and favourable overlap with the UV portion of the solar spectrum, making it an attractive option for solar applications.

To date, a multitude of dissolved organic, inorganic and organo-metallic compounds have been treated successfully. This has mainly been achieved at laboratory scale using small photocatalytic reactors operating as batch or flow systems (Blake, 1999). Complete degradation (mineralisation) of the parent molecule has been reported frequently. Colour and odour removal have been achieved with regard to the photocatalytic treatment of industrial effluent samples. The photocatalytic removal of disinfection by-products from drinking water were also reported. For PCO technologies to be competitive with conventional water treatment processes, the need exists to develop practical designs of photocatalytic reactors capable of being scaled-up. Such a development is very complex and requires comprehensive evaluation of the design of interest via two separate phases, viz. :

- Statistical optimisation of reactor and reaction parameters
- Reactor modelling (viz., momentum balances, mass balances, thermal energy balances, chemical kinetic and radiation transfer studies)

PCO exhibits marked potential for the complete oxidative removal of dissolved organic compounds in water, however it remains to be seen whether the technology could be exploited commercially. Scaling-up operations to date have been limited to a handful of pilot studies.

The treatment of raw drinking water containing industrial pollutants, cyanobacterial microcystin toxins and natural organic matter (NOM) is of relevance to the South African context of the provision of safe drinking water. This WRC sponsored project was therefore undertaken to assess the effectiveness of two novel photocatalytic reactors for the optimised removal of these groups of compounds from water. The project comprised two phases: an initial screening phase (August 1995 to December 1997) and a follow-up phase (January 1998 to June 2000). Experimental research was jointly conducted by the Department of Chemistry (University of Stellenbosch) and the Programme on Mycotoxins and Experimental Carcinogenesis (PROMEC) at the Medical Research Council (based in Tygerberg).

1.2 OBJECTIVES

The objectives of this research programme were to:

- Develop and establish the optimum performance characteristics of a novel design of photocatalytic reactors for purification of raw drinking water containing humic acids, clay colloids and other organic pollutants.
- Evaluate and establish the optimum performance characteristics of photocatalytic reactor designs for the decomposition of microcystins in various raw water samples.
- Establish optimal growth conditions for the microcystins by toxic cultures of cyanobacteria.
- Isolate and purify known and novel microcystin variants from freeze-dried culture material.
- Apply pure microcystin variants to the photocatalytic reactor(s), using the optimised conditions determined under the second objective.
- Identify the decomposition products derived from individual pure microcystin variants.

CHAPTER 2 : LITERATURE REVIEW

2.1 PHOTOCATALYTIC OXIDATION TECHNOLOGY

2.1.1 Fundamentals and Applications

Photocatalytic oxidation (PCO) involves the oxidative degradation of dissolved organic pollutants using UV irradiated dispersions of a suitable semiconductor, resulting in the complete mineralisation of the organic compounds to carbon dioxide, water and inorganic ions (mineral acids). Generation of reactive oxidising species such as hydroxyl radicals is considered to be the essence of the photocatalytic process. Oxidative degradation reactions mediated by hydroxyl radicals are adequately described in terms of three distinct mechanisms, viz., hydrogen abstraction, electron transfer and electrophilic addition (Legrini *et al.*, 1993).

Anatase TiO_2 has been the popular choice as semiconductor photocatalyst due to its non-toxicity, high photo-activity, low cost and favourable overlap with the UV portion of the solar spectrum, making it an attractive option for solar applications. The application of UV irradiation of appropriate wavelength (< 380 nm) to anatase TiO_2 results in the promotion of valence band electrons to the conduction band. The corresponding band gap energy is equivalent to approximately 3.2 eV. The ensuing charge separation leads to the formation of positively charged holes in the valence band which is neutralised through reaction with surface hydroxyl ions or water (depending on the pH of the medium), thus effecting hydroxyl radical formation. Excited electrons are trapped by molecular oxygen to form superoxide radical anions, thus preventing undesirable recombination of electrons and positive holes. The superoxide radicals and several other oxidant species may participate in a complex series of surface catalysed oxidation reactions to contribute to the overall oxidation of the pollutant molecule of interest. It is generally believed that PCO is surface catalysed and not induced in bulk aqueous solution. An ongoing global debate still exists on whether surface hydroxyl radicals of positively charged holes are directly responsible for PCO.

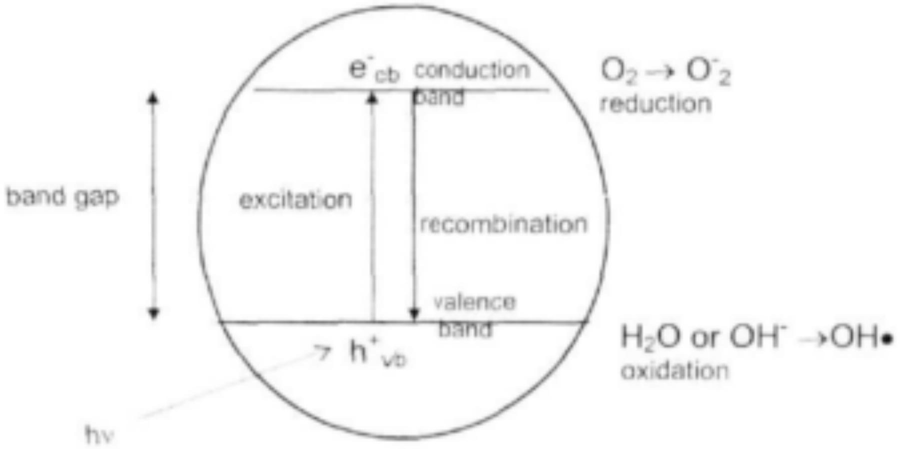

Figure 2.1: Hydroxyl radical formation via TiO_2 photocatalysis

Apart from using PCO in water treatment applications, the process of TiO_2 photocatalysis has also been applied in several other environmental, medical and industrial related sectors, viz. :

- Destruction of bacteria, viruses and fungi
- Destruction of tumor and cancer cells
- Destruction of mouth microbes and bacteria
- Oil spill clean-ups
- Self-cleaning devices and materials
- Super-hydrophilic materials
- Reductive separation of metals
- Organic synthesis
- Total organic carbon analysis
- Deodorising devices (air purification)
- UV sunscreens (rutile TiO_2 is used, though not as a photocatalyst)

A number of related advanced oxidation technologies are also currently being investigated for the remediation of aqueous waste streams. These technologies mostly involve hydroxyl radical chemistry in some form or another. Technical development has reached pilot and commercial scale in certain instances (Al-Ekabi, 1999; De Villiers, 2000). Some examples include:

- Chemical Oxidation Technologies
- Fenton and photo-Fenton Oxidation
- UV, Ozone and Hydrogen Peroxide based Technologies
- Vacuum Ultraviolet Technologies
- Supercritical Water Oxidation
- Electron Beam and Gamma Irradiation
- Electrohydraulic Cavitation and Sonolysis
- Non-Thermal Plasma Technologies (for air treatment)

2.1.2 Reactor Design

Research efforts pertaining to photocatalytic reactor design have mainly been directed towards slurry-phase or immobilised-bed (fixed-bed) reactors operating as batch or flow reactors. Slurried reactor configurations comprise the dispersion of TiO_2 colloidal particles in aqueous slurry medium. Immobilised configurations comprise the impregnation of TiO_2 on stationary supports such as quartz, glass, fibre glass, sand, ceramics, polymers, activated carbon, zeolites and optical fibres. They are usually operated as annular or falling film-type systems, but are less effective than slurried models in terms of reaction rates and photocatalytic efficiency due to inherent low catalytic surface-to-volume ratios. To their advantage is the fact that expensive secondary removal of catalyst is not required as in the case with slurries. Immobilized configurations are consequently favoured when scaling-up of designs are considered. For photocatalytic reduction processes, however, slurried reactors are required to facilitate reduction and deposition of metals onto catalyst particles. Furthermore, for organic syntheses via TiO_2 photocatalysis, slurried reactors are required to ensure high conversion rates.

Several types of small-scale photocatalytic reactors have been developed in laboratory studies using a variety of artificial light sources or solar irradiation. Ten examples were selected from literature and are presented below (Table 2.1):

Table 2.1: Literature survey of photocatalytic reactors examined for water purification

Configuration of TiO_2	Reactor Description	Operation Mode	Light Source	Reference
Immobilised (fibre glass)	Annular (Flow)	Recirculation	Low-pressure Mercury lamp	Ireland *et al.*, 1993
Immobilised (quartz sand)	Fluidised Bed (Flow)	Recirculation	Medium-pressure Mercury lamp	Haarstrick *et al.*, 1996
Immobilised (polyethylene)	Batch reactor	Not applicable	Solar irradiation	Naskar *et al.*, 1998
Immobilised (optical fibres)	Batch reactor	Not applicable	Xenon Arc UV lamp	Peill *et al.*, 1998
Immobilised (glass sheet)	Falling Film (Flow)	Recirculation	Fluorescent UV lamps	Sclafani *et al.*, 1999
Slurry-phase	Immersion (Flow)	Recirculation	Medium pressure Mercury lamps	Braun *et al.*, 1993
Slurry-phase	Parabolic Trough (flow)	Recirculation	Solar irradiation	Matthews, 1986
Slurry-phase	Laminar Falling Film (Flow)	Recirculation	UV-A and UV-C Mercury lamps	Puma *et al.*, 1999
Slurry-phase	Batch reactor	Not applicable	High-pressure Mercury lamp	Crittenden *et al.*, 1997
Immobilised (dune sand)	Batch (flow-through)	Recirculation	Solar irradiation	Matthews, 1991

Schematics of selected examples of photocatalytic reactors are presented below:

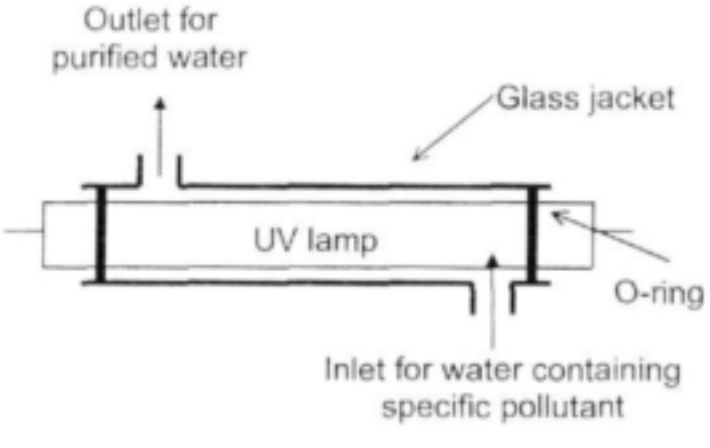

Figure 2.2: Conventional annular photocatalytic reactor (Cloete, 1999)

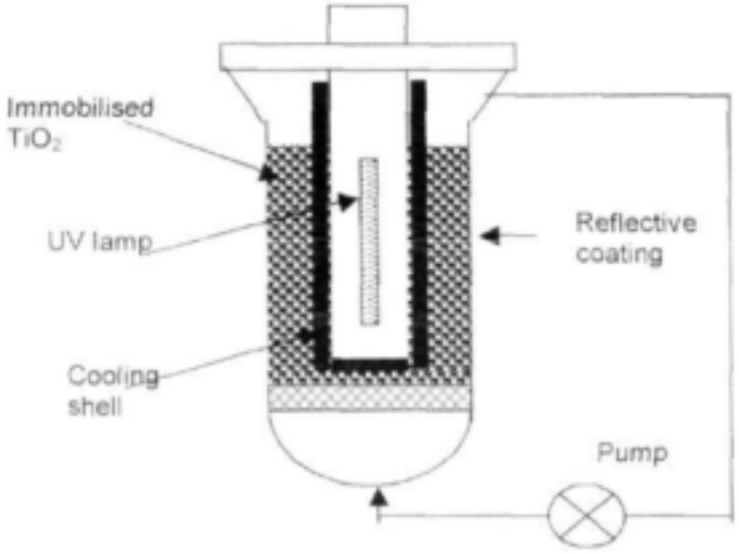

Figure 2.3: Immobilised-bed reactor (Haarstrick *et al.*, 1996)

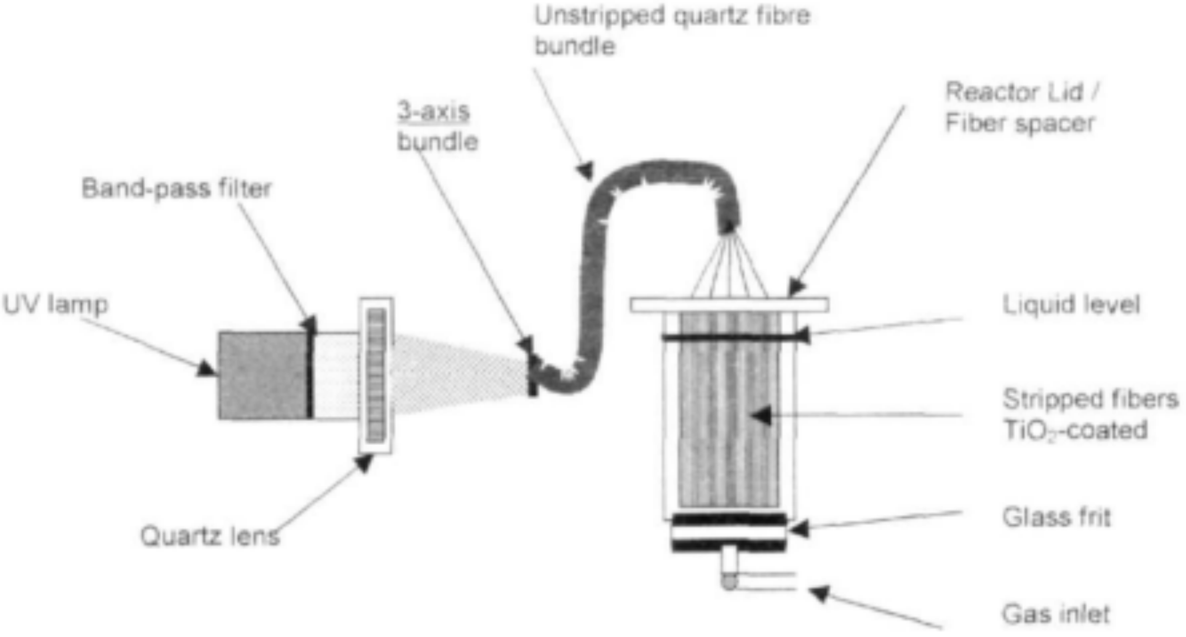

Figure 2.4: Fiber optic cable reactor (Peill and Hoffmann, 1998)

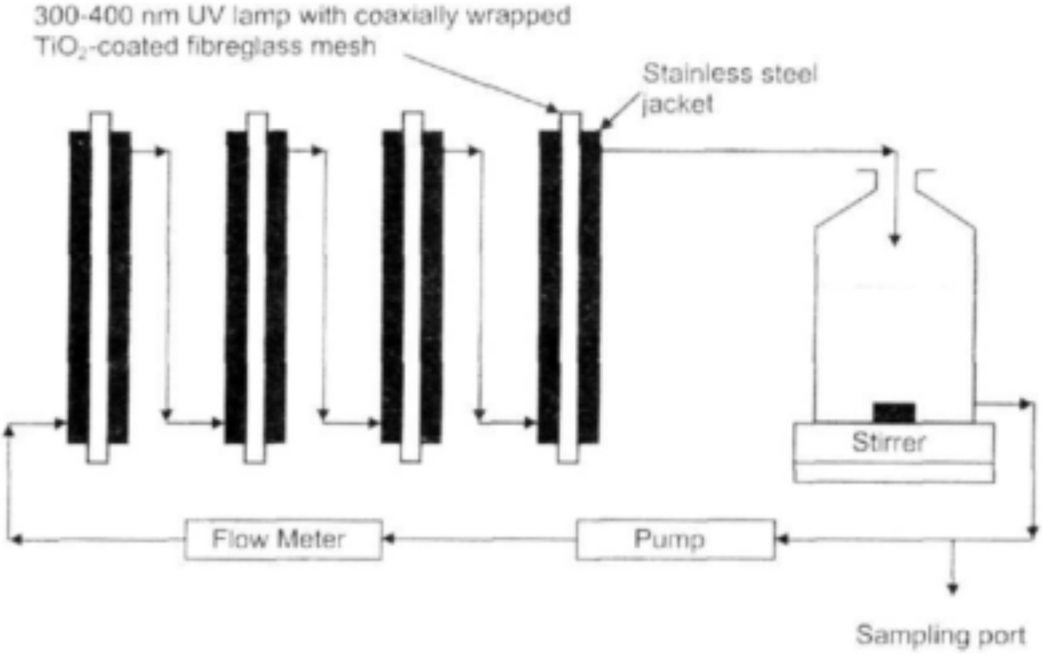

Figure 2.5: Direct contact flow-through reactor: Immobilised-bed and slurry-phase (Ireland *et al.*, 1993)

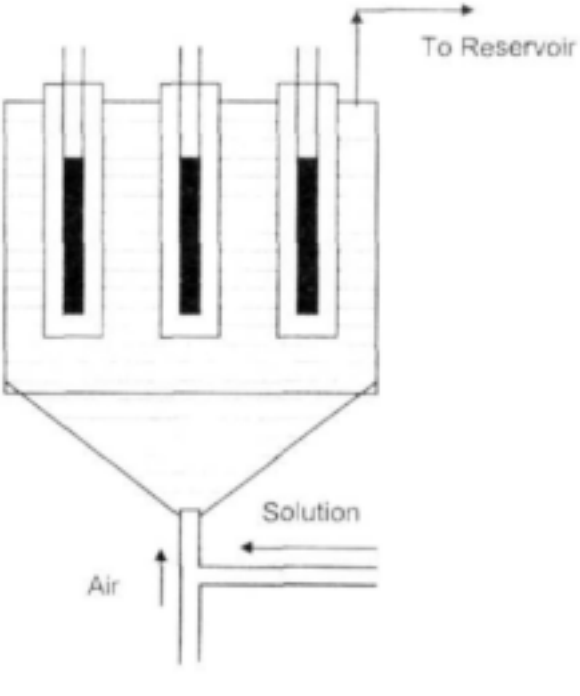

Figure 2.6: Multilamp immersion-type reactor (Braun *et al.*, 1993)

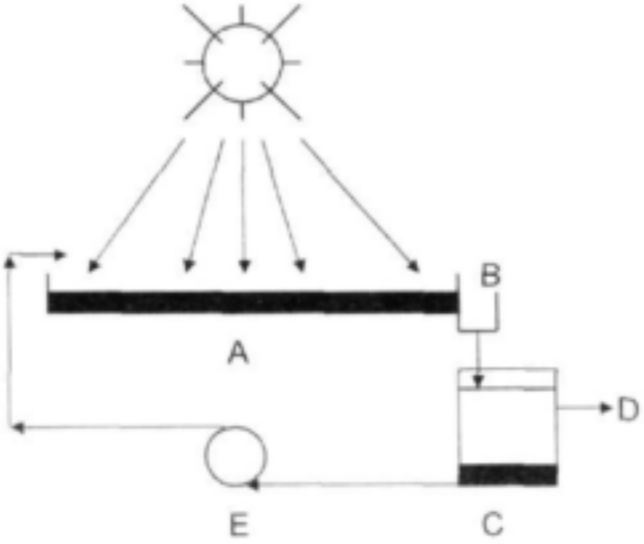

Figure 2.7: A solar-illuminated suspension pond reactor. (At sunset the suspension in lagoon A is dumped via dumping-trough B into an underground settling tank C. The suspension settles overnight and the clear water is pumped off through D. The settled suspension would be pumped back to the lagoon near sunrise, via a pump E, together with untreated water.) (Matthews, 1993)

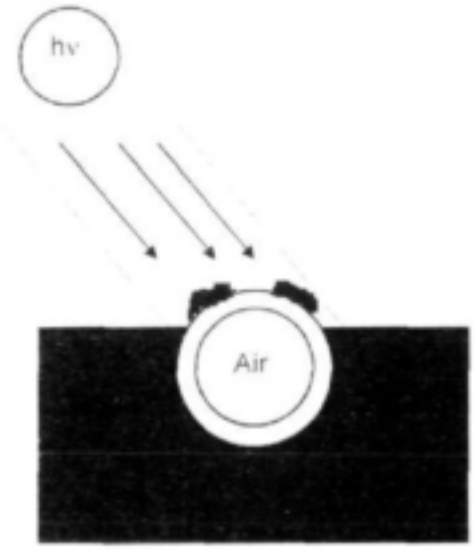

Figure 2.8: TiO_2 immobilised on glass microbeads (Jackson *et al.*, 1991)

2.1.3 Process Economics

With respect to investigating the scaling-up of photocatalytic reactors for treatment of polluted waters, a number of pilot-scale case studies have been completed, mostly in the United States and Canada. Cost calculations reported thus far have been variable and scaling-up projections were sensitive to the quality and volume of the untreated water. Comparisons are usually drawn with conventional treatments such as activated carbon adsorption and incineration. Rajeshwar (1996) projects a treatment cost of US$ 5.22 and 6.00 (per 1000 gallons) for UV photocatalysis and solar photocatalysis respectively. This amount compares favourably to granular activated carbon adsorption quoted at $ 6.20 (per 1000 gallons).

The cost to purify a small volume of highly contaminated water (e.g. 1000 L of wastewater containing 100 mg/L phenol) via UV photocatalysis has been projected to be in the vicinity of Aus$ 10. This calculation assumes 90 % mineralisation of phenol and takes into account electrical power consumption (per kWh), lamp replacement and catalyst cost. Lamp maintenance and plant amortization were disregarded. If the power was only consumed during off peak, costs would drop with approximately 50 %. The corresponding calculation when using granular activated carbon (GAC) amounted to Aus$ 6 taking disposal costs into account. The costs incurred in constructing a solar-based TiO_2 plant for treating 1 ML of water contaminated with 10 mg/L of phenol would amount to Aus$ 27500. Assuming 20 reuses of catalyst this amounts to Aus$ 1375/ML. Comparative GAC costs amounts to Aus$ 1000 (Matthews, 1993).

A more comprehensive calculation was conducted as part of an American Waterworks Association project on PCO (Hand *et al.*, 1995). Items such as catalyst cost, catalyst recovery, building materials, land and labour cost, lamp costs, lamp efficiency and life expectancy, electricity costs, contractor's profit, engineering administration costs and amortization periods were incorporated. Solar PCO treatment proved to be cheapest varying from US$ 0.48 per 1000 gallons for a 1 MGD plant to US$ 0.25 for a 100 MGD plant. Corresponding costs for systems operated by artificial UV light amounted to a maximum of around US$ 1 per 1000 gallons for a 100 MGD plant with an average UV contact time of 60 minutes. GAC costs reported in their study ranged from US$ 0.14 to US$ 2.21 per 1000 gallons.

The National Renewable Energy Laboratory in the United States reported a cost of US$ 10.90 per 1000 gallons for a 100 000 gallons per day TiO_2 slurry reactor operating as a solar trough system. Treatment costs are believed to be lowered considerably with the improvement in reactor designs and photocatalytic materials (Zhang *et al.*, 1994). Costs associated with the photocatalytic degradation of benzene, toluene, ethylbenzene and xylenes (BTEX) in groundwater was reported to be around US$ 1.75 per 1000 gallons without pretreatment. A British research group reported the following comparative costs in US Dollars for various system sizes (Mills *et al.*, 1993) :

Table 2.2: Estimated process costs for different water purification technologies

System size (MGD)	Carbon Adsorption	UV-Ozone Technology	UV-Photocatalytic Technology
0.029	$ 7.79	$13.00	$ 9.85
0.115	$ 4.25	$ 6.32	$ 4.36
0.23	$ 3.19	$ 4.92	$ 3.21
0.92	$ 2.21	$ 3.83	$ 2.32
2.44	$ 1.95	$ 3.10	$ 2.00

Trojan Technologies Inc. and Matrix Photocatalytic Inc. are both Canadian-based companies which are currently developing tailor-made UV and photocatalytic reactors for the treatment of contaminated groundwater, municipal wastewater and water for household purposes. Trojan's reactors are mainly designed as multiple annular UV reactors assembled in modules or coupled in series. They have several systems on the market operating at a variety of flow rates ranging from 2-12 gallons per minute (for small point-of-use drinking water application) to several hundred million gallons per day (for municipal wastewater disinfection). UV treatment in their systems occurs within 6-10 seconds in a flow-through channel in each segment of a module. Although Trojan specialises in disinfection of water by means of UV irradiation, they are also currently developing innovative photocatalytic technology in collaboration with KSE Inc., a US-based company.

Matrix Photocatalytic Inc. has commercialised and field tested annular photocatalytic reactors as far back as 1992. Their system (reactor cell) comprises an outer stainless steel jacket containing a UV lamp covered with a multi-layered sleeve of fibreglass mesh coated with TiO_2. Modular systems have been developed for high flow rates with capacity increments of 5 gallons per minute. Direct operating costs for raw effluent contaminated with organics, mainly BTEX and MTBE, are reported to be between $1-2 per 1000 gallons, with an average treatment time of 60 seconds. Several other in-house treatability tests yielded operating costs around $\$0.5/m^3$ for aromatics in water and around $\$0.3/m^3$ for THMs in drinking water. Matrix Photocatalytic technology was field-tested in the United States for groundwater remediation. A 60 gallon per minute parallel mode reactor system was employed. Based on the results achieved, the photocatalytic remediation costs were calculated to be much less compared to conventional groundwater remediation. For the treatment of 29 million gallons over a 2.5 year period at a flow rate of 24 gallons per minute, the costs projected to US$ 50.76 per 1000 gallons. For the treatment of 341 million gallons over a 30 year period at the equivalent flow rate, the costs projected to US$ 28.41 per 1000 gallons (Al-Ekabi, 1999).

Photocatalytic reactors are also currently been developed in Japan (for drinking water treatment) and in Germany, the Netherlands, Singapore and Hong Kong (for effluent treatment), however it is not sure whether commercial stage has been attained.

The task to develop and scale-up multi-phase photocatalytic reactors (particularly immobilised configurations) is significantly more complex than that of conventional homogeneous photochemical reactors. Factors to consider include mixing, mass transfer, reaction kinetics, catalyst immobilisation and illuminated specific surface area (κ). κ is an engineering parameter which is used to describe the efficiency of immobilised photocatalytic reactors in terms of the total illuminated surface area of catalyst within the reactor that is in contact with the reaction liquid (Ray and Beenackers, 1998). Other challenges relate to the practicality of reactor designs, optimal use of UV sources and the development of efficient photocatalysts. The high degree of interaction between transport processes, reaction kinetics and light absorption leads to a strong coupling of physicochemical phenomena, which complicates development via modeling. Chemical reaction engineering is required, ultimately spanning the entire development from molecular level (nanometer and femtosecond scale) to production scale. Reactor modeling will be complemented by results obtained from statistical optimisation of reactor and reaction parameters. A successful reactor, in conclusion, would consist of a unique configuration of light source, photocatalyst and reactor material. Such a development would inevitably require extensive collaboration between scientists, engineers and material specialists from a variety of backgrounds.

2.1.4 Figures-of-Merit

Globally acceptable "figures-of-merits" are required to evaluate different water treatment technologies on equal footing. For advanced oxidation technologies (AOTs) these parameters should be based on (1) electrical energy input, (2) water volumes to be treated, (3) volumetric flow rates (4) pollutant concentrations (5) level of purification required and (6) time of treatment.

A useful energy parameter for comparing the efficiency of AOTs in flow-reactor water purification systems has been established (Bolton *et al.*, 1996). This parameter is best used for situations where pollutant concentrations are low and overall first order degradation kinetics apply.

The Electrical Energy per Order (EE/O) is defined as the electrical energy in kWh required to effect the degradation of a pollutant by one order of magnitude in 1 m^3 (1000 L) of polluted water:

$$EE/O = P / F \times \log (c_o / c_f) \qquad (2.1)$$

Where:
P = Lamp power (in kW)
F = Volumetric water flow rate (in m^3/h)
c_o = Initial concentration
c_f = Final concentration
EE/O = kWh/order/m^3

Equation 2.1 is designed for idealised plug-flow reactors. Reactor volumes and first order kinetics can be accounted for, in which case the equation changes to:

$$EE/O = 38.4 \times P / V \times k_{1st} \qquad (2.2)$$

Where:
P = Lamp power (in kW)
V = Reactor Volume (in L)
k_{1st} = First order rate constant (in $mins^{-1}$)
EE/O = kWh/order/m^3

Eqn 2.2 is merely an equivalent version of eqn 2.1 and implies that EE/O can be calculated directly from kinetic rate constants, hence indirectly from UV contact times. In all cases, lower values of EE/O correspond to enhanced electrical efficiency and lower treatment costs. EE/O equations have also been suggested for idealised batch and continuously-stirred tank reactors (CSTRs).

In this project, cost calculations for experimental reactors were limited to a single pass mode of operation. The use of idealised plug-flow conditions facilitated the calculation in this regard. Recirculation mode of operation is more complex and relates to CSTR models.

In this instance the EE/O is not a constant per order and has to be determined for each destruction efficiency based on the hold-up time of liquid within the reactor (Bolton *et al.*, 1996).

Apart from the EE/O parameter, a second figure-of-merit has been suggested for evaluating the electrical efficiency based on mass removal of the pollutant (in kg) (Bolton *et al.*, 1996).

2.1.5 Tandem Technologies

Apart from using photocatalytic oxidation on its own for water purification, it has been suggested that the process be operated in tandem with other conventional treatment technologies. In this regard processes such as granular activated carbon adsorption (Crittenden *et al.*, 1997) and biological degradation (Li and Zhang, 1996) have been used in tandem with photocatalytic oxidation for the removal of organic compounds from water – the former process in each case used as workhorse to perform the bulk of the purification (i.e. COD, colour and organic carbon reduction) and the photocatalytic oxidation process introduced as a final polishing step or as a tool for the regeneration of spent adsorbents.

2.1.6 Fibrous Activated Carbon

A new formulation of activated carbon has recently been developed with potential application for water treatment, viz: fibrous activated carbon (FAC). The adsorption of organic water pollutants by FAC has been reported in scientific literature (Brasquet *et al.*, 1996; Le Cloirec *et al.*, 1997). FAC is manufactured from natural precursors (e.g. coconut) or synthetic precursors (phenolic resins or viscose). The raw material undergoes carbonisation at 1000 °C to eliminate volatiles. This is followed up by steam or CO_2 activation at 800 °C which produces the FAC product with a large specific surface area and a significant volume of micropores. The average pore diameter for FAC ranges from 5 to 21 Å. As a result, the total surface area may vary from 700 to approximately 2500 m^2/g depending on the manufactured grade. To date, FAC has not been engineered in industrial processes but recent laboratory studies (by Le Cloirec and co-workers) confirmed its superior adsorption potential for water pollutants (e.g. phenol) compared to GAC and PAC. The application of neural networks and statistical regression analysis to predict adsorbability of organic compounds onto FAC as a function of molecular structure is currently being addressed (Brasquet *et al.*, 1999).

A treatment strategy employing activated carbon adsorption in tandem with semiconductor photocatalysis was field tested at Tyndall Air Force Base (Florida, USA) for the removal and destruction of organic pollutants in groundwater (Crittenden *et al*, 1997). Although granular and powdered activated carbon are commonly used in water treatment, this report sparked the idea of combining FAC with TiO_2 photocatalysis for improved water purification. In this project a portion of the photocatalytic irradiation experiments will be conducted in a reactor with TiO_2 catalyst immobilised on a sheet of activated carbon (known as fibrous activated carbon). This approach will simulate a tandem process.

2.2 CYANOBACTERIAL MICROCYSTIN TOXINS

2.2.1 Origin

Cyanobacterial microcystins are a major group of natural biotoxins produced by several species of blue-green algae (cyanobacteria) in aquatic environments (Carmichael, 1992; Lawton and Robertson, 1999). The cyanobacteria are microscopic inhabitants of surface waters and known as a group of bacteria in which the cells contain chlorophyll and consequently participate in photosynthesis reactions. Individual algal cells are not visible to the naked eye, but do become visible when in concentrated form as suspended colonies (e.g. *Microcystis aeruginosa*) or filaments (e.g. *Anabaena*). Overabundant growths of algae result in the formation of dense green blooms which may resemble pea-soup suspended on water surfaces (Carmichael, 1994). Excessive nutrient enrichment of natural waters (eutrophication) are known to cause proliferative growth or blooms which may subsequently release microcystin toxins into water. The primary sources of nutrients (e.g phosphates and nitrates) are raw sewage spills, industrial effluents and run-offs from argricultural and urban regions. Warm summer conditions (high temperatures and light intensities) and calm, stable waters (low turbidity, no wind) also contribute to bloom formation. Blooms can spread from one shore-line to another in relatively short time on windy days.

2.2.2 Classification and Chemical Structure

Cyanobacterial toxins are classified into two main groups, viz. neurotoxins and hepatotoxins. Neurotoxins affect the nervous system and are fast-acting, small molecules. Examples include anatoxin and saxitoxin. Hepatotoxins affect the liver and are cyclic peptide molecules acting more slowly compared to neurotoxins. Examples include the microcystins and nodularins. The microcystins are cyclic heptapeptides containing 5 invariant amino acids and 2 variable L-amino acids. The toxins are labelled using one-letter abbreviations to indicate the 2 variable amino acids. Microcystin-LR, for example, contains leucine (L) and arginine (R) in the variable positions. More than 60 structural analogues (variants) are known (Carmichael, 1994; Lawton and Robertson, 1999).

2.2.3 Toxicity

At least one of the cyanobacterial species (*M. aeruginosa*) has been shown to produce hepatotoxic microcystins in South African waters. Wicks and Thiel (1990) determined the seasonal occurrence and distribution of 6 microcystin variants (LA, LR, YA, YR, FR and Laba) in the Hartebeespoort Dam, South Africa. The microcystins are capable of causing acute and chronic toxicosis in both humans and animals. Toxicological studies revealed LD_{50} values for the microcystins around 0.05 mg/kg in mice (by intra-peritoneal injection) compared to 4.3 mg/kg for sodium cyanide (Lam *et al.*, 1995). The microcystins have caused a number of livestock poisonings and deaths in South Africa to date (Van Halderen *et al.*, 1995). They have also been linked to the high incidence of liver cancer in areas of China where populations are dependent on surface drinking water (Nishiwaki-Matsushima et al., 1992). Moreover, the recent deaths of approximately 60 hospital patients in Caruaru, Brazil have been unequivocally linked to microcystin contamination of the water supply to the kidney dialysis unit of the local hospital (Hitzfeld *et al.*, 2000). Not all cyanobacterial blooms are toxic, but a significant number are. Health assessment studies have been scarce to date mainly due the variable toxicity of the blooms. The WHO has proposed a guideline value of 1μg/L for microcystin LR in drinking water (Chorus *et al.*, 1999) and 20μg/L for recreational water.

2.2.4 Analytical Detection

A validated method has been developed for the analytical determination of microcystins in water (Lawton *et al.*, 1994). The procedure comprises the following steps :

- Methanol extraction of the toxins from freeze-dried algal material
- Sample purification with Solid Phase Extraction (SPE)
- Separation and identification using isocratic reversed-phase HPLC with UV diode-array detection at 240 nm. Detection limit: below 250 ng/L (ppb) depending on the nature of the raw .and treated water analysed.

Other sensitive techniques (e.g. capillary electrophoresis and tandem-Mass Spectrometry) are being developed to reduce detection limits further within the ng/L range (Bateman *et al.*, 1995).

2.2.5 Treatment Options

Problems encountered with the treatment and subsequent removal of microcystins from drinking water sources are related to the chemical stability of these toxins with regard to temperature and pH variation. Conventional water treatment (e.g. coagulation) has been ineffective due to the relative small size of the toxin molecules (ca 800-1000 Daltons). Other treatment techniques (e.g. chlorination, carbon adsorption and UV irradiation) have all met with variable success and was limited to the treatment of small laboratory scale water samples (Nicholson *et al.*, 1994; Donati *et al.*, 1994; Tsuji *et al.*, 1995). Reverse osmosis retained the toxins successfully, however toxin enriched water had to be disposed of by other means. Chemical treatment methods such as ozonation and oxidation by hydrogen peroxide or permanganate have been investigated, but it remains uncertain whether oxidant stability as a function of water quality will render these processes economically viable (Lawton and Robertson, 1999).

The main objective of this project is to propose the use of photocatalytic oxidation as potential means for the complete oxidative destruction of microcystins in water. As a result, photocatalytic destruction was successfully demonstrated in this project in July 1995 and subsequently presented internationally (Stockenström *et al.*,1996). Recent results by Scottish and Australian groups (Robertson *et al.*, 1999; Feitz *et al.*, 1999) have confirmed complete photocatalytic destruction of microcystin toxin molecules with a resultant reduction in toxicity levels in water.

2.3 NATURAL ORGANIC MATTER

2.3.1 Origin

Surface and ground waters contain a complex variety of natural organic matter (NOM) characteristic to the natural vegetation of the environment within a specific catchment area. NOM present in water exert a significant effect on water treatment processes, the application of different disinfectants and the stability of the water. Water quality of potable waters (in terms of disinfection by-products (DBPs), biological regrowth in the distribution systems, colour, taste and odour) are directly influenced by NOM present in the water (Owen, 1995). For efficient water purification it is, therefore, of great importance that NOM is sufficiently characterised where it occurs.

2.3.2 Classification

Both insoluble and soluble organic matter contribute to NOM in raw water. Table 2.3 lists the most prominent groups of NOM compounds in water (Kunin, 1986)

Table 2.3: NOM compounds in water.

Insoluble Organic Matter	Soluble Organic Matter
Debris of vegetable origin Debris of animal origin Micro-organisms Oily matter Humic matter (substances)	Humic Matter (substances) Fatty acids Nitrogen-rich compounds (proteins, peptides, amino acids) Saccharides and sugars Dissolved organic gases (e.g CH_4) Soluble extracts of vegetable/animal origin Synthetic organic compounds

An alternative classification of NOM in raw water is based on the "humic character" of organic matter. NOM are divided into a humic (hydrophobic) and a non-humic (hydrophilic) category. Each main category is subdivided as presented in table 2.4 (Owen, 1995):

Table 2.4: NOM classification

Humic Matter	Non-Humic Matter
Humic Acids Fulvic Acids	Hydrophilic acids Proteins Amino Acids Carbohydrates

Most non-humic compounds are swiftly degraded by microorganisms, hence exhibit short life spans in soils and sediments. In the past, non-humic matter were discarded when addressing the overall topic of drinking water quality. A recent study has, however, indicated that these compounds (Owen, 1995) could contribute significantly to the formation of potential DBPs. Non-humic compounds also contribute to a greater percentage of the biodegradable organic carbon (BDOC), which is a water quality parameter of great concern when bacterial regrowth and bio-film formation in distribution systems are prevalent.

2.3.3 Humic Substances

(a) Origin, Structure and Molecular Weight Distribution

For many decades researchers have tried to determine the exact origin and composition of humic substances. Many papers have been published on this matter, but a great deal still remains to be interpreted. Humic substances are believed to originate from the chemical and biological degradation of plant and animal materials and from the synthesizing activities of micro-organisms. Contrary to the non-humic materials, humic substances are stable for longer periods. They exhibit weak physical and chemical characteristics, e.g. no well-defined (infrared) IR spectrum or melting point, which are normally associated with well-characterised organic compounds. Humic substances are defined as anionic, predominantly aromatic, polyelectrolytes, containing mainly carboxylic and phenolic functional groups. Molecular weights vary from a few hundred to several thousand mass units. The yellow-brown colour of surface waters can be attributed to the dark colour of the humic substances. This is confirmed and interpreted by UV spectrometric analysis of raw water containing humic substances (Cloete, 1999). The absorption of short wavelength light by these substances is coupled to a transmittance of longer wavelengths (500nm and beyond) which is explains the yellow-brown colour.

Humic substances consist of three main fractions, viz:

- **Fulvic acids** (FA) : the lowest molecular weight fraction; soluble regardless of pH; most susceptible to microbiological degradation
- **Humic acids** (HA) : intermediate molecular weights; soluble only in alkaline solution
- **Humin** (HU) : highest molecular weight fraction; insoluble regardless of pH; least susceptible to microbiological degradation.

(b) Characterisation

Characterisation of the functional groups in HA and FA is very important when different treatment processes are considered for e.g. surface water. Variation in functional group composition results in great differences in response to water treatment, e.g.

- FA have a higher combined carboxylic and phenolic acidity and therefore a higher charge density than HA, resulting in FA being more difficult to coagulate by charge neutralisation (Owen, 1995).

- Molecules with lower charge density can easily be removed by means of activated carbon adsorption. By reducing the pH, the charge density of FA can be lowered, thereby facilitating removal of both FA and HA (Owen, 1995).

- The solubility of HA and FA are influenced by the presence of different functional groups (Owen, 1995).

(c) Acid-Base Equilibria

The weak polyelectrolyte character of HA and FA contributes to buffering capabilities in soil and aqueous environments. By constructing pK distribution curves at specific ionic strengths, it is possible to demonstrate deprotonation of these compounds with increasing pH (Fukushima *et al.*, 1995). The behaviour of humic substances as a function of pH can therefore be predicted according to the state in which the functional groups are found.

(d) Complexation Properties

Since humic substances contain elements with lone pair electrons (e.g. nitrogen and oxygen), they are inclined to act as ligands in the formation of complexes with heavy metal ions (Fukushima *et al.*, 1995). FA and HA possess various binding sites for complexation, eg. -COOH, -COOH- (phenolic) and -OH (phenolic) functional groups. The binding capabilities of heavy metal ions can be correlated with the functional group distribution of humic substances (Warwick, 1994). Useful information concerning the complexation properties of humic substances with heavy metal ions can therefore be deduced from the acid-base equilibria (Fukushima *et al.*, 1995).

The behaviour of humic substances toward metal ions in water renders polarographic methods a potentially useful analytical tool whereby coloured waters could be characterised. By monitoring the complexation of humic substances with metal ions such as Fe^{3+}, Cu^{2+} and Zn^{2+} at various pH levels, humic substances (NOM) could be characterised.

The occurrence of metals in water originates mainly from natural sources, e.g. from minerals such as barite and limestone, or natural volcanic emissions. In recent times, discharges from factories, mining effluents and other industries have substantially increased the amount of metals in water sources. Complexation of humic substances with metals and/or clays in water have resulted in increased resistance against microbiological degradation and less efficient flocculation processes. Moreover, the presence of multivalent ions (such as ferric) in raw water may enhance complexation of humic substances with clay colloids (Kunin, 1986).

When considering the insoluble fractions of humic substances (HU), a possible explanation for their insolubility over the entire pH range may be found in their firm bonding to inorganic soil and sediment constituents.

(e) Adsorptive Properties

Kopinke *et al.* (1995) performed a series of experiments to investigate the sorption of organic pollutants onto the surface of humic matter. Adsorption constants (Log K) for several poli-aromatic hydrocarbons (PAHs) and poly-chlorobiphenyls (PCBs) were determined for sorption onto FA and HA. The results imply strong adsorption. With increasing industrial pollution of surface waters, this characteristic could cause several problems for standard water purification methods.

The hydrophobic properties of the aromatic rings and aliphatic chains contained within humic substances adsorb strongly onto the surface of mercury with a zero charge. The charged functional groups are oriented toward the aqueous medium. This phenomenon could facilitate the analysis of humic substances by means of voltammetry.

A recent study has shown that humic substances in water do not absorb onto fibrous activated carbon (FAC). Small organic micro-pollutants, however, were adsorbed readily and breakthrough curves for FAC could be determined accordingly (Le Cloirec *et al.*, 1997). The extent of absorption of larger organic water pollutants (such as microcystins and humic matter) onto these materials will be largely dependent on the degree of overlapping of molecular size with pore size/volume characteristics.

(f) Spectroscopic Properties

The standard humic acid chemical structure (long conjugated aromatic polymer chains) renders an efficient absorption of UV light. In general, aqueous humic samples exhibit a featureless increase in UV absorbance at shorter wavelengths. Through the absorption of UV light, humic substances are activated indirectly from a singlet state to a triplet electronic state. The activation allows humic substances to photo-induce the transformation of non-absorbing organic compounds. Various chromophores are responsible for the photoreactivity at a number of wavelengths (Aguer and Richard, 1996). Chin and co-workers (1994) have shown that the molar absorptivity (ε) of humic substances at specific wavelengths may be linked to aromaticity, the source of the humic substances, as well as the degree of humification. The study emphasised UV analysis at 280nm where $\pi \rightarrow \pi^*$ electron transitions occur for phenolic substances, aniline derivatives, benzoic acids, polyenes and polycyclic aromatic hydrocarbons. Many of these compounds are either precursors or components of humic substances. Based on these results, ε (280nm) may be considered a useful parameter for characterisation of humic substances.

The spectroscopic properties of humic substances may also be used to develop another useful method for characterisation of coloured waters. This is done by adding a UV in-active compound to coloured water, with the humic substances inducing fluorescence in this spiking compound. The resultant fluorescence spectrum could be recorded and used in the characterisation of coloured water.

Another potential method for water purification flows from the knowledge of the excited electronic states of humic substances that can be reached through initial radiative activation. Excited triplet states of the humic substances might have sufficient energy to activate dissolved oxygen in the ($X\ ^3\Sigma^-_g$) ground state to the first ($^1\Delta_g$) activated electronic state through intermolecular collisions. Singlet oxygen being a powerful oxidant can initiate the oxidation of organic pollutants as well as of humic substances (Lang *et al.*, 1992).

(g) Analytical Detection

The chemical and physical composition of humic substances can be determined by a series of experiments. Firstly, the humic substances can be extracted and separated by employing the knowledge of solubility of the various fractions. Each fraction may be categorised further according to their molecular weight using ultra-filtration.

Many non-degradative methods for the determination of the physical properties of humic substances exist (Schnitzer and Khan, 1987; Bekbolet, 1996; Liang *et al.*, 1999; Balnois *et al.*, 1999):

- Ultraviolet and Visible light spectrometry
- Infra-Red spectrometry
- Surface Enhanced Raman Spectrometry (SERS)
- X-Ray diffraction
- Atomic Force Microscopy (AFM)

Direct analytical monitoring of NOM constituents such as humic substances was achieved using Pyrolysis Gas Chromatography-Mass Spectrometry (Vilge-Ritter *et al.*, 1999). Gel Permeation Chromatography (GPC) was used to obtain separation of the various mass fractions prior to analysis.

(h) Treatment Options

Coagulation-flocculation procedures are used worldwide in conventional water treatment plants for the removal of humic substances in raw drinking water prior to chlorination. Flocculants used thus far include ferric chloride, aluminium sulphate and polychlorosulphate amongst others. Inefficient coagulation-flocculation results in the unwanted formation of DBPs since humic substances are precursors of THMs during chlorination. Alternative treatment strategies are based on the oxidative destruction of humic substances as opposed to phase transfer or physical separation of the compound. Advanced oxidation technologies such as TiO_2 photocatalysis and UV-Peroxide oxidation have been investigated on small scale for the mineralisation of humic substances in coloured waters. Colour and TOC reduction were achieved (Bekbolet, 1996; Eggins *et al.*, 1997; Martin *et al.*, 1999). A part of this project is devoted to the photocatalytic oxidative degradation of natural occurring humic matter in raw surface water.

2.4 Statistical Methods for Optimisation

2.4.1 Optimal experimental design

When complex experimental systems, consisting of many factors, must be optimised, varying each factor individually can become a very tedious and time-consuming process. The individual variation of factors does not allow for any interactions between the factors to be monitored (Braun, 1963).

An alternative approach to the *one-factor-at-a-time* method is to employ a statistical approach for the optimisation. Factors, which might influence the experiments, must be identified and an accurate response to variation in factor values must be measurable. If an experimental approach is well constructed, the number of experiments will be reduced dramatically (Braun, 1963). The basic approach can be divided into three steps, namely

Screening Designs: Screening is the initial step where little is known about the effect of the factors on the response measured. Many factors are examined in order to determine those which exert the greatest effect on the response. Statistical approaches, which can be employed, include the factorial statistical design and Plackett-Burman matrices (Braun, 1963).

Response Surface Designs: From the previous step, the important factors have been identified. These factors are now used to optimise the operating conditions of the system. A model is therefore constructed for optimal experimental results. Typical optimisation procedures include the simplex method and the central composite response surface design.

Verification: The final stage involves execution of the experiment at the predicted best settings to confirm the optimum value of the response predicted at these conditions. Reproducibility of the response can also be determined at these conditions.

Another approach to solving optimisation problems is the *Optimal Experimental Design Pyramid (OED pyramid)* (Ghosh, 1990). The screening design forms the basis of the pyramid and is employed in the initial stage of the investigation. Progress is made toward the top of the pyramid as more experimental information is generated.

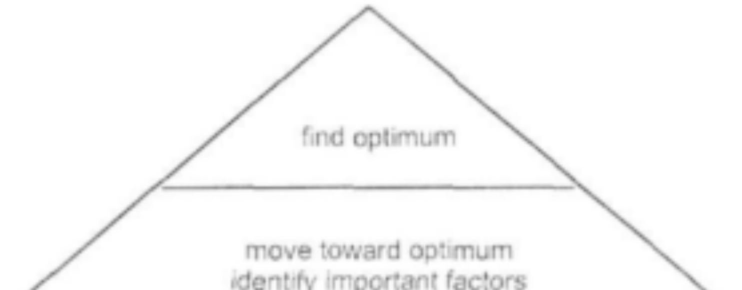

Figure 2.8: Optimal Experimental Design Pyramid (Ghosh, 1990, p.86)

Statistical optimisation of experimental conditions therefore involves much less effort. The sets of experiments are well constructed and the verified end results are reliable. Factor interactions are also investigated.

2.4.2 Experimental approach

2.4.2.1 Screening Design: Factorial Statistical Design

The factorial statistical design is one of the more common screening designs available. The purpose is to determine the relative individual influence of the qualitative and quantitative factors on the response measured, as well as the interactions between factors (Morgan, 1995). A *two level two factor factorial design*, for example, consists of two factors, each with a maximum and minimum value. The maximum and minimum levels must be chosen in such a way that a shift in factor value from minimum to maximum would result in a substantial change in the response measured. 2^k (where k = number of factors) experiments must be performed for each factorial design.

A two level two factor factorial (denoted by 2^2 factorial) would therefore consist of factors X_1 and X_2 and would require $2^2 = 4$ experiments. The experiments can be summarised by the following design matrix:

Table 2.5: A Typical Design Matrix for a 2^2 Factorial Design (- : minimum level, +: maximum level, Z: response measured)

Experiment	Factor		Response
	X_1	X_2	Z
1	-	-	Z_1
2	+	-	Z_2
3	-	+	Z_3
4	+	+	Z_4

By employing a statistical computer program, eg. STATGRAPHICS, SAS, QSCA, CARD or STATISTICA, these results can now be processed and interpreted. For our purposes STATISTICA Version 5.1 was employed.

2.4.2.2 Response Surface Design: Simplex Design

The simplex method can be used for the optimisation of quantitative factors in a particular experimental set-up (Yarbro, 1974). The set of factors, which resulted in the greatest positive response with e.g. a factorial design, is often used as the starting point of a simplex. However, when optimising an analytical reagent, it is preferable not to use the concentration of the reagent as a factor. Concentration effects, which involves movement of the simplex towards maximum concentration, should be avoided (Long, 1969).

The simplex is a geometric figure defined by a number of vertex points equal to one unit more in dimension than the number of factors chosen (Deming, 1973), e.g. a two factor simplex will be represented by a triangle. Each vertex point represents a set of experimental conditions for the entire set of factors. These values are determined in a set way (Long, 1969), namely

- choose the coordinates of vertex 1
- choose step-sizes for each factor

- multiply each step-size by the tabulated values (Table 2.6)
- add this result to vertex 1 to get the values of the new vertex point

Table 2.6: Initial Vertex Locations (Long, 1969)

Vertex	Factor									
No.	A	B	C	D	E	F	G	H	I	J
1	0	0	0	0	0	0	0	0	0	0
2	1.000	0	0	0	0	0	0	0	0	0
3	0.500	0.866	0	0	0	0	0	0	0	0
4	0.500	0.289	0.817	0	0	0	0	0	0	0
5	0.500	0.289	0.204	0.791	0	0	0	0	0	0
6	0.500	0.289	0.204	0.158	0.775	0	0	0	0	0
7	0.500	0.289	0.204	0.158	0.129	0.764	0	0	0	0
8	0.500	0.289	0.204	0.158	0.129	0.109	0.756	0	0	0
9	0.500	0.289	0.204	0.158	0.129	0.109	0.094	0.750	0	0
10	0.500	0.289	0.204	0.158	0.129	0.109	0.094	0.083	0.745	0
11	0.500	0.289	0.204	0.158	0.129	0.109	0.094	0.083	0.075	0.742

The simplex design is based on the principle of rejecting the worse vertex of the geometric figure and calculating a new vertex point (Figure 2.8), until an area of optimum response (a maximum or minimum) is reached. By decreasing the step-size for each factor, this optimum region can then be investigated even further until the exact optimum conditions are determined.

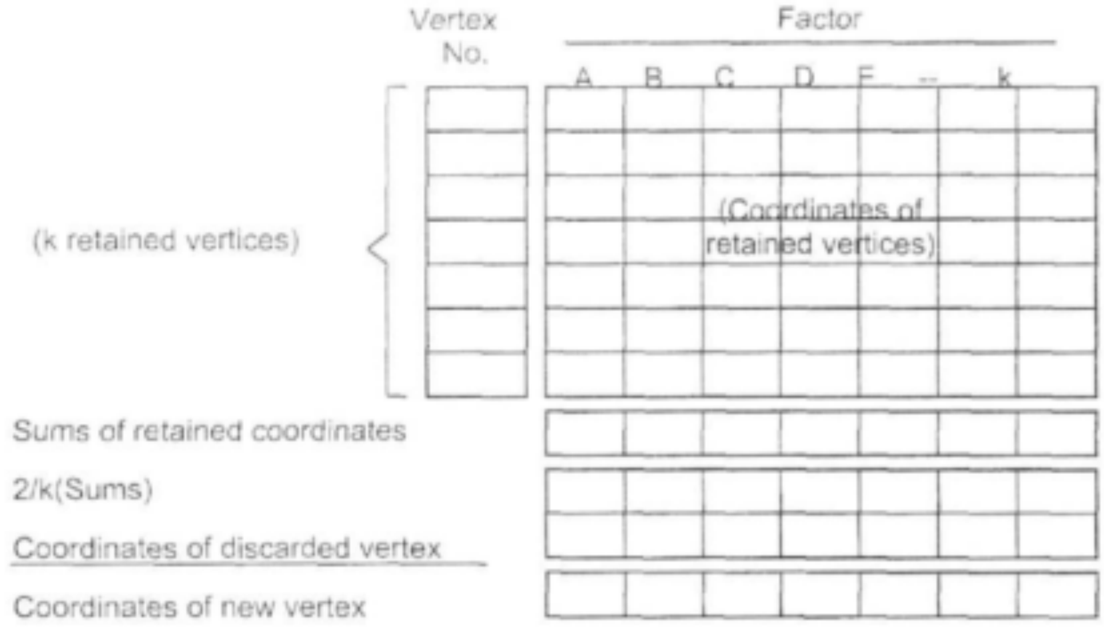

Figure 2.9: *Procedure for the Calculation of Succeeding Vertex Points* (Long, 1969)

2.4.2.3 Response Surface Designs: Central Composite Design

A well-known response surface design is the central composite design. This design consists of a complete 2^k factorial, with additional axial points (denoted by a) along the coordinate axes, as well as a center point. The center points is repeated two or three times in order to determine the reproducibility of the specific system under investigation.

The axial points can be located at arbitrary distances from the center point, depending on the analysis being performed. However, for the design to be rotatable, the axial distance from the center point must be $a=F^{1/4}$, where F is the number of factorial points ($F=2^k$). Rotatability is a desirable property for any design,allowing for the response to be estimated with equal precision at all points in the factor space that are equidistant from the centre of the design (Mason, 1989).

The following steps (Mason, 1989) construct a central composite design:

- a complete 2^k factorial layout (with k factors)
- 2k axial points along the coordinate axes
- m repeat observations at the design center
- randomise the experiment to eliminate "bias effects"

The total number of runs in a central composite design is based on the complete factorial design:

$$n=2^k + 2k + m$$

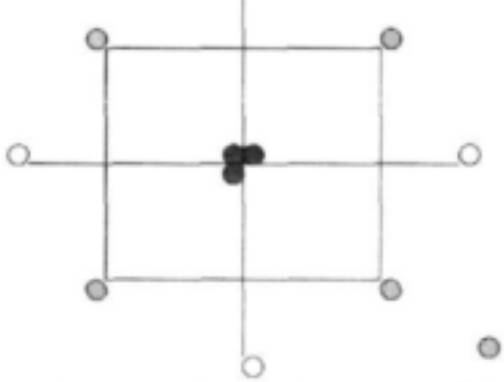

Figure 4.3: Typical Central Composite Design for two factors (2^k factorial design; ● center points; ○ axial points)

The data obtained can now be analysed by means of one of the above mentioned statistical programs.

2.4.2.3 Response Surface Methodology

The experimental region for a chosen system is characterised by the manner in which the factors influence the specific response function. Graphic representations of these experimental regions provide a clearer image of the variation of the response as a function of the chosen factors (Figure 2.11).

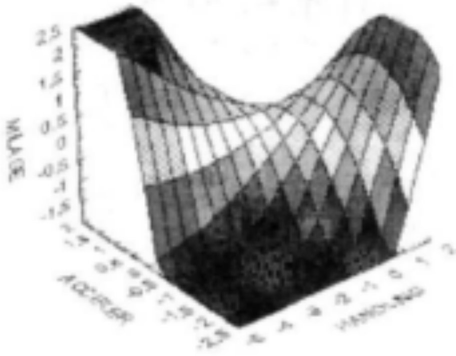

Figure 2.11: A Typical Saddle Response Surface

Mathematical modelling is employed to determine the basic shape of the response surface. This is done by constructing a quadratic polynomial for the response in terms of two factors (X_1 and X_2). The general form of a quadratic polynomial in terms of two factors can be represented by:

$$Z = \beta_0 + \beta_1 X_1 + \beta_2 X_2 + \beta_{11} X_1^2 + \beta_{22} X_2^2 + \beta_{12} X_1 X_2$$

where,

Z: response function
X_1, X_2: experimental factors
β_0: intercept on response axis
β_1, β_2: gradient for each factor
β_{11}, β_{22}: parabolic character of the surface for each factor
β_{12}: interaction term; combined effect of the two factors

These polynomials can be generated with any of the above mentioned statistical computer programs.

For further discussions of statistical methods of optimisation see:

- Box GEP, Draper NR (1986)
- DeVor RE., Chang TH., Sutherland JW (1992)
- Miller JC, Miller JN (1984)

CHAPTER 3 : MATERIALS AND METHODS

3.1 EXPERIMENTAL PHOTOCATALYTIC REACTORS

3.1.1 Design and Operation

Two types of experimental photocatalytic reactors were designed, constructed and optimised for the removal of low concentrations of organic contaminants in water. These reactors were operated as flow systems based on a "falling film" principle. The first (Reactor 1) was operated only as a slurry-phase reactor using aqueous suspensions of Anatase TiO_2 catalyst. The second (Reactors 2A and 2B) were operated either as immobilised-bed or combined slurry immobilised-bed systems.

Reactor 1 consisted of a cylindrical Pyrex glass tube (140 cm long, e.d = 8.5 cm., i.d. = 7.0 cm) equipped at the top with a receiver cup with 1 L volume capacity. The tube was mounted vertically in a base reservoir and encircled by a set of eight 30 W germicidal UV lamps (90 cm long) connected to an external framework.

Reactor 2 consisted of a vertically suspended rectangular sheet module (40 ×110 cm) with six 15 W UV lamps (45 cm long) assembled uniformly on both sides of the sheet for maximum irradiation. Both reactors were covered with a protective UV shield to prevent loss of UV radiation and to ensure operator safety. Electrical power input per unit area of irradiated surface amounted to 95.4 and 20.45m W/cm^2 for Reactors 1 and 2 respectively.

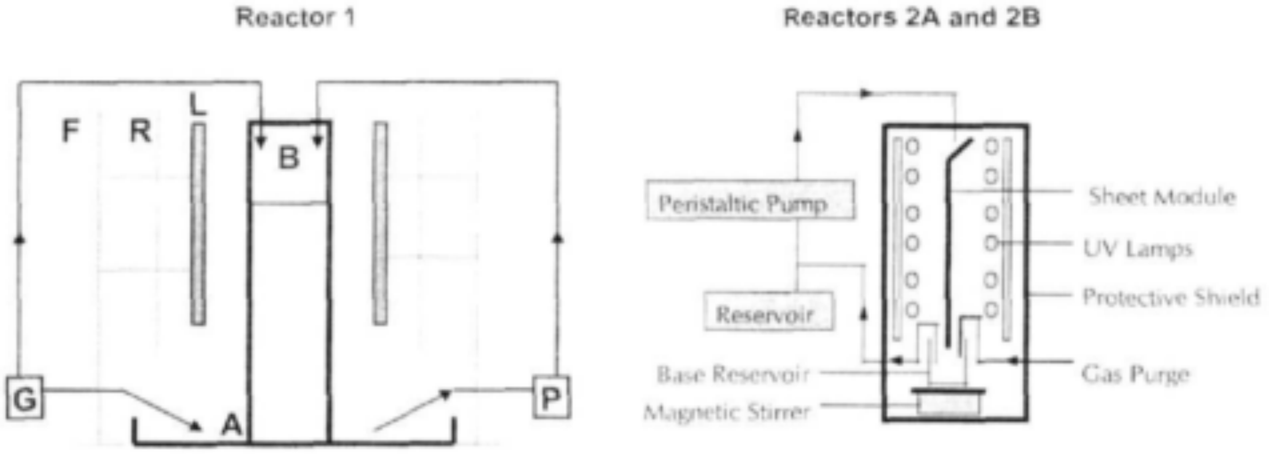

Figure 3.1: Schematics of experimental photocatalytic reactors.

Reactor 1 :	**Cylindrical glass tube reactor (A: Base reservoir; B: Glass tube with cup; F: External frame; G: Gas purge; L: Germicidal UV lamps; P: Peristaltic Pump; R: Shield and reflector)**
Reactor 2A:	**Fibre glass sheet module**
Reactor 2B:	**Fibrous Activated Carbon (FAC) sheet module**

The designs of the reactors were chosen to (1) facilitate the use of commercially available material for the construction (2) avoid the use of components prone to fouling during operation and (3) accommodate future developments in photocatalysts.

Reactor 2 was essentially designed with its scaling-up potential and overall capacity in mind - i.e. in the vertical direction by increasing the length of the sheet and the number of parallel UV lamps, in the lateral direction by increasing the width of the sheet and the length of the UV lamps, and in the horizontal direction by increasing the number of sheets sharing a set of UV lamps. Optimisation, however, could be performed at laboratory scale utilising one reactor consisting of a single sheet with a set of lamps on each side.

Three basic modes of operation existed for the falling film flow reactors, viz.:

- single pass mode
- sequential single pass mode
- recirculation mode

Aqueous TiO_2 suspensions (slurries) were prepared in 3 or 6 L batch containers by addition of the desired loading of catalyst to the water sample of choice. Magnetic stirring was conducted for 5 minutes prior to spiking the sample with the organic pollutant of choice. An additional 5 minutes of stirring were used to attain adsorption equilibrium prior to feeding the sample into the reactors.

Immobilisation of TiO_2 on reactor sheet modules was achieved by applying suspension coating or droplet spraying methods. Suspension coating was selected as standard method due to reliable statistical reproducibility.

A typical UV photocatalytic irradiation experiment (test run) comprised the spiked water sample (or slurry) of choice being introduced to the top section of the designated reactor from a batch reservoir using a peristaltic pump. A "falling film" is obtained from the top through laminar gravitational flow along the *exterior surface* of the cylindrical tube (Reactor 1) or *both sides* of the sheet module (Reactors 2A and B) while UV irradiation proceeds. Catalyst slurries were kept in suspension by incorporating a gas purge (oxygen or compressed air) in the receiver cup of the slurry reactor and in the base reservoirs of both reactors. The inclusion of oxygen is vital to the photocatalytic production of hydroxyl radicals.

During the course of any given experiment, fixed-volume aliquots of treated water were collected from the reactor base reservoir using peristaltic pumps. Where necessary, slurry aliquots were filtered in the dark to remove excess TiO_2 particles prior to analysis. Whatman 42 (Ashless, 110 mm ϕ, Catalogue number: 1442 110) and Whatman 44 (Ashless, 185 mm ϕ, Catalogue number: 1444 185) were used in para-chlorophenol and microcystin studies respectively.

Table 3.1: Summary of design parameters

Parameter	Reactor 1	Reactor 2A	Reactor 2B
Photocatalyst	Degussa P-25 TiO_2	Degussa P-25 TiO_2	Degussa P-25 TiO_2
Catalyst Immobilisation	Slurries only	Fibre glass sheets[c]	FAC sheets
UV-C lamps (germicidal; 254 nm)	Yes	Yes	Yes
UV-A lamps (fluorescent; ca 360 nm)	No	Yes	No
Surface area irradiated (m^2)	0.252	0.880	0.880
Max. Lamp power per unit area (mW/cm^2)	95.40	20.45	20.45
UV residence time per single pass (sec)	2.1 ± 0.1	4.1 ± 0.1	11.5 ± 0.2
Vertical distance of Irradiation (cm)	90	110	110
Linear Flow Velocity (cm/sec)	42.9	26.8	9.6
Horizontal distance of irradiation (cm)	2 to 8	5 to 15	5 to 15
Pump flow rates (L/min.)[b]	0.05 to 2	1 to 2	1 to 4
Surface Flow Rate per hour ($L / hr / m^2$)	12 to 475	70 to 135	70 to 270
Reaction Volumes (L)	3 to 6	3 to 6	3 to 12
Oxygen flow rate (L/min.)	5 and 20	5 and 20	5
Illuminated specific surface area ($m^2/m^3 = m^{-1}$)	3380	6620	2300-2600

3.1.2 Film Layer Thickness

Calculation of film layer thickness for falling film reactors depends on water flow rates, UV residence times (contact times) and the catalyst surface area covered by liquid during irradiation. These calculations imply that layer thickness varies inversely proportional to the illuminated specific surface area (κ). Film thickness for reactor 1 was calculated between 112 and 296 μm depending on the flow rate used. For reactor 2A film thickness varied between 75 and 150 μm and for reactor 2B between 218 and 436 μm. Thickening effects caused by catalyst slurries, turbulent flow or surface roughening were not accounted for.

3.1.3 UV Dosage

UV dosages may be calculated using the residence time of irradiation within the reactor and the level of UV irradiance (in mW/cm^2). These parameters will be determined by the reactor type and operation mode under investigation. The actual power output of commercial UV lamps are approximately one-third of the value specified as input power (Martin *et al.*, 1999). UV power output (levels of irradiance) is also referred to as "Radiant flux" and is normally determined with UV sensors, radiometers and actinometric analyses. Irradiance may vary markedly throughout a reactor, hence complex mathematical techniques such as multiple point source modelling is often required to calculate this parameter for a given design (Bolton, 1999). Moreover, UV lamps have a limited life-span (*ca* 5000 h for commercial low-pressure mercury arcs) which complicates the calculation. For the purpose of this project, only *theoretical* UV dosages (in mW-s/cm^2) were calculated in an effort to construct UV-dosage response curves. The determination of *absolute* UV dosages was precluded due to the (1) unavailability of radiometers and actinometers (2) extended use of the original batch of UV lamps and (3) lack of modelling studies addressing the true magnitude and spatial variation of UV irradiance within the reactors.

3.1.4 Reactor Materials

Germicidal and fluorescent (low pressure Mercury) UV lamps (Product Code: TUV G15T8) and starters (Product Code: S2/CEBEC74/BS3772/4JKLM) were supplied by Phillips (The Netherlands). Power ballasts (Catalogue no. CS/2201230) were supplied by Harper Electrical Industries (Pty) (Cape Town).

Variable-speed peristaltic pumps (Watson-Marlow 505S, Product Code: 050•4841•L0U) were supplied by Aeromix (Pty) Ltd (Cape Town).

Oxygen (99% pure), compressed air and argon were supplied by Afrox.

TiO_2 (Degussa P-25, FW 79.90 g/mole) was purchased in 10 kg batches from Degussa AG (Frankfurt, Germany) (CAS no. 13463-67-7) and used as received. Degussa's product consists of approximately 75% Anatase and 25% Rutile TiO_2.

Details pertaining to the reactor sheet materials used in this project are presented in Tables 3.2 and 3.3:

Table 3.2: Design details of reactor sheets

Sheet	Supplier	Product Code / Catalogue No.	Approximate Weight (g/m^2)
Fibre glass (reinforced)	Foyntech Africa cc (Stellenbosch)	GLASS COAT 60	60
Fibre glass tissue (non-reinforced)	Freudenberg Nonwovens Pty (Ltd) (Parow Industria)	DIN 60001-T01	26
FAC (Kuractive 15)	Kuraray (Japan) via Enviro Services cc (Somerset West)	CH700-15 K81006-701	118
FAC (Kuractive 20)	*ibid.*	CH700-20 K80314-603	60

Table 3.3: Product details of Kuractive FAC sheet materials

Property	Grade 10	Grade 15	Grade 20	Grade 25
Total Surface Area (m^2/g)	1000	1500	2000	2500
Pore Radius (angstrom)	9	12	16	22
Pore Volume (mL/g)	0.22	0.50	0.75	1.20
Benzene Adsorption (wt%)	22	45	65	90
Iodine Adsorption (mg/g)	950	1550	2000	2400
Ash Content (%)	0.03	0.03	0.04	0.05
Ignition Point ($^{\circ}C$)	470	470	470	470

3.1.5 Test Pollutants

(a) *para*-chlorophenol

Chlorophenols form a family of organic water pollutants that are omnipresent in wastewater as a result of their extensive use in industrial processes (De Villiers, 2000). From this group, *para*-chlorophenol (p-CP) was selected as test pollutant to conduct a series of parametric experiments as part of a *reactor development* strategy for the experimental photocatalytic reactors. p-CP has been selected as universal test pollutant in an effort to create a standard framework of conditions for figure-of-merit comparison of PCO technologies (Mills and Morris, 1993).

(b) cyanobacterial Toxins and Natural Organic Matter

For potential application of the proposed photocatalytic reactors to drinking water treatment, two naturally occurring groups of compounds were used as test pollutants. Cyanobacterial microcystin toxins (originating from various species of blue-green algae) and humic substances (originating from natural organic matter) have been selected due their potentially detrimental effect on drinking water quality. Inefficient removal of these compounds from raw waters by conventional processes such as coagulation/flocculation, filtration, carbon-adsorption and subsequent chlorination may give rise to (1) the presence of microcystin toxins and (2) high levels of disinfection by-products in treated waters (Pieterse, 1997).

3.2 ANALYTICAL METHODOLOGY

3.2.1 *para*-chlorophenol

(a) UV Spectrometry

p-CP dissolves readily in water and exhibits high molar absorption coefficients at two UV wavelengths (viz., 225 and 280 nm). In this project a GBC-920 double-beam UV-Visible spectrometer was used for quantitative detection of p-CP in aqueous samples. A standard linear calibration was used to convert absorbance signals to the equivalent p-CP concentrations. Limit of detection was determined as 1 mg/L. The following scanning parameters were used:

Cuvettes :	Quartz, 1cm x 1cm
Sample Volume :	*ca* 3 mL
Measurement mode :	Absorbance
Scan range :	200 – 400 nm
Scan Speed :	1000 nm/min.
Wavelength step :	1.25 nm
Monochromator slit width :	2 nm

(b) Stock Material

p-CP (FW 128.56 g/mole, 99% purity, CAS no. 106-48-9, Catalogue No. 18578-7) was obtained from Aldrich Chemical Co. and used as received without further purification.

(c) Water Sources

Distilled water (conductivity 2.4 uS/m) and de-ionised water (conductivity 1.5 uS/m) were prepared in-house using Aquatron and Milli-Q (Millipore Corporation, Bedford, Massachusetts, USA) systems, respectively. Tap water experiments were conducted using Stellenbosch tap water (conductivity 80 uS/m); total alkalinity 14 mg/L $CaCO_3$) treated by flocculation and chlorination processes. (Mansfield 2000).

3.2.2 Microcystins

(a) High-Performance Liquid Chromatography

In this project, 4 microcystin variants (viz., YR, LR, YA and RR) were used to spike water samples meant for photocatalytic experiments. For analytical purposes these toxins were separated and quantified by isocratic reversed-phase High-performance Liquid Chromatography (HPLC) with UV detection at 240 nm. Sample preparation comprised purification on C_{18} Solid Phase Extraction (SPE) cartridges. Identity of the HPLC peaks was confirmed by spectral comparison (over the range 200-300 nm) with authentic standards using UV diode-array detection. The authenticity of the various analytes was unequivocally confirmed by electrospray Liquid Chromatography- Mass Spectrometry (LC-MS) operated in single ion recording mode at $^{m}/_{z}$ = 1045, 995, 959 and 1038 for the YR, LR, YA and RR variants, respectively.

The HPLC analytical method for microcystin determinations included the following conditions : mobile phase (46 % acetonitrile in 0.05 % trifluoroacetic acid, TFA), flow rate (1 mL/min.) and isocratic programming. The analytical column used was a Phenomenex Ultremex C_{18} , 3μ (100 × 4.6 mm).

Clean-up and preparation of water samples prior to HPLC analysis involved the following steps:

- A 100 mL sample collected from the reactor for each determination was centrifuged at 3000 rpm for about 10 minutes to facilitate the separation of the water phase and any solid catalyst particles which might be present.
- The required amount of water sample was then added to an Erlenmeyer flask.
- The C_{18} end-capped SPE cartridges were then conditioned with methanol and water.
- The clear water sample was applied to the cartridge at a flow rate of 5 mL/min.
- The flask was rinsed with water.
- The column was washed with 10 mL each of 10%,20% and 30% methanol in water.
- The microcystins were then eluted with 3 mL of 0.1% TFA in methanol and dried under nitrogen.
- The microcystins were taken up in about 200 µL methanol, ready for HPLC analysis.

The concentrations of the microcystins were monitored and calculated using calibrated standards for each of the variants studied: YA, YR, LR and RR. Limit of detection in most instances was set as 10 ug/L (ppb) for all variants.

(b) Stock Material

Initial photocatalytic experiments with cyanobacterial toxins were performed using an algal extract containing microcystins YR, LR and YA. These toxins were extracted with methanol from freeze-dried algal material stored at PROMEC from previous studies. The freeze-dried material originated from a toxic strain of *Microcystis aeruginosa*.

In order to circumvent the need to seek natural sources of toxic strains (given that not all isolated strains produce toxins) several batches of cyanobacterial culture material were obtained from abroad, cultured and analysed for microcystin content, viz. :

- M. *aeruginosa* UV027
- *M. aeruginosa* PCC7820
- *M. aeruginosa* SAG 14.85
- *M. aeruginosa* PCC7806
- *M. aeruginosa* PCC7813

The culturing of these strains was problematic, mainly due to problems related to the transportation and contamination. Some strains, however, were revived and successfully cultured at the University of the Free State (Prof. JU Grobbelaar, Department of Botany and Genetics). Eventually, a natural source of toxins was located at Wildevoël Vlei (Noordhoek, Cape Peninsula) where an outbreak of cyanobacterial blooms yielded microcystins LR and RR in detectable amounts (viz. greater than 10 ug/L) in extracts from freeze-dried material. These extracts were used in the latter part of the microcystin studies.

(c) Water Sources

De-ionised water (conductivity 1.5 uS/m) was prepared in-house using a Milli-Q system. Raw lake water was obtained on a periodic basis from two hypertrophic lakes on the Cape Flats, viz.: Zeekoevlei and Rondevlei. The respective sampling areas were at Zeekoevlei Yacht Club and Rondevlei Nature Reserve. The properties of these samples are given below. No further chemical analyses was performed prior to use of these waters in reactor experiments.

Table 3.4: Characterisation of raw waters used in microcystin studies

Reactor	1	2A	2B
Water Source	Zeekoevlei	Zeekoevlei	Rondevlei
Sampling Date	8 Feb.1996	29 Aug.1999	25 Jan.1999
Temperature (°C)	23.7	14.2	23.8
Dissolved Oxygen (mg/L)	12.4	13.7	5.8
O_2 Saturation (%)	148	134	69
Total Suspended Solids (mg/L)	NA	43	64
pH	9.3	8.0**	8.1
Conductivity (mS/m)	124	87.7	143
Chemical Oxygen Demand (mg/L)	NA*	34	159
Total Persulphate Oxidisable Nitrogen(mg/L)	1.88	2.31	2.44
Ammonia (mg/L)	0.027	0.020	0.330
Nitrite + Nitrate (mg/L)	0.023	0.470	0.030
Total Phosphorous (mg/L)	0.539	0.752	0.293
Soluble Reactive Phosphorous (mg/L)	0.284	0.205	0.010
Chlorophyll-a (ug/L)	202.0	349.8	71.8
Phaeophytin (ug/L)	24.0	45.9	36.5

* NA = Not analysed

** Determined in-house at the Department of Chemistry, University of Stellenbosch.

3.2.3 Natural Organic Matter

(a) Colour

HA and FA compounds (as part of humic substances contained within NOM) exhibit pronounced UV absorption at 254 nm due to suitable chromophores in the organic structure of the molecules. UV spectroscopy may therefore be used to monitor the reduction of HA and FA content of coloured water. In this project, the reduction in UV absorbance at 254 nm was monitored and correlated with the removal of colour from the treated water. A double-beam GBC 920 UV/VIS spectrophotometer, equipped with a deuterium lamp, a quartz iodide lamp and 1 cm quartz cuvettes were used for all UV analysis.

(b) Total Organic Carbon

The destruction of NOM in water by photocatalytic oxidation was monitored in terms of total organic carbon (TOC) content of water. A low temperature TOC analyser (ANATOC) was used in this investigation (Bennett and Van der Merwe, 1995). ANATOC is operated on the principle of photocatalytic oxidation of the organic content of target samples. A catalyst suspension of 0.2% $^{w}/_{v}$ Degussa P-25 TiO_2 in combination with two 8 W blacklight fluorescent tubes forms the photocatalytic system within the instrument. Organic carbon content is decomposed in aqueous medium to yield CO_2, H_2O and the acid, base or salt of any inorganic constituents. The evolution of CO_2 is followed by capturing the gas in a conductivity cell. The corresponding conductivity signal is used to produce a reading in TOC units. $CO_2 - HCO_3^- - H_2CO_3$ equilibria as a function of pH is also taken into account.

Calibration was done with a standard 200 mg C/L solution of benzoic acid. pH dependency of CO_2 was an important factor. To ensure accurate and consistent TOC analyses, it was necessary to adjust the pH of each sample to a value below pH 5 to render a maximum yield of CO_2 from oxidation of TOC within each sample. Suggested pH levels were between 3.5 and 4.0. pH adjustments were done with 0.1 M solutions of perchloric acid and NaOH to obtain the required pH 3.5. A standard sample injection volume of 1000μL was used throughout. TOC measurements were expressed as mg C/L.

(c) Stock Material and Water Sources

Samples of raw natural water were obtained from Simonstown (via Mr. SA Pieterse of Cape Town Metropolitan Council) and also collected at a coastal lagoon near Betty's Bay in the Overberg region. Chemical analysis of both waters was conducted at Scientific Services Branch of the Cape Town Metropolitan Council and is presented in Table 3.5 (Pieterse, 1997):

Table 3.5: Characterisation of raw waters used in NOM studies

Determination	Raw Water	
	Betty's Bay	Simonstown
Physical and General		
Electrical Conductivity (mS/m @ 20°C)	26.7	24.6
pH	6.54	5.71
Turbidity (NTU)	1.15	1.35
Colour (Pt std)	200	280
Organic		
Oxygen Absorbed (4hrs at 27°C) (mg/L)	2.284	1.5
Alkalinity		
Total Alkalinity as $CaCO_3$ (mg/L)	6.0	3.0
Mineral		
Chloride (Cl^-) (mg/L)	73.0	68.0
Sulphate (SO_4^{2-}) (mg/L)		11.4
Calcium (Ca) (mg/L)	6.00	6.19
Magnesium (Mg) (mg/L)	5.15	4.25
Sodium (Na) (mg/L)	37.13	35.49
Potassium (K) (mg/L)	0.33	0.85
Trace Metals		
Aluminium (Al) (mg/L)	0.29	0.51
Iron (Fe) (mg/L)	0.397	0.518
Manganese (Mn) (mg/L)	0.002	0.023

3.2.4 Miscellaneous

Conductivities of water samples were determined using a Metrohm 644 conductometer. pH was measured with a Metrohm E520 pH-meter.

3.3 EXPERIMENTAL METHODOLOGY

3.3.1 Treatment of *para*-chlorophenol

p-CP was selected as test pollutant in a series of experimental runs aimed at evaluating the oxidation efficiency of the photocatalytic reactors in terms of all defined system parameters. Random parametric studies were conducted using a standard one-factor variation method and operating the reactor of choice in recirculation, single pass or sequential single pass mode. Screening and optimisation studies were conducted using multi-parameter experimental designs in similar fashion.

For *recirculation mode* of operation, exponential first order kinetics were used to model reaction rates. The corresponding observed rate constants (in $mins^{-1}$) and half-lives (in min) were obtained via normalisation and logarithmic conversion of temporal concentration data. Initial reaction rates were obtained by the product of initial concentration and the observed rate constant (eqn 3.1) :

$$r_o = -dc(t)/dt = k_{obs}\, c_o \qquad (3.1)$$

where :

r_o = initial rate (in concentration per time units)
$c(t)$ = Concentration as a function of time
c_o = Initial concentration
k_{obs} = Observed first order rate constant (in mins^{-1})
t = Time (min)

Where $10^2\, k_{obs}$ is used in this report, it refers to 100 x k_{obs}

For the *single pass mode* of operation, a standard statistical response function (denoting the percentage of pollutant degradation) was adopted (eqn 3.2):

$$\%\,D = 100 \times [(p\text{-}CP)_0 - (p\text{-}CP)_E\,] / (p\text{-}CP)_0 \qquad (3.2)$$

where:

$\%\,D$ = Percentage of degradation
$(p\text{-}CP)_0$ = Initial p-CP concentration
$(p\text{-}CP)_E$ = Final p-CP concentration (after one single pass)

For *sequential single pass mode* of operation, a response was constructed to denote the first order decay in concentration as a function of the number of single passes (N). This response is analogous to conventional first order decay as a function of time:

$$c(N) = c_o \exp(-k_{obs}N) \qquad (3.3)$$

where :

$c(N)$ = Concentration as a function of single pass number
c_o = Initial concentration
k_{obs} = Observed first order rate constant (in passes^{-1})
N = Single pass number

By incorporating the UV residence time (contact time) per single pass for each reactor, equation 3.3 can be converted to the conventional first order kinetic regime.

Analysis of Variance (ANOVA) was used as statistical aid to assess significance probabilities of parameters according to the null-hypothesis theory. A commercial software package (Statistica ®, Version 5, 1997) was used to conduct all experimental design, ANOVA and precision analyses.

3.3.2 Treatment of Cyanobacterial Microcystins

Experimental runs conducted with microcystins as test pollutant were limited to the recirculation mode of operation with the exception of one run (conducted in sequential single pass mode). Microcystin spiking material was limited throughout, hence comprehensive screening and optimisation studies were omitted and one-factor variation was adopted in a series of random parametric studies.

3.3.3 Treatment of Natural Organic Matter

All three modes of operation were studied viz., (1) single pass mode, (2) sequential single pass and (3) recirculation mode. Experimental design methods were used in screening and optimisation studies.

3.3.4 Summary

The oxidation efficiencies of three types of falling film photocatalytic reactor were optimised for recirculation , single pass and sequential single pass modes of operation. The slurry phase, immobilised bed (IMM) and combined slurry immobilised-bed (SLIMM) configurations were each optimised. Two types of glass fibre sheets and two types of FAC sheets as reactor material were investigated.

Three compounds or mixture of compounds representing different classes of water pollutants e.g. para-chlorophenol, a mixture of cyanobacterial microcystin toxins and natural organic matter were oxidised.

First order rate constants for the removal of pollutants, percentage degradation and first order rate constant in terms of number of passes were used as response functions.

Depending on the type of reactor various statistical approaches for optimisation have been employed. Generally system parameters e.g. catalyst suspension loading, volumetric flow rate, horizontal radiation distance, initial concentration of compound, reaction volume, water matrix, pH, purge gas, flow rate of purge gas and number of UV-C lamps were investigated at assigned levels.

In the following chapters the so-called reference level of a parameter indicates the assigned level when this was kept constant.

CHAPTER 4 : EVALUATION OF REACTOR 1

4.1 TREATMENT OF *para*-CHLOROPHENOL

4.1.1 Recirculation Mode

(a) System Parameters

The photocatalytic oxidation of p-CP in water was investigated in a random parametric study using one-factor variation for each experiment. The following system parameters were evaluated at discrete levels in terms of first order reaction kinetics (see Table 4.1):

Table 4.1: System parameters for p-CP study (Reactor 1; Recirculation Mode)

Parameter	Assigned Levels
Catalyst Suspension Loading (g/L)	0; 1*; 2.5; 5; 10; 20; 30
Volumetric Flow Rate (mL/min.)	225^{a}; 750^{*b}
Horizontal Irradiation Distance (cm)	2; 8*
p-CP Initial Concentration (mg/L)	5; 13; 40*; 70; 100
Reaction Volume (L)	3*; 6
Water Matrix	Distilled*; De-ionised; Tap
Initial Slurry pH	3; 5*; 7; 9; 11
Gas Purge	Oxygen*; Air; Argon
Oxygen Flow Rate (L/min.)	5*; 20
Number of UV-C lamps	2^{c}; 8^{*d}

Note: * Denotes standard reference level of parameters
a Surface flow rate = 53.5 L/hr/m^2
b Surface flow rate = 178.5 L/hr/m^2
c UV irradiance = 238 W/m^2 = 2 x 30W lamps (per 0.252 m^2)
d UV irradiance = 954 W/m^2 = 8 x 30W lamps (per 0.252 m^2)

(b) Catalyst Suspension Loading

Introduction and Objectives:

The effect of catalyst suspension loading was examined by comparing results for 7 different loadings of TiO_2 (0; 1; 2.5; 5; 10; 20 and 30 g/L). The objectives of this study were to (1) establish a region of maximum photocatalytic oxidation of p-CP and (2) assess the effect of UV photolysis.

Results and Discussion:

Table 4.2: p-CP concentration as a function of irradiation time and catalyst suspension loading

Irradiation Time (min)	Catalyst Suspension Loading (g/L TiO_2)						
	0	1*	2.5	5	10	20	30
0	40.0	40.0	40.0	40.0	40.0	40.0	40.0
5	37.1	34.2	26.9	24.0	21.8	20.5	24.4
10	35.5	29.0	22.5	15.5	15.0	10.5	16.1
15	32.9	22.2	18.2	11.0	9.8	7.6	11.9
30	30.0	12.3	4.5	3.9	2.1	0.9	4.1
45	27.2	6.5	ND	ND	ND	ND	ND
60	24.8	ND**					
10^2 k_{obs} (min^{-1})	0.76	4.10	7.12	7.60	9.63	12.44	7.43
Half-life (min)	91.2	16.9	9.7	9.1	7.2	5.6	9.3
R^2	0.98	0.99	0.97	0.99	0.99	0.99	0.99

Note: * Denotes standard reference level of parameter
ND = Not Detected; Limit of Detection = 1 mg/L**

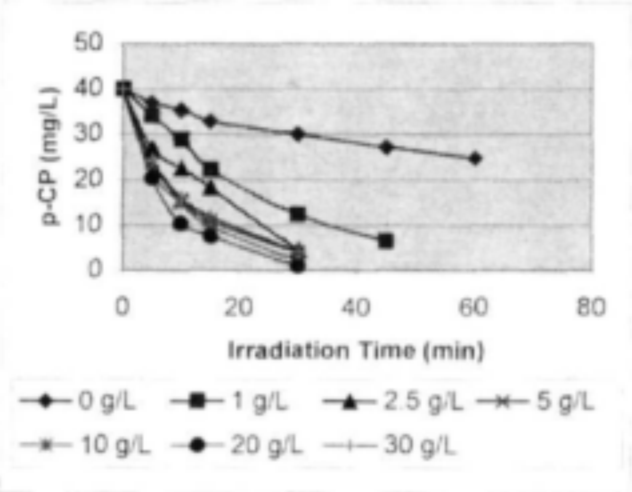

Figure 4.1: p-CP concentration as a unction of irradiation time and catalyst suspension loading

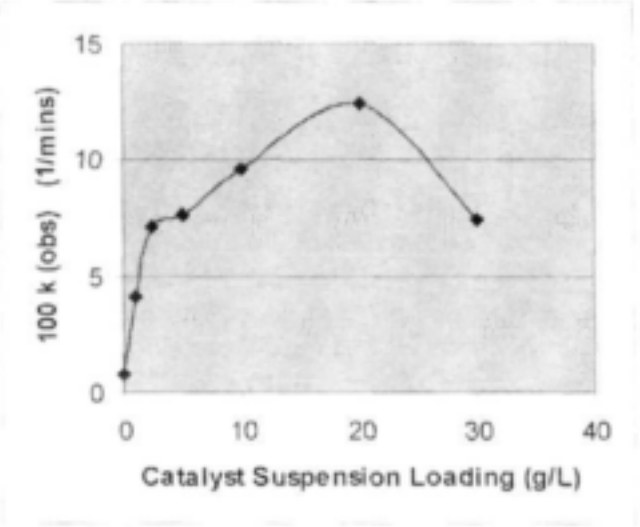

Figure 4.2: Reaction rate constant for p-CP oxidation as a function of catalyst suspension loading (g/L TiO_2)

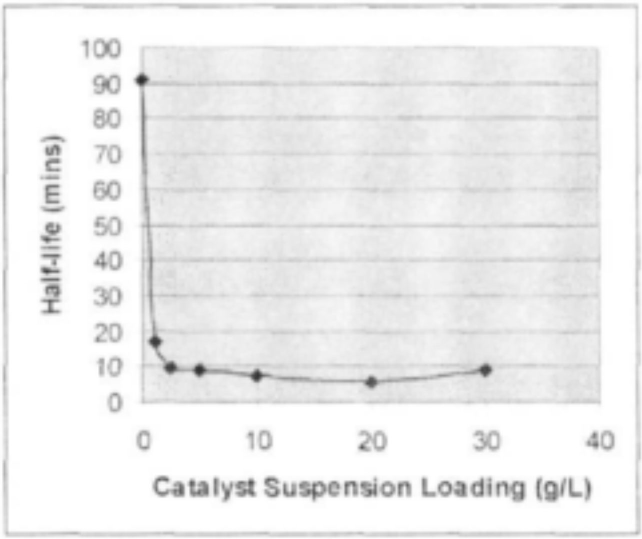

Figure 4.3: Half-life of p-CP as a function of catalyst suspension loading (g/L TiO_2)

The results obtained from these experiments (Table 4.2 and Figures 4.1-4.3) indicated that :

- first order exponential decay kinetics apply for the photocatalytic oxidation of p-CP;
- the observed first order rate constant (k_{obs}) increases with an increase in catalyst suspension loading, yielding a maximum rate around 20 g/L TiO_2 ;
- *beyond a loading of 20 g/L TiO_2 a marked decrease in rate is observed.* This is ascribed to pronounced UV shielding effects and problems related to maintaining catalyst particles in suspension;
- the half-lives for p-CP removal are significantly reduced (by one order of magnitude) when increasing the catalyst suspension loading from 0 to 2.5 g/L ;
- *UV photolysis of p-CP (at 0 g/L TiO_2) is possible, but at a significantly slower rate* compared to TiO_2 photocatalysis.

(c) Volumetric Flow Rate

Introduction and Objectives:

The effect of volumetric flow rate was examined by comparing results for a reduced flow rate (225 mL/min) against the standard flow rate (750 mL/min) used. The objectives of this study were to (1) assess the positive effect of a higher number of recycles (obtained when using higher flow rate) and (2) assess the auxiliary effect of a thin falling film (obtained when using lower flow rates).

Results and Discussion:

Table 4.3: p-CP concentration as a function of irradiation time and volumetric flow rate

Irradiation Time (min)	Volumetric Flow Rate (mL/min)	
	225	750*
0	40.0	40.0
5	32.7	34.2
10	26.1	29.0
15	25.0	22.2
30	19.8	12.3
45	16.3	6.5
60	11.8	ND**
10^2 k_{obs} (min^{-1})	1.83	4.10
Half-life (min)	37.9	16.9
R^2	0.96	0.99

Note: * Denotes standard reference level of parameter
ND = Not Detected; Limit of Detection = 1 mg/L**

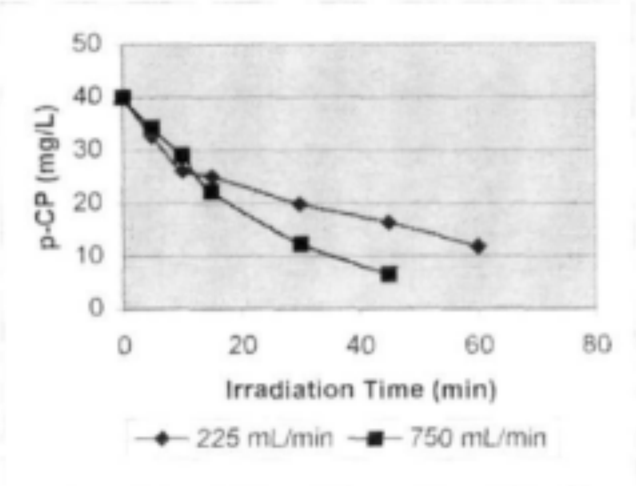

Figure 4.4: p-CP concentration as a function of irradiation time and volumetric flow rate (mL/min)

The results obtained from these experiments (Table 4.3 and Figure 4.4) indicated that :

- the observed first order rate constant (k_{obs}) increases with an increase in volumetric flow rate. This is ascribed to a higher recirculating rate obtained at higher flow rate;
- the effect of a thin falling film will be more pronounced when using low flow rates for shorter periods of irradiation, e.g. in a single pass reactor with UV contact times in the order of seconds.

(d) Horizontal Irradiation Distance

Introduction and Objectives:

Horizontal irradiation distance (HID) represents the mean distance between the configuration of UV lamps and the irradiated surface, viz. the cylindrical tube in Reactor 1. The effect of HID was examined by comparing results for a reduced distance (2 cm) against the standard distance (8 cm) used. The objective of this study was to determine whether it is beneficial to assemble the UV lamps at the closest distance possible.

Results and Discussion:

Table 4.4: p-CP concentration as a function of irradiation time and horizontal irradiation distance

Irradiation Time (min)	Horizontal Irradiation Distance (cm)	
	2	8*
0 5 10 15 30 45 60	40.0 35.8 33.0 28.7 21.2 15.8 12.1	40.0 34.2 29.0 22.2 12.3 6.5 ND**
10^2 k_{obs} (min^{-1})	2.01	4.10
Half-life (min)	34.5	16.9
R^2	0.99	0.99

Note: * Denotes standard reference level of parameter
ND** = Not Detected; Limit of Detection = 1 mg/L

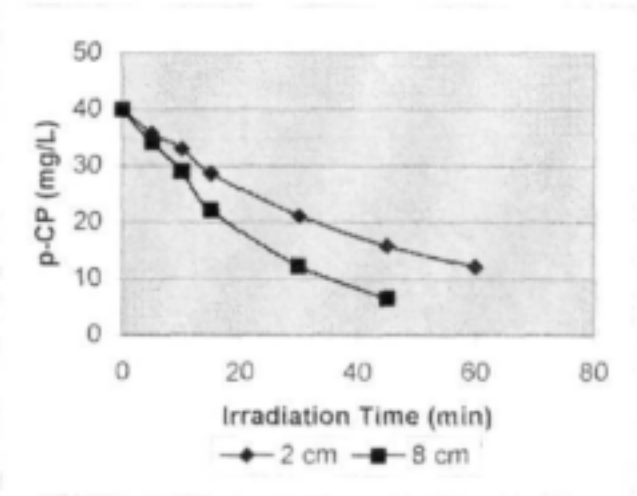

Figure 4.5: p-CP concentration as a function of irradiation time and horizontal irradiation distance

The results obtained from these experiments (Table 4.4 and Figure 4.5) indicated that :

- the observed first order rate constant (k_{obs}) decreases with a decrease in horizontal irradiation distance from 8 to 2 cm. This is ascribed to the inhibiting effect of localised

- irradiation and reduced reflection on isolated portions of the irradiated surface at 2 cm distance;
- unwanted lamp contamination occurs at 2 cm distance with minute droplets of catalyst slurry settling on lamp envelopes.

(e) p-CP Initial Concentration

Introduction and Objectives:

The effect of initial concentration was examined by comparing results for 5 different loadings of p-CP (5; 13; 40; 70 and 100 mg/L). The objective of this study was to establish a region of maximum photocatalytic oxidation of p-CP.

Results and Discussion:

Table 4.5: p-CP concentration as a function of irradiation time and initial p-CP concentration

Irradiation Time (min)	p-CP Initial Concentration (mg/L)				
	5	13	40*	70	100
0	5.0	13.0	40.0	70.0	100.0
5	1.9	8.1	34.2	59.1	85.1
10	0.9	5.8	29.0	53.5	79.9
15	ND**	4.5	22.2	47.2	72.2
30		1.0	12.3	37.5	60.2
45		ND	6.5	27.8	50.8
60			ND	20.8	43.1
75				13.5	38.9
90				8.5	34.5
120				ND	22.8
150					11.9
180					4.1
210					ND
10^2 k_{obs} (min^{-1})	17.15	8.38	4.10	2.19	1.51
Half-life (min)	4.0	8.3	16.9	31.7	45.9
R^2	0.99	0.99	0.99	0.99	0.95

Note: * Denotes standard reference level of parameter
ND = Not Detected; Limit of Detection = 1 mg/L**

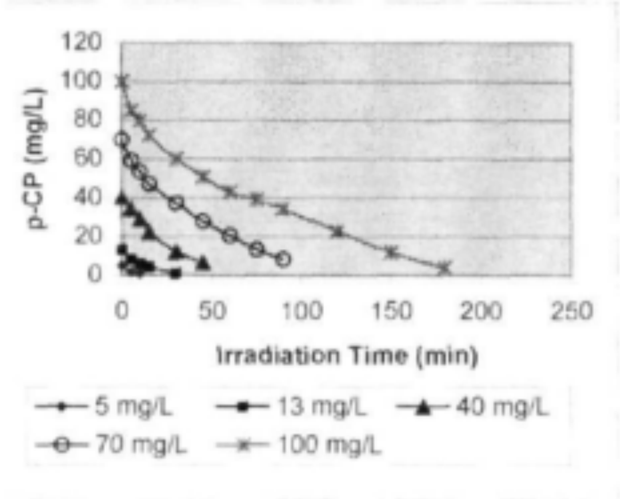

Figure 4.6: p-CP concentration as a function of irradiation time and initial p-CP concentration

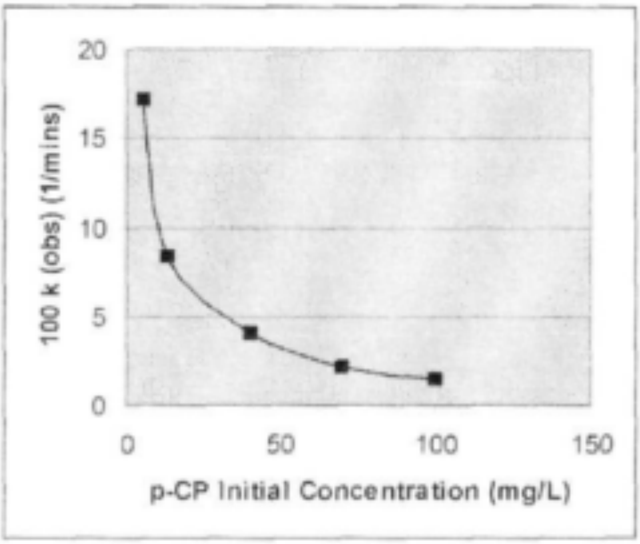

Figure 4.7: Reaction rate constant as a function of p-CP initial concentration (in mg/L).

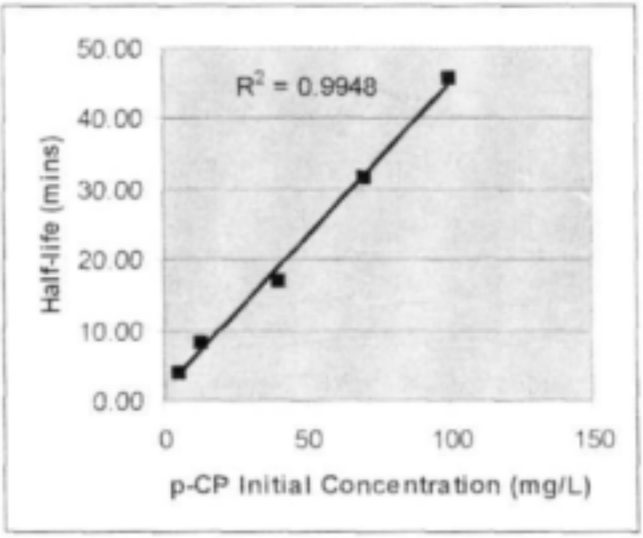

Figure 4.8: Half-life as a function of p-CP initial concentration (in mg/L).

The results obtained from these experiments (Table 4.5 and Figures 4.6-4.8) indicated that :

- the observed first order rate constants (k_{obs}) are inversely proportional to initial p-CP concentration. A hyperbolic dependence with increase in initial concentration from 5 to 100 mg/L is confirmed. The corresponding half-lives increased linearly as a function of concentration;
- the recirculation mode of operation is effective when treating low concentration levels of p-CP in water (viz.: *ca* 5 to 40 mg/L).

Langmuir-Hinshelwood kinetics were confirmed in a separate study, indicating the contribution of mass transfer (via surface adsorption onto TiO_2) toward the overall reaction rate (De Villiers, 2000). Adsorption contributed to approximately 5-10% loss in p-CP concentration in the absence of UV irradiation. This effect, however, is dependent on several parameters and needs to be studied in more detail.

(f) Reaction Volume

Introduction and Objectives:

The effect of reaction volume (volume of water treated) was examined by comparing results for a 6 L volume against the standard volume of water used (3 L). The objective of this study was to determine whether an increase in reaction volume exerted an inhibitory effect on the oxidation rate when operating Reactor 1 in recirculation mode.

Results and Discussion:

Table 4.6: p-CP concentration as a function of irradiation time and reaction volume

Irradiation Time (min)	Reaction Volume (L)	
	3*	6
0 5 10 15 30 45 60	40.0 34.2 29.0 22.2 12.3 6.5 ND**	40.0 36.5 32.5 29.1 23.3 18.6 14.4
10^2 k_{obs} (min^{-1})	4.10	1.67
Half-life (min)	16.9	41.5
R^2	0.99	0.99

Note: * Denotes standard reference level of parameter
ND** = Not Detected; Limit of Detection = 1 mg/L

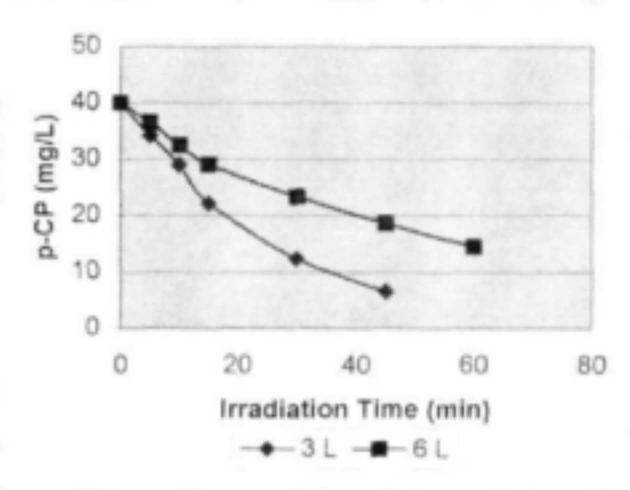

Figure 4.9: p-CP concentration as a function of irradiation time and reaction volume

The results obtained from these experiments (Table 4.6 and Figure 4.9) indicated that :

- the observed first order rate constant (k_{obs}) decreases markedly with a two-fold increase in reaction volume. This is ascribed to the larger amount of p-CP administered in the 6 L water sample and a lower recirculation rate achieved at constant volumetric flow rate;
- Reactor 1 is not suitable for treating large volumes of water in a recirculation mode of operation.

(g) Water Matrix Effects

Introduction and Objectives:

Water matrix effects were examined by comparing results for deionised and tap water (conductivity 80 μS/m; total alkalinity 14 mg/L (Mansfield, 2000)) against distilled water used as standard water. The objective of this study was to assess the effect of ionic strength (in terms of conductivity) on the photocatalytic oxidation rate.

Results and Discussion:

Table 4.7: p-CP concentration as a function of irradiation time and water matrix

Irradiation Time (min)	Water Matrix		
	Distilled Water*	Deionised Water	Tap Water
0	40.0	40.0	40
5	34.2	29.8	35.2
10	29.0	24.8	32.5
15	22.2	21.4	30.2
30	12.3	11.4	22.8
45	6.5	4.9	20.1
60	ND**	ND	16.1
10^2 k_{obs} (min^{-1})	4.10	4.49	1.47
Half-life (min)	16.9	15.4	47.2
R^2	0.99	0.99	0.98

Note: * Denotes standard reference level of parameter
ND = Not Detected; Limit of Detection = 1 mg/L**

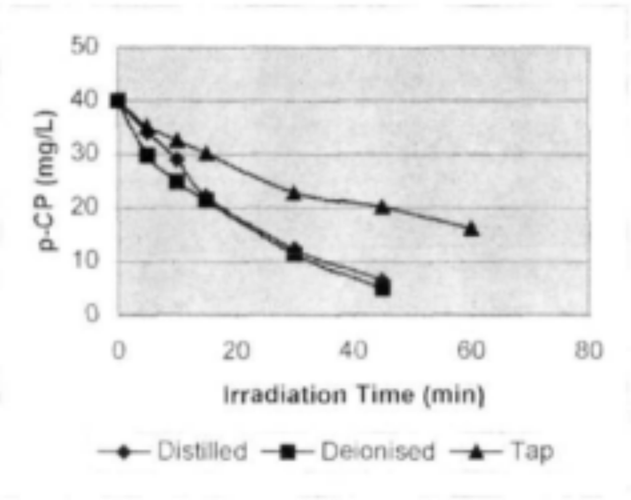

Figure 4.10: p-CP concentration as a function of irradiation time and water matrix

The results obtained from these experiments (Table 4.7 and Figure 4.10) indicated that :

- the observed first order rate constants (k_{obs}) increases marginally when using deionised water as spiking matrix for p-CP as opposed to distilled water. The observed increase is ascribed to the initial absence of radical scavenger ions in the deionised water matrix, which may be detrimental to the photocatalytic generation of hydroxyl radicals (deionised water conductivity: 1.5 uS/m; distilled water conductivity 2.4 uS/m);
- the disparity in reaction rate between deionised and distilled water is eliminated after about 15 minutes of reaction. This observation confirms the detrimental effect of chloride ions and HCl (as end-products of p-CP oxidation) on the oxidation rate *per se*;
- a reduction in reaction pH as a result of HCl formation is detrimental to photocatalytic oxidation and needs to be addressed in detail;
- the oxidation rate decreases markedly when using chlorinated tap water, indicating the inhibiting effect of inorganic ions and organic carbon as potential hydroxyl radical scavenger agents (tap water conductivity: 80 uS/m, total alkalinity 14 mg/L).
- waters with a higher alkalinity, will result in a decreased oxidation rate due to the scavenging effect of carbonate and bicarbonate ions (Glaze and Kang,1999)

(h) Initial pH

Introduction and Objectives:

The effect of pH was examined by comparing results for 4 different initial pH conditions against the standard pH of 5 for a 1 g/L TiO_2 slurry. 1M NaOH and 1M HCl (and dilutions thereof) were used as additives to adjust pH. The objectives of this study were to (1) confirm the detrimental effect of an acidic slurry pH on the photocatalytic oxidation rate and (2) investigate the behaviour of the photocatalytic system in alkaline conditions.

Results and Discussion:

Table 4.8: p-CP concentration as a function of irradiation time and initial slurry pH

Irradiation Time (min)	Initial Slurry pH				
	3	5*	7	9	11
0	40.0	40.0	40.0	40.0	40.0
5	35.1	34.2	34.9	37.2	36.5
10	30.3	29.0	29.9	34.3	34.1
15	23.5	22.2	22.5	29.4	32.5
30	14.5	12.3	13.3	21.8	28.5
45	7.2	6.5	6.8	16.8	25.6
60	ND**	ND	ND	12.6	22.5
10^2 k_{obs} (min^{-1})	3.81	4.10	3.98	1.96	0.91
Half-life (min)	18.2	16.9	17.4	35.4	76.2
R^2	0.99	0.99	0.99	0.99	0.98

Note: * Denotes standard reference level of parameter
ND = Not Detected; Limit of Detection = 1 mg/L**

Figure 4.11: p-CP concentration as a function of irradiation time and initial slurry pH

The results obtained from these experiments (Table 4.8 and Figure 4.11) indicated that :

- the observed first order rate constant (k_{obs}) is largely independent of pH in the range pH 3 to 7 (standard pH 5). This is ascribed to favourable adsorptive interaction of undissociated p-CP with TiO_2 (predominantly existing as TiOH species in this pH range);
- the rate decreases markedly when increasing the slurry pH to 9 and 11 respectively. This is ascribed to weak electrostatic repulsion between dissociated p-CP (present as fenolate anions) and TiO_2 (present as TiO^- anions).

(i) Gas Purge

Introduction and Objectives:

The effect of gas purge was examined by comparing results for compressed air and argon against pure oxygen used as standard gas purge. The objectives of this study were to (1) compare the rates of photocatalytic oxidation when using pure oxygen and air and (2) investigate the behaviour of the photocatalytic system in the absence of an oxygenated gas purge.

Table 4.9: p-CP concentration as a function of irradiation time and gas purge

Irradiation Time (min)	Gas Purge		
	Pure Oxygen*	Compressed Air	Argon
0 5 10 15 30 45 60	40.0 34.2 29.0 22.2 12.3 6.5 ND**	40.0 35.5 31.9 28 19.5 14.1 10.2	40.0 38.2 37.3 36.5 34.9 34.3 33.5
10^2 k_{obs} (min^{-1})	4.10	2.29	0.27
Half-life (min)	16.9	30.3	256.7
R^2	0.99	0.99	0.90

Note: * Denotes standard reference level of parameter
ND = Not Detected; Limit of Detection = 1 mg/L**

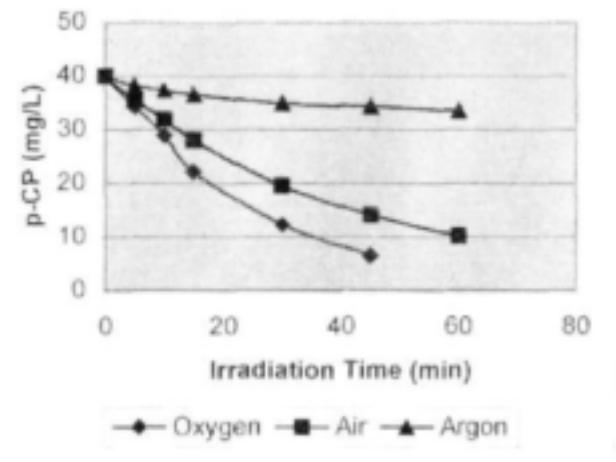

Figure 4.12: p-CP concentration as a function of irradiation time and gas purge.

The results obtained from these experiments (Table 4.9 and Figure 4.12) indicated that :

- the observed first order rate constant (k_{obs}) decreases with approximately 50% when using compressed air at the standard gas flow rate of 5 L/min This result is ascribed to the reduced oxygen content of air. Oxygen depletion may enhance charge recombination reactions and inhibit production of hydroxyl radicals;
- the rate constant decreases further by one order of magnitude when using an argon purge. The net removal of a small amount of p-CP is ascribed to UV photolytic effects;
- the use oxygen as gas purge is a prerequisite for photocatalytic oxidation.

(j) Gas Flow Rate

Introduction and Objectives:

The effect of gas flow rate was examined by comparing results for 20 L/min O_2 against the standard gas flow rate of 5 L/min O_2. The objectives of this study were to (1) establish whether an increased oxygen flow rate will enhance oxidation and (2) assess the observed effect in terms of reaction time, mode of operation and reactor type.

Results and Discussion:

Table 4.10: *p-CP concentration as a function of irradiation time and gas flow rate*

Irradiation Time (min)	Oxygen Gas Flow Rate (L/min)	
	5*	20
0	40.0	40.0
5	34.2	29.6
10	29.0	23.5
15	22.2	18.5
30	12.3	8.8
45	6.5	4.1
60	ND**	ND
10^2 k_{obs} (min^{-1})	4.10	5.00
Half-life (min)	16.9	13.9
R^2	0.99	0.99

Note: * Denotes standard reference level of parameter
ND = Not Detected; Limit of Detection = 1 mg/L**

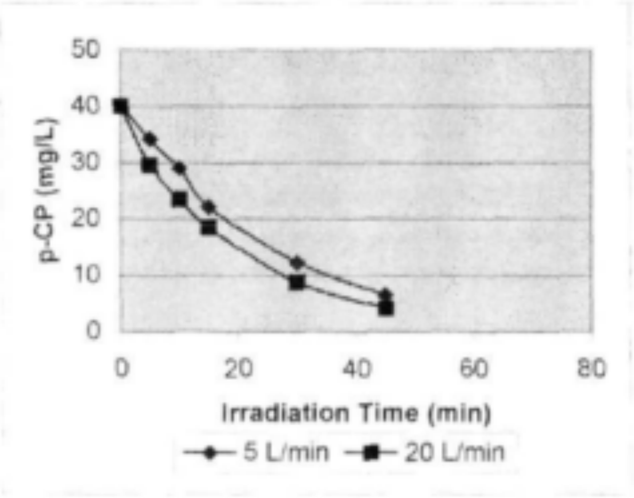

Figure 4.13: p-CP concentration as a function of irradiation time and gas flow rate

The results obtained from these experiments (Table 4.10 and Figure 4.13) indicated that :

- the observed first order rate constant (k_{obs}) increases only marginally when increasing the oxygen gas flow rate from 5 of 20 L/min, hence dependence of reaction rate on oxygen flow rate are less important in this instance. Oxygen concentration, however, is considered significant (as shown in the previous section);
- aqueous TiO_2 suspensions used for photocatalytic oxidation are sufficiently saturated with pure oxygen at low gas flow rates. This is possibly due to longer reaction times utilised in recirculation mode experiments;
- the positive auxiliary effect of increased oxygen flow rate may be more pronounced when using operation modes with shorter UV contact times (e.g. in single pass mode);
- a slurry-phased continuously stirred tank reactor (CSTR), such as Reactor 1, can be operated efficiently in recirculation mode using economical (low) oxygen flow rates;
- a reduction in operation cost for slurried configurations (such as Reactor 1) can probably be achieved in recirculation mode by using high air flow rates.

(k) UV Irradiance

Introduction and Objectives:

The effect of UV irradiance (radiant flux) was examined by comparing results for irradiation experiments conducted with two UV germicidal lamps against the standard (maximum) number of lamps used in Reactor 1 (eight). The irradiation experiment with two lamps comprised a 180° configuration viz., using lamps assembled at directly opposite ends of the circular array. The objectives of this study were to (1) determine whether a 75% reduction in UV irradiance (W/m^2) rendered a proportional reduction in oxidation rate and (2) explain the observed deterioration or improvement in performance.

Results and Discussion:

Table 4.11 p-CP concentration as a function of irradiation time and UV irradiance

Irradiation Time (min)	Number of UV lamps used for Irradiation	
	2 lamps (238.4 W/m^2)	8* (953.6 W/m^2)
0	40	40.0
5	36.3	34.2
10	33.9	29.0
15	31.5	22.2
30	27.5	12.3
45	23.4	6.5
60	20.4	ND**
10^2 k_{obs} (min^{-1})	1.08	4.10
Half-life (min)	64.2	16.9
R^2	0.99	0.99

Note: * Denotes standard reference level of parameter
ND = Not Detected; Limit of Detection = 1 mg/L**

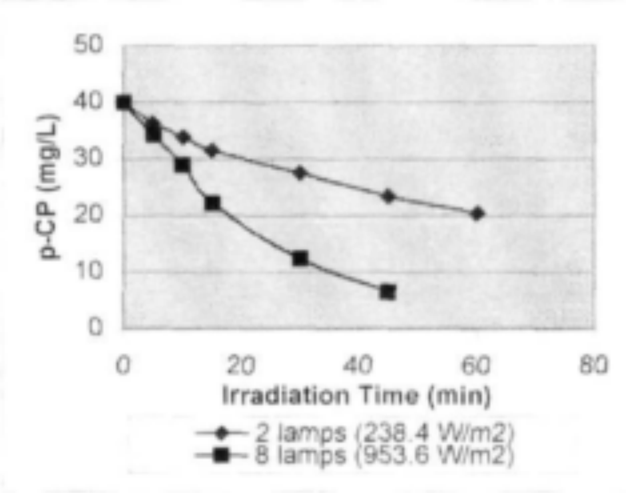

Figure 4.14: p-CP concentration as a function of irradiation time and UV irradiance

The results obtained from these experiments (Table 4.11 and Figure 4.14) indicated that :

- the observed first order rate constant (k_{obs}) is reduced by approximately 75% when applying 2 UV lamps for irradiation (in a 180° configuration) as opposed to the standard number of 8 lamps. This result correlates with the 75% reduction in UV irradiance (radiant flux), viz.: from 953.6 W/m^2 (8 lamps) to 238.4 W/m^2 (2 lamps);
- oxidation rate is linearly dependent on UV irradiance in the region examined (*ca* 240-950 W/m^2). A linear dependence indicates efficient utilisation of UV light photons for oxidation. This may be attributed to (1) minimised loss of UV radiation (2) efficient reflection characteristics (3) high illuminated specific surface area (κ) and (4) efficient catalyst-analyte interaction in the slurry-phased Reactor 1.

4.1.2 Single Pass Mode

(a) System Parameters

The photocatalytic oxidation of p-CP in water was investigated using (1) one-factor variation for random parametric studies (2) two-level experimental designs for screening studies and (3) response surface designs for optimisation studies. A global statistical formula was adopted as response function to denote the percentage of pollutant degradation (%D) (see Section 3.3). The following system parameters were evaluated as discrete levels in terms of the percentage degradation (Table 4.12):

Table 4.12: System parameters for p-CP study (Reactor 1; Single Pass Mode)

Parameter	Assigned Levels
Catalyst Suspension Loading (g/L)	0; 1; 5; 10; 20; 30
Volumetric Flow Rate (mL/min.)	50; 225[a]; 400; 575; 750*[b]
Horizontal Irradiation Distance (cm)	2; 8*
p-CP Initial Concentration (mg/L)	3; 5; 13; 27; 40*; 70; 100
Reaction Volume (L)	3*; 6
Water Matrix Effects	Distilled*
Solution pH	3; 5*; 7; 9; 11
Gas Purge	Oxygen*; Air
Gas Flow Rate (L/min.)	5*; 20
Number of UV-C lamps	0; 1; 2[c]; 4; 8*[d]

Note: * Denotes standard reference level of parameters
a Surface flow rate = 53.5 L/hr/m^2
b Surface flow rate = 178.5 L/hr/m^2
c UV irradiance = 238 W/m^2 = 2 x 30W lamps (per 0.252 m^2)
d UV irradiance = 954 W/m^2 = 8 x 30W lamps (per 0.252 m^2)

(b) Screening Study

Introduction and Objectives:

Seven parameters were identified for an initial screening study (see Tables 4.12-13). The objectives were to (1) obtain a rough estimate of the effects of the various parameters on the response function (2) eliminate insignificant parameters in accordance with the Pareto Principle (3) identify important parameters for optimisation purposes and (4) evaluate the application of a highly fractionated (1/16th) two-level factorial design in a screening study.

Results and Discussion:

Table 4.13: Design matrix for screening study (orthogonal array).

Run	Catalyst Suspension Loading (g/L)	Volumetric Flow Rate (mL/min.)	Gas Purge	Gas Flow Rate (L/min.)	Initial p-CP Conc. (mg/L)	Reaction Volume (L)	HID (cm)	D** (%)
1	1	225	Air	5	13	3	2	41.4
2	30	225	Oxygen	5	40	3	8	63.2
3	1	750	Oxygen	5	13	6	8	45.3
4	30	750	Air	5	40	6	2	35.5
5	1	225	Air	20	40	6	8	28.7
6*	30	225	Oxygen	20	13	6	2	68.9
7	1	750	Oxygen	20	40	3	2	36.1
8	30	750	Air	20	13	3	8	42.2

a HID = Horizontal Irradiation Distance; D = Degradation (%)**

*** Best result in terms reaction rate constant (run 6)**

**** D = Degradation of p-CP (%)**

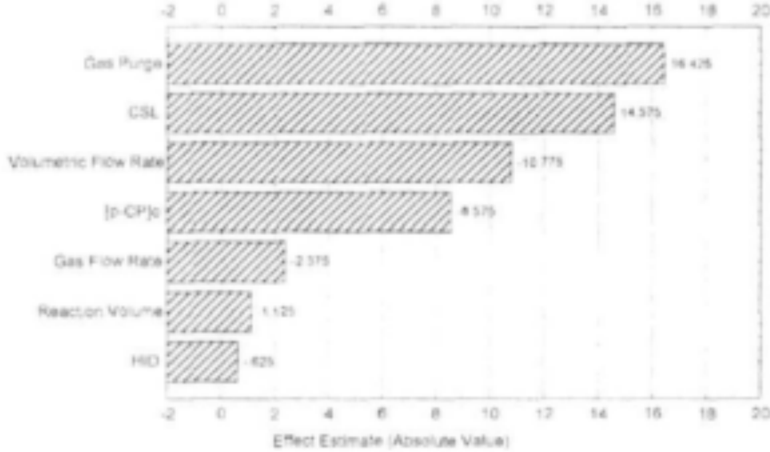

Figure 4.15: Pareto chart illustrating parameter effects with respect to % D response function. (CSL = Catalyst Suspension Loading; [p-CP]o = p-CP Initial Concentration in mg/L; HID = Horizontal Irradiation Distance in cm)

The results obtained from these experiments (Table 4.13 and Figure 4.15) indicated that :

- gas purge with oxygen has a highly beneficial effect on oxidation efficiency, while a higher gas purge flow rate does not have such a highly beneficial effect. More economical lower flow rates could be considered;
- a higher catalyst suspension loading has a highly beneficial effect on oxidation efficiency. An optimum loading would be necessary;
- a higher volumetric flow rate has a substantial negative effect on destruction efficiency for single pass mode of operation. This is ascribed to limited penetration of UV photons through a denser falling film when applying a higher flow rate;
- p-CP initial concentration has an intermediate negative effect on the destruction efficiency for the single pass mode of operation. This observation confirms the utility of Reactor 1 for the treatment of low concentrations of pollutant ;
- the volume of polluted water passed through the reactor has a negligible effect. This observation confirms the utility of Reactor 1 for treating large volumes of water when operated in single pass mode;
- the horizontal distance of the lamps has a negligible effect. Although this observation is in contrast with the result obtained for the analogous experiment in recirculation mode, it can be explained in terms of the physical constraints of the reactor design and the complex interaction that exists between parameters when conducting a multi-parameter experiment;
- parameter main effects are calculated successfully when using highly fractionated factorial designs in tandem with linear mathematical models. This observation indicates the utility of the selected design in terms of multi-parameter screening. ANOVA significance probabilities, however, are not calculated due to an insufficient number of degrees of freedom;
- parameter effects are confounded with each other when applying quadratic (polynomial) modelling. The calculation of parameter interactions is therefore precluded.

Based on the results obtained above, it was decided to (1) assess the effects of catalyst suspension loading, volumetric flow rate and initial p-CP concentration using one-factor variation studies and (2) to fix the remainder of the parameters at standard reference levels (presented in Table 4.12) which were considered to be economical or suitable for further experimentation.

(c) Catalyst Suspension Loading and Volumetric Flow Rate

Introduction and Objectives:

The effects of catalyst suspension loading and volumetric flow rate were examined in a series of one-factor variation experiments resembling a 5 x 4 block design. Five different loadings of TiO_2 were selected (1; 5; 10; 20 and 30 g/L) and treatment results thereof compared at four different volumetric flow rates (225; 400; 575 and 750 mL/min) for a p-CP initial concentration of 40 mg/L. The remainder of the system parameters were fixed at their standard reference levels. The objectives of this study were to (1) assess the individual effects of the parameters on the response function over their respective ranges and (2) assess the combined effects via a 3-dimensional representation.

Results and Discussion:

Table 4.14: Degradation (%) of p-CP as a function of volumetric flow rate for various catalyst suspension loadings (g/L TiO_2)

Volumetric Flow Rate (mL/min)	Catalyst Suspension Loading (g/L TiO_2)				
	1	5	10	20	30
225	44.9	55.1	64.2	68.4	63.2
400	35.3	46.2	54.3	54.5	55.0
575	30.1	37.8	43.8	44.2	44.3
750	30.2	33.1	35.2	35.9	40.3

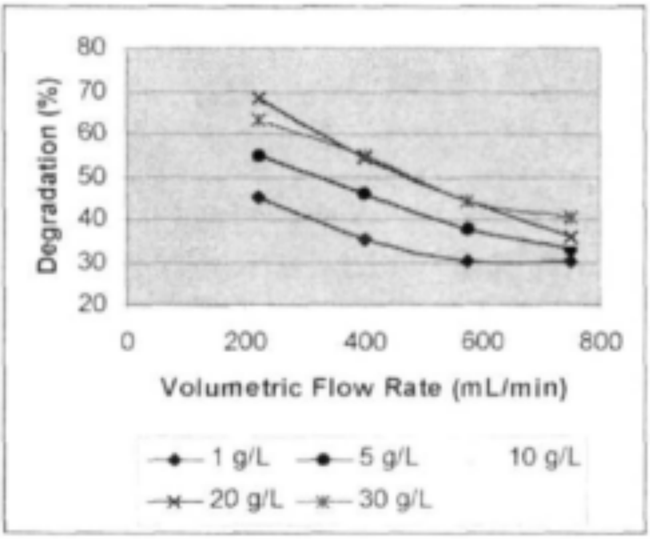

Figure 4.16: Degradation (%) of p-CP as a function of volumetric flow rate for various catalyst suspension loadings (g/L TiO_2)

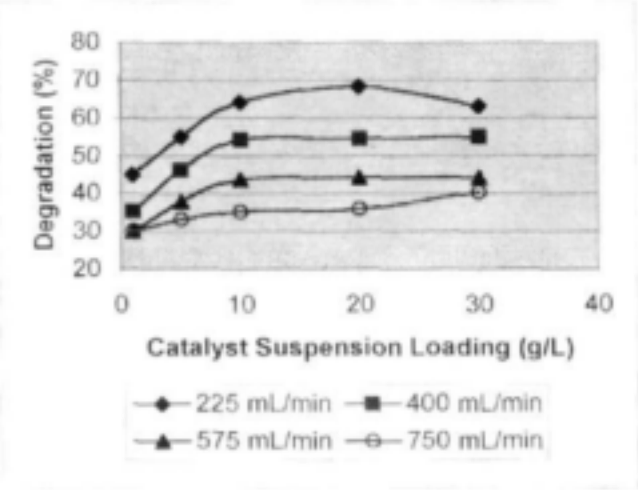

Figure 4.17: Degradation (%) of p-CP as a function catalyst suspension loading for various volumetric flow rates (mL/min).

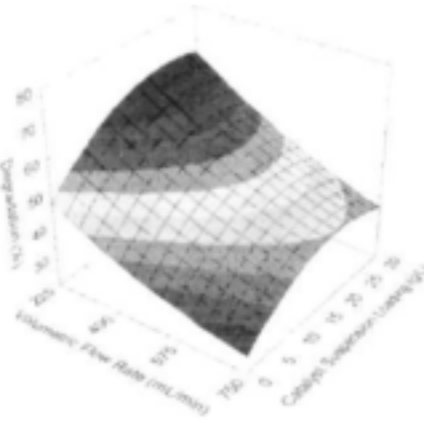

Figure 4.18: 3-Dimensional representation illustrating the combined effects of volumetric flow rate and catalyst suspension loading on the % degradation of 40 mg/L p-CP.

The results obtained from these experiments (Table 4.14 and Figures 4.16-4.18) indicated that:

- an increase in catalyst suspension loading generally enhances photocatalytic oxidation. This is in accordance with earlier results obtained in recirculation mode. The positive effect increases significantly with reduction in volumetric flow rate;
- a decrease in volumetric flow rate generally enhances oxidation. This is explained in terms of a thinner falling film attained at lower flow rate, which facilitates the penetration of UV light. The effect of flow rate is enhanced by increasing the catalyst suspension loading;

- the effect of catalyst suspension loading on the response is dependent on the magnitude of volumetric flow rate viz.: (1) for a relatively low flow rate (225 mL/minute) an optimum catalyst suspension loading (20 g/L) is attained from a quadratic response curve (2) for intermediate flow rates (400-575 mL/min) a plateau value (10 g/L) is attained from an asymptotic curve and (3) for a high flow rate (750 mL/min) the response curve is linear, indicating a steady increase in catalyst suspension loading. The latter result naturally implies that responses (viz.: oxidation efficiency) could be further increased at higher flow rate when applying loadings beyond 30 g/L TiO_2. This is an advantageous result in terms of practical application at high flow rate;
- the combined effect of the two parameters produces a saddle-like "rising ridge" curve when plotted in 3 dimensions against the response function (viz.: % Degradation).

(d) UV Photolysis

Introduction and Objectives:

The effect of UV photolysis (in the absence of TiO_2 catalyst) was examined for various volumetric flow rates. The objectives of this study were to (1) assess and compare the efficiency of UV photolysis to TiO_2 photocatalysis and (2) obtain information regarding the falling film effect as a function of volumetric flow rate under UV photolytic conditions.

Results and Discussion:

Table 4.15: Degradation (%) of p-CP as a function of volumetric flow rate under UV photolytic conditions

Volumetric Flow Rate (mL/min)	Degradation (%)
225	40.5
400	30.9
575	25.6
750	20.2

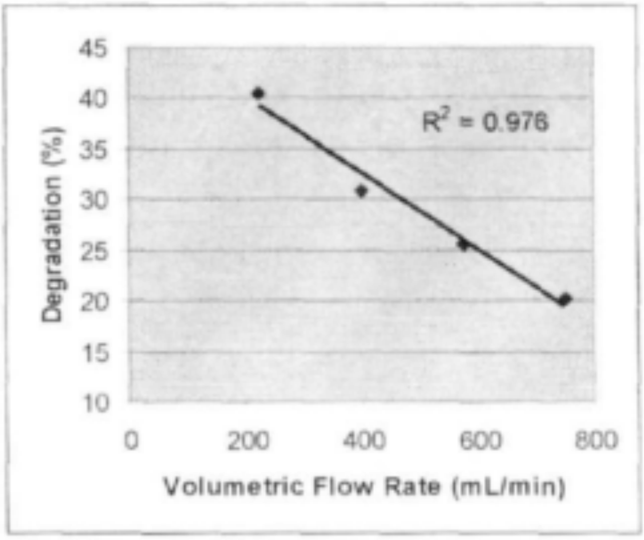

Figure 4.19: Degradation (%) of p-CP as a function of volumetric flow rate under UV photolytic *conditions*

The results obtained from these experiments (Table 4.15 and Figure 4.19) indicated that :

- UV photolysis of p-CP in water is feasible ;
- UV photolytic degradation efficiency increases linearly with a decrease in volumetric flow rate. This observation is in accordance with a thinner falling film obtained at low flow rate;
- TiO_2 photocatalysis is superior to UV photolysis under identical conditions, although the disparity is less pronounced at low flow rate as a result of the thin film effect.

(e) UV Irradiance

Introduction and Objectives:

The effect of UV irradiance (radiant flux) was examined by varying the number of UV lamps used for irradiation during a single pass experiment. A catalyst suspension loading of 10 g/L TiO_2 and a volumetric flow rate of 750 mL/minute were used. The objectives of this study were to (1) determine degradation efficiency as a function of UV irradiance and (2) to assess the efficiency of the reactor in terms of the nature of the UV irradiance response curve.

Results and Discussion:

Table 4.16: Degradation (%) of p-C as a function of UV irradiance

Number of UV lamps used for irradiation	Theoretical UV irradiance (W/m^2)	Initial p-CP Concentration (mg/L)	Final p-CP Concentration (mg/L)	Degradation (%)
0	0	40.0	38.5	3.8
1	119.2	40.0	37.1	7.3
2	238.4	40.0	36.0	10.0
4	476.8	40.0	33.4	16.5
8	953.6	40.0	25.9	35.3

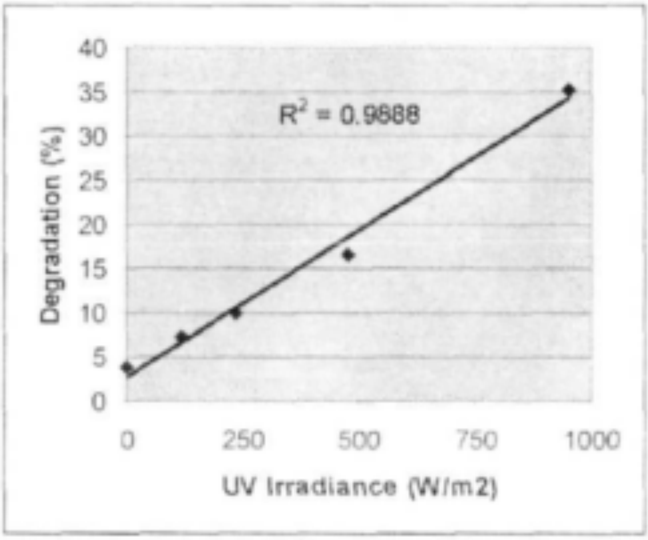

Figure 4.20: Degradation (%) of p-CP as a function of UV irradiance (in W/m^2)

The results obtained from these experiments (Table 4.16 and Figure 4.20) indicated that :

- degradation efficiency increases linearly with an increase in UV irradiance;
- less than 4% p-CP is lost due to mass transfer effects (in the absence of UV irradiation);
- based on the linear nature of the UV irradiance response curve, Reactor 1 represents an efficient photocatalytic design in terms of radiation characteristics.

(f) p-CP Initial Concentration

Introduction and Objectives:

The effect of initial concentration was examined by comparing results for 7 different loadings of p-CP (3; 5; 13; 27; 40; 70 and 100 mg/L). A catalyst suspension loading of 1 g/L TiO_2 and a volumetric flow rate of 750 mL/min were used. The objectives of this study were to (1) determine the efficiency of the single pass reactor for ultra-low and shock loadings respectively and (2) locate a region of maximum degradation efficiency, if possible.

Results and Discussion:

Table 4.17: Degradation (%) of p-CP as a function of initial concentration of p-CP (in mg/L)

Initial p-CP Concentration (mg/L)	Final p-CP Concentration (mg/L)	Degradation (%)
3.0	2.1	30.0
5.0	3.4	32.0
13.0	6.9	46.9
27.0	18.5	31.5
40.0	27.9	30.2
70.0	56.8	18.9
100.0	85.7	14.3

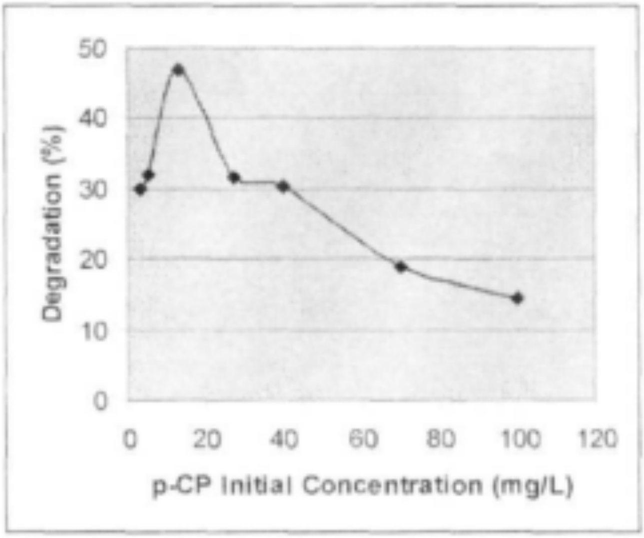

Figure 4.21: Degradation (%) of p-CP as a function of initial concentration of p-CP (in mg/L).

The results obtained from these experiments (Table 4.17 and Figure 4.21) indicated that :

- Reactor 1 is mostly suited for the removal of low concentrations of p-CP when operated in single pass mode. This is in accordance with results achieved earlier using the recirculation mode of operation;
- an optimum region of degradation exists when using an initial concentration of approximately 13 mg/L p-CP. This concentration is equivalent to 10^{-4} M.

(g) Initial pH

Introduction and Objectives:

The effect of pH was examined by comparing results for a range of initial pH conditions (pH 2.3-11.9) against the standard pH of 5 for a 1 g/L TiO_2 slurry. 1M NaOH and 1M HCl (and dilutions thereof) were used as additives to adjust pH. The experiments were conducted with the standard volumetric flow rate (750 mL/minute). The objectives of this study were to (1) confirm the detrimental effect of an acidic slurry pH on the photocatalytic oxidation rate and (2) investigate the behaviour of the photocatalytic system in alkaline conditions.

Results and Discussion:

Table 4.18: Degradation (%) of p-CP as a function of initial slurry pH

10^5 [HCl] (M)	10^5 [NaOH] (M)	Initial slurry pH	Degradation (%)
1000	Not App	2.3	15.0
100	Not App	3.0	23.3
50	Not App	3.4	24.3
10	Not App	4.2	26.9
5	Not App	4.4	27.9
1	NotApp	4.7	28.2
0	0	5.0	33.0
Not App*	1	5.2	30.2
Not App	5	6.4	27.7
Not App	10	7.3	27.1
Not App	50	9.8	25.8
Not App	100	10.5	17.8
Not App	1000	11.9	14.8

Note: NotApp* = Not applicable

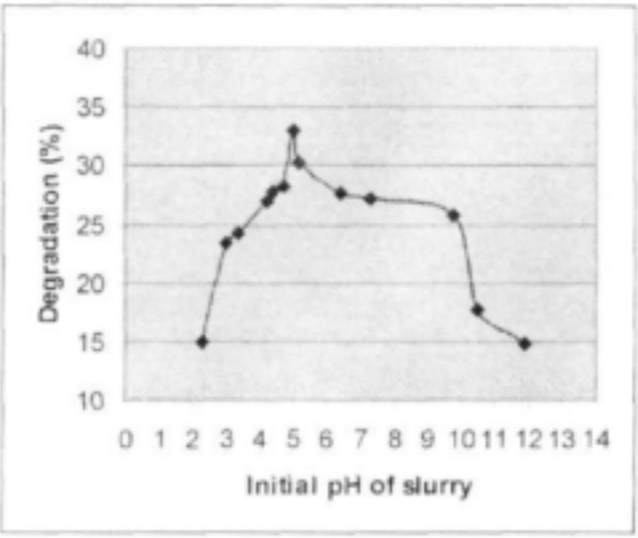

Figure 4.22: Degradation (%) of p-CP as a function of initial slurry pH

The results obtained from these experiments (Table 4.18 and Figure 4.22) indicated that :

- degradation efficiency is marginally affected by pH in the region pH 4 to10. This is ascribed to favourable adsorptive interaction of undissociated p-CP with TiO_2 (predominantly existing as TiOH species in this pH range);
- maximum efficiency is obtained at the natural pH of 5 for a 1 g/L TiO_2 slurry. It is concluded that the photocatalytic system is sensitive to the presence of inorganic ions in the reaction medium. This is possibly due to the fact that these species are blocking surface sites on the catalyst and thus hampering surface catalysed oxidation of p-CP;
- increasing the concentration of HCl or NaOH additive, thus moving further away from the natural slurry pH of 5, affects the degradation more substantially. The poor degradation efficiency around pH 2 is ascribed to the scavenging effects of excess chloride ions, while a similar result around pH 12 is ascribed to weak electrostatic repulsion between dissociated p-CP (present as fenolate anions) and TiO_2 (present as TiO^- anions) ;
- no drastic change in degradation efficiency occurs around the point of zero charge (PZC) of TiO_2 (viz.: at pH 6.2).

(h) Optimisation Example

Introduction and Objectives:

Based on all previous results, two parameters (viz. catalyst suspension loading and volumetric flow rate) were identified for an optimisation study using a response surface design in conjunction with a polynomial mathematical model (see Table 4.19). The initial concentration of p-CP was 40 mg/L, while the remainder of the system parameters were fixed at their standard reference levels (as listed in Table 4.12). The objectives of this study were to (1) monitor the behaviour of the response function in the optimal region (2) fine-tune the optimum conditions for catalyst suspension loading and volumetric flow rate and (3) assess the utility of a Doehlert uniform array as potential experimental design in optimisation procedures.

Results and Discussion:

Table 4.19: Design matrix for optimisation study (Doehlert uniform array)

Run	Catalyst Suspension Loading (g/L)	Volumetric Flow Rate (mL/min)	Degradation (%)
1	20	225.0	68.4
2	21	242.5	61.1
3	22	225.0	65.5
4	21	207.5	63.0
5	19	207.5	67.4
6	18	225.0	65.3
7	19	242.5	64.1

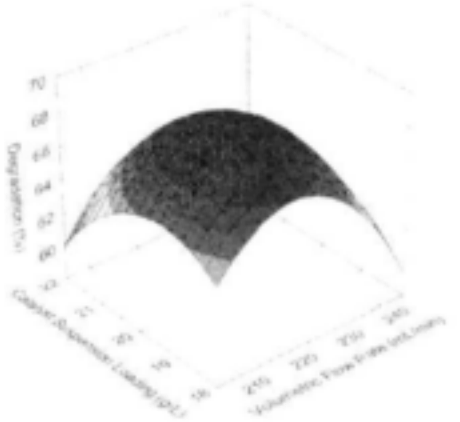

Figure 4.23: Three dimensional response surface illustrating the combined effects of volumetric flow rate and catalyst suspension loading on the % degradation of 40 mg/L p-CP

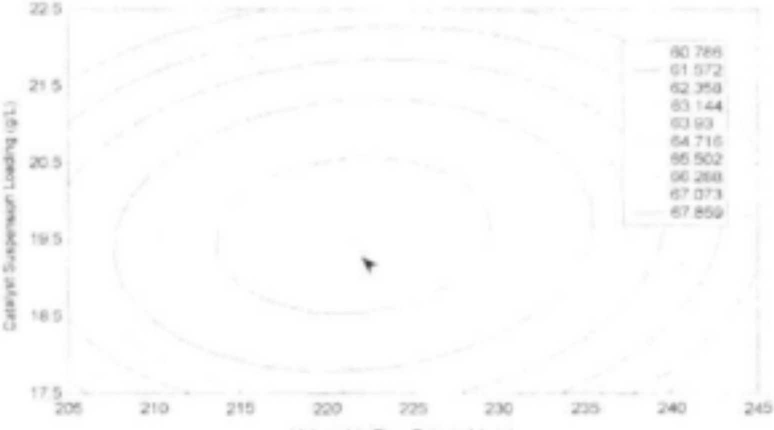

Figure 4.24: Two dimensional contour plot illustrating the existence of optimum conditions for catalyst suspension loading (*ca* 19.5 g/L TiO_2) and volumetric flow rate (*ca* 221.5 mL/min) for the degradation (%) of p-CP

The results obtained from these experiments (Table 4.19 and Figures 4.23-4.24) indicated that:

- a parabolic response surface (denoting the existence of optimum conditions) is successfully generated with the aid of a Doehlert uniform array ;
- the optimum conditions (see Figure 4.24) for catalyst suspension loading and volumetric flow rate are *ca* 19.5 g/L TiO_2 and *ca* 221.5 mL/minute for the single pass mode of operation ;
- despite the relative small variation in response values, the technique of Response Surface Methodology remains an efficient means for establishing optimum conditions.

4.1.3 Sequential Single Pass Mode

(a) System Parameters

The photocatalytic oxidation of p-CP in water was investigated in terms of the defined first order kinetic responses for sequential single pass mode of operation (see Section 3.3). The following system parameters were evaluated at discrete levels (Table 4.20):

Table 4.20: System parameters for p-CP study (Reactor 1; Sequential Single Pass Mode)

Parameter	Assigned Levels
Catalyst Suspension Loading (g/L)	20
Volumetric Flow Rate (mL/min)	225[a]
Horizontal Irradiation Distance (cm)	8
p-CP Initial Concentration (mg/L)	40
Reaction Volume (L)	3
Water Matrix Effects	Distilled
Gas Purge	Oxygen
Gas Flow Rate (L/min)	5
Number of UV-C lamps	8[b]

a Surface flow rate = 53.5 L/hr/m^2
b UV irradiance = 954 W/m^2 = 8 x 30W lamps (per 0.252 m^2)

(b) Representative Example

Introduction and Objectives:

The sequential single pass operation of Reactor 1 corresponds with a UV residence time (contact time) of 2.1 sec per single pass (N). Test runs were conducted by preparing fresh batches of catalyst for each single pass, thus eliminating catalyst deactivation effects as a function of pH. System parameters were fixed at the levels specified in Table 4.20. The objectives of this study were to (1) determine the theoretical number of passes required to reduce 40 mg/L of p-CP to below the limit of detection (1 mg/L) at near optimised conditions for catalyst suspension loading and volumetric flow rate and (2) compare the kinetic results with those obtained when operating the reactor in recirculation mode.

Results and Discussion:

Table 4.21: p-CP concentration and cumulative degradation (5) as functions of single pass number (N)

Number of Single Passes (N)	Cumulative Contact Time of Irradiation (sec)	p-CP Concentration (mg/L)	Cumulative Degradation (%)
0	0.0	40.0	0.0
1	2.1	12.8	68.0
2	4.2	4.1	89.8
3	6.3	1.5	96.3
4	8.4	ND*	>97.5
5	10.5	ND	>97.5
6	12.6	ND	>97.5
Independent Parameter	10^2 k_{obs}	Half-Life	R^2
Single Pass Number (N)	*ca* 110 passes^{-1}	*ca* 0.6 passes	0.99
Irradiation Time (sec)	*ca* 53.3 sec^{-1}	*ca* 1.3 sec	0.99
Irradiation Time (min)	*ca* 3200 min^{-1}	*ca* 0.02 min	0.99

ND*= Not detected; Limit of Detection = 1 mg/L

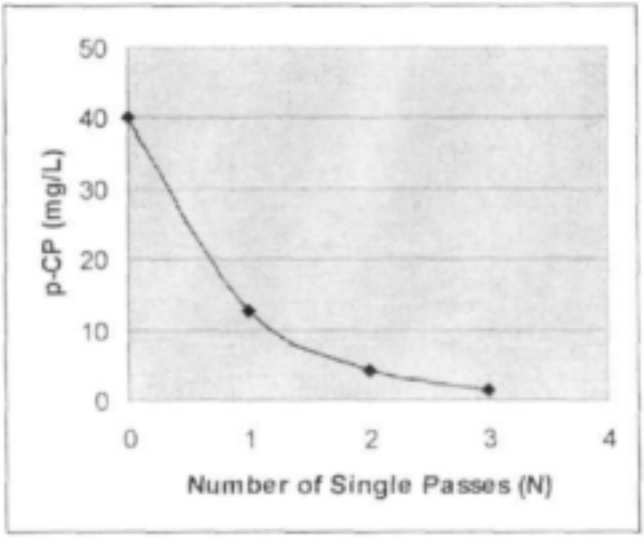

Figure 4.25: p-CP concentration as a function of single pass number (N) where N = 2.1 sec for *each* pass.

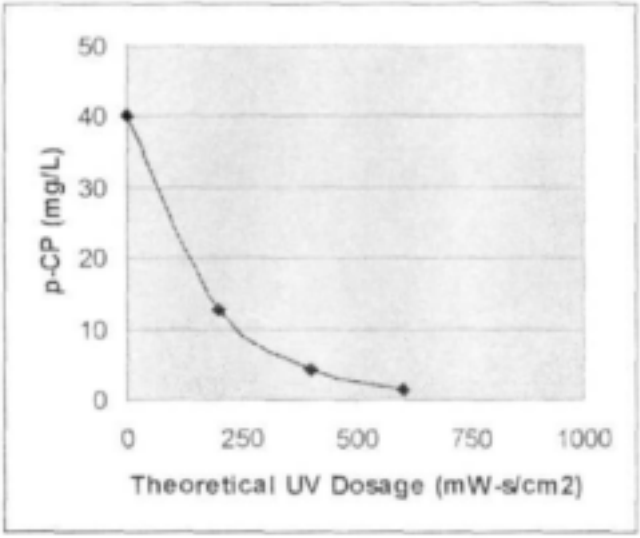

Figure 4.26: p-CP concentration as a function of theoretical UV dosage (in mW-sec/cm^2).

The results obtained from these experiments (Table 4.21 and Figures 4.23-4.24) indicated that:

- first order exponential decay kinetics apply to the photocatalytic oxidation of p-CP when operating Reactor 1 in sequential single pass mode ;
- the initial p-CP concentration of 40 mg/L decreases to below the detection limit (1 mg/L) within 4 single passes of the reactor ;
- the result mentioned above requires a theoretical UV dosage in the order of 800 mW-s/cm^2 . This dosage is equivalent to approximately 8.5 seconds of UV exposure in the reactor ;
- the first order rate constants (in min^{-1}) are generally 3 orders of magnitude greater than the analogous rate constants in recirculation mode, hence the sequential single

pass mode of operation is significantly more efficient in terms of UV dosages (viz.: irradiation times).

It was shown in a separate study that (1) the relative effects of catalyst suspension loading and volumetric flow rate diminish within the framework of a sequential single pass mode of operation and (2) variation in slurry pH (as a result of p-CP oxidation and the formation of HCl) suppresses the catalytic activity of TiO_2. These negative effects, however, were partially countered by pH adjustment and/or controlled periodic illumination (viz.: subjecting slurries to "dark recovery periods") (De Villiers, 2000).

(c) Cost Calculation

A preliminary cost calculation was made for the photocatalytic oxidative treatment of p-CP in distilled water, based on the operation of Reactor 1 as a slurried system in the sequential single pass mode. The calculation was done in view of the following assumptions :

- first order kinetics
- idealised plug-flow reactor conditions
- a constant electrical energy per order (EE/O)

Bolton's formula for EE/O in idealised plug-flow reactors has been defined earlier (in Section 2.1.3) :

$$EE/O = P / F \times \log (c_0 / c_f)$$

Where: P = Lamp power (in kW)
F = Volumetric water flow rate (in m^3/h)
c_0 = Initial concentration
c_f = Final concentration
EE/O = $kWh/order/m^3$

Thus, taking the above mentioned p-CP result as example, the EE/O and cost (per m^3) for the photocatalytic oxidation of an initial concentration of 40 mg/L to below the limit of detection (1 mg/L) can be calculated as follows :

- orders of removal = log (40/1) = 1.602
- P = 8 x 30 W = 240 W = 0.24 kW
- F = 0.225 L/minute = 13.5 L/h = 0.0135 m^3/h

EE/O amounts to: (0.24)/(0.0135 x 1.602) = 11.1 $kWh/order/m^3$. At a unit price of 11.8 c/kWh in the Stellenbosch area, the cost to reduce 40 mg/L p-CP with one order of magnitude (4 mg/L) amounts to 131c / m^3 of water. A further order of magnitude reduction (to 0.4 mg/L) will double the cost, since EE/O is a constant per order.

When applying a volumetric flow rate of 750 mL/minute, the cost changes to 39c / m^3, which demonstrates that a high volumetric throughput drastically reduces electrical costs in the single pass (plug-flow) reactor.

4.2 TREATMENT OF MICROCYSTINS

4.2.1 Recirculation Mode

(a) System Parameters

The photocatalytic oxidation of three variants of microcystins in water was investigated in a random parametric study using one-factor variation for each experiment. The following system parameters were evaluated at discrete levels in terms of first order reaction kinetics (see Table 4.22):

Table 4.22: System parameters for microcystin study (Reactor 1; Recirculation Mode)

Parameter	Assigned Levels
Catalyst Suspension Loading (g/L)	0; 0.2; 1; 5
Volumetric Flow Rate (L/min.)	1.5^{*a}; 2.0^{b}
Horizontal Irradiation Distance (cm)	8^{*}
Microcystin Variants	YR, LR and YA
Reaction Volume (L)	5^{*}
Water Matrix Effects	Distilled; Deionised*; Lake water
Gas Purge	Oxygen*; Air
Oxygen Flow Rate (L/min.)	5^{*}
Number of UV-C lamps for Irradiation	8^{*c}
Irradiation Time (min.)	20^{*}; 60^{d} and 180^{d}

Note: * Denotes standard reference level of parameters
a Surface flow rate = 357 L/hr/m^2
b Surface flow rate = 475 L/hr/m^2
c UV Irradiance = 954 W/m^2
d For initial screening studies

(b) Screening Study

Introduction and Objectives:

Three initial screening test runs were conducted to determine whether (1) photocatalytic oxidative destruction of microcystin toxins in water was feasible (2) surface adsorption (mass transfer) of microcystin molecules onto TiO_2 slurry particles occurred in the absence of UV irradiation and (3) first order exponential decay kinetics could be applied using a minimised standard time of irradiation.

Results and Discussion:

For the first test run an irradiation period of 3 hours was selected. System parameters included a catalyst suspension loading of 1 g/L TiO_2, a volumetric flow rate of 1500 mL/minute (using a double-headed peristaltic pump) and a distilled water matrix. The remainder of the system parameters were fixed at their reference levels (listed in Table 4.22). Aliquots of a 100 mL were collected from the reactor for each sampling time (specified in Table 4.23) and consequently analysed for microcystin content.

Table 4.23: Microcystin concentration as a function of irradiation time

Irradiation Time (min)	Microcystins (ug/L)		
	YA	YR	LR
0	ND*	92	46
30		10	ND
60		ND	
180			

Note: ND* = Not Detected; Limit of Detection = 10 ug/L

The results obtained from the first experiment (Table 4.23) indicated that:

- the concentration of microcystin YA is already below the 10 ug/L detection limit prior to commencement of the reaction. This observation proves that YA may be sensitive to catalyst adsorption;
- the initial concentration of microcystin YR (92 ug/L) decreases to 10 ug/L within 30 minutes of UV exposure and is not detected after 1 hour;
- the initial concentration of microcystin LR (46 ug/L) decreases to below the 10 ug/L limit within the first 30 minutes of reaction;
- no intermediate or final breakdown products are detected via HPLC analysis.

Although the first screening test run confirmed microcystin removal from the water sample, it was not clear whether the observed reduction in concentration levels could be attributed to photocatalytic oxidation of microcystins or merely mass transferred removal thereof from the aqueous phase via surface adsorption onto slurried TiO_2 catalyst. A "dark" adsorption experiment (in the absence of UV light) was conducted by recirculating 5 L of distilled water (spiked with algal extract) through the reactor for a period of 60 minutes. 100 mL aliquots were collected from the reactor at 0 and 60 minutes of reaction time. The remainder of the system parameters were fixed at their reference levels (Table 4.22). An oxygen gas purge (at 5 L/minute flow rate) was applied to ensure suspension of TiO_2 particles.

Table 4.24: Microcystin concentration as a function of irradiation time

Recirculation Time (min)	Microcystins (ug/L)		
	YA	YR	LR
0	22	102	52
60	21	93	41
Net Removal (%)	4.5	8.8	21.2

The results obtained from the second experiment (Table 4.24) indicated that:

- microcystin YA decreases from 22 to 21 ug/L (net removal of 4.5%);
- microcystin YR decreases from 102 to 93 ug/L (net removal of 8.8%);
- microcystin LR decreases from 52 to 41 ug/L (net removal of 21.2 %)
- the observed mean reduction of 11% (due to surface adsorption and partial oxidation via oxygen purging) is relative small compared to the reduction obtained by applying photocatalytic oxidation;

The effect of surface adsorption on the photocatalytic oxidation of microcystins is a complex function of several system parameters and needs to be addressed in more detail.

The third screening test run was conducted to establish a minimum standard irradiation period for reducing all microcystin levels below 10 ug/L (detection limit) and to assess the application of first order kinetics in this regard. System parameters were identical in comparison to the first test run (Table 4.22). Deionised water was used as spiking matrix.

Table 4.25: Microcystin concentration as a function of irradiation time

Irradiation Time (min)	Microcystins (ug/L)		
	YA	YR	LR
0	15	112	55
5	ND*	47	31
10		21	16
15		10	9
20		ND	ND
10^2 k_{obs} (mins^{-1})	NC**	16.11	12.18
Half-life (min)	-	4.3	5.7
R^2	-	0.99	0.99

Note: ND* = Not Detected; Limit of Detection = 10 ug/L
NC = Not calculated**

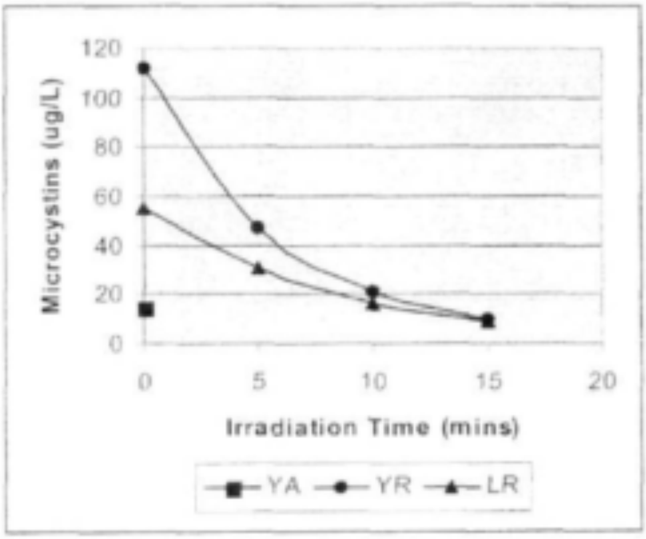

Figure 4.27: Microcystin concentration as a function of irradiation time and microcystin variant

The results obtained from the third experiment (Table 4.25 and Figure 4.27) indicated that:

- the decrease in microcystin levels adheres to first order exponential decay kinetics;
- the initial concentration of microcystin YA (15 ug/L) is reduced to below the detection limit within the first 5 minutes of photocatalytic treatment;
- microcystins YR and LR require approximately 20 minutes to achieve the same result. This result is attributed to higher initial concentrations;
- microcystin LR (with initial reaction rate of 6.7 ug/L/min.) is more resistant to photocatalytic oxidation than YR (reaction rate of 18 ug/L/min.), despite the disparity in initial concentration levels.

(c) Catalyst Suspension Loading (Deionised Water)

Introduction and Objectives:

The effect of catalyst suspension loading was examined in deionised water by comparing results for 3 different loadings of TiO_2 (0; 0.2 and 1 g/L). System parameters were evaluated at standard reference levels (see Table 4.22). The objectives of this study were to (1) establish whether an increase in catalyst suspension loading promotes photocatalytic oxidation of microcystins and (2) assess and compare the effects of UV photolysis against TiO_2 photocatalysis.

Results and Discussion:

Table 4.26: Microcystin concentration as a function of irradiation time and catalyst suspension loading

Irradiation Time (min)	Microcystins (ug/L)								
	YA			YR			LR		
	Catalyst Suspension Loading (g/L)			Catalyst Suspension Loading (g/L)			Catalyst Suspension Loading (g/L)		
	0	0.2	1	0	0.2	1	0	0.2	1
0	14	17	ND	82	63	58	28	26	26
2	46	21		63	46	43	26	22	23
4	43	13		50	41	10	24	16	12
6	38	13		56	36	ND	23	15	ND
8	37	ND*		46	16		18	11	
10	35	12		44	12		19	15	
12	31	14		39	ND		17	10	
14	25	ND		28			14	ND	
16	32	ND		33			14		
18	NA***	12		NA			NA		
20	26	NA		26			17		
10^2 k_{obs} (min^{-1})	NC**	NC	NC	6.25	16.56	43.95	4.72	7.16	19.33
Half-life (min)	-	-	-	11.1	4.2	1.6	14.7	9.7	3.6
R^2	-	-	-	0.90	0.92	0.87	0.95	0.82	0.87

Note: ND* = Not detected; Limit of Detection = 10 ug/L
NC = Not calculated**
NA* = Not analysed**

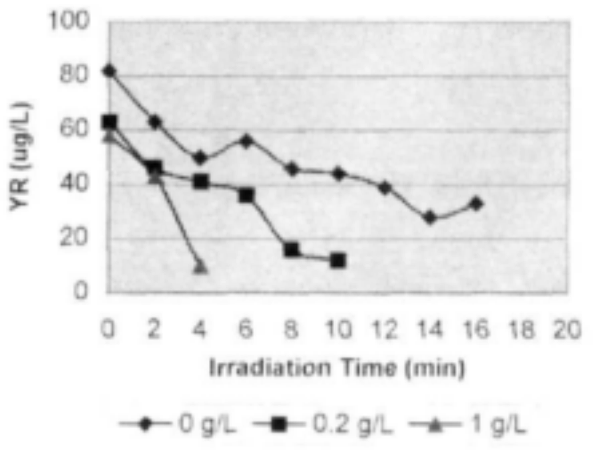

Figure 4.28: Microcystin YR concentration as a function of irradiation time and catalyst suspension loading

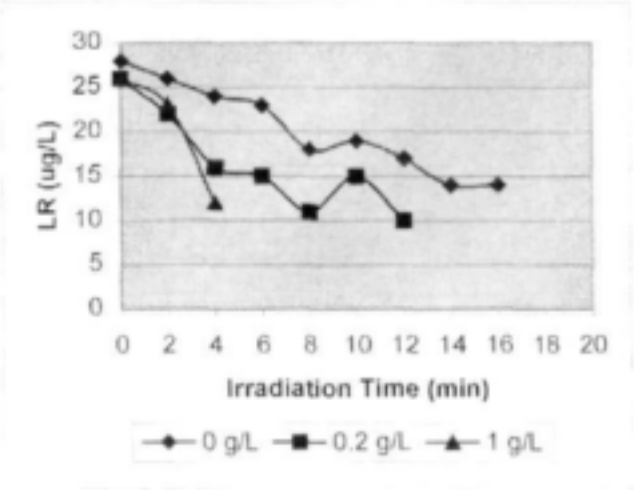

Figure 4.29: Microcystin LR concentration as a function of irradiation time and catalyst suspension loading.

The results obtained from these experiments (Table 4.26 and Figures 4.28-4.29) indicated that:

- the photocatalytic oxidation rate of microcystins increases by increasing the catalyst suspension loading;
- when using a deionised water matrix, the effect of catalyst suspension loading is amplified due to an absence of inorganic ions acting as oxidant scavengers;
- a catalyst suspension loading of 1 g/L TiO_2 reduces the microcystin YR and LR concentrations to a non-detectable level (ND) within 6 minutes of UV exposure. This observation is anticipated in terms of reduced starting concentrations used (e.g. 58 ug/L for YR) compared to earlier runs (test run 3 : 112 ug/L for YR);
- the addition TiO_2 catalyst significantly enhanced degradation of microcystin YR, compared to UV photolysis;
- microcystin LR is considerably more resistant to photocatalytic oxidation than YR;
- surface adsorption of microcystin YA is favoured by an increase in catalyst suspension loading.

(d) Gas Purge

Introduction and Objectives:

The effect of gas purge was examined by comparing results for compressed air against pure oxygen used as standard gas purge. The economic implications of such an experiment would become significant in a scaling-up situation. Catalyst suspension loading was set at 0.2 g/L TiO_2. The remainder of the system parameters were evaluated at standard reference levels (see Table 4.22). The objective of this study was to compare rates of photocatalytic oxidation for the two gas purges used.

Results and Discussion:

Table 4.27: Microcystin YR concentration as a function of irradiation time and gas purge

Irradiation Time (min)	Microcystins (ug/L)					
	YA		YR		LR	
	Oxygen	Air	Oxygen	Air	Oxygen	Air
0 2 4 6 8 10 12 14 16 18 20	17 21 13 13 ND* 12 14 ND ND 12 NA***	15 ND	63 46 41 36 16 12 ND	53 52 31 32 23 17 14 11 ND ND ND	26 22 16 15 11 15 10 ND	19 18 10 ND 10 ND
10^2 k_{obs} (mins^{-1})	NC**	NC	16.56	11.73	7.16	8.94
Half-life (min)	-	-	4.2	5.9	9.7	7.8
R^2	-	-	0.92	0.97	0.82	0.74

Note: ND* = Not detected; Limit of Detection = 10 ug/L
NC = Not calculated**

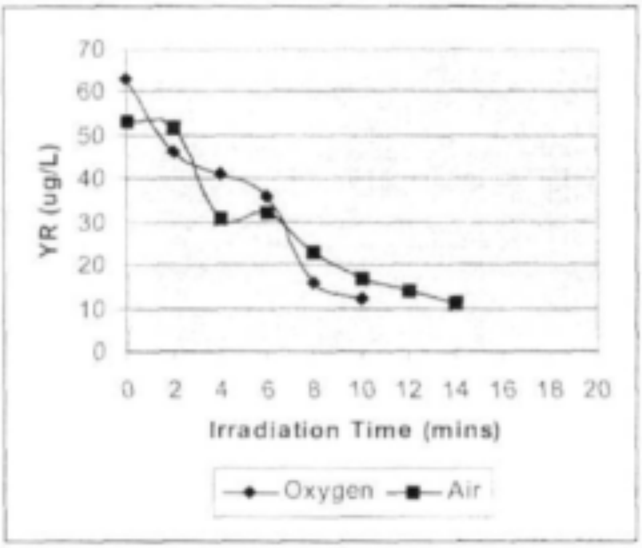

NA* = Not analysed**

Figure 4.30: Microcystin YR concentration as a function of irradiation time and gas purge

The results obtained from these experiments (Table 4.27 and Figure 4.30) indicated that:

- the oxidation rate for microcystin LR is largely unaffected by switching the gas purge from oxygen to compressed air. This observation is coupled to high resistance of LR towards photocatalytic oxidation in general;
- the oxidation rate for microcystin YR is marginally reduced when switching gas purge to air. This observation is coupled to the greater susceptibility of YR towards photocatalytic oxidation;
- *the utilisation of air as gas purge in photocatalytic oxidations is to be considered when treating recalcitrant organic pollutants in water.*

(e) Water Matrix Effects

Introduction and Objectives:

Water matrix effects were examined by comparing results for the treatment of microcystins in deionised water and natural lake water. Lake water was sampled at Zeekoevlei (a hypertrophic coastal lake on the Cape Flats) which has experienced seasonal outbreaks of cyanobacterial blooms. Catalyst suspension loading was set at 0.2 g/L TiO_2. The remainder of the system parameters were evaluated at standard reference levels (see Table 4.22). *The objectives of this study were to (1) compare rates of photocatalytic oxidation for the two water matrixes used and (2) assess the effect of inorganic ions on the photocatalytic oxidation of microcystins in untreated natural water.*

Results and Discussion:

Table 4.28: Microcystin concentration as a function of irradiation time, variant and water matrix

Irradiation Time (min.)	Microcystins (ug/L)					
	YA		YR		LR	
	Deionised Water	Lake Water*	Deionised Water	Lake Water*	Deionised Water	Lake Water*
0	17	21	63	64	26	35
2	21	17	46	58	22	30
4	13	15	41	50	16	31
6	13	12	36	41	15	26
8	ND*	11	16	38	11	25
10	12	11	12	41	15	32

12	14	ND	ND	32	10	22
14	ND			35	ND	22
16	ND			34		25
18	12			31		22
20	NA***			34		26
10^2 k_{obs} (min^{-1})	NC**	6.80	16.56	4.68	7.16	1.74
Half-life (min)	-	10.2	4.2	14.8	9.7	39.8
R^2	-	0.93	0.92	0.88	0.82	0.51

Note: # See Table 3.4
ND* = Not detected; Limit of Detection = 10 ug/L
NC = Not calculated**
NA* = Not analysed**

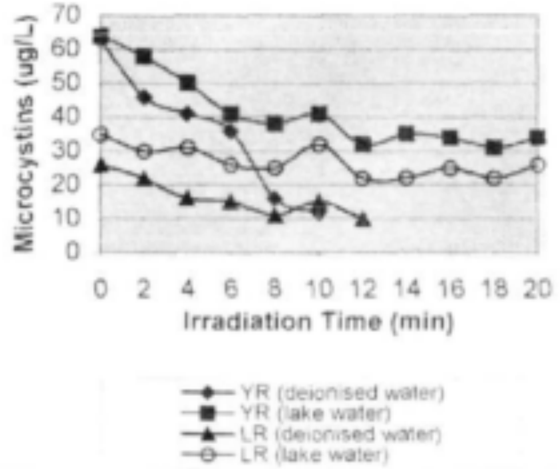

Figure 4.31: Microcystin concentration as a function of irradiation time, variant and water matrix

The results obtained from these experiments (Table 4.28 and Figures 4.31) indicated that:

- the utilisation of untreated lake water (as opposed to deionised water) results in significantly slower oxidation of microcystins. This result is attributed to the presence of pigments and inorganic ions (e.g. nitrates and phosphates) which can act as hydroxyl radical scavengers during photocatalytic oxidation;
- the conductivity is 3 orders of magnitude greater for the lake water used in this study compared to deionised water (1.1 mS/m versus 1.4 uS/m). This result confirms the higher concentration of inorganic species in the former water matrix ;
- the oxidation susceptibilities of microcystins YR and LR are dissimilar, despite observed first order rate constants decreasing with more than 70% for both variants when using lake water as spiking matrix.

(f) Catalyst Suspension Loading (Lake Water)

Introduction and Objectives:

The effect of catalyst suspension loading was examined in lake water by comparing results for 3 different loadings of TiO_2 (0.2; 2 and 5 g/L). System parameters were evaluated at standard reference levels according to Table 4.22. The objectives of this study were to (1) establish whether an increase in catalyst suspension loading promoted photocatalytic oxidation of microcystins in lake water and (2) monitor whether the oxidation rate could be enhanced to a level comparative with oxidation in deionised water.

Results and Discussion:

Table 4.29: Microcystin concentration as a function of irradiation time, variant and catalyst suspension loading

Irradiation Time (min)	Microcystins (ug/L)								
	YA			YR			LR		
	Catalyst Suspension Loading (g/L)			Catalyst Suspension Loading (g/L)			Catalyst Suspension Loading (g/L)		
	0.2	2	5	0.2	2	5	0.2	2	5
0	21	14	18	64	44	66	35	22	37
2	17	15	16	58	49	54	30	22	30
4	15	ND	13	50	26	45	31	13	30
6	12	10	12	41	31	39	26	15	17
8	11	ND	10	38	36	33	25	27	17
10	11		ND	41	27	29	32	29	15
12	ND*			32	30	26	22	24	12
14				35	24	21	22	21	12
16				34	23	21	25	19	13
18				31	22	18	22	14	11
20				34	18	15	26	19	ND
10^2 k_{obs} (min^{-1})	6.80	6.01	7.32	4.68	4.33	7.83	1.74	NC**	6.82
Half-life (min)	10.2	11.5	9.5	14.8	16.0	8.9	39.8	-	10.2
R^2	0.93	0.89	0.99	0.88	0.97	0.99	0.51	-	0.88

Note: ND* = Not detected (Limit of Detection = 10 ug/L)
NC** = Not calculated

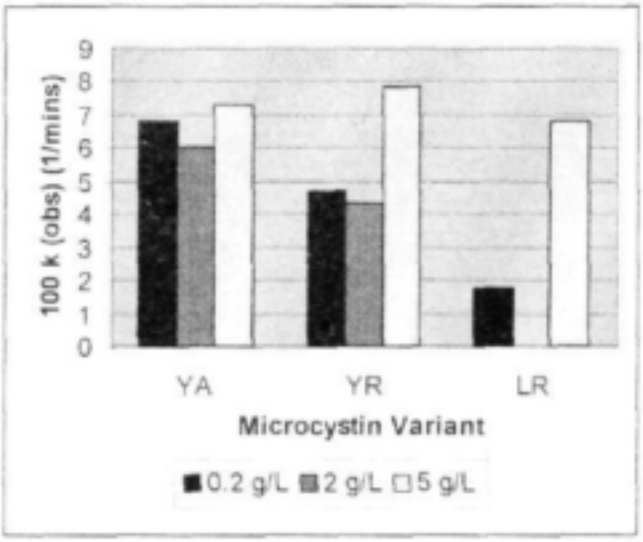

Figure 4.32: First order rate constants as a function microcystin variant and catalyst suspension loading

The results obtained from these experiments (Table 4.29 and Figure 4.32) indicated that :

- an increase in catalyst suspension loading from 0.2 to 5 g/L does not significantly promote the oxidation of microcystins YA and YR;
- an increase in catalyst loading from 0.2 to 5 g/L enhances the oxidation of microcystin LR considerably;
- photocatalytic oxidation performed at elevated catalyst loading is advised when treating recalcitrant organic compounds in the presence of inorganic ions (radical scavengers).

(g) Volumetric Flow Rate

Introduction and Objectives:

The effect of volumetric flow rate was examined by comparing results for 2 different rates (viz.: the standard reference rate of 1.5 L/minute and 2 L/minute). The corresponding surface flow rates are presented in table 4.22. Catalyst suspension loading was fixed at 5 g/L TiO_2 and the experiments were conducted in lake water. The remainder of the system parameters were evaluated at standard reference levels. The objectives of this study were to (1) assess the falling film effect at high flow rates and (2) determine whether the application of high flow rates is beneficial for oxidation when applying a recirculation mode of operation.

Results and Discussion:

Table 4.29: Microcystin concentration as a function of irradiation time, variant and catalyst suspension loading

Irradiation Time (min)	Microcystins (ug/L)								
	YA			YR			LR		
	Catalyst Suspension Loading (g/L)			Catalyst Suspension Loading (g/L)			Catalyst Suspension Loading (g/L)		
	0.2	2	5	0.2	2	5	0.2	2	5
0	21	14	18	64	44	66	35	22	37
2	17	15	16	58	49	54	30	22	30
4	15	ND	13	50	26	45	31	13	30
6	12	10	12	41	31	39	26	15	17
8	11	ND	10	38	36	33	25	27	17
10	11		ND	41	27	29	32	29	15
12	ND*			32	30	26	22	24	12
14				35	24	21	22	21	12
16				34	23	21	25	19	13
18				31	22	18	22	14	11
20				34	18	15	26	19	ND
10^2 k_{obs} (min^{-1})	6.80	6.01	7.32	4.68	4.33	7.83	1.74	NC**	6.82
Half-life (min)	10.2	11.5	9.5	14.8	16.0	8.9	39.8	-	10.2
R^2	0.93	0.89	0.99	0.88	0.97	0.99	0.51	-	0.88

Note: **ND* = Not detected (Limit of Detection = 10 ug/L)**
NC = Not calculated**

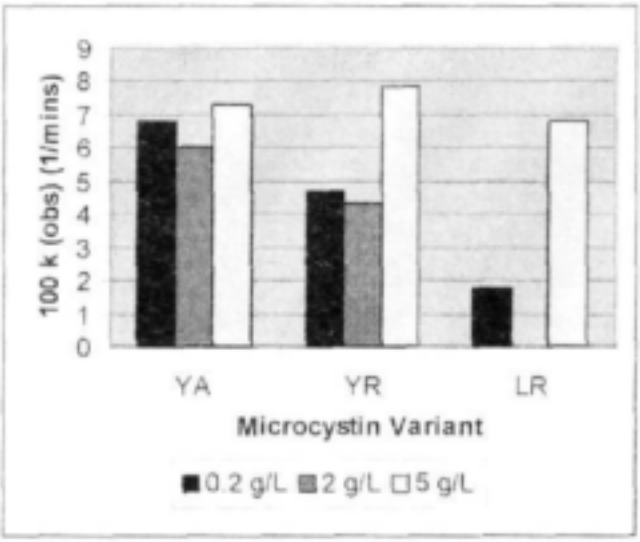

Figure 4.32: First order rate constants as a function microcystin variant and catalyst suspension loading

The results obtained from these experiments (Table 4.29 and Figure 4.32) indicated that :

- an increase in catalyst suspension loading from 0.2 to 5 g/L does not significantly promote the oxidation of microcystins YA and YR;
- an increase in catalyst loading from 0.2 to 5 g/L enhances the oxidation of microcystin LR considerably;
- photocatalytic oxidation performed at elevated catalyst loading is advised when treating recalcitrant organic compounds in the presence of inorganic ions (radical scavengers).

(g) Volumetric Flow Rate

Introduction and Objectives:

The effect of volumetric flow rate was examined by comparing results for 2 different rates (viz.: the standard reference rate of 1.5 L/minute and 2 L/minute). The corresponding surface flow rates are presented in table 4.22. Catalyst suspension loading was fixed at 5 g/L TiO_2 and the experiments were conducted in lake water. The remainder of the system parameters were evaluated at standard reference levels. The objectives of this study were to (1) assess the falling film effect at high flow rates and (2) determine whether the application of high flow rates is beneficial for oxidation when applying a recirculation mode of operation.

Table 4.30: Concentration of microcystins as a function of irradiation time, variant and volumetric flow rate

Irradiation Time (min)	Microcystins (ug/L)					
	YA		YR		LR	
	Flow Rate 1.5 L/min	Flow Rate 2 L/min	Flow Rate 1.5 L/min	Flow Rate 2 L/min	Flow Rate 1.5 L/min	Flow Rate 2 L/min
0	18	18	66	69	37	30
2	16	18	54	60	30	25
4	13	17	45	56	30	22
6	12	14	39	50	17	21
8	10	11	33	47	17	21
10	ND*	11	29	45	15	20
12		ND	26	36	12	19
14			21	30	12	13
16			21	31	13	14
18			18	27	11	13
20			15	26	ND	15
10^2 k_{obs} (min^{-1})	7.32	5.91	7.83	5.42	6.82	3.86
Half-life (min)	9.5	11.7	8.9	12.8	10.2	18.0
R^2	0.99	0.90	0.99	0.96	0.88	0.86

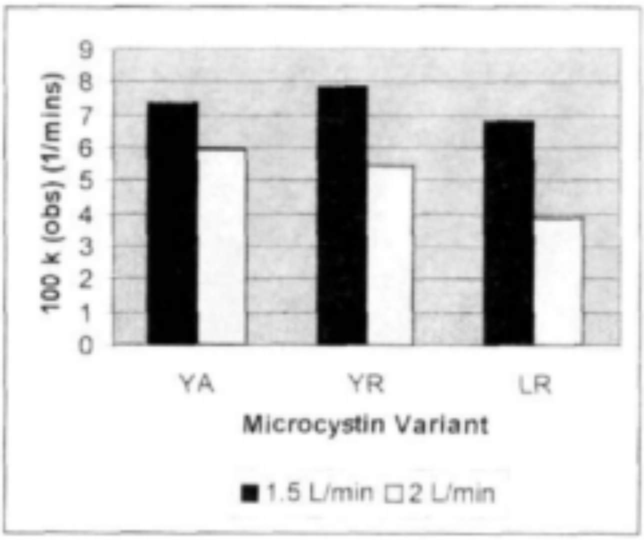

Figure 4.33: First order rate constant for the oxidation of microcystins as a function of variant and volumetric flow rate

The results obtained from these experiments (Table 4.30 and Figure 4.33) indicated that :

- the rate of oxidation of microcystins YA and YR is marginally reduced when applying the higher volumetric flow rate.
- the rate of oxidation of microcystin LR is reduced by approximately 50% when applying the higher volumetric flow rate;
- the falling film effect is detrimental to oxidation at high flow rates, particularly in the case of recalcitrant organic compounds;
- a higher rate of recirculation is not necessarily efficient enough to compensate for the inhibiting effect of a denser falling film.

(h) Reproducibility Study

Introduction and Objectives:

The statistical reproducibility of photocatalytic oxidation rates was examined for a fixed set of experimental conditions. Experiments were conducted in triplicate using a catalyst suspension loading of 5 g/L TiO_2 and a volumetric flow rate of 2 L/minute. Lake water (spiked with microcystin algal extract) was used. The remainder of the system parameters were evaluated at their standard reference levels (table 4.22). The objective of this study was to evaluate the reproducibility of the observed rate constants in terms of (1) standard deviation (SD) (2) relative standard deviation (RSD) and (3) microcystin variant.

Results and Discussion:

Table 4.31: Concentration of microcystins as a function of irradiation time, variant and replicate number

Irradiation Time (min)	Microcystins (ug/L)								
	YA			YR			LR		
	Replicate Run Number			Replicate Run Number			Replicate Run Number		
	1	2	3	1	2	3	1	2	3
0	18	18	22	69	71	76	30	31	32
2	18	16	16	60	61	62	25	23	26
4	17	14	15	56	50	55	22	22	24
6	14	15	15	50	55	56	21	26	23
8	11	13	14	47	46	48	21	20	19
10	11	10	10	45	41	41	20	19	17
12	ND*	ND	10	36	38	41	19	18	19
14			ND	30	35	36	13	16	16
16				31	32	35	14	17	15
18				27	27	31	13	14	14
20				26	24	28	15	15	16
10^2 k_{obs} (min^{-1})	5.91	4.99	6.03	5.42	4.82	4.96	3.86	3.39	3.67
Half-life (min)	11.7	13.9	11.5	12.8	14.4	14.0	18.0	20.4	18.9
R^2	0.90	0.85	0.89	0.96	0.95	0.96	0.86	0.87	0.88

Note: ND* = Not detected (Limit of Detection = 10 ug/L)

Table 4.32: Statistical analysis of response reproducibility for data in Table 4.31

Microcystin Variant	Measured Response	Mean	Standard Deviation	Relative Standard Deviation (%)
YA	10^2 k (obs)*	5.6	0.6*	10.7
YA	Half-life**	12.4	1.3**	10.5
YR	10^2 k (obs)	5.1	0.3	5.9
YR	Half-life	13.7	0.8	5.8
LR	10^2 k (obs)	3.6	0.2	5.6
LR	Half-life	19.1	1.2	6.3

*** in min^{-1} ; ** in min**

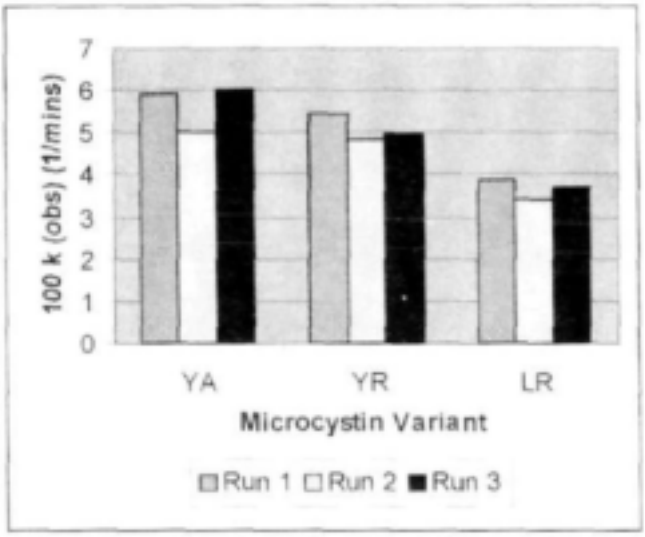

Figure 4.34: Reproducibility of observed first order rate constants for oxidation of microcystins as a function of variant

The results obtained from these experiments (Tables 4.31-4.32 and Figure 4.34) indicated that:

- the mean observed first order rate constants for oxidation of microcystins YA and YR are largely similar;
- the rate constants for LR are slightly smaller compared to YA and YR. This result demonstrates the more resistant nature of LR towards photocatalytic oxidative treatment ;
- the relative standard deviation (RSD) of results is equal to or below 10% for all 3 variants, which is considered acceptable taking into account possible error variations in sample preparation, reactor efficiency and analytical methodology ;
- RSD is slightly worse for the oxidation of microcystin YA. This result is explained in terms of (1) an earlier observation related to the mass transfer adsorption of YA at higher catalyst suspension loadings and (2) practical problems related to the HPLC analysis of this variant.

Based on the results obtained above, it was considered to investigate the effect of slurry pH and solution pH on the photocatalytic oxidation rate of microcystins. These studies were executed for Reactor 2A where immobilised TiO_2 configurations applied (see Section 5.2).

4.2.2 Single Pass Modes

The application of Reactor 1 for studying the photocatalytic oxidation of microcystin toxins was limited to the recirculation mode of operation.

CHAPTER 5 : EVALUATION OF REACTOR 2A

5.1 TREATMENT of *para*-CHLOROPHENOL

5.1.1 Recirculation Mode

(a) System Parameters

The photocatalytic oxidation of p-CP in water was investigated by operating Reactor 2A as (1) immobilised-bed (IMM) and (2) combined slurry-immobilised bed (SLIMM) reactors. One-factor variation (for random parametric studies) and two-level experimental designs (for screening studies) were employed as before. The following system parameters were evaluated at discrete levels in terms of first order reaction kinetics (see Table 5.1):

Table 5.1: System parameters for p-CP study (Reactor 2A; Recirculation Mode)

Parameter	Assigned Levels
Catalyst Loading for Impregnation (g/L)	1; 5*; 10; 20; 30
Volumetric Flow Rate (L/min)	1^a; 2^{*b}
Horizontal Irradiation Distance (cm)	5; 15*
p-CP Initial Concentration (mg/L)	13; 40*
Reaction Volume (L)	3*; 6
Water Matrix	Distilled
Initial Solution pH	3; 5; 6.2; 7.5*; 9; 11
Gas Purge	Oxygen
Gas Flow Rate (L/min O_2)	5*; 20
UV lamps^c	Blacklight (UV-A); Germicidal (UV-C)*

Note: * Denotes standard reference level of parameters
a Surface flow rate = 70 L/hr/m^2
b Surface flow rate = 135 L/hr/m^2
c UV irradiance = 204.5 W/m^2 = 12 x 15W lamps (per 0.88 m^2)

(b) Fibre Glass Examination

Introduction and Objectives:

Two types of locally available fibre glass sheet materials were examined for maximum impregnation of TiO_2 photocatalyst and their photochemical stability. Mechanical strength and fineness of the individual fibres were of primary concern in the selection of the sheets. The first sheet type (obtained from Foyntech Africa cc, Stellenbosch) was reinforced with a grid-like mesh on the surface. The second sheet type (obtained from Freudenberg Nonwovens Pty. Ltd., Parow Industria) was a glass tissue and resembled the Foyntech product without a reinforced mesh.

A dynamic contact angle analyser (DCAA) was used to conduct a preliminary study of the TiO_2 impregnation properties of the two types of fibre glass materials (Engelbrecht *et al.*, 1998). The procedure entailed dipping square samples of each (impregnation area: 5.6 cm^2) in 30 mL of TiO_2 suspension for a fixed period of time. The objectives of this study were to ascertain conditions for maximum catalyst impregnation as a function of (1) catalyst suspension loading (2) fibre glass type (3) impregnation time and (4) pH treatment of sheets. Standard one-factor variation and 2^3 factorial experiments were used for this purpose. These parameters will ultimately influence the optimised performance of the immobilised-bed reactor in terms of its photocatalytic destruction efficiency.

Results and Discussion :

Table 5.2: Catalyst impregnation loading as a function of catalyst suspension loading and type

Catalyst suspension loading (g/L)	Catalyst impregnation loading*** (in mg/cm^2)	
	Type 1 (reinforced)	Type 2 (non-reinforced)
0	0*	0**
1	0.6	0.5
5	0.8	0.7
10	0.9	0.8
20	1.1	1.0
30	1.2	1.2
50	1.3	1.2
75	1.4	1.3
100	1.5	1.3

*** Water adsorption (at 0 g/L TiO_2) = 13.2 mg/cm^2**

**** Water adsorption (at 0 g/L TiO_2) = 11.2 mg/cm^2**

***** Results corrected in terms of net uptake of water**

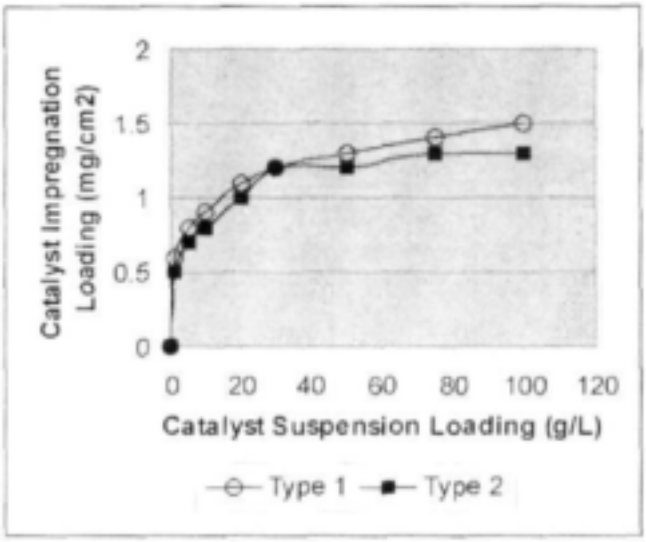

Figure 5.1: Catalyst impregnation loading as a function of catalyst suspension loading and type

The results obtained from these experiments (Table 5.2 and Figure 5.1) indicated that :

- the catalyst impregnation loading (CIL, in mg/cm^2) increases steadily with increasing catalyst suspension loading (CSL, in g/L) and reaches a plateau value of approximately 1.5 mg/cm^2 beyond 40 g/L TiO_2 used. This impregnation loading corresponds to a theoretical sheet module loading of 15 g/m^2 ;
- the two types of fibre glass materials display similar wetting properties with respect to TiO_2 suspension coating and wetting with clear water. Perfect wetting is observed for all analyses (advancing and receding contact angles are 0° throughout);
- CIL is not significantly affected by increasing the time of impregnation (Engelbrecht *et al.*, 1998) ;
- treating the sheets with acidic media (pH4) marginally improves catalyst impregnation of TiO_2 (Engelbrecht *et al.*, 1998) ;
- treating the sheets with alkaline media (pH 9.5) results in a significant decrease of CIL. This is ascribed to the adverse effects of electrostatic repulsion between fibre glass surface hydroxyl ions and TiO^- species at high pH ;
- the mechanical stability of the reinforced fibre glass (Type 1) is significantly greater under wetting conditions, compared to Type 2. This observation is ascribed to the presence of the grid-like mesh.

Based on the results obtained above, it was anticipated that most of Reactor 2A's studies would probably have to be conducted with fibre glass sheet materials that are (1) mechanically very stable under wetting conditions or (2) reinforced by some structural means. As a result, the TiO_2 suspension coating and impregnation properties of the *reinforced fibre glass sheet module* (Type 1) was investigated in an effort to assess its utility as stationary support in Reactor 2A.

(c) TiO_2 Impregnation of Sheet Modules

Introduction and Objectives:

Suspension coating of the reinforced fibre glass sheet module (coating surface area: 0.88 m^2) was performed in triplicate. The coating procedure entailed dark recirculation of suspensions of TiO_2 (in 3 L of *distilled* water) through the system (across the sheet module) using (1) a 2 L/min volumetric flow rate (2) natural suspension pH (4-5) and (3) magnetic stirring for a period of 30 minutes. Sheet modules were weighed before and after coating. Coated sheets were air-dried at room temperature for 24 hr prior to determining the increase in weight. The objective of this study was to assess the reproducibility of catalyst impregnation loading as a function of suspension loading when using this particular procedure for sheet coating.

Results and Discussion:

Table 5.3: Statistical analysis for suspension coating of fibre glass sheet module (Type 1)

Catalyst Suspension Loading (g/L)	Catalyst Impregnation Loading (g/sheet*)					
	Coating Replicate 1	Coating Replicate 2	Coating Replicate 3	Mean	Standard Deviation	RSD** (%)
1	1.8	1.0	1.4	1.4	0.40	28.6
5	7.4	8.1	6.5	7.3	0.80	10.9
10	13.9	14.1	15.9	14.6	1.10	7.5
20	23.4	21.6	19.5	21.5	1.95	9.1
30	25.3	24.8	27.3	25.8	1.32	5.1

Note: * Total impregnation area on sheet = 0.88 m^2
RSD = Relative standard deviation**

Table 5.4: Catalyst impregnation loading (*in g TiO_2 / m^2*) as a function of catalyst suspension loading

Catalyst Suspension Loading (g/L TiO_2)	Mean Catalyst Impregnation Loading (g TiO_2 /m^2)
1	1.6 ± 0.4
5	8.3 ± 0.8
10	16.6 ± 1.1
20	24.4 ± 2.0
30	29.3 ± 1.3

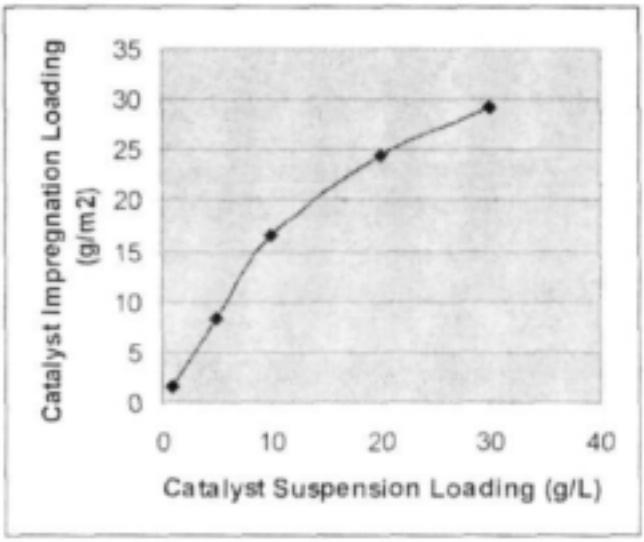

Figure 5.2: Catalyst impregnation loading (in g TiO_2 /m^2) as a function of catalyst suspension loading

The results obtained from these experiments (Tables 5.3-4 and Figure 5.2) indicated that :

- the average dry weight of the non-coated sheet modules is 28.9 ± 0.9 g (RSD = 3.2%);
- increasing the loading of catalyst used for suspension coating steadily increases the mass of TiO_2 impregnated onto the sheet module, albeit striving towards a saturation value (viz.: maximum impregnation capacity);
- the mass transfer (%) of catalyst from the aqueous coating suspension to the sheet module decreases with an increase in catalyst suspension loading. This result is anticipated in view of the maximum impregnation capacity of the module;
- the reproducibility of the coating procedure improves with elevation in catalyst suspension loading. Acceptable RSD (*ca* 10 % or less) is attained when using loadings equal to or greater than 5 g/L ;
- the sheet module maintains mechanical stability, even at high catalyst suspension loadings;
- catalyst suspension loadings in excess of 30 g/L TiO_2 are unsuited for suspension coating. Problems are encountered with maintaining TiO_2 in suspension, hence the recirculation thereof through the reactor is problematical ;
- suspension coating cannot be scaled-up linearly as a function of catalyst suspension loading and impregnation area (compare results from Tables 5.2-4);

Based on the results obtained above, it was decided to adopt a *standard suspension coating procedure* for further work. This procedure entailed the use of (1) a catalyst suspension loading of 5 g/L TiO_2 in 3 L of distilled water and (2) identical system parameters as specified in the introductory paragraph of this study. The equivalent catalyst impregnation loading amounts to 8.3 g/m^2 (viz.: 0.83 mg/cm^2) which is in the optimum range reported for immobilised-bed photocatalytic reactors (Herrmann, 1995).

Droplet spraying was also assessed as potential coating procedure. This study, however, was limited to the TiO_2 impregnation of a fibrous activated carbon (FAC) sheet module, as explained in the next chapter (see Reactor 2B in Chapter 6).

(d) Sheet Modifications

Introduction and Objectives:

Two compounded sheet modules were prepared in-house from the two types of fibre glass materials purchased originally. The first compounded module comprised the reinforced fibre glass sheet (Type 1) modified with a number of additional rectangular strips of the same material which were attached at intermittent positions (10 cm apart) as depicted below (Figure 5.3). The second compounded module comprised the non-reinforced sheet (Type 2) altered similarly using the reinforced material as intermittent strips.

The compounded modules were prepared in an effort to (1) enhance the coating ability of the existing sheet modules (2) create a turbulence (stirring) effect during the falling film irradiation procedure and (3) increase the water residence time on the sheet module, thereby prolonging contact with UV irradiation.

The main objective of this study was to compare the utility of the 4 sheet modules (viz.: the two original and two compounded modules) in terms of the photocatalytic oxidation of p-CP in water by using (1) immobilised-bed (IMM) and (2) combined slurry-immobilised (SLIMM) reactor configurations. System parameters were evaluated at standard reference levels (Table 5.1) and an irradiation period of 30 minutes was selected. The standard suspension coating procedure was applied to all sheet modules (viz.: using a catalyst suspension loading of 5 g/L TiO_2).

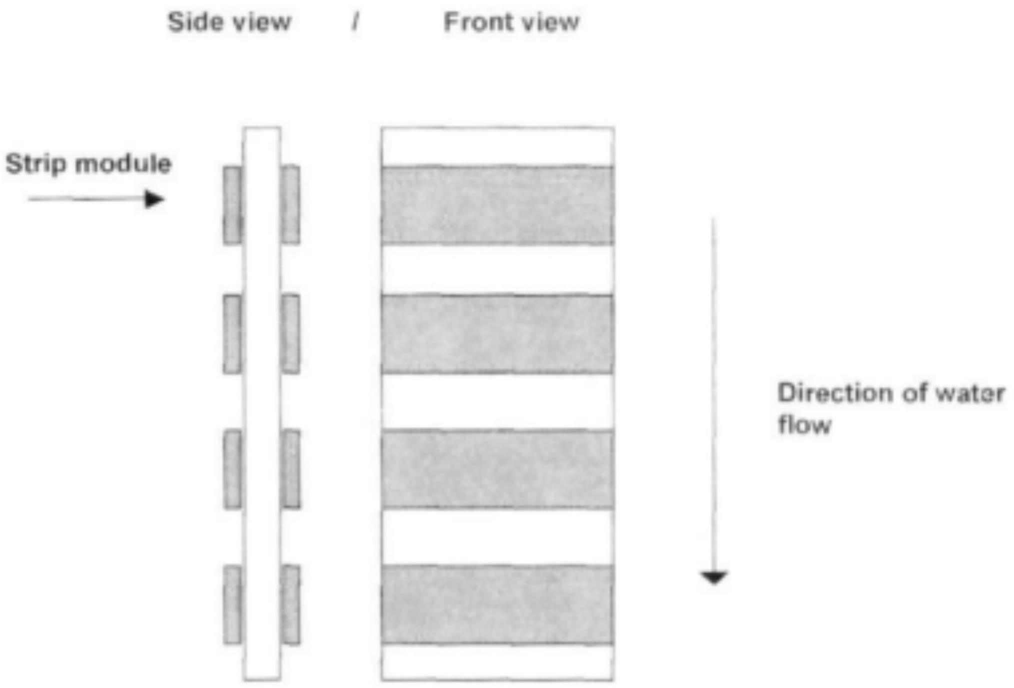

Figure 5.3: Schematic of the designed compounded sheet module

Table 5.5: p-CP concentration as a function of irradiation time and sheet module used (IMM reactor)

Irradiation Time (min)	Fibre Glass 1 (reinforced sheet)		Compound 1 (reinforced + reinforced strips)		Fibre Glass 2 (non-reinforced tissue sheet)		Compound 2 (non-reinforced + reinforced strips)	
	IMM** Reactor	SLIMM*** Reactor	IMM Reactor	SLIMM Reactor	IMM Reactor	SLIMM Reactor	IMM Reactor	SLIMM Reactor
0	40.0	40.0	40.0	40.0	40.0	40.0	40.0	40.0
5	26.2	25.3	25.0	24.8	32.5	30.2	27.4	26.1
10	17.1	16.9	17.9	15.5	25.4	22.5	21.2	19.2
15	11.5	11.0	13.2	10.3	21.6	18.3	16.0	13.5
20	8.9	6.9	8.9	6.7	17.9	14.4	12.9	10.0
25	6.8	3.2	6.2	3.1	13.1	9.7	10.3	7.8
30	ND*	ND	ND	ND	9.7	5.1	7.5	4.0
$10^2\ k_{obs}$ (min^{-1})	7.14	9.69	7.27	9.78	4.58	6.35	5.34	7.13
Half-life (min)	9.7	7.2	9.5	7.1	15.1	10.9	13.0	9.7
R^2	0.99	0.99	0.99	0.99	0.99	0.96	0.99	0.98

ND* = Not Detected; Limit of Detection = 1 mg/L
IMM** = Immobilised-Bed Reactor (no suspended TiO_2 after coating)
SLIMM*** = Combined Slurry-Immobilised Reactor (suspension loading of 1 g/L TiO_2 after coating)

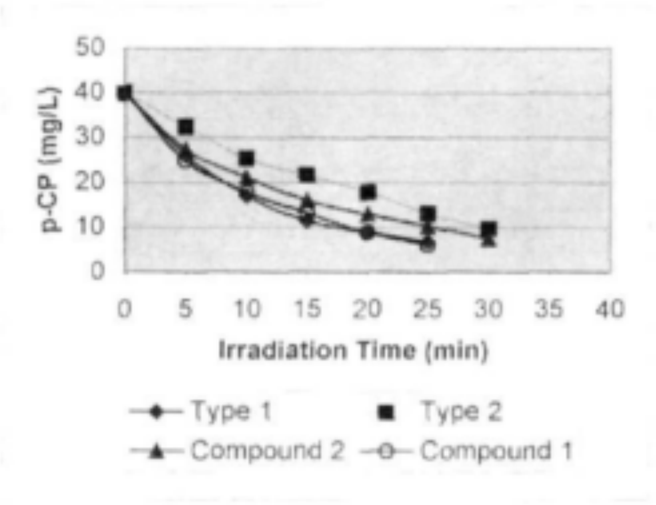

Figure 5.4: p-CP concentration as a function of irradiation time and sheet module used (IMM reactor)

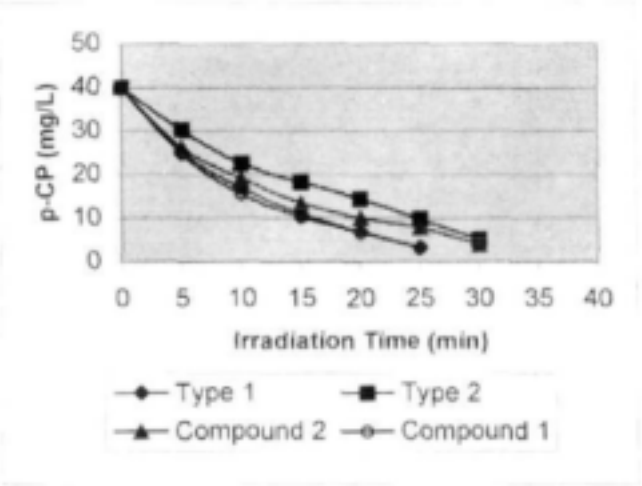

Figure 5.5: p-CP concentration as a function of irradiation time and sheet module used (SLIMM reactor)

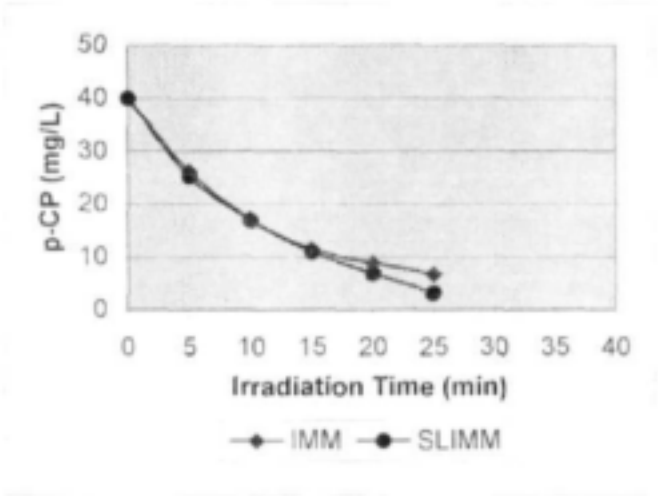

Figure 5.6: p-CP concentration as a function of irradiation time and reactor configuration (IMM and SLIMM reactor results when using *Fibre Glass Type 1* as sheet module)

The results obtained from these experiments (Table 5.5 and Figures 5.4-6) indicated that :

- first order exponential decay kinetics apply for the photocatalytic oxidation of p-CP in Reactor 2A ;
- the first order rate constants are higher for the modules which incorporate reinforced mesh (viz.: fibre glass Type 1 and Compound 1). This result is independent of reactor configuration and can be attributed to the positive auxiliary effect created by turbulence and additional mixing as a function of the surface roughness;
- the first order rate constant (for each sheet module used) increases marginally when switching from Immobilised-Bed (IMM) to Slurry-Immobilised (SLIMM) configuration. The result implies that additional suspended catalyst (viz.: 1 g/L TiO_2 in this study) do not significantly enhance p-CP oxidation in the presence of immobilised catalyst;

- the UV residence time of the falling film (*ca* 4.1 sec) is not increased through modification of the original sheets, hence vertical elongation of the existing modules (1.1 m) presents the only alternative for increasing this critical design parameter.

Based on the results obtained above, it was decided to discard sheet modification and to conduct all further experimentation of Reactor 2A with the original fibre glass material (Type 1) as stationary support for TiO_2.

(e) Screening Study (Immobilised-Bed Reactor)

Introduction and Objectives:

Seven parameters were identified for an initial screening study of Reactor 2A operated as an Immobilised-Bed (IMM) reactor (see Tables 5.1 and 6). The objectives were to (1) obtain a rough estimate of the effects of the various parameters on the response functions (2) eliminate insignificant parameters in accordance with the Pareto Principle (3) identify important parameters for optimisation purposes and (4) evaluate the application of a highly fractionated (1/16th) two-level factorial design in a screening study.

Results and Discussion:

Table 5.6: Design matrix for IMM screening study (orthogonal array).

Run	CSL[a] (g/L)	Volumetric Flow Rate (L/min)	Gas Flow Rate[b] (L/min)	$[p\text{-CP}]_o$[c] (mg/L)	UV[d] Source	HID[e] (cm)	Reaction Volume (L)	10^2 k_{obs} (min^{-1})	Half-life (min)	R^2
1	1	1	5	13	1	5	3	1.22	56.8	0.98
2	20	1	20	13	2	5	6	2.76	25.1	0.99
3	1	2	20	13	1	15	6	0.86	80.6	0.98
4*	20	2	5	13	2	15	3	4.22	16.4	0.99
5	1	1	5	40	2	15	6	1.35	51.3	0.98
6	20	1	20	40	1	15	3	1.18	58.7	0.99
7	1	2	20	40	2	5	3	2.51	27.6	0.98
8	20	2	5	40	1	5	6	0.50	138.6	0.97

a CSL = Catalyst suspension loading *used for impregnation* (see Table 5.4 for conversion factors)
b Oxygen gas purge only
c $[p\text{-CP}]_o$ = Initial concentration of p-CP
d UV source : 1 = Fluorescent Blacklight (UV-A); 2 = Germicidal (UV-C)
e HID = Horizontal irradiation distance
*** Best result in terms of reaction rate constant (run 4)**

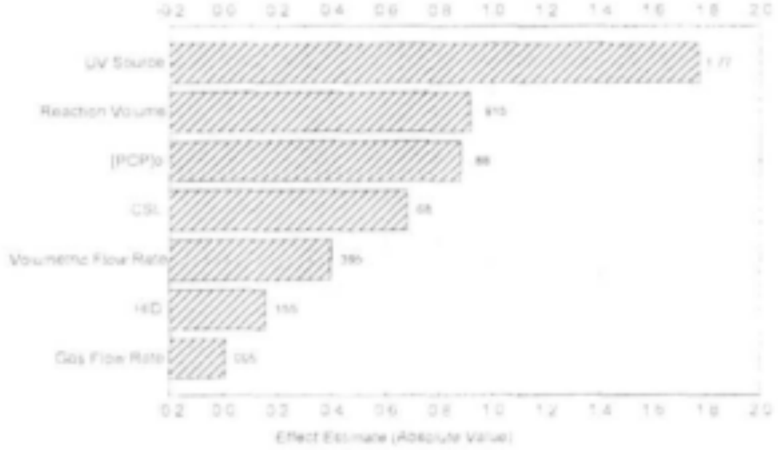

Figure 5.7: Pareto chart illustrating parameter effects with respect to first order rate constant (k_{obs}) as response function. (CSL = Catalyst Suspension Loading *used for impregnation of sheet*; [p-CP]o = p-CP Initial Concentration *in mg/L*; HID = Horizontal Irradiation Distance in cm)

The results obtained from these experiments (Table 5.6 and Figure 5.7) indicated that :

- first order exponential decay kinetics apply for the photocatalytic oxidation of p-CP;
- operating the IMM reactor with germicidal UV-C lamps has a highly beneficial effect on the oxidation rate of p-CP. This observation is attributed to the shorter wavelength (and thus higher energy) of UV-C radiation (254 nm) compared to fluorescent UV-A radiation (*ca* 315-400 nm). Theoretical power input in terms of radiant flux is identical for both types of lamps used (viz.: 15 W per lamp);
- an increase in reaction volume inhibits the oxidation rate. This result confirms the limitation of the Reactor 2A in terms of volume of water treated in recirculation mode;
- p-CP initial concentration has an intermediate negative effect on the oxidation rate. This observation confirms the utility of Reactor 2A for the treatment of low concentrations of pollutant ;
- the oxidation rate is marginally influenced by the amount of TiO_2 immobilised on the reactor sheet module. This result proves the utility of the reactor for economical operation using small amounts of catalyst ;
- the effects of volumetric flow rate, horizontal irradiation distance and oxygen flow rate are negligible within the framework of the selected experimental design ;
- parameter main effects are calculated successfully when using highly fractionated factorial designs in tandem with linear mathematical models. This observation indicates the utility of the selected design in terms of multi-parameter screening. ANOVA significance probabilities, however, are not calculated due to an insufficient number of degrees of freedom;
- parameter effects are confounded with each other when applying quadratic (polynomial) modelling. The calculation of parameter interactions is therefore precluded.

Based on the results obtained above, it became evident that the Pareto Principle applied, viz.: (1) one or two parameters exerted predominant effects on the response and (2) several parameters are insignificant and could therefore be kept constant at convenient experimental levels. It remained to be seen what the absolute effect of catalyst impregnation loading is when applying a standard set of conditions to the operation of Reactor 2A as an immobilised-bed (IMM) reactor.

(f) Catalyst Impregnation Loading (Immobilised-Bed Reactor)

Introduction and Objectives:

The effect of catalyst impregnation loading was examined by comparing results for 5 different suspension loadings of TiO_2 (1; 5; 10; 20 and 30). The corresponding impregnation loadings amounted to 1.0, 8.1, 14.1, 21.6 and 24.8 g TiO_2 per sheet module (0.88 m^2). The remainder of the system parameters were evaluated at standard reference levels (Table 5.1). The objectives of this study were to (1) assess the effect of catalyst impregnation loading on the rate of oxidation of 40 mg/L p-CP in the recirculation mode and (2) to determine an optimum or plateau value for this parameter in terms of first order rate constants.

Results and Discussion:

Table 5.7: First order rate constant for p-CP oxidation as a function of catalyst impregnation loading

Catalyst Suspension Loading (g/L TiO_2) *(used for sheet coating)*	Catalyst Impregnation Loading (g TiO_2 per sheet*)	Catalyst Impregnation Loading (g TiO_2 per m^2)	Observed first order rate constant (k_{obs} in min^{-1})
1	1.0	1.1	2.55
5	8.1	9.2	7.14
10	14.1	16.0	5.75
20	21.6	24.5	3.90
30	24.8	28.2	3.80

*** Sheet coating area = 0.88 m^2**

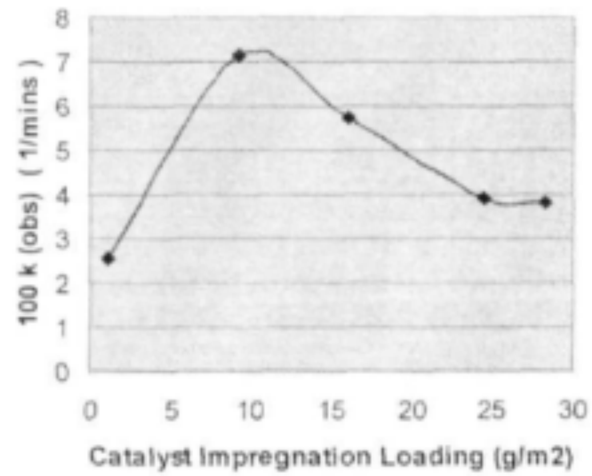

Figure 5.8: First order rate constant for p-CP oxidation as a function of catalyst impregnation loading

The results obtained from these experiments (Table 5.7 and Figure 5.8) indicated that :

- an optimum catalyst impregnation loading exists for the oxidation of 40 mg/L of p-CP using Reactor 2A in recirculation mode. This observation is in contrast to literature examples which state that an asymptotic dependence of rate on catalyst mass exists for immobilised photocatalytic reactors (Herrmann, 1995). This result can probably be ascribed to the novel configuration of Reactor 2A. It is however an acceptable price to pay in order to circumvent the filtration problem associated with slurry phase reactors ;
- the optimum loading of 9.2 g/m^2 is obtained by applying a suspension loading of 5 g/L TiO_2 according to the specified standard suspension coating procedure. This value (equivalent to 0.92 mg/cm^2) is in good agreement with Herrmann's optimum value of 1.3 mg/cm^2 ;
- higher catalyst impregnation loadings are detrimental to the efficiency of the immobilised-bed reactor. This effect could possibly be ascribed to a change in mass transfer characteristics of the system as a function of the amount of immobilised catalyst ;
- the catalytic activity of TiO_2 is suppressed when operating Reactor 2A as an immobilised reactor in recirculation mode

Based on the results obtained above, it was evident that the surface-catalysed nature of photocatalytic oxidation processes should be addressed through comprehensive kinetic studies. Moreover, the contributing effect of mass transfer is dependent on several parameters such as (1) the initial concentration of p-CP (2) the amount of immobilised catalyst (3) by-product interferences and (4) pH variations.

(g) pH Effects (Immobilised-Bed Reactor)

Introduction and Objectives:

The effect of pH was examined by operating Reactor 2A as an immobilised-bed reactor in recirculation mode and comparing results for 5 different initial pH conditions against the standard (neutral) pH of 7.5 for distilled water spiked with p-CP. 1M NaOH and 1M HCl (and dilutions thereof) were used as additives to adjust the initial pH. The catalyst suspension loading used for coating was 20 g/L TiO_2 (equivalent impregnation loading of approximately 24.4 g/m^2). The remainder of the system parameters were evaluated at their standard reference levels (Table 5.1). These levels (in combination with an initial p-CP concentration of 13 mg/L) were selected to ensure the *highest* oxidation rate possible. An equivalent dark adsorption experiment was conducted in tandem with each oxidation reactions by employing identical parametric conditions.

The objectives of this study were to (1) assess the oxidation efficiency of the immobilised reactor as a function of initial pH and (2) determine variations in p-CP mass transfer at high impregnation loading, low initial concentration (13 mg/L) and in the absence of UV irradiation.

Results and Discussion:

Table 5.8: First order rate constant for oxidation (k_{obs}) and mass transfer (%) of p-CP as a function of initial pH

Initial solution pH	10^{2} k_{obs} (min^{-1})	Dark adsorption (%)**
3.0	2.82	10.1
5.0	4.15	10.6
6.2*	4.18	10.2
7.5 (neutral)	4.22	9.5
9.0	3.99	5.2
11.0	2.49	3.1

***pH 6.2 is the point of zero charge (PZC) for TiO_2**
**** Dark adsorption = mass transfer**

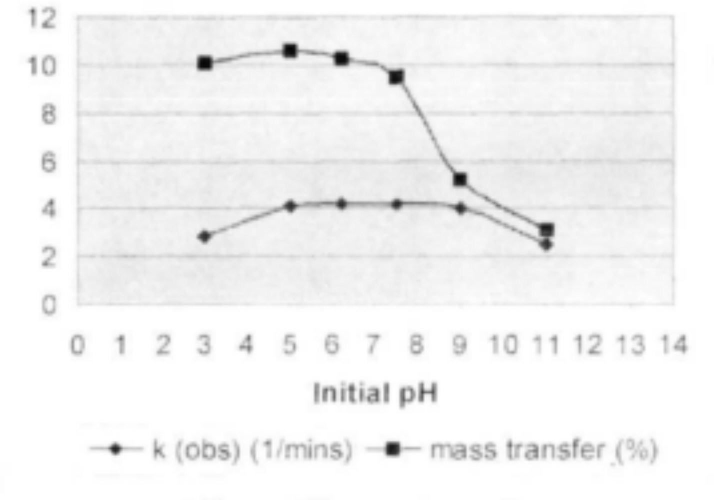

Figure 5.9: First order rate constant for oxidation (k_{obs}) and mass transfer (%) of p-CP as a function of initial pH

The results obtained from these experiments (Table 5.8 and Figure 5.9) indicated that :

- the observed first order rate constant is largely independent of initial solution pH in the range pH 5 to 9. This result is ascribed to favourable adsorption kinetics attained for p-CP and TiO_2 in this region ;
- the degree of p-CP mass transfer to immobilised TiO_2 is generally in the order 10% (w/w) ;
- the rate of p-CP oxidation is markedly suppressed at an initial pH of 3. The additive in this instance (HCl) is probably responsible for providing an excess chloride ions in solution which could (1) block active sites on the surface of the TiO_2 particles, thus hampering surface adsorption of p-CP and its surface catalysed oxidation and (2) act as hydroxyl radical scavengers, producing chlorine radicals (a less efficient oxidant);
- the rate of p-CP oxidation is markedly suppressed at an initial pH of 11. This result is ascribed to reduced mass transfer of p-CP caused by weak electrostatic interaction

- between dissociated p-CP (present as fenolate anions) and TiO_2 (present as TiO^- anions) ($pK_a = 9.4$ for p-CP) ;
- p-CP mass transfer in the order of 10% (w/w) is a good measure for efficient photocatalytic oxidation in immobilised reactors.

Based on the results obtained above, it is clear that the phenomenon of mass transfer is a very complex one with regard to the efficiency and rate kinetics of surface catalysed photocatalytic reactions. These aspects require more detailed investigation.

(h) Screening Study (Combined Slurry-Immobilised Reactor)

Introduction and Objectives:

Eight parameters were identified for an initial screening study of Reactor 2A operated as a combined Slurry-Immobilised (SLIMM) reactor (see Tables 5.1 and 9). The objectives were to (1) obtain a rough estimate of the effects of the various parameters on the response functions (2) eliminate insignificant parameters in accordance with the Pareto Principle (3) identify important parameters for optimisation purposes and (4) evaluate the application of a highly fractionated (1/16th) two-level factorial design in a screening study.

Results and Discussion:

Table 5.9: Design matrix for SLIMM screening study (orthogonal array)

Run	CIL[a] (g/L)	CSL[b] (g/L)	VFR[c] (L/min)	Gas[d] Flow Rate (L/min)	$[p\text{-}CP]_o$[e] (mg/L)	UV[f] Source	HID[g] (cm)	Reaction Volume (L)	$10^2\ k_{obs}$ (min^{-1})	Half-life (min)	R^2
1	1	1	1	5	13	1	5	3	2.14	32.4	0.98
2	1	20	1	20	13	2	5	6	3.58	19.4	0.99
3	1	1	2	20	13	1	15	6	2.38	29.1	0.97
4	1	20	2	5	13	2	15	3	7.24	9.60	0.98
5	1	1	1	5	40	2	15	6	1.88	36.9	0.99
6	1	20	1	20	40	1	15	3	1.42	48.8	0.99
7	1	1	2	20	40	2	5	3	6.84	10.1	0.97
8	1	20	2	5	40	1	5	6	1.87	37.1	0.98
9	20	20	2	20	40	2	15	6	3.91	17.7	0.99
10	20	1	2	5	40	1	15	3	2.08	33.3	0.98
11*	20	20	1	5	40	2	5	3	7.90	8.80	0.96
12	20	1	1	20	40	1	5	6	0.94	73.7	0.92
13	20	20	2	20	13	1	5	3	3.87	17.9	0.99
14	20	1	2	5	13	2	5	6	4.57	15.2	0.99
15	20	20	1	5	13	1	15	6	2.08	33.3	0.99
16	20	1	1	20	13	2	15	3	6.93	10.0	0.97

a CIL = Catalyst impregnation loading (expressed as suspension loading used for coating)
b CSL = True Catalyst suspension loading (in addition to immobilised catalyst)
c VFR = Volumetric Flow Rate
d Oxygen gas purge only
e $[p\text{-}CP]_o$ = Initial concentration of p-CP
f UV source : 1 = Fluorescent Blacklight (UV-A); 2 = Germicidal (UV-C)
g HID = Horizontal irradiation distance
*** Best result in terms of reaction rate constant (run 11)**

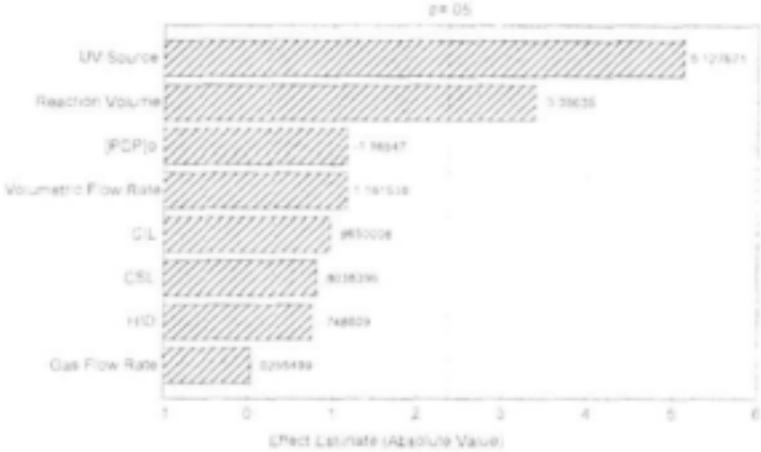

Figure 5.10: Pareto chart illustrating standardised parameter effects with respect to first order rate (k_{obs}) as response function. (CIL = Catalyst Suspension Loading *used for impregnation of sheet*; CSL = True Catalyst Suspension Loading in addition to CIL; [p-CP]o = p-CP Initial Concentration in mg/L; HID = Horizontal Irradiation Distance in cm)

The results obtained from these experiments (Table 5.9 and Figure 5.10) indicated that :

- first order exponential decay kinetics apply for the photocatalytic oxidation of p-CP;
- operating the SLIMM reactor with germicidal UV-C lamps has a highly beneficial effect on the oxidation rate of p-CP. This result was also obtained with the IMM reactor and the same reasoning applies ;
- increase in reaction volume inhibits the oxidation rate significantly. This result confirms the limitation of the Reactor 2A in terms of treating TiO_2 suspensions of polluted water in recirculation mode (SLIMM) ;
- the relative contributions of the remainder of the parameters (viz.: p-CP initial concentration, volumetric flow rate, both catalyst loadings, horizontal irradiation distance and oxygen flow rate) are statistically insignificant with respect to the constraints of the chosen experimental design ; the effects of volumetric flow rate, horizontal irradiation distance and oxygen flow rate are negligible within the framework of the selected experimental design ;
- parameter main effects are calculated successfully when using highly fractionated factorial designs in tandem with linear mathematical models. This observation indicates the utility of the selected design in terms of multi-parameter screening.
- ANOVA significance probabilities are successfully calculated due to a sufficient number of degrees of freedom. The main effects for UV source and reaction volume are statistically significant (with null hypothesis probability less than 5%) ;
- second order parameter interactions are not confounded with other effects and are successfully calculated by applying a quadratic (polynomial) model. The results show a similar trend to linear modelling, however an interesting interaction between volumetric flow rate and catalyst impregnation loading is noted. This result confirms the importance of efficient contact between the falling film layer and the immobilised catalyst ;
- the Pareto Principle applies for the operation of Reactor 2A as a SLIMM reactor.

(i) Endurance Tests

A number of endurance tests were conducted to assess the reproducibility of p-CP oxidation rates through the operation of Reactor 2A as SLIMM or IMM reactors in recirculation mode. The results (De Villiers, 2000) indicated that :

- reproducible results (RSM $\leq$ *ca* 10%) are achieved for the oxidation of 40 mg/L p-CP when using different sheets modules of the same product batch (coated under identical conditions according to the *standard* coating procedure). This result is observed for both reactor configurations (IMM and SLIMM) using a triplicate analysis ;
- a single TiO_2 coated fibre glass sheet maintains catalytic activity (hence statistical reproducibility) for at least 5 consecutive recirculation treatments of 40 mg/L p-CP (at the standard reference levels for the system parameters). This result is also observed for both configurations ;
- catalytic activity is markedly suppressed when reusing the original aqueous solution or slurry matrix (spiked with fresh p-CP) ;
- recirculation of a sample of clean distilled water over the sheet module (between successive oxidation runs) assists the retention of catalytic activity
- *almost no impregnated catalyst is lost from sheet modules during or after the execution* of a falling film experiment.

The results mentioned above, implies that a more detailed study is required to monitor and improve (where necessary) the catalytic activity of TiO_2 immobilised on the fibre glass sheet modules. Catalyst reactivation procedures (such as controlled periodic illumination) and physico-chemical treatment of sheet modules.

5.1.2 Single Pass Modes

(a) System Parameters

The photocatalytic oxidation of p-CP in water was investigated by operating Reactor 2A as (1) immobilised-bed (IMM) and (2) combined slurry-immobilised bed (SLIMM) reactors. One-factor variation (for random parametric studies) and two-level experimental designs (for screening studies) were employed as before. The following system parameters were evaluated at discrete levels in terms of the response functions defined for these operation modes (see Section 3.3 and Table 5.10 below):

Table 5.10: System parameters for p-CP study (Reactor 2A; Single Pass Modes)

Parameter	Assigned Levels
Catalyst Loading for Impregnation (g/L)	1; 5*; 10; 20; 30
Volumetric Flow Rate (L/min)	1[a]; 2*[b]
Horizontal Irradiation Distance (cm)	5; 15*
p-CP Initial Concentration (mg/L)	13; 40*
Reaction Volume (L)	3*; 6
Water Matrix	Distilled
Initial Solution pH	3; 5; 6.2; 7.5*; 9; 11
Gas Purge	Oxygen
Gas Flow Rate (L/min O_2)	5*; 20
UV lamps[c]	Blacklight (UV-A); Germicidal (UV-C)*

Note: * Denotes standard reference level of parameters
a Surface flow rate = 70 L/hr/m^2
b Surface flow rate = 135 L/hr/m^2
c UV irradiance = 204.5 W/m^2 = 12 x 15W lamps (per 0.88 m^2) = 20.45 mW/cm^2

(b) Representative Example

Introduction and Objectives:

The effects of reactor configuration and fibre glass module type were examined by operating Reactor 2A as (1) immobilised-bed (IMM) and (2) combined slurry-immobilised (SLIMM) reactors. System parameters were evaluated at standard reference levels (Table 5.10) and an irradiation period of 30 minutes was selected. The *standard* suspension *coating procedure was applied to all sheet modules (viz.: using a catalyst suspension* loading of 5 g/L TiO_2).

The objectives of this study were to (1) compare the utility of the 2 original sheet modules (viz.: the reinforced and tissue-like fibre glass modules) for the photocatalytic oxidation of p-CP in single pass modes (2) assess the auxiliary effect of additional suspended TiO_2 when switching from IMM to SLIMM reactor configuration and (3) investigate the utility of 2^2 factorial designs for determining main effects and interactions with respect to the defined response functions.

Results and Discussion:

Table 5.11: **p-CP concentration as a function of sheet module, reactor configuration and single pass number (N) - where each N equals 4.1 seconds of UV irradiation**

	Fibre Glass Type 1 (reinforced sheet)		Fibre Glass Type 2 (non-reinforced tissue sheet)	
Single Pass Number (N)	IMM Reactor	SLIMM*** Reactor	IMM Reactor	SLIMM Reactor
0	40.0	40.0	40.0	40.0
1	32.1	31.5	32.5	32.1
2	25.9	24.5	27.5	26.3
3	20.2	18.9	22.2	20.8
4	15.2	13.4	19.1	16.6
5	11.9	10.1	16.2	12.9
6	8.9	6.9	14.5	10.8
7	6.8	4.8	12.5	8.0
8	5.0	ND	12.4	6.9
9	2.9		11.9	4.9
10**	ND*		10.4	ND

ND* = Not detected; Limit of Detection = 1 mg/L

** **Cumulative UV irradiation time = 41.0 sec (theoretical UV dosage = *ca* 838 mW-s/cm^2)**

*** **Additional suspended catalyst = 1 g/L TiO_2**

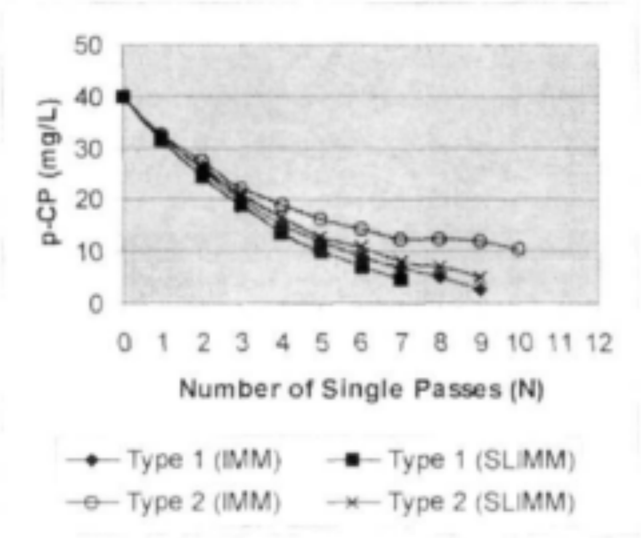

Figure 5.11: p-CP concentration as a function of sheet module, reactor configuration and single pass number (N) - where each N equals 4.1 seconds of UV irradiation

Table 5.12: First order rate constants for p-CP oxidation as a function of sheet module and reactor configuration

Kinetic Response Function	Fibre Glass Type 1 (reinforced sheet)		Fibre Glass Type 2 (non-reinforced tissue sheet)	
	IMM Reactor	SLIMM Reactor	IMM Reactor	SLIMM Reactor
10^2 k_{obs} (N)* (pass^{-1})	27.9	30.3	13.2	22.9
Half-life (passes)	2.5	2.3	5.3	3.0
10^2 k_{obs} (t)** (sec^{-1})	6.73	7.37	3.19	5.64
Half-life (sec)	10.3	9.4	21.7	12.3
10^2 k_{obs} (t) (min^{-1})	403.8	442.4	191.4	338.1
Half-life (min)	0.17	0.15	0.36	0.21
R^2	0.99	0.99	0.96	0.99

k_{obs} (N)* = Observed first order rate constant as a function of single pass number (N) (each single pass is equivalent to a UV contact time of 4.1 sec)

k_{obs} (t) = Observed first order rate constant as a function of irradiation time (in sec or min)**

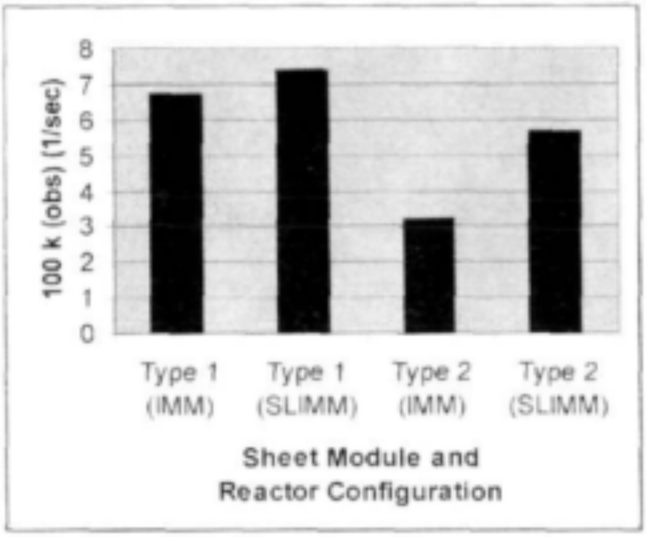

Figure 5.12: First order rate constants for p-CP oxidation as a function of sheet module and reactor configuration

Table 5.13: Design matrix for factorial study

Sheet Module Type	Reactor Configuration	10^2 k_{obs} * (sec^{-1})
1	IMM	6.73
2	IMM	3.19
1	SLIMM	7.37
2	SLIMM	5.64

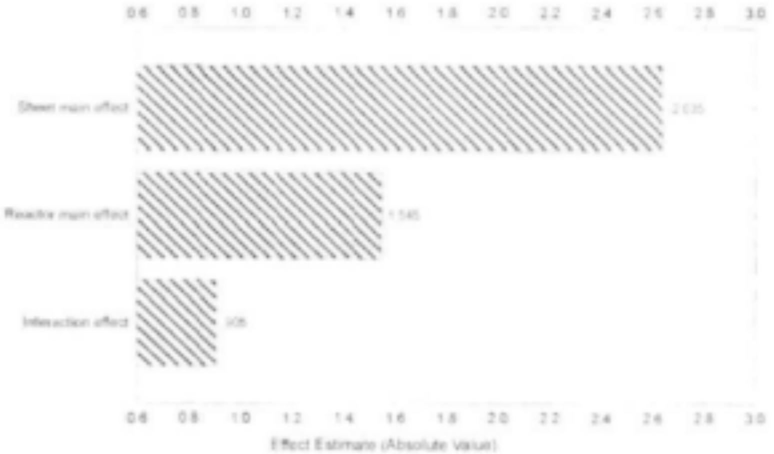

Figure 5.13: Pareto chart illustrating parameter main effects and second order interaction effect with respect to first order rate for p-CP oxidation (k_{obs}) as response function

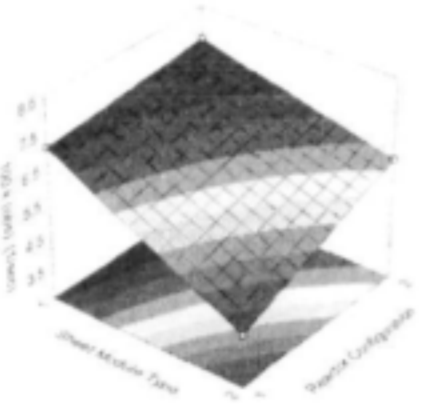

Figure 5.14: Second order response surface illustrating parameter effects and second order interaction effect with respect to first order rate constant for p-CP oxidation (k_{obs}). (Reactor configurations: 1 = IMM and 2 = SLIMM)

The results obtained from these experiments (Tables 5.11-5.13 and Figures 5.11-5.14) indicated that :

- first order decay kinetics apply for the photocatalytic oxidation of p-CP when operating Reactor 2A in sequential single pass mode ;
- the oxidation rate is substantially higher when using the original reinforced fibre glass sheet module (Type 1) as stationary support for TiO_2. This result is attributed to the surface roughness of the first material, which may result in beneficial mixing and turbulence effects during falling film flow. The effect of sheet type used is also fairly independent of reactor configuration, which means that both IMM and SLIMM reactors will benefit from surface roughened supports ;
- for fibre glass Type 1 as sheet module, the oxidation rate increases marginally when switching from the IMM to SLIMM reactor configuration. This result demonstrates that the auxiliary effect of slurried catalyst (1 g/L in this study) is insignificant when surface roughness of the support is pronounced ;
- for fibre glass Type 1 as sheet module, the oxidation rate increases considerably when switching from IMM to SLIMM configuration. This result demonstrates that additional suspended TiO_2 is beneficial for oxidation when using a relatively smooth support (under laminar flow conditions) ;
- parameter main effects and interactions are calculated successfully using a quadratic polynomial model in conjunction with a 2 x 2 factorial design ;
- the interaction effect between reactor sheet type and configuration is insignificant compared to the individual main effects.

Based on the results obtained above, it is evident that the physical characteristics of the TiO_2 support is of critical importance when evaluating immobilised-bed (IMM) reactor configurations and combinations thereof with slurried systems (SLIMM). The operation of Reactor 2A as IMM reactor for efficient oxidative removal of p-CP is justified.

(c) Screening Study (Immobilised-Bed Reactor)

Introduction and Objectives:

Seven parameters were identified for an initial screening study of Reactor 2A operated as an Immobilised-Bed (IMM) reactor (see Tables 5.10 and 14). The objectives were to (1) obtain a rough estimate of the effects of the various parameters on the response functions (2) eliminate insignificant parameters in accordance with the Pareto Principle (3) identify important parameters for optimisation purposes and (4) evaluate the application of a highly fractionated (1/16th) two-level factorial design in a screening study.

Results and Discussion:

Table 5.14: Design matrix for IMM screening study (orthogonal array)

Run	CSL (g/L)	Volumetric Flow Rate (L/min)	Gas Flow Rate[b] (L/min)	$[p\text{-CP}]_o$[c] (mg/L)	UV[d] Source	HID[e] (cm)	Reaction Volume (L)	D* (%)	$10^2\,k_{obs}(N)$** (pass^{-1})
1	1	1	5	13	1	5	3	10.6	6.42
2***	20	1	20	13	2	5	6	23.8	25.74
3	1	2	20	13	1	15	6	6.0	5.66
4	20	2	5	13	2	15	3	22.9	18.40
5	1	1	5	40	2	15	6	13.8	12.02
6	20	1	20	40	1	15	3	4.3	4.88
7	1	2	20	40	2	5	3	15.7	11.66
8	20	2	5	40	1	5	6	3.3	3.28

a CSL = Catalyst suspension loading *used for impregnation* (see Table 5.4 for conversion factors)
b Oxygen gas purge only
c $[p\text{-CP}]_o$ = Initial concentration of p-CP
d UV source : 1 = Fluorescent Blacklight (UV-A); 2 = Germicidal (UV-C)
e HID = Horizontal irradiation distance
*** D = Degradation of p-CP (%)**
**** k_{obs} (N) = First order rate constant as a function of single pass number**
***** Best *result in terms of reaction rate constant (run 2)***

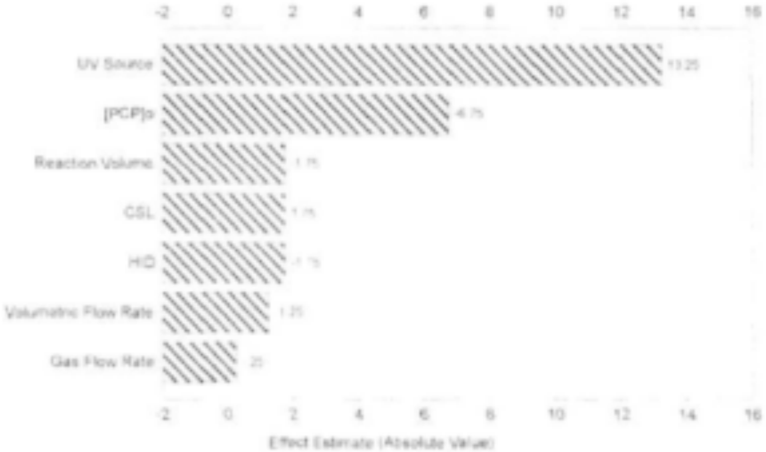

Figure 5.15: Pareto chart illustrating parameter main effects with respect to p-CP degradation (%) as response function. (CSL = Catalyst Suspension Loading *used for impregnation of sheet*; [p-CP]o = p-CP Initial Concentration in mg/L; HID = Horizontal Irradiation Distance in cm)

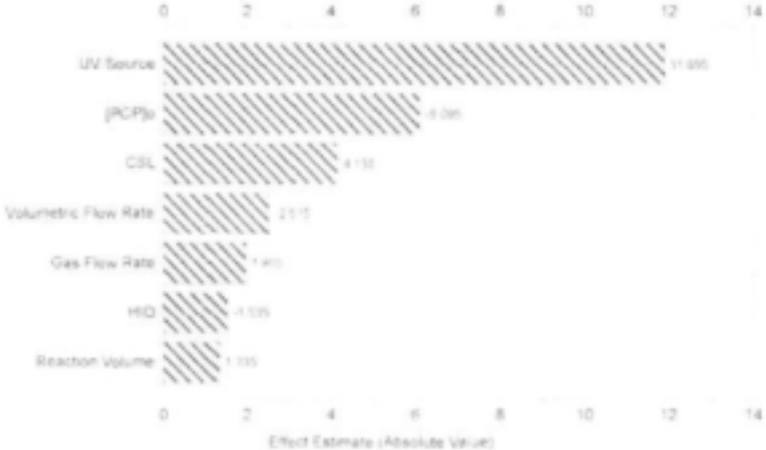

Figure 5.16: Pareto chart illustrating parameter main effects with respect to the first order rate constant (k_{obs}) as a function of sequential single pass number. (CSL = Catalyst Suspension Loading *used for impregnation of sheet*; [p-CP]o = p-CP Initial Concentration in mg/L; HID = Horizontal Irradiation Distance in cm)

The results obtained from these experiments (Table 5.14 and Figures 5.15-5.16) indicated that :

- first order exponential decay kinetics apply for the photocatalytic oxidation of p-CP when operating Reactor 2A as IMM reactor in sequential single pass mode ;
- operating the IMM reactor with germicidal UV-C lamps has a highly beneficial effect on the oxidation rate of p-CP in both single pass modes ;
- p-CP initial concentration has an intermediate negative effect on the oxidation rate for *both* modes. This observation confirms the utility of Reactor 2A for the treatment of low concentrations of pollutant ;
- the effect of volumetric flow rate is negligible in single pass mode and diminishes further for the sequential mode. These observations confirm the potential use of the reactor for treating large volumes of polluted water efficiently.
- the effects of horizontal irradiation distance and oxygen flow rate are negligible within the framework of the selected experimental design. These results demonstrate the practical benefits of Reactor 2A ;

- the effect of immobilised catalyst (expressed in terms of the suspension loading used for coating) becomes more significant when switching from single pass to sequential single pass mode. This result confirms the importance of attaining optimised conditions for the *first* single pass in a network of sequential single pass reactors ;
- parameter main effects are calculated successfully when using highly fractionated factorial designs in tandem with linear mathematical models ;
- the Pareto Principle applies, viz.: (1) one or two parameters exert predominant effects on the response and (2) several parameters are insignificant and could therefore be kept constant at convenient experimental levels.

Based on the results obtained above, it remained to be seen how significantly the degradation efficiency of the single pass reactor (2A) depended on the amount of immobilised catalyst.

(d) Catalyst Impregnation Loading (Immobilised-Bed Reactor)

Introduction and Objectives:

The effect of catalyst impregnation loading was examined by comparing results for 5 different suspension loadings of TiO_2 (1; 5; 10; 20 and 30). The corresponding impregnation loadings amounted to 1.0, 8.1, 14.1, 21.6 and 24.8 g TiO_2 per sheet module (0.88 m^2). This specific batch of sheet modules were also used for the equivalent study in recirculation mode (see Section 5.1.1(f)). The remainder of the system parameters were evaluated at standard reference levels (Table 5.10). The objectives of this study were to (1) assess the effect of catalyst impregnation loading on the rate of oxidation of 40 mg/L p-CP in the single pass mode and (2) to determine an optimum or plateau value for this parameter in terms of the defined response function (viz.: percentage of p-CP degradation).

Results and Discussion:

Table 5.15: Degradation (%) of p-CP as a function of catalyst impregnation loading

Catalyst Suspension Loading (g/L TiO_2) *(used for sheet coating)*	Catalyst Impregnation Loading (g TiO_2 per sheet*)	Catalyst Impregnation Loading (g TiO_2 per m^2)	p-CP Degradation (%)
1	1.0	1.1	11.3
5	8.1	9.2	19.1
10	14.1	16.0	19.6
20	21.6	24.5	19.7
30	24.8	28.2	19.8

*** Sheet coating area = 0.88 m^2**

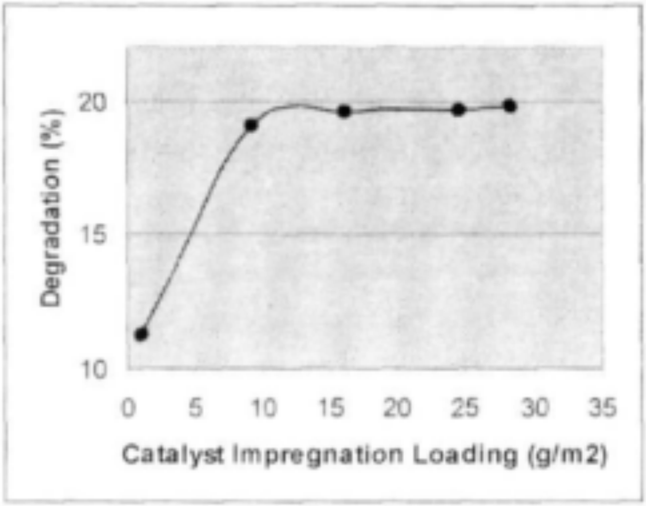

Figure 5.17: Degradation (%) of p-CP as a function of catalyst impregnation loading

The results obtained from these experiments (Table 5.15 and Figure 5.17) indicated that :

- the degradation efficiency increases with approximately 10% when increasing the impregnation loading from ca 1 to 9 g TiO_2 /m^2 ;
- beyond loadings of 10 g/m^2 a plateau value exists for the amount of p-CP oxidised as a function of catalyst impregnation loading (p-CP initial concentration: 40 mg/L). This result implies that oxidation efficiency becomes independent of the mass of immobilised TiO_2 when operating Reactor 2A in single pass mode ;
- maximum degradation (*ca* 19%) is attained for a catalyst impregnation loading of between 9 and 16 g/m^2 TiO_2 (viz.: between 0.9 and 1.6 mg/cm^2). This value is in good agreement with literature values for typical immobilised-bed photoreactors (Herrmann, 1995).

Based on the results obtained above, it is evident that the existence of a plateau in the catalyst impregnation loading would result in an easier procedure to optimise other configurations of immobilised photocatalytic reactors (e.g. a single pass horizontal flow system).

(e) pH Effects (Immobilised-Bed Reactor)

Introduction and Objectives:

The effect of pH was examined by operating Reactor 2A as an immobilised-bed reactor in the single pass mode and comparing results for 5 different initial pH conditions against the standard (neutral) pH of 7.5 for distilled water spiked with p-CP. 1M NaOH and 1M HCl (and dilutions thereof) were used as additives to adjust the initial pH. The catalyst suspension loading used for coating was 20 g/L TiO_2 (equivalent impregnation loading of approximately 24.4 g/m^2). The remainder of the system parameters were evaluated at their standard reference levels (Table 5.10). These levels (in combination with an initial p-CP concentration of 13 mg/L) were selected to complement an analogous study for the recirculation mode of operation. An equivalent dark adsorption experiment was conducted in tandem with each oxidation reaction by employing identical parametric conditions.

The objectives of this study were to (1) assess the oxidation efficiency of the immobilised reactor as a function of initial pH and (2) determine variations in p-CP mass transfer at high impregnation loading, low initial concentration (13 mg/L) and in the absence of UV irradiation.

Results and Discussion:

Table 5.16: Degradation (%) of p-CP and mass transfer (%) as a function of initial pH

Initial solution pH	Degradation (%)	Dark adsorption (%)
3.0	8.5	10.1
5.0	22.7	10.2
6.2	22.2	9.8
7.5 (neutral)	22.9	9.9
9.0	17.8	5.6
11.0	10.4	3.0

*pH 6.2 is the point of zero charge (PZC) for TiO_2

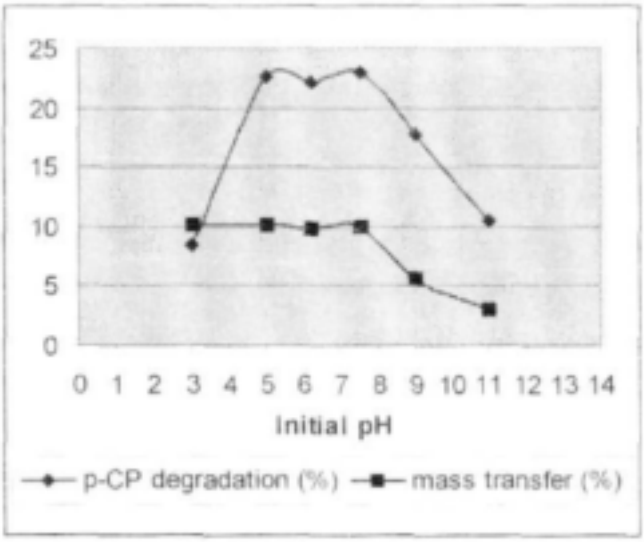

Figure 5.18: Degradation (%) of p-CP and mass transfer (%) as a function of initial pH

The results obtained from these experiments (Table 5.16 and Figure 5.18) indicated that :

- the degradation of p-CP is largely independent of initial solution pH in the range pH 5 to 7.5 when utilising the single pass mode of operation. This result is ascribed to

- favourable adsorption kinetics attained for p-CP and TiO_2 in this region. The degree of p-CP mass transfer to immobilised TiO_2 is generally in the order 10% (w/w) ;
- the oxidation efficiency is markedly suppressed at an initial pH of 3. The additive in this instance (HCl) is probably responsible for interfering with the photocatalytic process (as explained before) although mass transfer of p-CP remains constant ;
- the oxidation efficiency is suppressed when increasing the initial pH to 9 and 11, respectively. This result is ascribed to reduced mass transfer of p-CP as explained earlier ;
- p-CP mass transfer in the order of 10% (w/w) is a good measure for efficient photocatalytic oxidation in single pass immobilised reactors ;
- the superior degradation efficiency of Reactor 2A in single pass mode over recirculation mode is clearly demonstrated (compare Figures 5.9 and 5.18).

(f) Screening Study (Combined Slurry-Immobilised Reactor)

Introduction and Objectives:

Eight parameters were identified for an initial screening study of Reactor 2A operated as a combined Slurry-Immobilised (SLIMM) reactor (see Tables 5.10 and 17). The objectives were to (1) obtain a rough estimate of the effects of the various parameters on the response functions (2) eliminate insignificant parameters in accordance with the Pareto Principle (3) identify important parameters for optimisation purposes and (4) evaluate the application of a highly fractionated (1/16th) two-level factorial design in a screening study.

Results and Discussion:

Table 5.17: Design matrix for SLIMM screening study (orthogonal array)

Run	CIL^a (g/L)	CSL^b (g/L)	VFR^c (L/min)	Gas^d Flow Rate (L/min)	$[p\text{-CP}]_o^e$ (mg/L)	UV^f Source	HID^g (cm)	Reaction Volume (L)	D* (%)	10^2 k (N)** (pass^{-1})
1	1	1	1	5	13	1	5	3	8.1	7.4
2***	1	20	1	20	13	2	5	6	46.2	35.14
3	1	1	2	20	13	1	15	6	6.2	6.84
4	1	20	2	5	13	2	15	3	40.0	27.5
5	1	1	1	5	40	2	15	6	30.3	21.47
6	1	20	1	20	40	1	15	3	9.9	14.16
7	1	1	2	20	40	2	5	3	17.8	12.64
8	1	20	2	5	40	1	5	6	13.2	11.68
9	20	20	2	20	40	2	15	6	18.0	21.91
10	20	1	2	5	40	1	15	3	11.9	8.36
11	20	20	1	5	40	2	5	3	38.8	33.68
12	20	1	1	20	40	1	5	6	6.1	7.31
13	20	20	2	20	13	1	5	3	20.5	12.15
14	20	1	2	5	13	2	5	6	18.5	28.26
15	20	20	1	5	13	1	15	6	18.6	17.17
16	20	1	1	20	13	2	15	3	42.7	28.4

a CIL = Catalyst impregnation loading (expressed as suspension loading used for coating)
b CSL = True Catalyst suspension loading (in addition to immobilised catalyst)
c VFR = Volumetric Flow Rate
d Oxygen gas purge only
e $[p\text{-CP}]_o$ = Initial concentration of p-CP
f UV source : 1 = Fluorescent Blacklight (UV-A); 2 = Germicidal (UV-C)
g HID = Horizontal irradiation distance
* D = Degradation of p-CP (%)
** k_{obs} (N) = First order rate constant as a function of single pass number
*** Best result in terms of reaction rate constant (run 2)

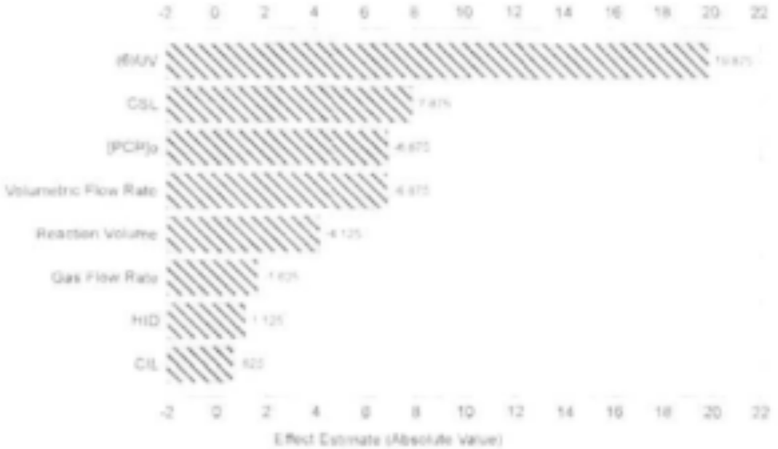

Figure 5.19: Pareto chart illustrating parameter main effects with respect to p-CP degradation (%) as response function. (CIL = Catalyst Suspension Loading *used for impregnation of sheet*; CSL = True catalyst suspension loading in addition to CIL; [p-CP]o = p-CP Initial Concentration in mg/L; HID = Horizontal Irradiation Distance in cm)

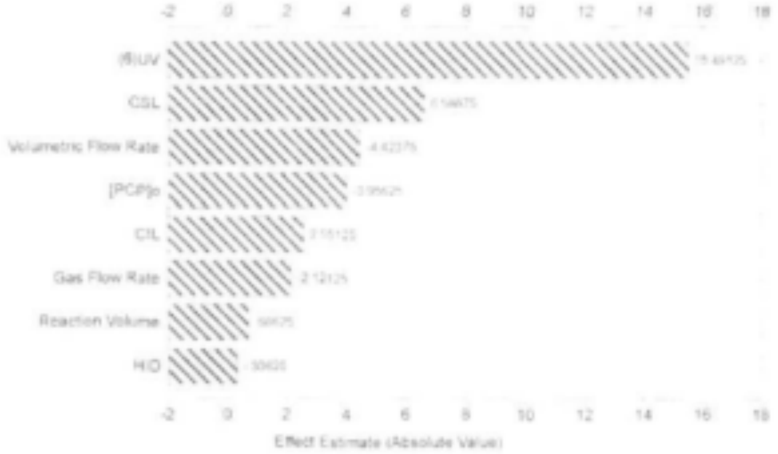

Figure 5.20: Pareto chart illustrating parameter main effects with respect to the first order rate constant (k_{obs}) as a function of sequential single pass number. (CIL = Catalyst Suspension Loading *used for impregnation of sheet*; CSL = True catalyst suspension loading in addition to CIL; [p-CP]o = p-CP Initial Concentration in mg/L; HID = Horizontal Irradiation Distance in cm)

The results obtained from these experiments (Table 5.17 and Figures 5.19-20) indicated that :

- first order exponential decay kinetics apply for the photocatalytic oxidation of p-CP when operating Reactor 2A as a SLIMM reactor in sequential single pass mode ;
- operating the SLIMM reactor with germicidal UV-C lamps has a highly beneficial effect on the oxidation rate of p-CP in both single pass modes ;
- p-CP initial concentration has an intermediate negative effect on the oxidation rate for *both* modes. This observation confirms the utility of Reactor 2A for the treatment of low concentrations of pollutant in single pass mode ;
- the intermediate negative effect of volumetric flow rate is applicable to both single pass modes. This observation implies that penetration of UV light through suspension films may be problematical when operating SLIMM reactors at high flow rate ;
- the effects of horizontal irradiation distance, oxygen flow rate and reaction volume are negligible for both modes within the framework of the selected experimental design. These results demonstrate the practical benefits of Reactor 2A (apart from filtration problems) operated as a SLIMM reactor ;
- the effect of immobilised catalyst (expressed in terms of the suspension loading used for coating) is negligible for the single pass mode, with marginal elevation in significance when switching to sequential single pass mode ;
- the effect of true catalyst suspension loading (in addition to immobilised catalyst) remains positive throughout and is considerably more significant than the amount of immobilised catalyst. This observation is expected for a slurried system ;
- parameter main effects are calculated successfully when using highly fractionated factorial designs in tandem with linear mathematical models ;
- standardised effects are also generated as a result of a sufficient number of degrees of freedom ;
- the Pareto Principle applies, viz.: (1) one or two parameters exert predominant effects on the response and (2) several parameters are insignificant and could therefore be kept constant at convenient experimental levels.

Based on the results obtained above and the knowledge of the insurmountable problems associated with the filtration of TiO_2 slurries , it is clear that (1) the operation of Reactor 2A should be limited to the IMM reactor configuration and (2) optimised single pass conditions for IMM will render comparative oxidation efficiencies to the SLIMM reactor.

(g) Endurance Tests

A number of endurance tests were conducted to assess the reproducibility of p-CP oxidation rates through the operation of Reactor 2A as SLIMM or IMM reactors in the single pass mode. The results (De Villiers, 2000) indicated that :

- reproducible results (RSM $\leq$ *ca* 10%) are achieved for the oxidation of 40 mg/L p-CP when using different sheets modules of the same product batch (coated under identical conditions according to the *standard* coating procedure). This result is observed for both reactor configurations (IMM and SLIMM) ;
- a single TiO_2 coated fibre glass sheet maintains catalytic activity (hence statistical reproducibility) for at least 10 consecutive single passes of 40 mg/L p-CP (at standard reference levels for the system parameters). This result is also observed for both configurations ;
- *catalytic activity is mildly suppressed when reusing the original aqueous solution or* slurry matrix (spiked with fresh p-CP);
- recirculation of a sample of clean distilled water over the sheet module (between *successive oxidation runs) assists the retention of catalytic activity*
- almost no impregnated catalyst was lost from sheet modules during or after the execution of a falling film experiment.

The results mentioned above, implies that a more detailed study is required to monitor and improve (where necessary) the catalytic activity of TiO_2 immobilised on the fibre glass sheet modules. Catalyst reactivation procedures and sheet module treatment should be addressed.

(h) Cost Calculation

A preliminary cost calculation was made for the photocatalytic oxidative treatment of p-CP in distilled water, based on the operation of Reactor 2A as IMM reactor in the sequential single pass mode. The calculation was done in view of the following assumptions :

- first order kinetics
- idealised plug-flow reactor conditions
- a constant electrical energy per order (EE/O)

Bolton's formula for EE/O in idealised plug-flow reactors has been defined earlier (in Section 2.1.3) :

$$EE/O = P / F \times \log (c_o / c_f)$$

Where: P = Lamp power (in kW)
F = Volumetric water flow rate (in m^3/h)
c_o = Initial concentration
c_f = Final concentration
EE/O = kWh/order/m^3

Thus, taking the above mentioned p-CP result as example, the EE/O and cost (per m^3) for the photocatalytic oxidation of an initial concentration of 40 mg/L to below the limit of detection (1 mg/L) can be calculated as follows :

- orders of removal = log (40/1) = 1.602
- P = 12 x 15 W = 180 W = 0.18 kW
- F = 2 L/minute = 120 L/h = 0.12 m^3/h

EE/O amounts to: (0.18)/(0.12 x 1.602) = 0.94 kWh/order/m^3. At a unit price of 11.8 c/kWh in the Stellenbosch area, the cost to reduce 40 mg/L p-CP with one order of magnitude (4 mg/L) amounts to 11c / m^3 of water. A further order of magnitude reduction (to 0.4 mg/L) will double the cost, since EE/O is a constant per order.

When applying a volumetric flow rate of 1 L/minute, the cost changes to 22c / m^3, which demonstrates that a low volumetric throughput increases electrical costs in the single pass (plug-flow) reactor.

5.2 TREATMENT OF MICROCYSTINS

5.2.1 Recirculation Mode

(a) System Parameters

The photocatalytic oxidation of four variants of microcystins in water was investigated by operating Reactor 2A as (1) immobilised-bed (IMM) and (2) combined slurry-immobilised (SLIMM) reactor. One-factor variation methods were employed to conduct random parametric studies. The following system parameters were evaluated at discrete levels in terms of first order reaction kinetics (see Table 5.18):

Table 5.18: System parameters for microcystin study (Reactor 2A; Recirculation Mode)

Parameter	Assigned Levels
Catalyst Suspension Loading (g/L)	0; 1^{a}; 5^{*a}
Catalyst Loading for Impregnation (g/L)	5^{*}; 20
Volumetric Flow Rate (L/min)	2.0^{*b}
Horizontal Irradiation Distance (cm)	15^{*}
Microcystin Variants	YA, YR, LR and RR
Reaction Volume (L)	5^{*}
Water Matrix	De-ionised water; Lake water*
Gas Purge	Oxygen*
Gas Flow Rate (L/min O_2)	5^{*}; 20
Number of UV-C lamps for Irradiation	12^{*c}
Irradiation Time (min.)	20^{*}

Note: * Denotes standard reference level of parameters
a For SLIMM reactor configuration
b Surface flow rate = 136 L/hr/m^2
c UV irradiance = 204.5 W/m^2

(b) TiO_2 Impregnation of Sheet Modules

Based on coating and impregnation results obtained earlier (see Section 5.1.1), the reinforced fibre glass material (Type 1) was used as stationary support for TiO_2 in the evaluation of Reactor 2A for the photocatalytic oxidation of microcystins. The *standard coating procedure* was followed as explained before. This entailed "dark" recirculation of suspensions of TiO_2 (in 3 L of distilled water) through the system (across the sheet module) using (1) a 2 L/min volumetric flow rate (2) natural suspension pH (4-5) and (3) magnetic stirring for a period of 30 minutes. Sheet modules were weighed before and after coating. Coated sheets were air-dried at room temperature for 24 hr prior to determining the net increase in weight. A suspension loading of 5 g/L TiO_2 was used as *standard reference level* and yielded an impregnation loading of about 7.5 g TiO_2 per sheet (viz.: 8.5 g/m^2). The effect of increased impregnation loading was assessed during experimentation (see Table 5.18).

(c) Catalyst Suspension Loading (Lake Water)

Introduction and Objectives:

The effect of catalyst suspension loading was examined in natural water (Zeekoevlei, Cape Flats) by comparing results for 3 different loadings of TiO_2 (0; 1 and 5 g/L). System parameters were evaluated at standard reference levels (Table 5.18). The objectives of this study were to (1) establish whether an increase in catalyst suspension loading promotes the photocatalytic oxidation of microcystins and (2) assess oxidation efficiency as a function of reactor configuration (viz.: operating Reactor 2A as an IMM or a SLIMM reactor).

Results and Discussion:

Table 5.19 **Concentration of microcystins YA, YR and LR as functions of irradiation time and catalyst suspension loading**

Irradiation Time (min)	Microcystins (ug/L)								
	YA			YR			LR		
	Catalyst Suspension Loading (g/L)			Catalyst Suspension Loading (g/L)			Catalyst Suspension Loading (g/L)		
	0	1	5	0	1	5	0	1	5
0	18	21	21	53	66	71	23	31	30
2	16	17	12	48	62	55	19	39	27
4	15	13	11	44	48	47	18	26	23
6	13	ND*	ND	39	NA***	32	14	10	19
8	10			29	NA	25	11	10	15
10	ND			25	29	19	11	10	14
12				20	23	16	ND	11	11
14				21	15	ND		12	ND
16				17	14			ND	
18				14	13				
20				11	11				
10^2 k_{obs} (min^{-1})	6.92	11.99	16.17	7.65	10.15	12.91	7.97	NC**	8.48
Half-life (min)	10.0	5.8	4.3	9.1	6.8	5.4	8.7	NC	8.2
R^2	0.94	0.99	0.85	0.96	0.97	0.99	0.96	NC	0.99

Note: **ND* = Not detected; Limit of Detection = 10 ug/L**
NC = Not calculated**
NA* = Not analysed**

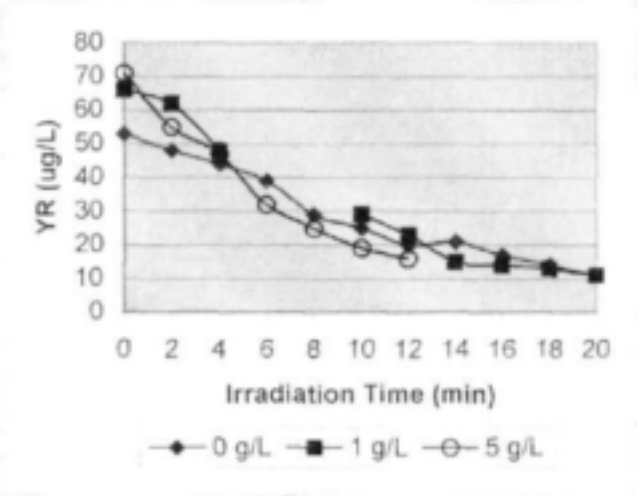

Figure 5.21: Concentration of microcystin YR as a function of irradiation time and catalyst suspension loading

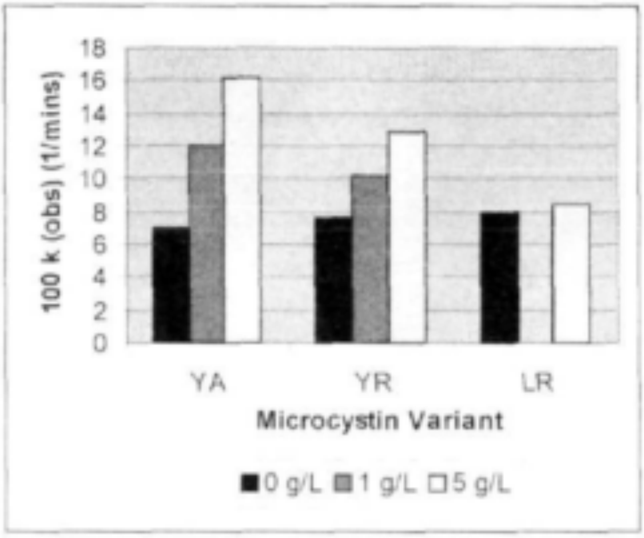

Figure 5.22: First order rate constants for the oxidation of microcystins as a function microcystin variant and catalyst suspension loading (in g/L TiO_2)

The results obtained from these experiments (Table 5.19 and Figures 5.21-5.22) indicated that :

- an increase in catalyst suspension loading from 0 to 5 g/L promotes the oxidation of microcystins YA and YR. This result confirms the (1) superior destruction efficiency of the SLIMM reactor for these variants (2) auxiliary oxidation effect of slurried catalyst in the presence of immobilised catalyst and low starting concentrations (viz.: *ca* 20 ug/L) ;
- an increase in catalyst loading from 0 to 5 g/L does not enhance oxidation of microcystin LR significantly. This result demonstrates the (1) higher resistance of LR towards oxidation and (2) utility of the IMM reactor for treatment of LR ;
- the high RSD for initial concentration data can be remedied by normalisation (viz.: expressing data as fraction percentages of the observed initial concentration ;
- the use of IMM reactor configurations is suitable when treating recalcitrant organic compounds in natural lake water (viz.: in the presence of inorganic ions and NOM as radical scavengers).

(d) Reproducibility Study (Slurry-Immobilised Reactor)

Introduction and Objectives:

The statistical reproducibility of photocatalytic oxidation rates was examined by operating Reactor 2A as combined slurry-immobilised reactor (SLIMM) at the standard reference levels for all parameters (Table 5.18). Test runs were conducted in triplicate using a catalyst suspension loading of 5 g/L TiO_2 *after* sheet coating (according to the standard procedure). Lake water (spiked with microcystin algal extract) was used in this instance. The objective of this study was to evaluate the reproducibility of the observed rate constants in terms of (1) standard deviation (SD) (2) relative standard deviation (RSD) and (3) microcystin variant.

Results and Discussion:

Table 5.20: Concentrations of microcystins as functions of irradiation time, variant and replicate number

Irradiation Time (min)	Microcystins (ug/L)								
	YA			YR			LR		
	Replicate Run Number			Replicate Run Number			Replicate Run Number		
	1	2	3	1	2	3	1	2	3
0	24	22	21	77	72	71	32	25	30
2	17	15	12	61	56	55	26	24	27
4	14	14	11	49	48	47	23	21	23
6	12	ND	ND	47	33	32	23	21	19
8	10			34	25	25	19	17	15
10	11			26	20	19	15	14	14
12	10			19	16	16	14	13	11
14	ND*			11	ND	ND	10	ND	ND
16				12			10		
18				ND			11		
20							ND		
$10^2\ k_{obs}$ (min^{-1})	6.85	11.30	16.17	12.90	12.90	12.91	6.72	5.81	8.48
Half-life (min)	10.1	6.1	4.3	5.4	5.4	5.4	10.3	11.9	8.2
R^2	0.85	0.86	0.85	0.95	0.99	0.99	0.94	0.95	0.99

Note: ND* = Not detected; Limit of Detection = 10 ug/L

Table 5.21: Statistical analysis of reproducibility of observed first order rate constants for oxidation of microcystins as a function of microcystin variant.

Microcystin Variant	Measured Response	Mean	Standard Deviation	Relative Standard Deviation (%)
YA	10^2 k (obs)*	11.4	4.7*	41.2
YA	Half-life**	6.8	3.0**	44.1
YR	10^2 k (obs)	12.9	0.0	0.0
YR	Half-life	5.4	0.0	0.0
LR	10^2 k (obs)	7.0	1.4	20.0
LR	Half-life	10.1	1.9	18.8

*** in min^{-1} ; ** in min**

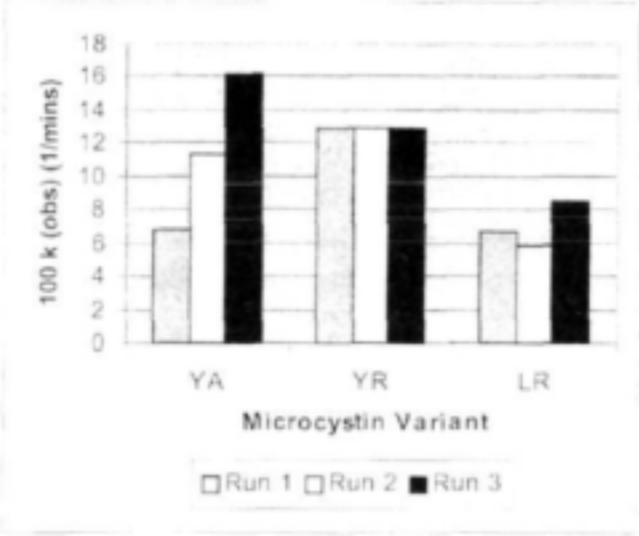

Figure 5.23: Reproducibility of observed first order rate constants for oxidation of microcystins as a function of microcystin variant

The results obtained from these experiments (Tables 5.20-5.21 and Figure 5.23) indicated that:

- the mean observed first order rate constants for oxidation of microcystins YA and YR are largely similar. This result suggests that YA is more resistant to oxidation than YR due to first order kinetics prescribing higher rate constants for lower initial concentrations (see Section 4.1) ;
- the rate constants for LR are slightly smaller compared to YA and YR. This result demonstrates the more resistant nature of LR towards photocatalytic oxidative treatment ;
- the relative standard deviation (RSD) of the first order rate constant is close to 0% for the YR variant. This is considered a good result taking into account possible error variations in sample preparation, reactor efficiency and analytical methodology ;
- RSD is very high for the oxidation of microcystins YA and LR. This result is explained in terms of (1) variable mass transferred adsorption as a function of catalyst suspension loading and (2) practical problems related to the HPLC analysis of these variants ;
- the overall oxidation susceptibility of the three variants is in the order: YR>YA>LR.

Based on the results obtained above, a more detailed study would be required to link the organic structure of microcystin toxins to their respective photocatalytic reactivities.

(e) Mass Transfer Effects

Introduction and Objectives:

A dark control experiment was performed by operating Reactor 2A as an immobilised-bed reactor (IMM) using the standard reference levels for all system parameters (Table 5.18). Lake water from Zeekoevlei (spiked with microcystin algal extract) was used in this experiment. The objective of this study was to determine the extent of adsorptive mass transfer of microcystin YR and LR molecules to TiO_2 immobilised on the fibre glass support of the reactor.

Results and Discussion:

Table 5.22 Microcystin concentration as a function of recirculation time

Recirculation Time (min)	Microcystins (ug/L)	
	YR	LR
0 20	84 83	46 42
Mass Transfer (%)	1.2	8.7

The results obtained from this experiment (Table 5.22) indicated that:

- less than 10% mass transfer (via adsorption) of microcystins YR and LR occurs to immobilised TiO_2 on the fibre glass sheet module ;
- photocatalytic oxidation is most probably responsible for the overall removal of microcystin toxins from water treated in this experimental reactor.

Based on the result obtained above, it is evident that although the effect of mass transfer is very small (*ca* 10% or less), the surface-catalysed nature of photocatalytic oxidation reactions still require a degree of mass transfer of the target pollutant. This reasoning is based on Langmuir-Hinshelwood kinetics for photocatalytic oxidation (Legrini *et al.*, 1993).

(f) Stability Study

Introduction and Objectives:

Two batches of blue-green algal extracts were used during the evaluation of Reactor 2A. Initial photocatalytic experiments were performed using an algal extract containing microcystins YA, YR and LR in detectable amounts (viz.: greater than 10 ug/L). These toxin variants were extracted with methanol from freeze-dried algal material stored at PROMEC from previous studies. The freeze-dried material originated from a toxic strain of *Microcystis aeruginosa*. The second extract (containing LR and RR in detectable amounts) was prepared from a natural bloom obtained at Wildevoëlvlei near Noordhoek in the Cape Peninsula.

A stability study was conducted on these extracts by spiking 10 mL of each in 5 L of natural lake water in a continuously stirred reservoir. Lake water from Zeekoevlei and Rondevlei was used for this purpose (see Section 3.2.2). The experiments were conducted in the dark to eliminate UV effects. A 100 mL aliquot of water was collected at fixed sampling intervals and analysed for microcystin content. The objectives of this study were to (1) confirm the stability of the toxins in natural water (2) show that the removal of microcystins from water treated by the reactor is mainly due to photocatalytic oxidation.

Results and Discussion:

Table 5.23: Stability study for first extract spiked in natural water (from Zeekoevlei)

Sampling Time (min)	Microcystins (ug/L)		
	YA	YR	LR
0 (not spiked)	ND*	ND	ND
0 (spiked)	42	107	43
5	42	107	44
10	44	117	48
15	45	111	46
20	45	114	52
30	44	111	52
60	31	102	43
1440 (24hr)	41	106	46
8640 (6 days)	42	108	45

Note: ND* = Not detected ; Limit of detection = 10 ug/L

Table 5.24 Stability study for second extract (Wildevoëlvlei) spiked in natural water (from Rondevlei)

Sampling Time (min)	Microcystins (ug/L)	
	LR	RR
0	80	NC*
10	86	NC
20	77	NC
60	78	NC
1440 (24hr)	79	NC
2880 (48 hr)	80	NC

Note: NC* = Not calculated

The results obtained from this experiment (Tables 5.23-24) indicated that:

- the algal extracts used in this project remain stable when spiked into natural water ;
- the microcystins toxins are not decomposed naturally as a result of the water matrix used ;
- the removal of microcystins from water treated in the experimental reactors (1 and 2A) is primarily effected by photocatalytic oxidation.

Based on the results obtained above, it was decided to conduct more parametric studies in order to assess the performance of Reactor 2A as immobilised-bed (IMM) and slurry-immobilised (SLIMM) reactor for the photocatalytic oxidation of microcystins in natural water. System parameters were mainly evaluated at their standard reference levels (unless stated otherwise). Sheet modules were prepared using the standard coating procedure as before.

(g) Water Matrix Effects (Immobilised-Bed Reactor)

Introduction and Objectives:

Water matrix effects were examined by operating Reactor 2A as immobilised-bed (IMM) reactor and comparing results for the treatment of microcystins LR and RR in deionised water and natural lake water. Lake water from Zeekoevlei was used in this study. All system parameters were evaluated at standard reference levels (Table 5.18). The objectives of this study were to (1) compare rates of photocatalytic oxidation as a function of water matrix and microcystin variant and (2) assess the impeding effect of inorganic ions on oxidation rate.

Results and Discussion:

Table 5.25 **Microcystin concentration as a function of irradiation time, variant and water matrix**

Irradiation Time (min)	Microcystins (ug/L)			
	LR		RR	
	Deionised Water	Lake Water	Deionised Water	Lake Water
0	48	59	55	66
2	25	43	32	53
4	17	35	23	43
6	10	34	18	36
8		32	10	35
10		23	ND	31
12		13		23
14		10		16
16		ND*		ND
18				
20	ND			
10^2 k_{obs} (min^{-1})	25.46	11.74	19.92	8.99
Half-life (min)	2.7	5.9	3.5	7.7
R^2	0.99	0.92	0.98	0.96

Note: ND* = Not detected; Limit of Detection = 10 ug/L

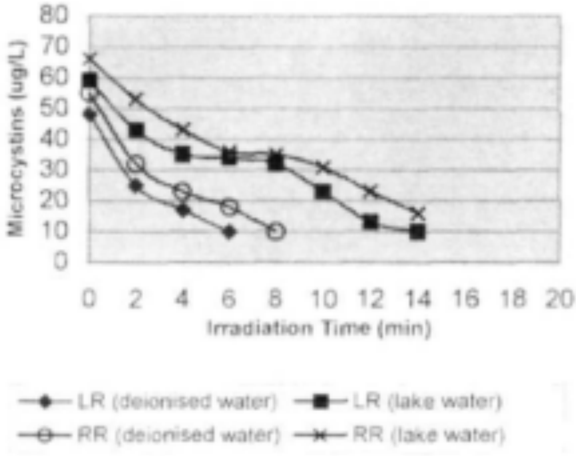

Figure 5.24: Microcystin concentration as a function of irradiation time, variant and water matrix

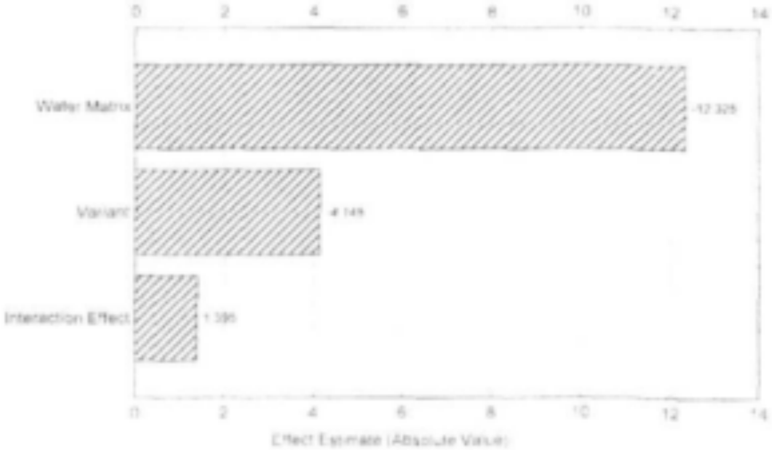

Figure 5.25: Pareto chart illustrating parameter main effects and second order interaction effect for water matrix and microcystin variant

The results obtained from this experiment (Table 5.25 and Figures 5.24-5.25) indicated that:

- the photocatalytic oxidation rate constants for both microcystin variants decrease markedly when switching from deionised water to natural lake water. This result is anticipated in view of (1) pronounced scavenging of hydroxyl radicals by NOM and inorganic ions (such as phosphate) in natural water and (2) inference effects caused by inorganic ions in terms of the blocking of active surface sites on TiO_2 ;
- the photocatalytic oxidation rate constant for microcystin RR is marginally lower than for LR for both water matrices (at comparative initial concentration). Hence, RR and LR exhibit similar oxidation susceptibility ;
- the interaction effect between the 2 parameters is negligible compared to individual main effects. This observation implies that the inherent oxidation susceptibility of a microcystin variant could be linked to organic structure and water quality on a *separate* basis. The application of (1) quantum mechanical modelling (2) neural network simulation and (3) multivariate experimental design is envisaged as part of this exercise.

Based on the results obtained above, it is evident that by using deionised water as spiking matrix for microcystins, it is possible to conduct an absolute comparison of oxidation susceptibility as a function of variant.

(h) Solution pH (Immobilised-Bed Reactor)

Introduction and Objectives:

The effect of pH was examined by operating Reactor 2A as an immobilised-bed (IMM) reactor and comparing results for 2 different initial solution pH conditions against the standard (neutral) pH of 8. 1M NaOH, 1M HCl and 1M H_2SO_4 (and dilutions thereof) were used as additives to adjust pH. Microcystins LR and RR were spiked in lake water from Zeekoevlei (pH 8) prior to photocatalytic treatment. All system parameters were evaluated at standard reference levels (Table 5.18) and the standard coating procedure applied for the sheet module. The objectives of this study were to (1) compare rates of photocatalytic oxidation as a function of initial solution pH and microcystin variant and (2) assess the impeding effect of inorganic ions on the oxidation rate.

Results and Discussion:

Table 5.26: **Microcystin concentration as a function of irradiation time and initial solution pH**

Irradiation Time (min)	Microcystins (ug/L)							
	LR				RR			
	pH 3 (HCl)	pH 3 (H_2SO_4)	pH 8 (neutral)	pH 11 (NaOH)	pH 3 (HCl)	pH 3 (H_2SO_4)	pH 8 (neutral)	pH 11 (NaOH)
0	49	32	59	45	54	44	66	57
2	NA	31	43	32	28	33	53	42
4	32	20	35	26	19	23	43	35
6	20	19	34	24	12	19	36	35
8	19	NA	32	21	ND	17	35	26
10	14	NA**	23	NA		15	31	26
12	ND*	11	13	13		ND	23	16
14		ND	10	ND			16	ND
16			ND				ND	
18								
20								
10^2 k_{obs} (min^{-1})	12.61	9.26	11.74	9.49	24.50	10.80	8.99	9.05
Half-life (min)	5.5	7.5	5.9	7.3	2.8	6.4	7.7	7.7
R^2	0.97	0.96	0.92	0.97	0.99	0.95	0.96	0.93

Note: ND* = Not detected; Limit of Detection = 10 ug/L
NA = Not analysed**

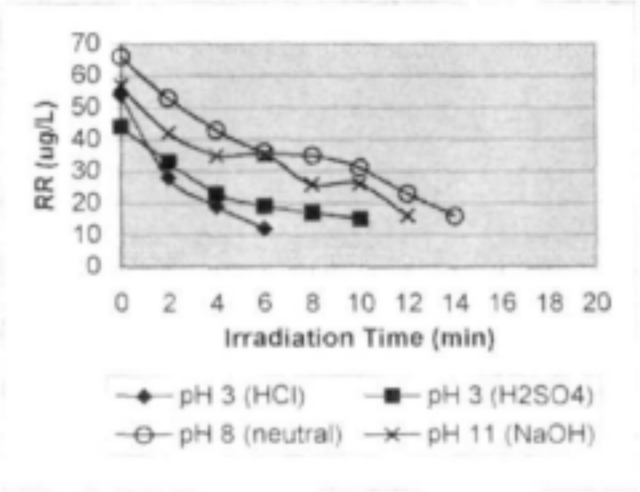

Figure 5.26: Microcystin RR concentration as a function of irradiation time and initial solution pH

The results obtained from this experiment (Table 5.26 and Figure 5.26) indicated that:

- the oxidation rate constant for microcystin LR increases marginally when adjusting the initial pH to 3 using HCl as additive. This result is ascribed to favourable adsorptive interaction between negatively charged microcystin molecules and positively charged TiO_2 species (existing as $TiOH_2^+$) at pH 3. The effect is markedly amplified for the oxidation of RR under the same conditions ;
- when using H_2SO_4 as acidic additive, the rate constant for LR drops marginally compared to HCl. This result is ascribed to the inhibiting effect of sulphate ions acting as hydroxyl radical scavengers. The effect is markedly amplified for RR oxidation with a more than 50 % reduction in rate constant for H_2SO_4 addition ;
- the oxidation rate remains relatively unchanged when adjusting the initial pH to 11. This result is unexpected in view of pronounced electrostatic repulsion existing between TiO^- species and negatively charged microcystin molecules in this pH range. The utility of the reactor for microcystin oxidation in waters of high pH is therefore demonstrated ;
- the oxidation rate constant for microcystin LR is relatively insensitive to pH variation, whereas the oxidation of RR reveals a marked dependence on pH ;
- the treatment of LR in an IMM reactor configuration is of practical importance.

Based on the results obtained above, it is evident that the photocatalytic oxidation of microcystins is a complex process which depends on the (1) organic structure (2) relative pH sensitivity (3) adsorption kinetics as a function of pH and (4) oxidation susceptibility, of the variant under investigation.

(i) Slurry pH (Combined Slurry-Immobilised Reactor)

Introduction and Objectives:

The effect of slurry pH was examined by operating Reactor 2A as a slurry-immobilised (SLIMM) reactor and comparing results for 2 different initial slurry pH conditions against the standard (neutral) pH of 7 (for a 5 g/L TiO_2 suspension in lake water). 1M H_2SO_4 (and dilutions thereof) were used as additive to adjust pH. Algal extract (containing microcystin LR) was added to 5 L lake water (Zeekoevlei) with the addition of a catalyst suspension loading of 5 g/L TiO_2 prior to photocatalytic treatment. All system parameters were evaluated at standard reference levels (Table 5.18) and the standard coating procedure applied for the sheet module.

The objectives of this study were to (1) assess the efficiency of LR photocatalytic oxidation as a function of initial slurry pH (2) monitor the inhibiting effect of sulphate ions and (3) compare oxidation results as a function of reactor configuration (viz.: SLIMM versus IMM reactor).

Results and Discussion:

Table 5.27: **Microcystin LR concentration as a function of irradiation time and initial slurry pH. (Concentrations normalised)**

Irradiation Time (min)	Microcystin LR (ug/L)	
	Slurry pH 7 (neutral)	Slurry pH 3
0	30	42
2	27	36
4	23	28
6	19	23
8	15	18
10	14	15
12	11	ND
14	ND*	
16		
18		
20		
$10^2\ k_{obs}$ (min^{-1})	8.48	10.61
Half-life (min)	8.2	6.5
R^2	0.99	0.99

Note: ND* = Not detected; Limit of Detection = 10 ug/L

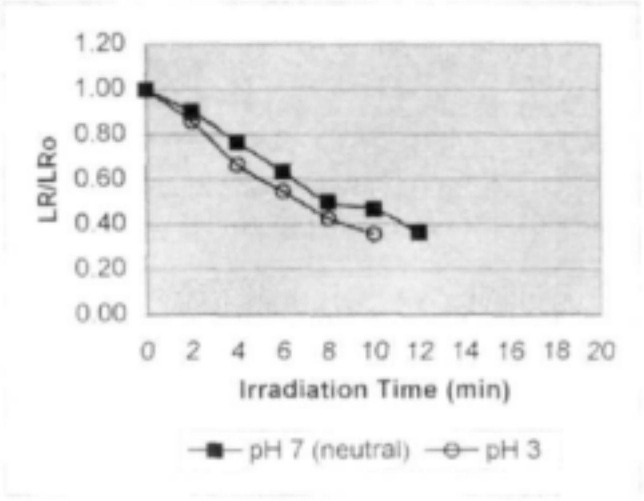

Figure 5.27: Microcystin LR concentration as a function of irradiation time and initial slurry pH. (Concentrations normalised)

The results obtained from this experiment (Table 5.27 and Figure 5.27) indicated that :

- the first order oxidation rate constant increases with approximately 10% when adjusting the initial pH of the 5g/L TiO_2 slurry from 7 to 3 with H_2SO_4. This result indicates the utility of the SLIMM reactor to enhance oxidation of microcystin LR, which is otherwise relatively insensitive to pH variation in IMM reactor configuration ;
- the detrimental effect of sulphate ions is countered when operating the SLIMM reactor ;
- the first order rate constant for LR oxidation is fairly independent of reactor configuration (viz.: SLIMM rates are similar to IMM rates). This result is also obtained for RR using identical conditions and demonstrates the utility of the IMM reactor configuration for treating recalcitrant microcystins such as LR and RR.

Based on the results obtained above, it is concluded that Reactor 2A can be successfully operated as an immobilised-bed system for the treatment of microcystins in natural waters. The operation of slurry-phase reactors do not present a significant improvement on the former configuration.

(j) Gas Flow Rate (Immobilised-Bed Reactor)

Introduction and Objectives:

The effect of oxygen gas flow rate was examined by operating Reactor 2A as an immobilised-bed (IMM) reactor and comparing results for an elevated rate of 20 L/minute against the standard rate applied (5 L/minute O_2). Algal extract (containing microcystins LR and RR) was spiked in lake water from Zeekoevlei (natural pH 8) prior to photocatalytic treatment. All system parameters were evaluated at standard reference levels (Table 5.18) and the standard coating procedure applied for the sheet module. The objectives of this study were to (1) compare rates of photocatalytic oxidation as a function oxygen flow rate and (2) assess the change in oxidation susceptibility for each variant.

Results and Discussion:

Table 5.28: **Microcystin concentration as a function of irradiation time and oxygen flow rate (in L/min). (Concentrations normalised)**

Irradiation Time (min)	Microcystins (ug/L)			
	LR		RR	
	Gas Flow Rate (L/min O_2)		Gas Flow Rate (L/min O_2)	
	5	20	5	20
0	59	60	66	145
2	43	40	53	109
4	35	NA**	43	86
6	34	30	36	68
8	32	15	35	40
10	23	NA	31	41
12	13	ND	23	21
14	10		16	11
16	ND*		ND	ND
18				
20				
10^2 k_{obs} (min^{-1})	11.74	15.30	8.99	17.29
Half-life (min)	5.9	4.5	7.7	4.0
R^2	0.92	0.92	0.96	0.95

Note: **ND* = Not detected; Limit of Detection = 10 ug/L**
NA = Not analysed**

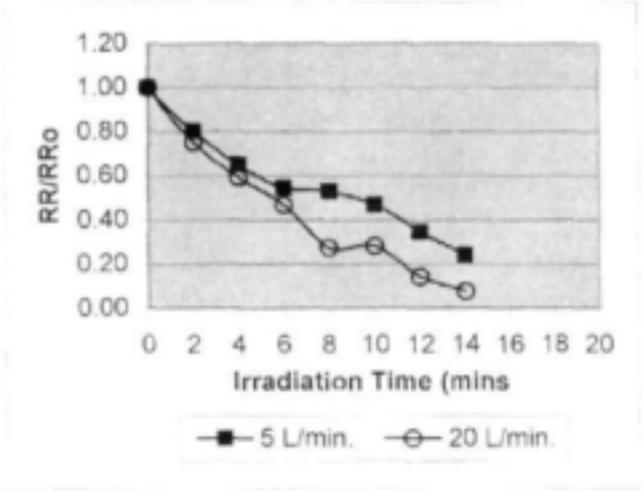

Figure 5.28: Microcystin RR concentration as a function of irradiation time and oxygen flow rate (in L/min). (Concentrations normalised)

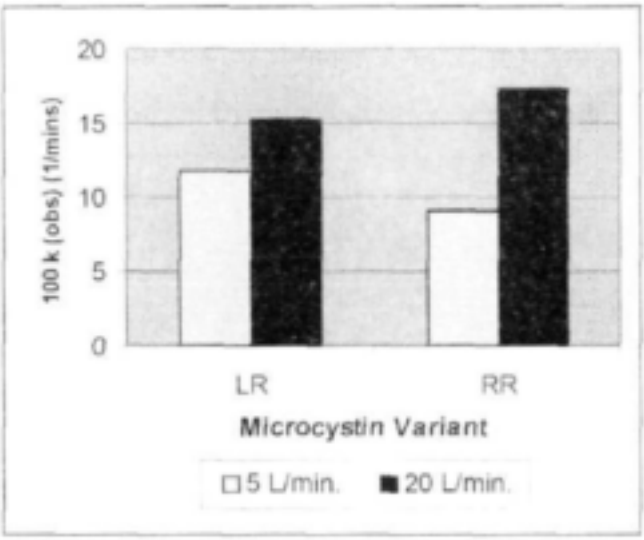

Figure 5.29: Observed first order rate constants for oxidation of microcystins as a function of microcystin variant and oxygen flow rate (in L/min)

The results obtained from this experiment (Table 5.28 and Figures 5.28-5.9) indicated that :

- the first order rate constants for oxidation of both variants (LR and RR) increase substantially when increasing the oxygen flow rate from 5 to 20 L/minute. This result confirms the importance of oxygen for efficient photocatalytic oxidation ;

- the observed increase is non-linear which indicates that the aqueous solution becomes saturated with oxygen during prolonged recirculation time. This result motivates the use of a convenient lower flow rate for photocatalytic oxidation ;
- the rate constant for LR oxidation increases with approximately 30%, while the corresponding RR constant is almost doubled. This comparison indicates that RR may be more susceptible to photocatalytic oxidation than LR. This is in contrast to earlier results ;
- the discrepancy in initial concentration of RR is due to underlying interferences experienced during the HPLC analytical procedure ;
- the normalisation of concentration data facilitates comparison of experimental runs using identical theoretical starting concentrations, but with variable observed starting concentration (see Figure 5.28).

Based on the results obtained above, it is evident that variation in the oxygen gas purge rate presents another useful parameter for comparing photocatalytic oxidation susceptibility of different microcystin variants.

(k) Catalyst Impregnation Loading (Immobilised-Bed Reactor)

Introduction and Objectives:

The effect of catalyst impregnation loading was examined by operating Reactor 2A as an immobilised-bed (IMM) reactor and comparing results for an elevated impregnation loading against the standard loading of the fibre glass sheet module. The conditions for enhanced coating were similar to the standard coating procedure with the exception of a 20 g/L TiO_2 suspension used in stead of the standard 5 g/L. This alteration resulted in a net mass loading of 21.6 g TiO_2 on the sheet module (viz.: 24.5 g/m^2) compared to the original loading of 7.5 g/sheet (viz.: 8.5 g/mm^2). Algal extract (containing microcystins LR and RR) was spiked in lake water from Zeekoevlei (natural pH 8) prior to photocatalytic treatment. The remainder of the system parameters were evaluated at standard reference levels (Table 5.18). The objectives of this study were to (1) compare rates of photocatalytic oxidation as a function catalyst impregnation loading and (2) assess the change in oxidation susceptibility for each variant.

Table 5.29: Microcystin concentration a function of irradiation time, microcystin variant and catalyst impregnation loading (in g TiO_2/m^2)

Irradiation Time (min)	Microcystins (ug/L)			
	LR		RR	
	Catalyst Impregnation Loading (g/m^2)		Catalyst Impregnation Loading (g/m^2)	
	8.5*	24.5**	8.5	24.5
0	59	60	66	127
2	43	43	53	90
4	35	34	43	70
6	34	32	36	65
8	32	24	35	56
10	23	19	31	41
12	13	ND	23	21
14	10		16	ND
16	ND***		ND	
18				
20				
10^2 k_{obs} (min^{-1})	11.74	10.80	8.99	12.85
Half-life (min)	5.9	6.4	7.7	5.4
R^2	0.92	0.98	0.96	0.92

** Catalyst suspension loading = 5 g/L TiO_2*

** Catalyst suspension loading = 20 g/L TiO_2

***ND = Not detected ; Limit of detection = 10 ug/L

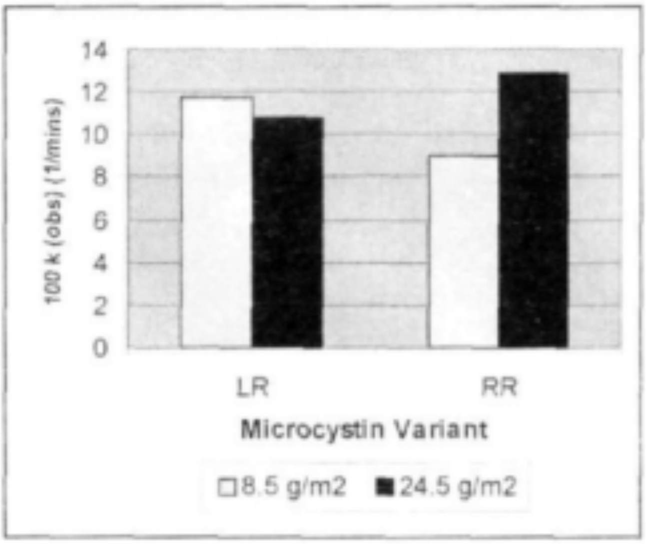

Figure 5.30: Observed first order rate constant for oxidation of microcystins as a function microcystin variant and catalyst impregnation loading (in g TiO_2/m^2)

The results obtained from this experiment (Table 5.29 and Figure 5.30) indicated that :

- the rate constants for oxidation of microcystins LR and RR changes marginally with a threefold increase in catalyst impregnation loading of the sheet module. This result demonstrates the utility of Reactor 2A to be operated as IMM reactor with economical (low) impregnation loadings of TiO_2 .

Based on the results obtained above, it is evident that the degree of interaction between microcystin molecules and TiO_2 on a stationary support is an important factor for scaling-up of immobilised-bed reactor configurations. The attainment of sufficient interaction at the lowest practical impregnation loading should yield high conversion (oxidation) rates when the reactor is optimised for microcystin removal via statistical techniques and comprehensive reactor modelling.

5.2.2 Sequential Single Pass Mode

(a) System Parameters

The photocatalytic oxidation of three variants of microcystins in water was investigated by operating Reactor 2A as an immobilised-bed (IMM) reactor. The following system parameters were evaluated at discrete levels in terms of the defined kinetic response functions for this mode of operation (see Section 3.3 and Table 5.30):

Table 5.30: System parameters for microcystin study (Reactor 2A; Sequential Single Pass Mode)

Parameter	Assigned Levels
Catalyst Loading for Impregnation (g/L)	5
Volumetric Flow Rate (L/min)	2.0[a]
Horizontal Irradiation Distance (cm)	15
Microcystin Variants	YA, YR and LR
Reaction Volume (L)	5
Water Matrix	Lake water
Gas Purge	Oxygen
Gas Flow Rate (L/min O_2)	5
Number of UV-C lamps for Irradiation	12[b]
UV Contact Time (sec)	4.1

Note: * Denotes standard reference level of parameters
a Surface flow rate = 136 L/hr/m^2
b UV Irradiance = 204.5 W/m^2 (=20.45 mW/cm^2)

(b) Representative Example (Immobilised-Bed Reactor)

Introduction and Objectives:

The sequential single pass operation was examined for the treatment of microcystins in Reactor 2A by executing a series of 10 consecutive single passes. The corresponding UV residence time (contact time) amounted to 4.1 sec per single pass (N). Algal extract (containing microcystins YA, YR and LR) was spiked in lake water from Zeekoevlei (natural pH 8) prior to photocatalytic treatment. The experiment entailed the reuse of the original water sample for each consecutive single pass without pre-treatment. A 100 mL aliquot of water was collected for analysis between each single pass. All system parameters were evaluated at standard reference levels (Table 5.30) and the standard coating procedure was applied to the sheet module.

The objectives of this study were to (1) determine the number of passes required for complete removal of the three variants as a function of relative initial concentration (2) compare the oxidation susceptibilities of the respective variants via normalisation of data and (3) compare the kinetic results with those obtained when operating the reactor in recirculation mode.

Results and Discussion:

Table 5.31: : Microcystin concentration as a variant and single pass number (N).,(where each N = 4.1 sec of UV irradiation)

Single Pass Number (N)	Microcystins (ug/L)		
	YA	YR	LR
0	21	71	49
1	17	57	18
2	NA**	47	14
3	9	30	10
4	ND*	20	ND
5		19	
6		16	
7		15	
8		ND	
9			
10			
10^2 k (N) ($pass^{-1}$)	28.75	24.23	50.19
Half-Life (passes)	2.4	2.9	1.4
R^2	0.99	0.95	0.90

Note: ND* = Not detected; Limit of Detection = 10 ug/L
NA** = Not analysed

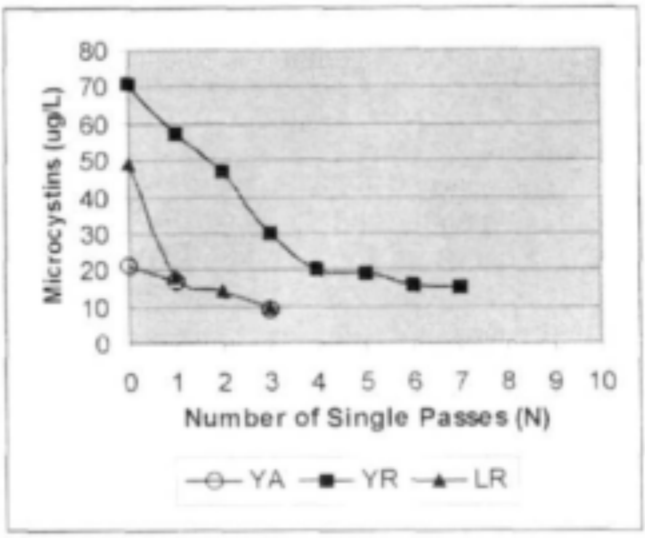

Figure 5.31: Microcystin concentration as a function of variant and single pass number (N)..(where each N = 4.1 sec of UV irradiation)

Table 5.32: Microcystin concentration as a function of cumulative time of irradiation **and variant in sequential single pass experiments**

Cumulative Time of Irradiation (sec)	Microcystins (ug/L)		
	YA	YR	LR
0.0	21	71	49
4.1	17	57	18
8.2	NA**	47	14
12.3	9	30	10
16.4	ND*	20	ND
20.5		19	
24.6		16	
28.7		15	
32.8		ND	
36.9			
41.0			
10^2 k (sec^{-1})	7.01	5.91	12.24
Half-life (sec)	9.9	11.7	5.7
R^2	0.99	0.95	0.90
Initial Rate (ugL^{-1}sec^{-1})	1.47	4.20	6.00

Note: **ND* = Not detected ; Limit of detection = 10 ug/L**
NA = Not analysed**

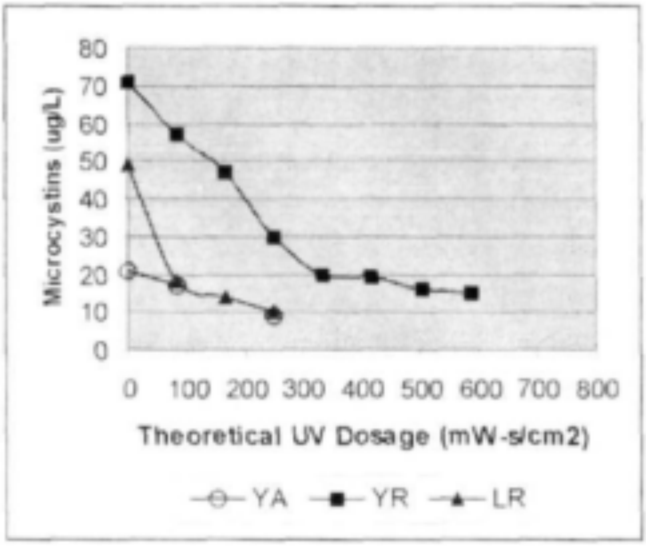

Figure 5.32: Microcystin concentration as a function of theoretical UV dosage (in mW-sec/cm²). (where each N = 4.1 sec of UV irradiation)

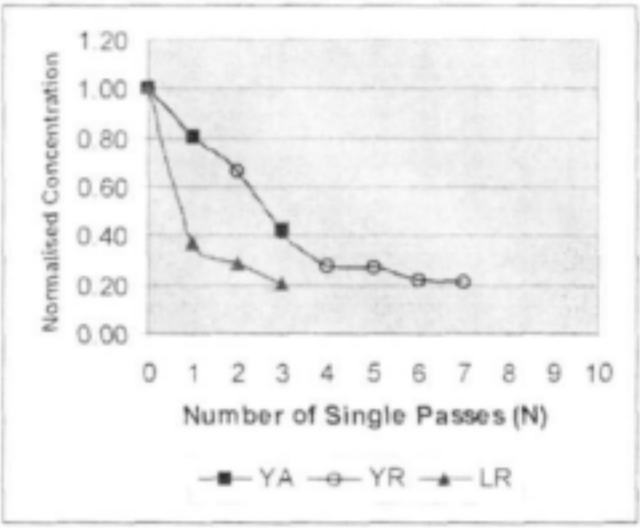

Figure 5.33: Microcystin concentration as a function of variant and single pass number (N). (Concentrations normalised)

The results obtained from this experiment (Tables 5.31-5.32 and Figures 5.31-5.33) indicated that :

- first order exponential decay kinetics apply for the oxidation of microcystins YA, YR and LR when operating Reactor 2A as an IMM reactor in sequential single pass mode ;
- the initial YA concentration (21 ug/L) decreases to below the detection limit (10 ug/L) within 4 single passes ;

- the initial LR concentration (49 ug/L) decreases to below the detection limit (10 ug/L) within 4 single passes ;
- removal of all 3 variants to below the detection limit requires a theoretical UV dosage in the order of 670 mW-s/cm^2 . This dosage is equivalent to approximately 33 seconds of UV exposure in the reactor ;
- the oxidation susceptibility of LR in natural water is markedly enhanced when operating Reactor 2A in sequential single pass mode. Both the first order rate constant and initial reaction rate (expressed in ug/L/sec) are higher for LR compared to YA and YR. This result is auspicious in terms of using an IMM reactor configuration for large-scale treatment of recalcitrant microcystins such as LR ;
- normalisation of concentration data facilitates comparison of microcystin variants in terms of rate constants and oxidation rates. This procedure should be used to evaluate the oxidation susceptibility of all variants under conditions of similar starting concentrations (viz.: at ultra-low ug/L levels ;
- the first order rate constants for treatment of microcystins in sequential single pass mode are generally 2 orders of magnitude greater than the analogous rate constants in recirculation mode. For example, the rate constant for LR oxidation in the IMM reactor increases from *ca* 0.08 min^{-1} (recirculation mode) to *ca* 7.3 min^{-1} (sequential single pass mode). The corresponding initial reaction rate increases from ca 1.8 to 260 ug/L/minute (thus with a factor of 200).

Based on the results obtained above, it is evident that Reactor 2A can be efficiently operated as an IMM reactor in sequential single pass mode for the photocatalytic oxidation of microcystins in natural water. Moreover, the utility of the reactor for treatment of recalcitrant microcystins (such as LR) is clearly demonstrated in the sequential single pass mode.

(c) Cost Calculation

A preliminary cost calculation was made for the photocatalytic oxidative treatment of microcystins YA, YR and LR in natural waters, based on the operation of Reactor 2A as an immobilised-bed system in the sequential single pass mode. The calculation was done in view of the following assumptions :

- first order kinetics
- idealised plug-flow reactor conditions
- a constant electrical energy per order (EE/O)

Bolton's formula for EE/O in idealised plug-flow reactors has been defined earlier (in Section 2.1.3) :

$$EE/O = P / F \times \log (c_0 / c_f)$$

Where:
P = Lamp power (in kW)
F = Volumetric water flow rate (in m^3/h)
c_o = Initial concentration
c_f = Final concentration
EE/O = $kWh/order/m^3$

Thus, for microcystin YA as example, the EE/O and cost (per m^3) for the photocatalytic oxidation of an initial concentration of 21 ug/L to below the limit of detection (10 ug/L) can be calculated as follows :

- orders of removal = log (21/10) = 0.322
- P = 12 x 15 W = 180 W = 0.18 kW
- F = 2 L/minute = 120 L/h = 0.12 m^3/h

EE/O amounts to: (0.18)/(0.12 x 0.322) = 4.66 $kWh/order/m^3$. At a unit price of 11.8 c/kWh in the Stellenbosch area, the cost to reduce 21 ug/L YA with one order of magnitude (2.1 ug/L) amounts to 55c / m^3 of water. A further order of magnitude reduction (to 0.21 ug/L) will double the cost, since EE/O is a constant per order.

Calculations for YR and LR are done similarly (as summarised in Table 5.33).

Table 5.33: EE/O and cost (per m^3) calculations for the photocatalytic treatment of microcystins in Reactor 2A (Lamp power = 0.18 kW ; .flow rate = 0.12 m^3/h)

Microcystin Variant	Initial Concentration (ug/L)	Final Concentration (ug/L)	Orders of Removal	EE/O ($kWh/order/m^3$)	Operation Cost (per order removal)
YA	21	10	0.322	4.66	55c / m^3
YR	71	10	0.851	1.76	21c / m^3
LR	49	10	0.690	2.17	26c / m^3
YA + YR + LR	141	10+10+10	0.672	2.23	26c / m^3

This figures quoted above are only with regard to the electrical energy cost incurred in the photocatalytic oxidation process. A complete cost analysis will require the inclusion of other cost factors such as (1) capital cost (2) operation/maintenance of reactor utilities (3) amortised investment and several more (Bolton *et al.*, 1996).

5.3 TREATMENT OF NOM IN WATER

5.3.1 Recirculation Mode

(a) System Parameters

The photocatalytic oxidation of NOM in raw natural water was investigated by operating Reactor 2A as (1) immobilised-bed (IMM) and (2) combined slurry-immobilised (SLIMM) reactor. A highly coloured water (mean initial TOC 26.4 mgC/L) from the Simonstown *reservoir in the Cape peninsula was used for the experiments. Experimental design* methods were employed in parametric studies. The following system parameters were evaluated at discrete levels in terms of first order reaction kinetics and % mineralisation of TOC (see Table 5.34):

Table 5.34: System Parameters for NOM study (Reactor 2A; Recirculation Mode)

Parameter	Assigned Levels
Catalyst Suspension Loading (g/L)	0; 1; 10
Volumetric Flow Rate (L/min)	1[a]; 2*[b]
Horizontal Irradiation Distance (cm)	15*
Initial TOC (mgC/L)	26.4
Reaction Volume (L)	3*
Water Matrix	SimonsTown raw water
pH range studied	3 to 9
Gas Purge	Oxygen*
Gas Flow Rate (L/minO_2)	2.5*
UV lamps[c]	Germicidal (UV-C)*

Note: * Denotes standard reference level of parameters
a Surface flow rate = 70 L/hr/m^2
b Surface flow rate = 135 L/hr/m^2
c Power input/area = 204.5 W/m^2 = 12 x 15W lamps (per 0.88 m^2)

(b) UV Absorbance and TOC Calibrations

Introduction and Objectives:

UV (254 nm) absorbance and TOC determinations were used to monitor the photocatalytic oxidation of NOM.

A calibration series was constructed with 100% concentration representing the undiluted raw water and the corresponding lower percentages represented by distilled water dilutions. Analytical determinations for UV absorbance and TOC were executed according to standard methodology described elsewhere (Cloete, 1999).

The trihalomethane formation potential (THMFP) determination of NOM was also considered to monitor the photocatalytic oxidation of NOM. Being a very time-consuming process, it was eventually discarded.

Results and Discussion :

Table 5.35: UV absorbance and TOC of NOM as functions of raw water concentration

Raw water Concentration (%)	UV Absorbance* (254 nm)	TOC content (mg C / L)
0**	0	0
20	0.150	6.5
40	0.382	11.9
60	0.664	16.3
80	0.880	20.3
100	1.139	26.4

* Absorbance as determined with an 1 cm quartz cell

** Distilled water

The following calibration graphs were constructed :

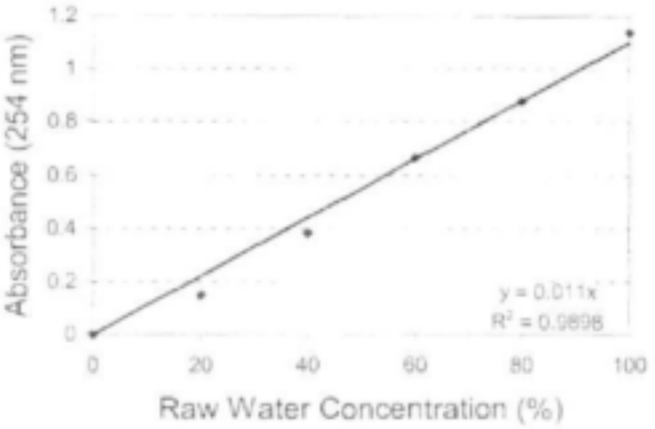

Figure 5.34: Absorbance of NOM as a function of raw water concentration

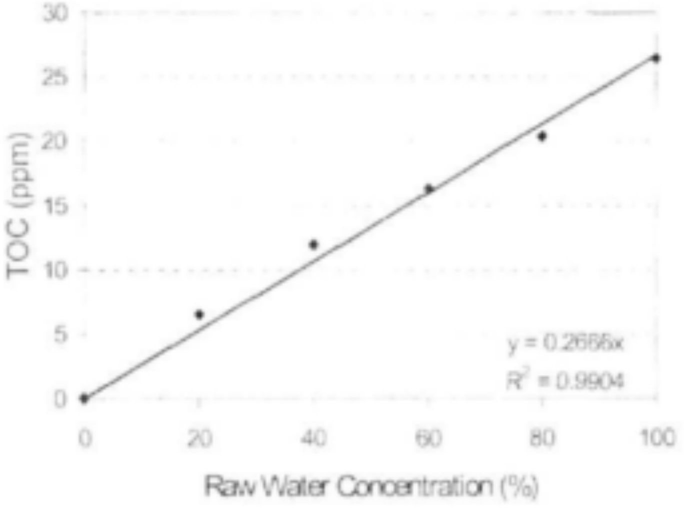

Figure 5.35: TOC as a function of raw water concentration

The results obtained from these experiments (Table 5.35 and Figures 5.34-5.35) indicated that :

- a linear relationship exists between UV absorbance at 254 nm and the TOC of a specific NOM containing water sample.

(c) Screening Study (Immobilised-Bed Reactor)

Introduction and Objectives:

A series of 8 experiments were conducted. 3 Parameters were varied according to a 2^3 factorial design format to create a systematic variation in experimental conditions. These parameters were:

- TiO_2 impregnation loading (expressed in terms of suspension loading)
- Solution pH
- Volumetric Flow Rate through the reactor

The screening design matrix below (Table 5.36) contains the combination of parameter levels for each of the 8 runs.

Results and Discussion :

Table 5.36: Screening design matrix for IMM reactor study

Run	Parameter		
	Catalyst Impregnation Loading (g/L TiO_2)*	Solution pH	Volumetric Flow Rate (L/min)
1	10	8	2
2	10	8	1
3	10	3	2
4	10	3	1
5	1	8	2
6	1	8	1
7	1	3	2
8	1	3	1

50 mL samples were collected at various time intervals, including a zero-time sample, which was collected prior to commencement of a particular irradiation run. Samples were filtered with Whatman No.42 filter paper prior to UV absorbance and TOC determinations.

Results for e.g. UV measurement are summarised in Table 5.37:

Table 5.37: Results of UV measurement by 2^3 Factorial Design

Run	Sampling Time (min)				
	0	5	10	20	30
1	1	0.666	0.509	0.337	0.128
2	1	0.465	0.459	0.166	0.076
3	1	0.312	0.273	0.195	0.124
4	1	0.326	0.307	0.195	0.110
5	1	0.513	0.500	0.238	0.149
6	1	0.657	0.587	0.399	0.245
7	1	0.291	0.306	0.176	0.141
8	1	0.287	0.281	0.200	0.122

All UV absorbance and TOC measurements were normalised in order to facilitate comparisons. Normalisation was performed as follows:

$$\text{Normalised Signal} = \frac{C_t}{C_0}$$

where,

C_t =Response measurement at time t

C_0 =Response measurement at time 0

Table 5.38: Normalised UV(254 nm) absorbencies of NOM

Run	Normalised UV$_{254}$ Absorbencies				
	Irradiation Time (min)				
	0	5	10	20	30
1	1	0.666	0.509	0.337	0.128
2	1	0.465	0.459	0.166	0.076
3	1	0.312	0.273	0.195	0.124
4	1	0.326	0.307	0.195	0.110
5	1	0.513	0.500	0.238	0.149
6	1	0.657	0.587	0.399	0.245
7	1	0.291	0.306	0.176	0.141
8	1	0.287	0.281	0.200	0.122

The table above was converted to yield mineralisation percentages (see Table 5.39):

Table 5.39: Mineralisation percentages of NOM

Run	Mineralisation %				
	Irradiation Time (min)				
	0	5	10	20	30
1	0	33.4	49.1	66.3	87.2
2	0	53.5	54.1	83.4	92.4
3	0	68.8	72.7	80.5	87.6
4	0	67.4	69.3	80.5	89.0
5	0	48.7	50.0	76.2	85.1
6	0	34.3	41.3	60.1	75.5
7	0	70.9	69.4	82.4	85.9
8	0	71.3	71.9	80.0	87.8

The results obtained from these experiments (Table 5.35 and Figures 5.34-35) indicated that NOM can be removed by photocatalytic oxidation in Reactor 2A.

(d) Optimisation Study A (Combined Slurry-Immobilised Reactor)

Introduction and Objectives:

A 2^3 factorial design was chosen for the optimisation of parameters that could possibly influence the photocatalytic efficiency of the reactor

The following factors were selected for the factorial experiment:

- TiO_2 Slurry Concentration
- Raw water Concentration
- Slurry pH

TiO_2 impregnation of fibre glass sheet modules were not executed prior to commencement of runs, thus rendering an initial catalyst impregnation loading of 0 g/L. The absolute loading would be determined by the reaction conditions and time of recirculation.

The response used was the TOC reduction (%) after a pre-selected time interval. The response function can be defined by the following equation:

$$\%\,\text{Reduction} = \frac{C_0 - C_t}{C_0} \text{x} 100$$

where

C_0= TOC content at time interval t=0 (in ppm C)
C_t= TOC content at time interval t=t (in ppm C)

The factorial design matrix is presented in Table 5.40, 50 mL samples were collected, at set intervals as before, including a zero-time sample. Samples were filtered with a double layer of Whatman No.42 filter paper.

Results and Discussion:

Table 5.40: Factorial design matrix for optimisation study

Run	Parameter		
	Catalyst Suspension Loading ($g/L\ TiO_2$)*	Slurry pH	Raw Water Concentration (%)
1	10	6.5	100
2	10	6.5	50
3	10	3	100
4	10	3	50
5	1	6.5	100
6	1	6.5	50
7	1	3	100
8	1	3	50

Response values are summarised in Table 5.41:

Table 5.41: Factorial Design Response Values

Run	TOC (0 min.) (mg C / L)	TOC (120 min.) (mg C / L)	Mineralisation (%)
1	25.06	3.70	85.2
2	10.97	4.16	62.1
3	21.39	4.60	78.5
4	7.89	4.07	48.4
5*	16.39	2.03	87.6
6	7.89	4.69	40.6
7	14.19	4.93	65.3
8	8.33	3.03	63.6

***Best result**

An ANOVA analysis was performed to determine the significance of the various parameters under investigation. The significance was described in terms of a null-hypothesis probability (p), where the boundary level of significance was assigned to be $p=0.05$. For $p<0.05$, the null hypothesis is proved to be invalid with a certainty of 95%. Variation of such a parameter would exert a significant effect on the response measured. If $p>0.05$, the opposite is proved, and the corresponding parameter can be discarded within the constraints of the particular experimental design with a certainty factor of 95%.

Response surface methodology (RSM) usually requires the combination of a mathematical model with the chosen experimental design and corresponding response data. Polynomials of linear or quadratic form can be used. In this case, a quadratic polynomial model indicated no significant factors via the ANOVA analysis. By using a linear model for data processing, we assumed that no interactions occurred between the relevant factors. The response measured could be expressed in terms of the following equation:

$$Z = \beta_0 + \beta_1X_1 + \beta_2X_2$$

where
Z=response function
X_1,X_2=experimental factors
β_0=intercept on response axis
β_1, β_2=gradient for each factor

The following null-hypothesis probabilities were calculated by STATISTICA (See Table 5.42):

Table 5.42: ANOVA results for parameter significance testing

Parameters	p-Value
TiO_2	0.51
pH	0.72
NOM concentration	0.04*

*** statistically significant effect**

The results obtained from these experiments (Tables 5.35-35.9) indicated that :

- Only the NOM concentration reveals an ANOVA probability less than 0.05 and can therefore be classified as being significant. Therefore, an increase in NOM content results in greater % TOC reduction. Similar response increases with increase in pollutant concentration(s) have been observed for other photocatalytic oxidation investigations.

- Relative to the NOM concentration, the other 2 parameters exert insignificant effects on the response within their respective regions of variation. This observation suggests that the high TOC levels of the water used negated the relative effects of the other parameters.

In order to investigate the effects of the other 2 parameters in the absence of the dominating effect of the NOM concentration parameter, the existing 2^3 factorial design was divided into two separate 2^2 fractional factorial designs. Each 2^2 fractional matrix represented only one of the 2 selected NOM concentration levels.

The fractional factorial matrices consisted of the following runs (see Table 5.40):

- 100% NOM content: runs 1, 3, 5, 7
- 50% NOM content: runs 2, 4, 6, 8

The results were processed and interpreted via STATISTICA 5.0, assuming a linear mathematical model:

$Z = \beta_0 + \beta_1 X_1 + \beta_2 X_2$

where
Z=response function
X_1, X_2=experimental factors
β_0=intercept on response axis
β_1, β_2=gradient for each factor

Table 5.43: ANOVA results from fractional factorial design

Parameters	p-Value	
	100% NOM Content	50% NOM Content
TiO_2 suspension loading	0.61	0.73
pH	0.31	0.68

The statistical results obtained from this experiment (Tables 5.40 and 5.43) indicated that :

- Both NOM concentration scenarios yield null-hypothesis probabilities with values greater than 0.05, indicating the insignificance of the individual factors within the constraints of the design ;

- the TiO_2 concentration has a positive main effect, which implies that an increase in TiO_2 concentration yields an increase in the % TOC reduction ;

- the pH parameter exhibits conflicting trends as a function of NOM content. A positive main effect is present at high NOM content, while the opposite effect is applicable at low NOM levels ;
- In summary: At high NOM content an increase in both TiO_2 and pH lead to improved reduction in TOC levels, while high TiO_2 and low pH levels yield optimum destruction of NOM substances at low NOM content ;
- The variation in optimum pH could be explained in terms of the ionisation of the functional groups on NOM molecules . In addition, TiO_2 exhibits a charge variation as a function of pH according to the following equilibria :

$$-\text{Ti-OH}_2^+ \overset{H^+}{\Leftrightarrow} -\text{Ti-OH} \overset{H^+}{\Leftrightarrow} -\text{Ti-O}^-$$

Interaction between these ionised species explains the observed behaviour of the system as a function of pH.

(e) Optimisation Study B (Combined Slurry-Immobilised Reactor)

Introduction and Objectives:

The unusual effect of pH on the trend toward optimum TOC reduction indicated that pH variation affect either (1) the ionisation of the TiO_2 particles or (2) the functional groups on the NOM substances. In this study, response surface methodology (RSM) was used for in an attempt to locate and fine-tune a condition for maximum TOC reduction. Hence, the main objective of this study was to optimise the TOC reduction rate in terms of pH and TiO_2 suspension concentration as experimental parameters. The RSM design used was a central composite design (CCD).

Since the fulvic acid (FA) fraction of NOM is soluble over the entire pH range, and the humic acid (HA) fraction is only soluble from pH greater than 7 , two regions of interest were identified for the optimisation of the pH level, namely pH 3-6 and pH 6-9. This was combined with the variation in TiO_2 concentration. Two CCDs were therefore generated. The corresponding α-parameter was set at $\alpha=2^{0.5}$, indicating the span of the design.

A shorter sampling time interval was used compared to previous experiments. This was done in view of optimising the initial rate of photocatalytic oxidation with respect to the undiluted NOM water sample containing a theoretical HA content of 100%.

The system parameters were evaluated at the following levels :

TiO_2 suspension concentration : See Table 5.44
Water Matrix : Betty's Bay raw water
Reaction Volume : 3 litres
Slurry pH : See Table 5.44
Volumetric Flow Rate : 2 L/minute
Reactor Configuration : Combined slurry immobilised bed (SLIMM)
Operation Mode : Recirculation
O_2 flow rate : 2.5L/minute
Sampling Intervals (min) : 0 and 15
Analytical Method : TOC analysis
Response : % Reduction in TOC

The reproducibility of the CCD is determined in triplicate by performing 3 runs in the centre of the experimental region, i.e. Runs 1, 6 and 11 (see Table 5.44).

The response function selected was similar to that used for the factorial design, namely the % reduction of TOC achieved within 15 minutes of reaction. Since it was already known that parameter interactions are mainly insignificantly, a linear mathematical model was chosen for each pH region, with the aim of generating the corresponding response surfaces.

Table 5.44: Design matrix for optimisation study (2-parameter Central Composite Design)

Run	pH Range 3-6		pH Range 6-9	
	Slurry pH	Catalyst Suspension Loading (g/L TiO_2)	Slurry pH	Catalyst Suspension Loading (g/L TiO_2)
1	4.50	6.00	7.50	6.00
2	3.00	2.00	7.50	11.66
3	6.00	2.00	9.00	2.00
4	3.00	10.00	9.62	6.00
5	6.00	10.00	9.00	10.00
6	4.50	6.00	7.50	6.00
7	2.38	6.00	6.00	40.00
8	6.62	6.00	5.38	6.00
9	4.50	0.34	6.00	2.00
10	4.50	11.66	7.50	0.34
11	4.50	6.00	7.50	6.00

The results obtained for the pH range 3 – 6 are presented in Table 5.45.

Table 5.45: Experimental Results for pH range 3 – 6

Run	TOC (0 min.) (mg C / L)	TOC (15 min.) (mg C / L)	Mineralisation (%)
1	23.7	15.9	32.9
2	26.6	16.3	38.7
3	27.6	17.2	37.7
4	24.8	23.0	7.3
5	25.8	17.7	31.4
6	27.7	18.7	32.5
7	27.9	22.5	19.4
8	23.0	16.6	27.8
9	27.3	18.2	33.3
10	25.4	19.0	25.2
11*	27.5	16.5	40.0

*Best result

Table 5.46: ANOVA results (pH 3-6)

Parameter	p-Value
Slurry pH	0.73
TiO_2 suspension concentration	0.08

The statistical results obtained for the pH 3-6 range (Table 5.46) indicated that :

- the TiO_2 suspension loading parameter is significant for a 0.1 null-hypothesis probability, but not for a 0.05 level ;
- the effect of slurry pH is insignificant in terms of TOC removal ;
- the TiO_2 parameter exerts a negative main effect. This results implies that lowering the catalyst loading will increase the removal rate of TOC, which is contradictory to the findings from the fractional factorial designs used earlier.

The results obtained for the pH range 6-9 are presented in Table 5.47:

Table 5.47: Experimental Results for pH range 6 – 9

Run	TOC (0 min.) (mg C / L)	TOC (15 min.) (mg C / L)	Mineralisation (%)
1	20.9	17.7	15.3
2	16.8	14.6	13.1
3	16.9	15.0	11.2
4	22.2	15.2	31.5
5	23.1	18.5	19.9
6*	24.0	12.8	46.7
7	18.9	12.4	34.4
8	20.5	18.2	11.2
9	22.0	18.2	17.3
10	24.1	15.6	35.3
11	23.7	18.4	22.4

* Best result

Table 5.48: ANOVA results (pH 6-9)

Parameter	p-Value
Slurry pH	0.13
TiO_2 suspension concentration	0.09

The statistical results obtained for the pH 6-9 range (Table 5.48) indicated that :

- both parameters exert a statistically significant effect on the response function if a null-hypothesis probability level of 0.1 is adopted ;
- the effect of slurry pH reduces substantially if a probability level of 0.05 is adopted.
- a negative main effect exists for the slurry pH parameter. This result could be explained in terms of the reduced adsorption of pollutant species and surface hydroxyl ions at high pH values (where TiO_2 exists as TiO^- species).

(f) Optimisation Study C (Combined Slurry-Immobilised Reactor)

Introduction and Objectives:

A more thorough picture of the response variation as a function of pH was required in view of the variable effects observed earlier. The entire pH range (i.e. from pH 3 to pH 9) was scanned by merging the 2 central composite designs (used in the previous section), thus generating an unique superimposed model. The objective of this study was therefore to assess the utility of a user-defined superimposed design for locating optimised pH conditions via response surface methodology (RSM).

The responses from the central composite designs (Tables 5.45 and 57) were combined and the corresponding parameter main and interaction effects re-calculated using STATISTICA.

Results and Discussion:

A linear-quadratic model was selected to calculate 2-way interactions in addition to parameter main effects. The corresponding response function was represented by the following polynomial equation:

$$Z = \beta_0 + \beta_1 X_1 + \beta_2 X_2 + \beta_{11} X_1^2 + \beta_{22} X_2^2 + \beta_{12} X_1 X_2$$

where,
Z: response function
X_1, X_2: experimental parameters
β_0: intercept on response axis
β_1, β_2: gradient for each parameter main effect
β_{11}, β_{22}: coefficients for quadratic main effects
β_{12}: interaction term; combined effect of the two parameters

The corresponding ANOVA results are presented in table 5.49 :

Table 5.49: Anova Results (L: linear; Q: quadratic)

Factors	p-Value
pH (L)	0.10
pH (Q)	0.002*
TiO_2 Concentration (L)	0.61
TiO_2 Concentration (Q)	0.51
pH - TiO_2 Interaction (Q)	0.006*

***indicates statistical significance**

The following regression equation was generated:

$$Z=17.15+11.47*X_1 - 1.48*X_1^2 - 4.07*X_2 - 0.09*X_2^2+0.82*X_1*X_2$$

Where : X_1 = slurry pH
X_2 = TiO_2 suspension concentration (viz.: catalyst suspension loading)

A rising ridge type response surface is generated (Figure 5.36), which clearly illustrates the statistical significance of the 2-way interaction as calculated. The corresponding contour plot (Figure 5.37) confirms the existence of the ridge and an optimised pH-TiO_2 condition.

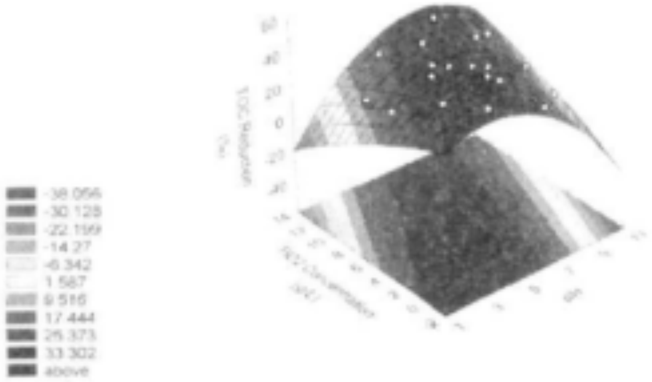

Figure 5.36: Response surface illustrating TOC removal as a function of slurry pH and TiO_2

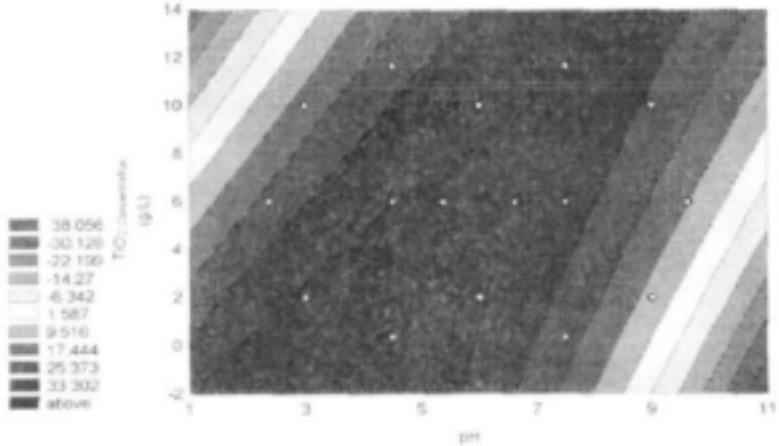

Figure 5.37: Contour plot illustrating a cross-section of the rising ridge response surface

The results obtained from these experiments (Table 5.49 and Figures 5.36-5.37) indicated that :

- from Table 5.49, the significance of both the quadratic pH effect (X_1^2), as well as the 2-way effect between pH and TiO_2 (X_1X_2) is clear ;
- the significance of these factors facilitate the curved nature of the response surface;
- the β_{11} and β_{22} coefficients characterise the parabolic nature of the response surface. The calculated negative values for these coefficients correspond with the rising ridge nature of the response surface (Figure 5.36) ;
- β_{12} (the interaction term) is significant and effects the asymmetry of the ridge across the surface. An optimised range exists for the TOC removal response function and stretches diagonally across the surface, from low pH (at low TiO_2) to high pH (at high TiO_2) ;
- The observed optimum condition (Figure 5.37) is :
- TiO_2 = 7.80 g/L
- pH = 6.20

5.3.2 Single Pass Modes

(a) System Parameters

The photocatalytic oxidation of NOM in raw natural water with a TOC of 41.6 mg C / L was investigated by operating Reactor 2A as an immobilised-bed (IMM) reactor. The following system parameters were evaluated at discrete levels in terms of the defined first order kinetic responses for these modes of operation (Table 5.50) :

Table 5.50: System Parameters for NOM study (Reactor 2A; Single Pass Modes)

Parameter	Assigned Levels
Catalyst Suspension Loading used for impregnation (g/L)	1*
Volumetric Flow Rate (L/min)	2*a
Horizontal Irradiation Distance (cm)	15*
Initial TOC (mgC/L)	41.6
Reaction Volume (L)	3*
Water Matrix Effects	Simonstown raw water
pH region	natural
Gas Purge	Oxygen*
Gas Flow Rate (L/min O_2)	2.5*
UV lamps	Germicidal (UV-C)*b

Note: * Denotes standard reference level of parameters
a Surface flow rate ≈ 135 L/hr/m^2
B UV irradiance = 204.5 W/m^2 = 12 x 15W lamps (per 0.88 m^2)

(b) Representative Example (Immobilised-Bed Reactor)

Introduction and Objectives:

In view of a prospective scaling-up of the existing photocatalytic reactor for potable water treatment, it is essential to optimise the shortest pathway for the production of purified water. The recirculation mode of operation restricts the volume of water to be treated, hence only the single pass (and sequential single pass) modes are regarded as feasible for potential scaling-up operations. The objectives of this study was to (1) determine the number of passes required in Reactor 2A to reach an acceptable level of NOM purified water and (2) assess the magnitude of the mass transfer component by conducting a "dark adsorption" run in tandem with the corresponding UV irradiation experiment.

Results and Discussion:

Table 5.51: TOC and UV absorbance data for single pass experiment

Single Pass Number (N)	TOC (mg C / L)		UV Absorbance (254 nm)	
	UV Photocatalysis	Dark Adsorption	UV Photocatalysis	Dark Adsorption
0	41.6	33.9	1.230	1.188
1	37.7	30.6	0.795	0.742
2	27.0	28.7	0.463	0.642
3	21.2	25.6	0.289	0.648
4	21.6	25.5	0.178	0.678
5	18.9	25.4	0.139	0.728
6	18.1	26.7	0.104	0.798
7	17.2	28.4	0.090	0.683
8	17.3	27.7	0.095	0.704
9	17.4	28.0	0.080	0.865
10	19.4	28.4	0.080	0.758

The table above can be converted to mineralisation efficiencies (see Table 5.52).

Table 5.52: Mineralisation of NOM via TOC and UV absorbance measurements

Single Pass Number (N)	TOC (mg C / L)		UV Absorbance (254 nm)	
	UV Photocatalysis	Mineralisation %	UV Photocatalysis	Mineralisation %
0	41.6	0	1.230	0
1	37.7	9.4	0.795	35.4
2	27.0	35.1	0.463	60.7
3	21.2	49.0	0.289	76.5
4	21.6	48.1	0.178	85.5
5	18.9	54.6	0.139	88.7
6	18.1	56.5	0.104	91.5
7	17.2	58.7	0.090	92.7
8	17.3	58.4	0.095	92.3
9	17.4	58.2	0.080	93.5
10	19.4	53.4	0.080	93.5

The results obtained from these experiments (Tables 5.51-2) indicate that :

- a discrepancy exists between the degree (or %) of mineralisation obtained from UV absorbance and TOC measurements. This could be explained on the basis that photocatalytic oxidation is a stepwise process. In the case of NOM, the large molecular species responsible for the UV absorbance are broken down to smaller species without UV absorbance but a contribution to TOC.

Normalised values of TOC were used to generate the following curve (Figure 5.38).

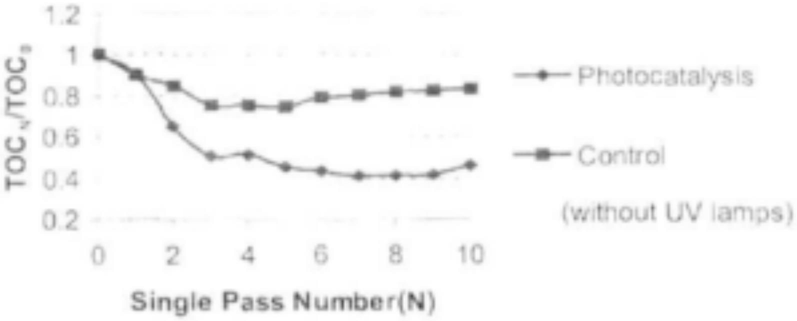

Figure 5.38: Normalised TOC Response Results

The results (as depicted in Figure 5.38) indicated that :

- enhanced removal rates of NOM from the water sample by is due to photocatalytic oxidation ;
- mass transfer of NOM to the fibre glass sheet module (via adsorption) occurs during the first 3 passes of the control experiment. Single passes 4 to 10 show no further adsorption ;
- The corresponding photocatalytic degradation rate adheres to first order exponential decay according to the following equations (as defined in Chapter 3) :

$C(N) = C_0.e^{-kN}$
$\ln C(N)/C_0 = -k N$
where: k = first order decay constant
N = single pass number

Based on the results obtained above, it is clear that Reactor 2A (using an immobilised-bed configuration) is able to oxidise NOM in raw water through TiO_2 photocatalysis.

It was also demonstrated that :

- the reduction in NOM is successfully monitored using TOC analysis ;
- the NOM content is the dominant parameter in attaining optimum degradation efficiency in Reactor 2A. An increase in relative NOM concentration improves the degradation efficiency. Furthermore, scientific publications have advised the use of a constant levels when concentration is considered as parameter in experimental design type optimisations, since the maximum response will invariably proceed in the direction of increasing concentration (Long, 1969) ;
- since the structural characteristics of both TiO_2 and NOM substances facilitated surface modification by pH variation, pH has been identified as an important factor to consider for optimum TOC degradation in NOM laden water. From the superimposed model, a rising ridge was observed as response surface. The ridge stretched diagonally across the pH range 3 to approximately 7. The amount of TiO_2 that was required for optimum TOC degradation was therefore dependent on the pH of the raw water.

These results indicated that Reactor 2A is able to photocatalytically oxidise NOM in raw water with a very high TOC of 41.6 mg C / L. No further work was done on the photocatalytic oxidation of NOM because it became clear from the investigation of the other phases of photocatalytic reactor development that Reactor 2A did not have the potential for upscaling to a commercial reactor due too an inefficient UV contact time.

Cost calculations were not done on the removal of NOM with Reactor 2A due to the relatively high initial TOC values of the raw water used.

It was realised however that reactor 2A (operating in the IMM configuration and in the recirculation mode) should be an excellent system to obtain relative rate constants for the photocatalytic destruction of pollutants in various water matrixes.

(c) Cost Calculation

A preliminary cost calculation was made for the photocatalytic oxidative treatment of NOM (with initial TOC of 41.6 mg C/L) in raw natural water, based on Reactor 2A operated as IMM reactor in the sequential single pass mode. The calculation was done in view of the following assumptions :

- first order kinetics
- idealised plug-flow reactor conditions
- a constant electrical energy per order (EE/O)

Bolton's formula for EE/O in idealised plug-flow reactors has been defined earlier (in Section 2.1.3) :

$$EE/O = P / F \times \log (c_o / c_f)$$

Where: P = Lamp power (in kW)
F = Volumetric water flow rate (in m^3/h)
c_o = Initial concentration
c_f = Final concentration
EE/O = kWh/order/m^3

Thus, taking the above mentioned NOM result as example, the EE/O and cost (per m^3) for the photocatalytic oxidation of an initial TOC concentration (41.6 mg C/L) to 19.4 mg C/L after 10 single passes, can be calculated as follows :

- orders of removal = log (41.6/19.4) = 0.331
- P = 12 x 15 W = 180 W = 0.18 kW
- F = 2 L/minute = 120 L/h = 0.12 m^3/h

EE/O amounts to: (0.18)/(0.12 x 0.331) = 4.53 kWh/order/m^3. At a unit price of 11.8 c/kWh in the Stellenbosch area, the cost to reduce a TOC of 41.6 mg C/L with one order of magnitude (4.16 mg C/L) amounts to 53c / m^3 of water. A further order of magnitude reduction (to 0.4 mg C/L) will double the cost, since EE/O is a constant per order.

CHAPTER 6 : EVALUATION OF REACTOR 2B

6.1 TREATMENT of *para*-CHLOROPHENOL

6.1.1 Recirculation Mode

(a) System Parameters

The photocatalytic oxidation of p-CP in water was investigated by operating Reactor 2B as an immobilised-bed (IMM) reactor. One-factor variation (for random parametric studies) and two-level experimental designs (for screening and optimisation studies) were employed as before. The following system parameters were evaluated at discrete levels in terms of first order reaction kinetics (Table 6.1):

Table 6.1: System parameters for p-CP study (Reactor 2B; Recirculation Mode)

Parameter	Assigned Levels
Catalyst Loading for Impregnation (g/L)	0; 1; 5*; 10; 20; 30
Volumetric Flow Rate (L/min)	2*[a]
Horizontal Irradiation Distance (cm)	15*
p-CP Initial Concentration (mg/L)	40*
Reaction Volume (L)	3*
Water Matrix	Distilled*
Initial solution pH	7.5*
Gas Purge	Oxygen*
Gas Flow Rate (L/min O_2)	5*
UV lamps used for irradiation	Germicidal (UV-C)*[b]

Note: * Denotes standard reference level of parameters
a Surface flow rate = 135 L/hr/m^2
b UV irradiance = 204.5 W/m^2 = 12 x 15W lamps (per 0.88 m^2)

(b) Fibrous Activated Carbon Examination

Introduction and Objectives :

Two grades of commercially available fibrous activated carbon (FAC) sheet materials were examined for maximum impregnation of TiO_2 photocatalyst and their photochemical stability. Mechanical strength and fineness of the individual fibres were of primary concern in the selection of the sheets. Batches of FAC (commercial name: Kuractive) were obtained from Kuraray (Japan) via a local supplier (Enviro Services cc, Somerset West). Details pertaining to their physical characteristics are presented in Chapter 3 (Table 3.3). The grades used in this project (Kuractive 15 and 20) were similar in appearance despite a marked difference in weight per m^2 (see Table 3.2).

A dynamic contact angle analyser (DCAA) was used to conduct a preliminary study of the TiO_2 impregnation properties of the two types of FAC materials (Engelbrecht *et al.*, 1998). The procedure entailed dipping square samples of each (impregnation area: 5.6 cm^2) in 30 mL of TiO_2 suspension for a fixed period of time. The objectives of this study were to ascertain conditions for maximum catalyst impregnation as a function of (1) catalyst suspension loading (2) FAC grade and (3) impregnation time. Standard one-factor variation and 2^3 factorial experiments were used for this purpose. These parameters will ultimately influence the optimised performance of the immobilised-bed FAC reactor (2B) in terms of its photocatalytic destruction efficiency.

Results and Discussion:

Table 6.2: Catalyst impregnation loading as a function of catalyst suspension loading and FAC grade

Catalyst suspension loading (g/L)	Catalyst impregnation loading*** (in mg/cm^2)	
	FAC grade 15 (1500 m^2/g)	FAC grade 20 (2000 m^2/g)
0	0.0*	0**
1	1.4	0.8
5	4.3	1.1
10	5.6	2.6
20	6.2	3.9
30	6.9	5.2
50	8.5	6.2
75	10.6	9.7
100	11.1	11.6

*** Water adsorption (at 0 g/L TiO_2) = 31.4 mg/cm^2**
**** Water adsorption (at 0 g/L TiO_2) = 35.3 mg/cm^2**
***** *Results corrected in terms of net uptake of water***

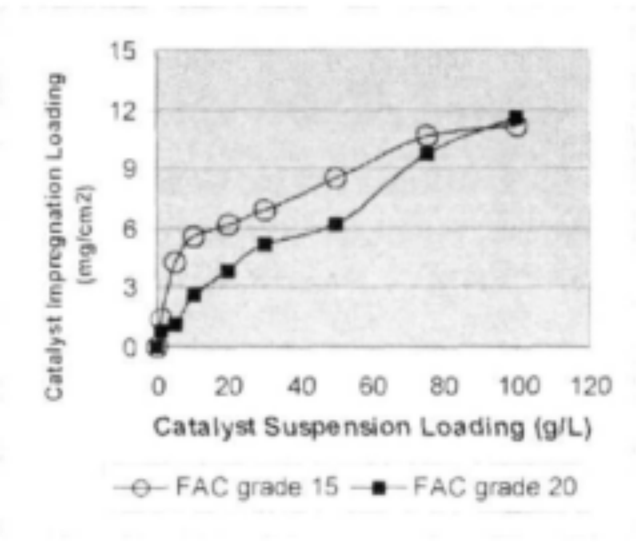

Figure 6.1: Catalyst impregnation loading as a function of catalyst suspension loading and FAC grade

The results obtained from these experiments (Table 6.2 and Figure 6.1) indicated that :

- the catalyst impregnation loading (CIL) for FAC grade 15 attains a plateau value of approximately 11 mg/cm^2 beyond catalyst suspension loadings of 40 g/L TiO_2. This result demonstrates the limited impregnation capacity of grade 15 on a small scale and is probably linked to a lower degree of porosity compared to grade 20 (see Table 3.3) ;
- the CIL response for grade 20 increases steadily with increasing suspension loading from 0 to 100 g/L TiO_2. This result is dependent on the scale of experimentation and is explained in terms the higher degree of porosity of Grade 20, as reflected by its larger total surface area, pore radii and pore volumes (see Table 3.3) ;
- the two FAC grades display similar wetting properties with respect to TiO_2 suspension coating and wetting with clear water. Perfect wetting is observed for all analyses (advancing and receding contact angles are 0° throughout) ;
- the impregnation loading does not significantly change by increasing the time of impregnation (Engelbrecht *et al.*, 1998). This result implies that a relatively short impregnation time could be adopted as standard ;
- the mechanical stability of grade 15 is significantly greater under wetting conditions, compared to grade 20. This observation is ascribed to the considerable difference in porosity and weight per unit area ;
- the catalyst impregnation loading is similar for FAC and fibre glass (Type 1 and 2) when using suspension loadings in the order of 1 g/L TiO_2. This effect, however, changes dramatically at higher suspension loadings where a 1 order of magnitude difference is observed in favour of FAC (Tables 5.2 and 6.2) as a result of its markedly higher total surface area.

Based on the results obtained above, it was anticipated that most of Reactor 2B's studies would probably have to be conducted with FAC grade 15 which is (1) mechanically more stable under wetting conditions and (2) displays a saturation-type dependence on TiO_2 impregnation loading which should be beneficial for steady-state kinetic studies. However, the DCAA results were not necessarily applicable to reactor-scale coating and a study of the impregnation properties of both grades was required to assess their respective utilities as a stationary support for TiO_2 in Reactor 2A.

(c) TiO_2 Impregnation of Sheet Modules

Introduction and Objectives:

The techniques of *suspension coating* and *droplet spraying* were assessed for the impregnation of TiO_2 on sheet modules (coating surface area 0.88 m^2) of both FAC grades. The standard suspension coating procedure entailed dark recirculation of suspensions of TiO_2 (in 3 L of distilled water) through the reactor (across the sheet module) using (1) a 2 L/min volumetric flow rate, (2) natural suspension pH (4-5) and (3) magnetic stirring for a period of 30 minutes. The droplet spraying procedure entailed administering a 1.5 L TiO_2 suspension (of the desired catalyst loading) to each side of a sheet module via a spraying canister (thus 3 L in total). These conditions rendered an identical mass of TiO_2 being applied for both procedures. Sheet modules were weighed before and after coating. Coated sheets were air-dried at room temperature for 24 hr prior to determining net mass increase. Experiments were not repeated due to a limited amount of FAC material available.

The objectives of this study were to (1) compare the impregnation properties of the FAC sheet modules as a function of catalyst suspension loading, FAC grade and impregnation method used (2) compare impregnation loadings for the FAC sheet modules with results obtained from the small-scale DCAA study and (3) compare the impregnation loading of FAC against the standard fibre glass used previously.

Results and Discussion:

Table 6.3 Catalyst impregnation loading as a function of catalyst suspension loading, impregnation method and FAC grade

Catalyst Suspension Loading (g/L TiO_2)	Catalyst impregnation loading of sheet module* (in g TiO_2 /m^2)			
	Suspension Coating		Droplet Spraying	
	FAC grade 15	FAC grade 20	FAC grade 15	FAC grade20
1	2.4	1.3	3.3	2.2
5	12.8	10.7	16.8	11.5
10	22.8	12.8	32.6	17.3
20	35.6	15.9	64.1	24.8
30	50.6	17.2	91.0	29.0

***Sheet module coating area = 0.88 m^2 (8800 cm^2)**

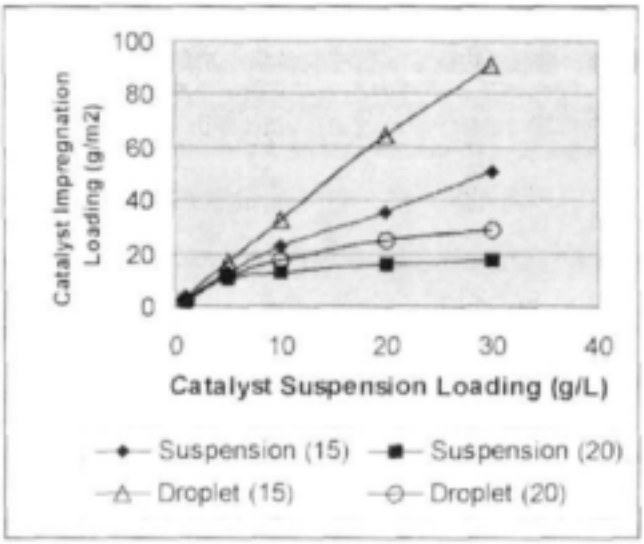

Figure 6.2: Catalyst impregnation loading as a function of catalyst suspension loading, impregnation method and FAC grade

Table 6.4: Design matrix for 2^3 factorial study.

Run	Catalyst Suspension Loading (g/L TiO_2)	Impregnation Method	FAC Grade	Catalyst Impregnation Loading (g TiO_2/m^2)
1	1	Suspension coating	15	2.4
2	30	Suspension coating	15	50.6
3	1	Droplet spraying	15	3.3
4	30	Droplet spraying	15	91.0
5	1	Suspension coating	20	1.3
6	30	Suspension coating	20	17.2
7	1	Droplet spraying	20	2.2
8	30	Droplet spraying	20	29.0

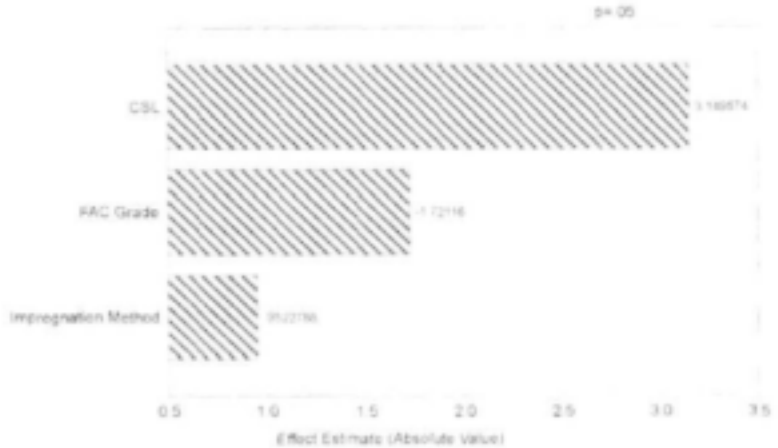

Figure 6.3: Pareto chart illustrating parameter main effects with respect to catalyst impregnation loading as response function. (CSL = Catalyst Suspension Loading *used for impregnation of FAC sheet)*

The results obtained from these experiments (Tables 6.3-6.4 and Figures 6.2-6.3) indicated that :

- the catalyst impregnation loading (CIL) for FAC grade 15 increases linearly as a function of catalyst suspension loading (CSL). The linear trend is fairly independent of the impregnation method used and demonstrates the pronounced adsorption ability of grade 15 for large quantities of TiO_2. The trend is in contrast to the earlier DCAA results, which demonstrated a saturation-type effect for CIL. These results prove that, when applying FAC on reactor scale, the porosity of the grade becomes less important when steady-state conditions have not yet been attained. The marked advantage of FAC grade 15 (in terms of sheet weight per unit area) is also an important factor (see Table 3.2) to note ;
- the CIL response for grade 20 modules displays a saturation-type plateau value when applying suspension loadings greater than 20 g/L. This result is in contrast to the linear impregnation response observed in the DCAA study (Figure 6.1), which indicates (again) that porosity is less significant when conducting a scaled-up coating of FAC. It is evident that impregnation coating conducted on small-scale
- the absolute value for CIL is higher for droplet spraying than suspension coating. This effect is observed for both grades at each suspension loading used. The result is attributed to a higher mass transfer of TiO_2 effected during droplet spraying, as opposed to suspension coating ;
- the relative main effects of impregnation method and FAC grade is negated within the framework of an experimental design, while the catalyst suspension loading is the only significant parameter in terms of impregnation (Figure 6.3) ;
- when using suspension coating for reactor sheet modules, the CIL parameter (as a function of CSL) varies roughly in the order: FAC grade 15 > fibre glass (Type 1) > FAC grade 20 ;
- droplet spraying of FAC 20 renders a similar impregnation loading compared to the suspension coating fibre glass Type 1. This result demonstrated the utility of the method for improved impregnation. However, additional precision analyses are required to confirm the reproducibility this effect.

Based on the results obtained above, it is evident that impregnation studies of TiO_2 supports cannot be linearly extrapolated, particularly when highly adsorptive supports (such as FAC) are used. It was also demonstrated that FAC grade 15 (with superior mechanical stability under wetting conditions) can be used as an efficient TiO_2 immobiliser. Consequently, a series of parametric studies were conducted using *grade 15* in Reactor 2B to examine the TiO_2 photocatalytic oxidation of p-CP in water.

It was envisaged that the oxidative kinetics for p-CP treatment would be enhanced markedly by using FAC as TiO_2 support in the existing Reactor 2. This assumption would inevitably mean that the first order rate constant for *total rate of removal* (k_T) will be determined by two components, viz. : the *true photocatalytic oxidation rate constant* (k_P) and the *mass transfer* rate constant (k_A) as a result of p-CP adsorption onto FAC (k_A). It was further anticipated that k_A would be the predominant factor due to the very high surface area of FAC grade 15 (1500 m^2/g).

(d) Catalyst Impregnation Loading

Introduction and Objectives:

The effect of catalyst impregnation loading was examined by comparing results for 6 different suspension loadings of TiO_2 used for impregnation (0; 1; 5; 10; 20 and 30 g/L TiO_2). The *standard* suspension coating procedure (as described earlier in Section 5.1.1) was adopted throughout and only the immobilised-bed (IMM) reactor configuration applied. The corresponding impregnation loadings amounted to 0; 2.4; 12.8; 22.8; 35.6 and 50.6 g/m^2, respectively (see Table 6.3). The remainder of the system parameters were evaluated at standard reference levels (Table 6.1). Oxygen purge was only used during UV photocatalytic experiments. A total reaction time of 15 minutes was selected.

Temporal concentration data from each UV irradiation experiment was used to calculate the rate constant for total removal (k_T), assuming that first order exponential decay kinetics had been confirmed. A "dark adsorption" control run was conducted in tandem with each UV experiment to calculate the p-CP adsorption rate constant (k_A) from which the photocatalytic rate constant (k_P) was calculated as the difference between k_T and k_A . The objectives of this study were to (1) assess the magnitudes of the various rate constants as a function of catalyst impregnation loading and (2) comment on the utility of FAC as immobiliser for TiO_2 .

Results and Discussion:

Table 6.5: **p-CP removal as a function of dark adsorption time and catalyst impregnation loading (expressed as catalyst suspension loading used for FAC impregnation)**, (p-CP concentration in mg/L)

recirculation Time (min)	Catalyst Impregnation Loading (expressed as g/L TiO_2)**					
	0^a	1^b	5^c	10^d	20^e	30^f
0	40.0	40.0	40.0	40.0	40.0	40.0
1	18.6	19.5	23.5	24.5	28.2	32.2
2	10.4	11.4	14.4	15.9	18.9	23.2
3	5.6	6.6	9.1	11.6	14.2	17.7
4	3.0	3.6	6.6	8.2	9.9	14.5
5	1.5	2.2	4.1	6.0	8.1	12.1
6	ND*	0.9	3.0	4.4	6.1	10.2
7		ND	2.1	3.1	4.9	8.2
8			1.0	2.1	3.9	6.7
9			ND	1.5	3.0	5.5
10				0.9	2.5	4.5
11				ND	2.1	3.6
12					1.6	3.0
13					1.0	2.6
14					ND	2.3
15						1.9
10^2 k_A (min^{-1})	64.31	60.35	43.23	35.89	26.34	20.12
R^2	0.99	0.99	0.99	0.99	0.99	0.99

Note : ND* = Not detected ; Limit of detection = 1 mg/L
****True impregnation loading: (a) 2.4 (b) 12.8 (c) 22.8 (d) 35.6 (e) 50.6 g/m^2**

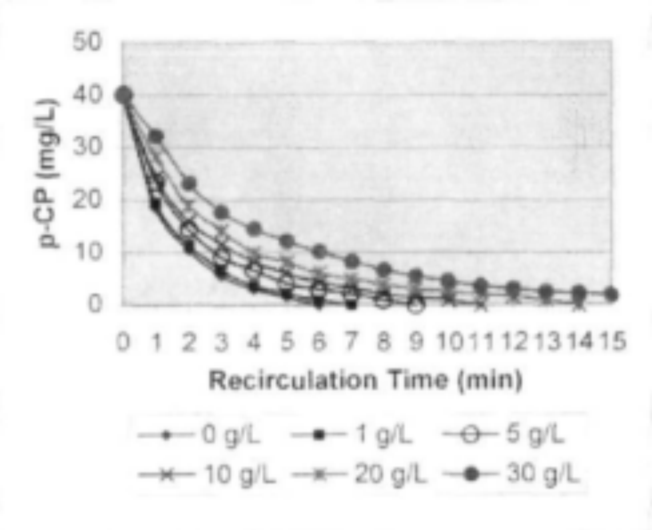

Figure 6.4: p-CP removal as a function of dark adsorption time and catalyst impregnation loading (expressed as catalyst suspension loading used for FAC impregnation)

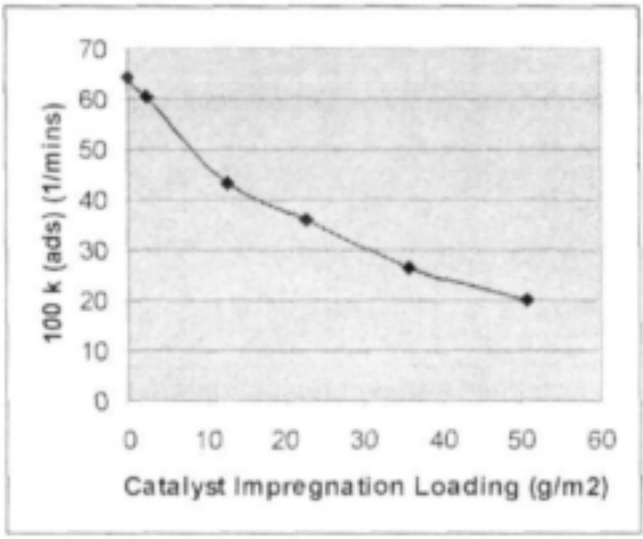

Figure 6.5: First order adsorption rate constant as a function of catalyst impregnation loading

Table 6.6: **p-CP removal as a function of UV irradiation time and catalyst impregnation loading *(expressed as catalyst suspension loading used for FAC impregnation)***

Irradiation Time (min)	Catalyst Impregnation Loading (expressed as g/L TiO_2)					
	0[a]	1[b]	5[c]	10[d]	20[e]	30[f]
0	40.0	40.0	40.0	40.0	40.0	40.0
1	19.1	18.9	18.6	22.2	24.8	29.5
2	9.8	10.1	9.9	12.4	16.5	23.9
3	4.1	5.4	3.0	7.2	11.0	18.8
4	2.0	3.0	ND	4.6	7.1	13.5
5	ND*	1.5		2.6	4.5	9.9
6		ND		1.4	3.1	7.3
7				ND	2.2	5.9
8					0.9	4.2
9					ND	3.2
10						2.1
11						1.0
12						ND
$10^2\ k_T$ *(min^{-1})*	75.30	64.47	84.01	54.78	44.47	31.02
R^2	0.99	0.99	0.98	0.99	0.99	0.98

Note : ND* = Not detected ; Limit of detection = 1 mg/L

****True impregnation loading: (a) 2.4 (b) 12.8 (c) 22.8 (d) 35.6 (e) 50.6 g/m^2**

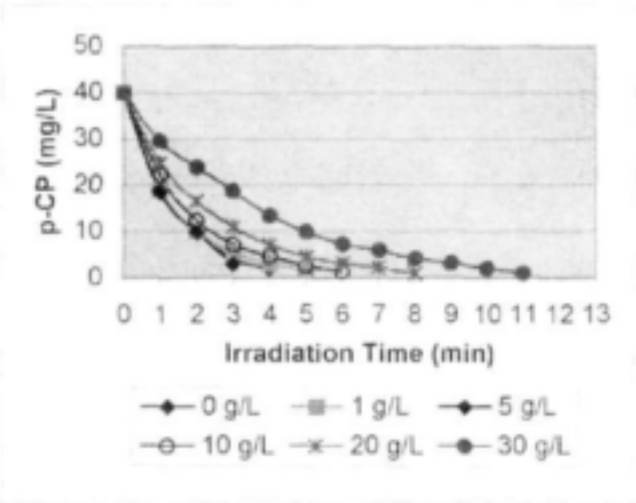

Figure 6.6: p-CP removal as a function of UV irradiation time and catalyst impregnation loading (expressed as catalyst suspension loading used for FAC impregnation)

Table 6.7: First order rate constants for total removal and photocatalytic oxidation as a function of catalyst impregnation loading. (k_T = total removal ; k_P = photocatalytic oxidation)

Catalyst Impregnation Loading		10^2 k_T	10^2 k_A	10^2 k_P	Gain*
(g/L TiO_2)	(g TiO_2 / m^2)	(min^{-1})	(min^{-1})	(min^{-1})	(%)
0	0.0	75.30	64.31	10.99	14.6
1	2.4	64.47	60.35	4.12	6.4
5	12.8	84.01	43.23	40.78	48.5**
10	22.8	54.78	35.89	18.89	34.5
20	35.6	44.47	26.34	18.13	40.8
30	50.6	31.02	20.12	10.90	35.1

Note: * Gain (%) = (k_P / k_T) x 100
**** Observed optimum gain**

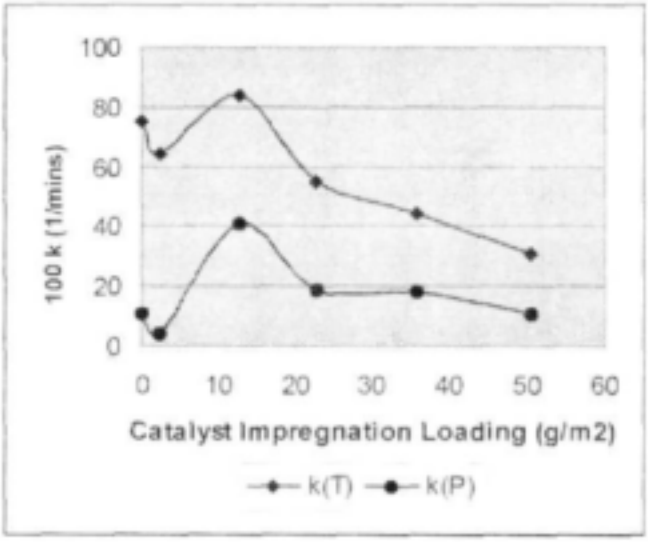

Figure 6.7: First order rate constants for total removal and photocatalytic oxidation as a function of catalyst impregnation loading. (k_T = total removal ; k_P = photocatalytic oxidation)

The results obtained from these experiments (Tables 6.5-6.7 and Figures 6.4-6.7) indicated that :

- first order exponential kinetics apply to the removal rate of p-CP in Reactor 2B ;
- the first order adsorption rate constant (k_A) decreases steadily with an increase in catalyst impregnation loading. This result confirms the inhibiting effect of an increased amount of immobilised TiO_2 on the adsorptive capacity of the micro-porous FAC ;
- non-coated FAC yields the highest adsorption rate for 40 mg/L p-CP (viz.: 120 mg in total). This result demonstrates the utility of FAC for the adsorptive removal of organic micro-pollutants ;

- the rate constant for total removal of p-CP (k_T) is constantly higher than the equivalent adsorption constant. This result indicates a marginal net improvement in removal rate due to the addition of UV irradiation, thus rendering UV photolytic (0 g/L TiO_2) and TiO_2 photocatalytic effects ;
- the net increase in rate constant (denoted by %Gain) is at a maximum of *ca* 49% when a catalyst impregnation loading of 12.8 g/m^2 (viz.: 1.28 mg/cm^2) is applied. This loading was achieved by using a suspension of 5 g/L TiO_2. This result is in excellent agreement with optimum loadings reported elsewhere for immobilised-reactors (Herrmann, 1995) ;
- it might be possible to balance the effects of adsorptive mass transfer and photocatalytic oxidation, albeit at non-steady state.

Based on the results obtained above, the auxiliary effect of photocatalysis is mostly very small compared to FAC adsorption (mass transfer) when operating Reactor 2B as an IMM reactor for the oxidative removal of p-CP from water.

(e) Intermittent Impregnation of Sheet Modules

Introduction and Objectives:

The effect of intermittent TiO_2 impregnation was examined by conducting a series of multi-variable screening design experiments with both grades of FAC (viz.: grades 15 and 20). The system parameters were evaluated at standard reference levels (Table 6.1) and a standard reaction time of 15 minutes was selected. All experiments (including dark adsorption runs) were conducted in duplicate to check reproducibility. Non-steady state conditions were assumed for p-CP adsorption onto FAC. This was based on the high initial adsorptive capacity of FAC (as demonstrated in the previous study) and implied (1) a constant adsorption rate of p-CP onto each module and (2) the absence of breakthrough conditions.

The 8 FAC sheet modules used in this study were impregnated with TiO_2 suspension using the droplet-spraying method as described before. Intermittent rectangular segments of each sheet module were sprayed on both sides with 1.5 L of the desired catalyst suspension loading. The designated non-coated segments were shielded during impregnation. Impregnated sheets were allowed to air-dry for at least 48 hours prior to use.

The main objective of this study was to significantly enhance photocatalytic oxidation of p-CP in water at the expense of FAC adsorption by using periodic photocatalysis. This effort entailed the evaluation of 4 sheet module parameters, viz.: (1) number of intermittent TiO_2 segments per sheet (vertical length :1.1 m) (2) vertical length of each TiO_2 segment (3) catalyst impregnation loading and (4) FAC grade, in terms of the first order rate constants defined in the previous section (k_T , k_A , k_P and Gain). Parameters levels are presented in Table 6.8:

Table 6.8: Sheet module parameters for study of intermittent impregnation.

Parameter	Code	Minimum level (0)	Maximum level (1)
Number of intermittent TiO_2 segments per sheet	n	3	6
Vertical length of TiO_2 segment* (in cm)	L	6.75	13.5
Catalyst impregnation loading (in g/L TiO_2)	CIL	5**	30**
FAC Grade	GRADE	15	20

Note: * Width = 40 cm = Sheet module width

** True catalyst impregnation loading depends on choice of n and L levels (hence 4 levels).

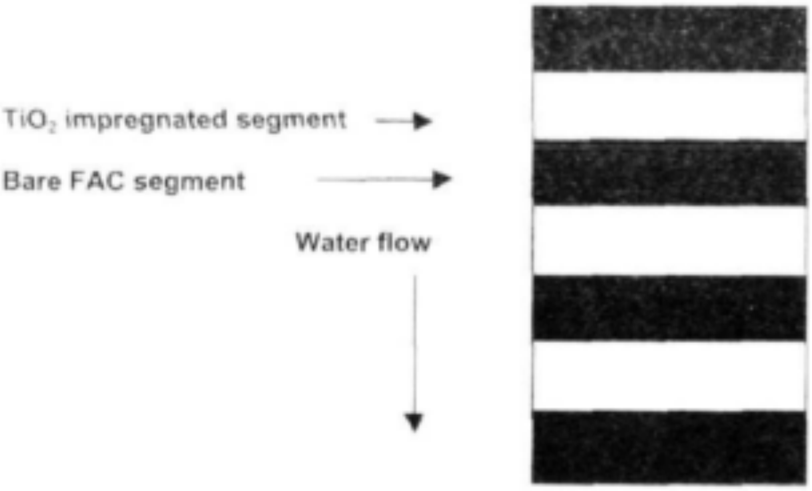

Fig.6.8: Design of FAC sheet with rectangular intermittent TiO_2 segments.

Results and Discussion:

Table 6.9: Design matrix for catalyst impregnation loading analysis (CIL, in g/m^2) of sheet modules

Sheet	Design Code	n	L (cm)	CSL (g/L)	GRADE	Impregnation** area (m^2)	Net Increase (g TiO_2)	CIL (g/m^2)
1	[0000]	3	6.75	5	15	0.162	2.6	16.0
2	[0101]	3	13.5	5	20	0.324	3.5	10.8
3	[1111]	6	13.5	30	20	0.648	18.9	29.2
4	[1100]	6	13.5	5	15	0.648	11.1	17.1
5	[0011]	3	6.75	30	20	0.162	5.0	30.9
6	[1001]	6	6.75	5	20	0.324	4.0	12.3
7	[1010]	6	6.75	30	15	0.324	29.7	91.6
8	[0110]	3	13.5	30	15	0.324	30.1	92.9

Note: * Design code is orthogonal
**Total impregnation area (per sheet) according to sheet module width (40 cm)

Table 6.10. Dimensions of bare (non-coated) FAC areas per sheet

n	L (cm)	nL (cm)	110-nL (cm)	(110-n)/L*
3	6.75	20.25	89.8	29.1
3	13.5	40.5	69.5	23.1
6	6.75	40.5	69.5	11.5
6	13.5	81	29	4.8

Note: *The vertical length for each bare (non-coated) segment were calculated taking into account the total vertical module length for irradiation (110 cm) and using an *equal* number of coated and non-coated segments per sheet.

Table 6.11: Design matrix for screening study (orthogonal array)

Sheet	Design Code	n[a]	L[b] (cm)	CSL[c] (g/L)	GRADE (15;20)	10^2 k_T (min^{-1})	10^2 k_A (min^{-1})	10^2 k_P (min^{-1})	(k_P/ k_T) Gain (%)
1	[0000]	3	6.75	5	15	38.46	37.00	1.46	3.8
2	[0101]	3	13.5	5	20	36.21	34.39	1.82	5.0
3	[1111]	6	13.5	30	20	32.04	30.75	1.29	4.0
4	[1100]	6	13.5	5	15	36.54	35.96	0.58	1.6
5	[0011]	3	6.75	30	20	34.50	33.79	0.71	2.1
6	[1001]	6	6.75	5	20	35.11	35.00	0.11	0.3
7	[1010]	6	6.75	30	15	37.04	35.89	1.15	3.1
8	[0110]	3	13.5	30	15	35.54	32.07	3.47	9.8

a n = Number of intermittent TiO_2 segments
b L = Vertical length of TiO_2 segment
c CSL = Catalyst suspension loading used for FAC impregnation
(k_T = Total removal rate ; k_A = Adsorption rate alone ; k_P = Photocatalytic oxidation rate
$k_T = k_A + k_P$)

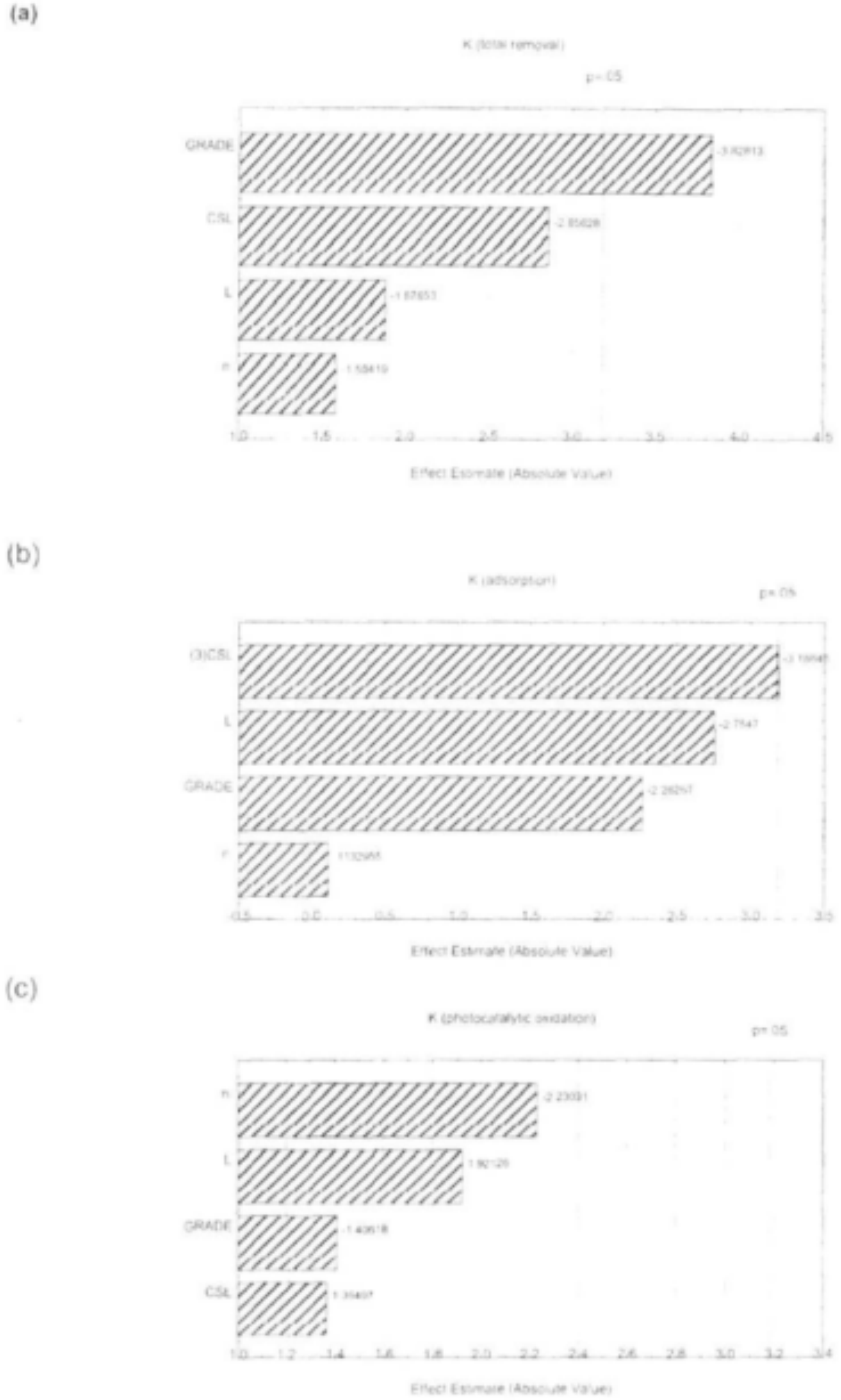

Figure 6.9: Pareto chart illustrating standardised parameter main effects for the 3 first order rate constant responses. (Grade = Type of FAC sheet, CSL = Catalyst suspension loading, L = Vertical length of TiO_2 impregnated segment, n = Number of TiO_2 segments per sheet.)

The results obtained from these experiments (Tables 6.8-6.11 and Figures 6.9a-6.9c) indicated that :

- first order exponential kinetics apply to the removal rate of p-CP in Reactor 2B when intermittent impregnation is applied to FAC sheet modules ;
- catalyst impregnation loadings for the intermittent approach (in g TiO_2 /m^2) are in good agreement with results obtained earlier for droplet-spraying of full-length sheet modules (compare Tables 6.3 and 6.9).

A statistical analysis was conducted to ascertain whether the 4 parameters concerned exerted meaningful effects on the defined response functions. ANOVA was used for this purpose, adopting a maximum null-hypothesis probability of 0.05 to confirm significance of the parameter under investigation. A linear mathematical model was selected in combination with the selected orthogonal design matrix. The linear model precluded the calculation of parameter interactions.

The results for the 8 experimental treatments generally indicated that :

- the observed total removal rate constants (k_T) are largely similar, with sheet 1 yielding the best response (viz.: using 3 intermittent TiO_2 areas of vertical length 6.75 cm on FAC grade 15 impregnated with a suspension loading of 5 g/L) ;
- the observed adsorption rate constants (k_A) are generally one order of magnitude greater than the corresponding photocatalytic oxidation rate constants ;
- the observed oxidation rate constants are suppressed to the degree that they are largely independent of any parameter variation. This result is ascribed to the overriding nature of FAC adsorption in terms of p-CP removal from the aqueous phase ;
- the gain in total removal rate constant as a result of using photocatalytic oxidation is maximised using sheet 8 (viz.: *ca* 10% for using 3 intermittent TiO_2 areas of vertical length 13.5 cm on FAC grade 15 impregnated with a 30 g/L TiO_2).

Results for the *total removal rate constant* response (Figure 6.9a) indicated that :

- all 4 parameters exert negative main effects, hence confirming that the conditions for sheet 1 (viz.: using 3 intermittent TiO_2 areas of vertical length 6.75 cm on FAC grade 15 impregnated with a suspension of 5 g/L TiO_2) produce the highest removal rate constant ;
- the FAC grade parameter exhibits a statistically significant negative main effect, hence the utility of FAC grade 15 is confirmed ;
- the full-length impregnation of FAC sheet modules is preferred to intermittent impregnation. The original choice of grade 15 (impregnated entirely with a catalyst suspension loading of 5 g/L TiO_2) seems to have been the better one (minimising the amount of intermittent coated areas).

Results for the *adsorption rate constant* response (Figure 6.9b) indicated that :

- the catalyst suspension loading (CSL) is the predominant parameter and exerts a statistically significant main effect, hence confirming the earlier observation that adsorption decreases significantly with an increase in catalyst loading ;
- the use of FAC grade 15 favours the adsorption rate. This result is conflicting with the relative pore characteristics of the 2 grades used, but confirms again that the net sheet weight is more important at reactor scale.

Results for the *photocatalytic oxidation rate constant* (Figure 6.9c) indicated that :

- no parameter variation exerts a statistically significant effect on the observed response. This result is explained in terms of the overriding effect of adsorptive mass transfer of p-CP which negates the effect of photocatalytic oxidation.

Based on the results above, it is evident that using FAC materials as primary adsorbent (stationary support) for TiO_2 is not beneficial for rendering a sufficient photocatalytic effect. It was therefore decided to investigate whether a change in operation mode would render a marked photocatalytic effect in terms of the oxidative treatment of p-CP in Reactor 2B.

6.1.2 Single Pass Modes

(a) System Parameters

The photocatalytic oxidation of p-CP in water was investigated by operating Reactor 2B as an immobilised-bed (IMM) reactor. One-factor variation methods were employed in a series of random parametric studies. The following system parameters were evaluated at discrete levels in terms of the defined response function for the operation modes (see Table 6.12) :

Table 6.12: System parameters for p-CP study (Reactor 2B; Single Pass Modes)

Parameter	Assigned Levels
Catalyst Loading for Impregnation (g/L)	0; 1; 5*; 10; 20; 30
Volumetric Flow Rate (L/min)	2^{*a}; 4^{b}
Horizontal Irradiation Distance (cm)	15*
p-CP Initial Concentration (mg/L)	40*
Reaction Volume (L)	3*; 6; 12
Water Matrix	Distilled*
Solution pH	7.5*
Gas Purge	Oxygen*
Oxygen Flow Rate (L/min)	5*
UV lamps used for irradiation	Germicidal (UV-C)^{*c}

Note: * Denotes standard reference level of parameters
a Surface flow rate = 135 L/hr/m^2
b Surface flow rate = 272 L/hr/m^2
c UV irradiance = 204.5 W/m^2 = 12 x 15W lamps (per 0.88 m^2)

(b) Choice of FAC Grade

Grade 15 was the only brand of FAC available at the time of studying the photocatalytic oxidation of p-CP with regard to Reactor 2B operated in the single pass modes.

(c) Catalyst Impregnation Loading

Introduction and Objectives:

The effect of catalyst impregnation loading was examined by using FAC grade 15 as TiO_2 support and comparing results for 6 different suspension loadings of TiO_2 used for impregnation (0; 1; 5; 10; 20 and 30 g/L TiO_2). The *standard* suspension coating procedure (as described earlier in Section 5.1.1) was applied to each sheet module and only the immobilised-bed (IMM) reactor configuration was studied. The corresponding impregnation loadings amounted to 0; 2.4; 12.8; 22.8; 35.6 and 50.6 g/m^2, respectively (see Table 6.3). The remainder of the system parameters were evaluated at standard reference levels (Table 6.12). Oxygen purging was only used during UV photocatalytic experiments.

The mean residence time (UV contact time) per single pass amounted to 11.5 sec (see Table 3.1) for FAC grade 15 sheet module. This is substantially longer than the corresponding time for fibre glass (Type 1) sheet modules used in Reactor 2A. The elongated time is attributed to the retarding effect created by the highly porous FAC surface.

p-CP concentrations were determined before and after each single pass and used to calculate the amount of removal as a function of single pass number. All UV irradiation experiments were conducted in tandem with a "dark adsorption" control experiment. The latter was used to calculate the net mass transferred removal as before. The objectives of this study were to (1) determine whether TiO_2 photocatalytic oxidation contributes significantly to the removal of 40 mg/L p-CP in the single pass modes (2) determine an optimum impregnation loading of TiO_2 , if possible and (3) assess the utility of Reactor 2B in terms of theoretical UV dosages.

Results and Discussion:

Table 6.13: p-CP concentration data (in mg/L)

Catalyst Impregnation Loading (as g/L TiO_2)	UV Source	Initial p-CP Concentration (mg/L)	p-CP Concentration (after 1st single pass) (mg/L)	Removal (%)	Gain (%)
0	off	40.0	4.0	90.0	-
0	on	40.0	3.6	91.0	1.0
1	off	40.0	4.0	90.0	-
1	on	40.0	3.0	92.5	2.5
5	off	40.0	4.1	89.8	-
5	on	40.0	ND*	*ca* 99.9	*ca 10*
10	off	40.0	4.6	88.5	-
10	on	40.0	4.0	90.0	1.5
20	off	40.0	5.0	87.5	-
20	on	40.0	4.6	88.5	1.0
30	off	40.0	5.2	87.0	-
30	on	40.0	4.8	88.0	1.0

Note: ND* = Not detected ; Limit of detection = 1 mg/L

The results obtained from these experiments (Table 6.13) indicated that :

- for all experiments, a maximum of two single pass procedures (corresponding to a total residence time of about 23 seconds) are required to attain removal of 40 mg/L of p-CP to below the detection limit. The equivalent theoretical UV dosage amounts to 470 mW-s/cm^2 ;
- reactor performance (% removal) generally increases with less than 5% with the addition of UV light, thereby re-confirming the relatively small auxiliary effect of photocatalytic oxidation with regard to FAC adsorption ;
- reactor performance yields an optimum gain when applying a suspension loading of 5 g/L TiO_2 (impregnation loading: 12.8 g/m^2). The approximate 10% gain in performance is related to the only experiment which yielded total removal of p-CP after the 1st single pass (theoretical UV dosage: 235 mW-s/cm^2).

Based on the results obtained above, it is evident that (1) the adsorption of FAC is too strong throughout and negates the effect of photocatalysis to a large extent (2) photocatalytic oxidation will only become significant when attaining breakthrough (or steady-state) conditions for FAC (viz.: when the FAC surface is fully saturated with TiO_2 particles). Theoretical UV dosages observed for the total removal of p-CP in Reactor 2B should not compared to the dosages required by immobilised-bed reactors based on non-adsorptive supports.

(d) Volumetric Flow Rate

Introduction and Objectives:

The effect of volumetric flow rate was examined in the single pass mode by comparing results for an elevated flow rate (4 L/minute) against the standard rate used (2 L/minute). The corresponding surface flow rate (per hour) amounted to 272 and 135 L/min/m^2, respectively. The higher flow rate was attained by the parallel coupling of 2 peristaltic pumps and operating both at maximum flow rate (viz.: 2 L/minute). The *standard* suspension coating procedure was applied to a fresh FAC grade 15 sheet module (as before) and only the immobilised-bed (IMM) reactor configuration was studied. The corresponding catalyst impregnation loading amounted to 13.1 g/m^2 (suspension loading: 5 g/L). The remainder of the system parameters were evaluated at standard reference levels (Table 6.12). Oxygen purging was only used during UV photocatalytic experiments.

p-CP concentrations were determined before and after the single pass and used to calculate the amount of removal as a function of single pass number. All UV irradiation experiments were conducted in tandem with a "dark adsorption" control experiment. The latter was used to calculate the net mass transferred removal as before. The objectives of this study were to (1) determine whether TiO$_2$ photocatalytic oxidation contributes significantly to the removal of 40 mg/L p-CP at higher volumetric flow rates and (2) determine the extent of mass transfer at high flow rate.

Results and Discussion:

Table 6.14: p-CP concentration data (in mg/L)

Volumetric Flow Rate (L/min)	UV Source	Initial p-CP Concentration (mg/L)	p-CP Concentration (after 1st single pass) (mg/L)	Removal (%)	Gain (%)
2	off	40.0	4.1	89.8	-
2	on	40.0	ND*	*ca* 99.9	*ca* 10
4	off	40.0	7.4	81.5	-
4	on	40.0	5.5	86.3	4.8

Note: ND* = Not detected ; Limit of detection = 1 mg/L

The results obtained from these experiments (Table 6.14) indicated that :

- reactor performance (% removal) decreases with approximately 10-15% when operating at the higher volumetric flow rate. This result applies to both mass transferred removal and photocatalytic oxidation of p-CP ;
- a practical limitation might exist for applying falling film reactor designs to the treatment of water at high flow rate. The efficiency of these reactors are mainly defined in terms of falling film thickness, which is dependent on volumetric water flow rate, irradiated surface area and UV residence time of the reactor. The inhibiting effect of reduced UV penetration through denser falling films (attained at high flow rate) has been demonstrated throughout this project.

(e) **Reaction Volume**

Introduction and Objectives:

The effect of reaction volume was examined in the single pass mode by comparing results for a two-fold (6 L) and four-fold (12 L) increase compared to the standard volume used (3L). Although the initial concentration of p-CP remained constant at 40 mg/L, the reaction volume increases implied the use of proportionally higher mass dosage, viz.: ranging from 120 mg (for 3 L) to 480 mg (for 6L). The *standard* suspension coating procedure was applied to a fresh FAC grade 15 sheet module (as before) and only the immobilised-bed (IMM) reactor configuration was studied. The corresponding catalyst impregnation loading amounted to 11.9 g/m^2 (suspension loading: 5 g/L). The remainder of the system parameters were evaluated at standard reference levels (Table 6.12). Oxygen purging was only used during UV photocatalytic experiments.

p-CP concentrations were determined before and after the single pass and used to calculate the amount of removal as a function of single pass number. All UV irradiation experiments were conducted in tandem with a "dark adsorption" control experiment. The latter was used to calculate the net mass transferred removal as before. The objectives of this study were to (1) determine whether TiO_2 photocatalytic oxidation contributes significantly to the removal of 40 mg/L p-CP at higher mass dosages (reactor volumes) and (2) determine the extent of mass transfer at under these conditions.

Results and Discussion:

Table 6.15: p-CP concentration data (in mg/L)

Reaction Volume (L)	UV Source	Initial p-CP Concentration (mg/L)	p-CP Concentration (after 1stsingle pass) (mg/L)	Removal (%)	Gain (%)
3	off	40.0	4.1	89.8	-
3	on	40.0	ND*	99.9	10
6	off	40.0	4.2	89.5	-
6	on	40.0	ND	99.9	10
12	off	40.0	5.5	86.3	-
12	on	40.0	2.6	93.5	7.2

Note: ND* = Not detected ; Limit of detection = 1 mg/L

The results obtained from these experiments (Table 6.15) indicated that :

- the 10% gain in reactor performance (due to photocatalysis) is sustained when doubling the reaction volume p-CP mass dosage ;
- the 10% gain in performance (due to photocatalysis) decreases marginally when quadrupling the volume and p-CP mass dosage ;
- mass transfer of p-CP to the FAC sheet module is fairly independent of reaction volume at low volumetric flow rate (2 L/minute). This result do not apply to the application of higher flow rates (as demonstrated in the previous study).

Based on all results obtained above, it is concluded that FAC is too strong an adsorbent of both TiO_2 particles and p-CP molecules to render practical (steady-state) conditions for the monitoring of photocatalytic effects. It is suggested that the problem be remedied by (1) studying the adsorption of other grades of FAC with lower adsorption capacity (2) determining the breakthrough curves for each grade of FAC using a range of organic micro-pollutants (3) study the FAC photocatalytic process for large bio-organic molecules in an attempt to counter adsorption as a function of molecular size.

6.1.3 Scanning Electron Microscopy

Introduction and Objectives:

Scanning Electron Microscopy (SEM) analyses of non-coated and TiO_2-coated FAC samples were conducted using a facility at the Department of Physics, University of Stellenbosch. The objectives of this study were to (1) view the micro-structure of individual FAC bundles and (2) assess the utility of the existing suspension coating process for efficient impregnation of TiO_2 particles on FAC bundles. The presence of titanium (hence TiO_2) on the coated samples was confirmed using EDAX (Energy Dispersive Analysis of X-rays).

Results and Discussion:

See Appendix 6.

The results obtained from these experiments indicated that :

- non-coated FAC grades 15 and 20 have a grid-like woven structure consisting of parallel bundles of individual fibres (viewed at a magnification factor of 60) ;
- the individual fibres are cylindrically shaped with an estimated diameter ranging from 10-15 μm (viewed at a magnification factor of 1000) ;
- TiO_2 coated FAC grades 15 and 20 (prepared via the standard suspension-coating with 5 g/L TiO_2) show a random (non-uniform) distribution of TiO_2 clusters between individual fibres and bundles. The observed catalyst clusters are highly variable in size, which indicates that existing coating procedure should be refined ;
- EDAX (Energy Dispersive Analysis of X-rays) confirms the presence of the elemental Titanium (hence TiO_2) on the impregnated FAC samples.

Based on the results obtained above, it is evident that the existing catalyst impregnation procedure needs to be refined in order to maximise utilisation of the micro-porous FAC structure. The application of droplet-spraying and painting procedures should be assessed in more detail using techniques such as SEM as screening tool.

6.1.4 Diffuse Reflectance Spectrometry

Introduction and Objectives:

Diffuse Reflectance Spectrometry (DRS) is a spectrometric technique often used to record diffuse reflectance and absorbance spectra of solid, powdered and fibrous samples in the UV-visible region. In this project it was suggested to develop a photometric technique for *direct quantitative* analysis of the amount of adsorbed organic pollutant (viz.: p-CP) on a sample of fibrous activated carbon (FAC).

A number of non-coated FAC *grade 15* samples (cut in 25 cm^2 squares) were saturated with different amounts of p-CP. Diffuse reflectance data for these samples were recorded over a wavelength region of 200-800 nm against a non-treated fibrous sample as reference material. Adsorption experiments were conducted in the dark (in 500 mL beakers) by stirring the FAC squares in 100 mL of distilled water spiked to the required concentration. Saturation generally occurred within 5-45 minutes. The adsorption process was followed by measuring the decrease in concentration of the pollutant in the water phase (p-CP absorbance measured at 225 nm). FAC samples saturated with p-CP were dried for 24 hours (in petri-dishes) prior to recording DRS data. The main objectives of this study were to (1) assess the utility of DRS for quantitative detection of p-CP adsorbed on FAC and (2) construct a calibration curve, if possible.

Results and Discussion:

Table 6.16: Saturation times for non-coated FAC grade 15 (25 cm^2) as a function p-CP mass loading

[p-CP] (mg/L) used for adsorption	p-CP Mass loading for adsorption (mg)	Saturation time (min.)
5	0.5	3
10	1	5
20	2	8
30	3	10
40	4	15
50	5	22
100	10	42

The results obtained from these experiments indicated that :

- diffuse reflectance signals (expressed in absorbance units) are generally very low and incorporate a high degree of background noise, most probably due to light scattering ;
- the observed analytical signals for of all samples analysed display insignificant variance over the designated wavelength area. This observation implied that a standard calibration curve could not be constructed for p-CP adsorption under the current experimental conditions.

Based on the results obtained above, it is evident that the lack of sensitivity of the DRS technique hampers direct monitoring of adsorbed p-CP. Further investigations will be required at altered reaction conditions (viz.: higher p-CP mass loadings) to render more pronounced mass transferred adsorption onto FAC.

6.2 TREATMENT OF MICROCYSTINS

6.2.1 Recirculation Mode

(a) System Parameters

The photocatalytic oxidation of two variants of microcystins in water was investigated by operating Reactor 2B as an immobilised-bed (IMM) reactor. A screening study was conducted using a 2^3 factorial experimental design. The following system parameters were evaluated at discrete levels in terms of first order reaction kinetics (see Table 6.16):

Table 6.17: System parameters for microcystin study (Reactor 2B; Recirculation Mode)

Parameter	Assigned Levels
Catalyst Loading for Impregnation (g/L)	0; 5*; 20
Volumetric Flow Rate (L/min)	2.0^{*a}
Horizontal Irradiation Distance (cm)	15*
Microcystin Variants	LR , RR and unknown compound
Reaction Volume (L)	5*
Water Matrix	Lake water*
Gas Purge	Oxygen*
Gas Flow Rate (L/min)	5*
Number of UV-C lamps for Irradiation	12^{*b}
Irradiation Time (min.)	20*

Note: * Denotes standard reference level of parameters
a Surface flow rate = 136 L/hr/m^2
b UV irradiance = 204.5 W/m^2 = 12 x 15W (per 0.88 m^2)

(b) Representative Example

Introduction and Objectives:

Earlier work (in collaboration with PROMEC) confirmed the photocatalytic oxidation of 3 microcystin toxin variants (YA, YR and LR) in natural lake water, by using a fibre glass sheet module impregnated with TiO_2 (see Reactor 2A : Chapter 5). The existing immobilised-bed (IMM) FAC photocatalytic reactor (Reactor 2B) was subsequently investigated as a potential means for enhanced removal/oxidative destruction of the microcystin toxins in eutrophic lake water.

This study comprised 4 experiments conducted in the recirculation mode, viz.: two UV irradiation and two "dark control" experiments. All system parameters were evaluated at standard reference levels (Table 6.17). An algal extract (containing microcystins LR and RR) was prepared from a natural bloom (see Section 3.2.2) and used to spike a 5 L sample of natural lake water (as before). Lake water (natural pH 8) was collected at Rondevlei Nature Reserve on the Cape Flats and used without pH adjustment. Rondevlei is a hypertrophic lake adjacent to Zeekoevlei.

Two FAC grade 15 sheet modules were used in this investigation. The first sheet module was used *without* TiO_2 impregnation, while the second module was impregnated according to the standard suspension coating procedure with 5 g/L TiO_2. The corresponding catalyst impregnation loading amounted to 12.2 g/m^2 TiO_2. FAC grade 15 was the only grade available at this stage.

Using the catalyst loadings (as described above) afforded the following 4 IMM reactor scenarios to be studied :

FAC reactor	(FAC adsorption only, UV irradiation excluded)
FAC-UV reactor	(FAC adsorption and UV photolysis)
FAC-TiO_2 reactor	(TiO_2 coated FAC adsorption only, UV irradiation excluded)
FAC-UV-TiO_2 reactor	(FAC adsorption and UV photocatalytic oxidation)

The objectives of this study were to (1) assess the efficiency of Reactor 2B for the removal of microcystins as a function of the 4 reactor scenarios used (2) study the auxiliary effect of UV irradiation in tandem with FAC mass transfer effects and (3) compare the oxidation susceptibilities of the microcystin variants in Reactor 2B.

Results and Discussion:

Table 6.18: (a) Microcystin concentrations and (b) normalised concentrations (%) as functions of reaction time

(a) Reaction Time (min)	Microcystins (ug/L)							
	LR				RR			
	FAC	FAC-UV	FAC-TiO_2	FAC-UV-TiO_2	FAC	FAC-UV	FAC-TiO_2	FAC-UV-TiO_2
0	86	97	92	118	120	116	135	159
2	71	85	91	114	88	92	136	148
4	62	69	85	88	79	83	130	131
6	65	57	93	93	74	82	138	128
8	61	36	88	79	56	38	136	98
10	62	44	85	63	64	33	141	69
12	69	35	86	74	53	38	128	91
14	54	47	109	57	56	27	161	71
16	54	38	104	41	33	41	126	56
18	54	34	108	36	58	34	144	51
20	55	NA*	99	23	50	NA*	178	40
$10^2\ k_{obs}$ (min^{-1})	NC**	NC	NC	7.37	NC	NC	NC	6.82
Half-life (min)	-	-	-	9.4	-	-	-	10.2
R^2	-	-	-	0.90	-	-	-	0.94

(b) Reaction Time (min)	Normalised Concentration (%)							
	LR				RR			
	FAC	FAC-UV	FAC-TiO_2	FAC-UV-TiO_2	FAC	FAC-UV	FAC-TiO_2	FAC-UV-TiO_2
0	100	100	100	100	100	100	100	100
2	83	88	98	96	73	79	101	93
4	72	71	92	75	66	72	96	82
6	75	59	101	79	62	71	102	81
8	71	37	96	70	47	33	101	62
10	72	45	92	53	53	28	104	43
12	80	36	93	63	44	33	95	57
14	63	48	118	48	47	23	119	45
16	63	39	113	35	28	35	93	35
18	63	35	117	31	48	29	107	32
20	64	NA*	108	19	42	NA*	132	25
%Removal (at 18 min)	37	65	0	69	52	71	0	68

Note: **NA*** = *Not analysed*
NC** = **Not calculated**

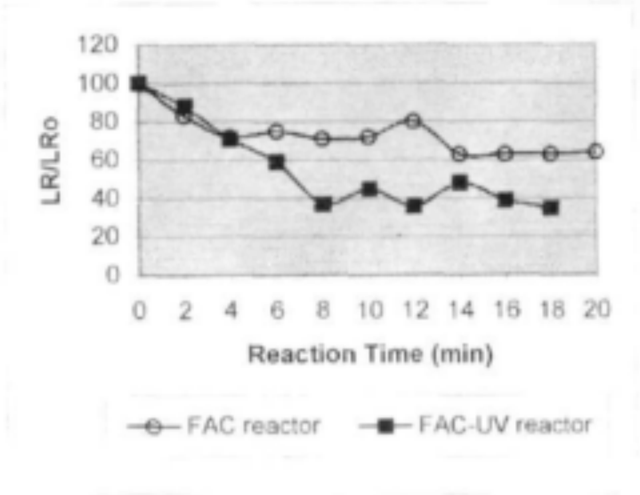

Figure 6.10: Microcystin LR normalised concentration a function of time in FAC and FAC-UV (photolytic) reactors

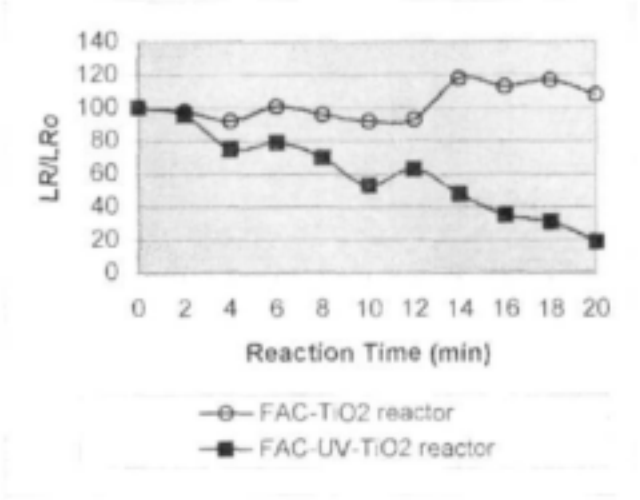

Figure 6.11: Microcystin LR normalised concentration as a function of time in FAC-TiO_2 and FAC-UV-TiO_2 (photocatalytic) reactors

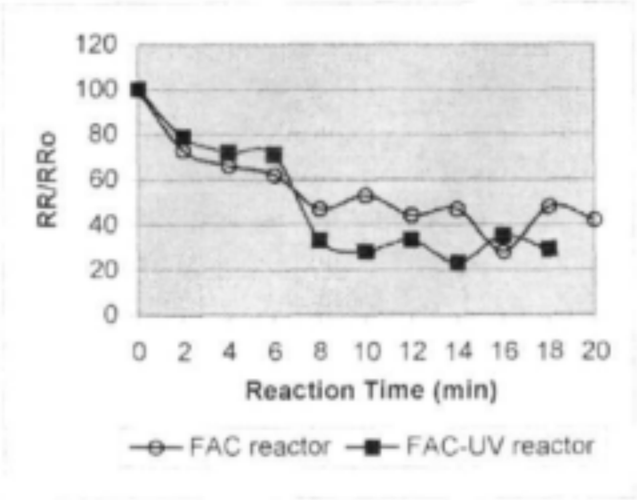

Figure 6.12: Microcystin RR normalised concentration as a function of time in FAC and FAC-UV (photolytic) reactors

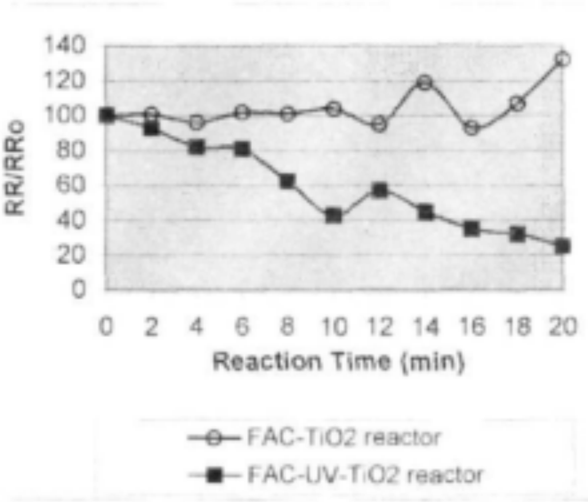

Figure 6.13: Microcystin RR normalised concentration as a function of time in FAC-TiO_2 and FAC-UV-TiO_2 (photocatalytic) reactors

Table 6.19: Design matrix for 2^3 factorial study (Reaction time = 18 min.)

Run	FAC* Status	UV** Status	Microcystin Variant	Removal (%) [at 18 *min.*]
1	FAC	0	LR	37
2	FAC-TiO_2	0	LR	0
3	FAC	UV	LR	65
4	FAC-TiO_2	UV	LR	69
5	FAC	0	RR	52
6	FAC-TiO_2	0	RR	0
7	FAC	UV	RR	71
8	FAC-TiO_2	UV	RR	68

Note: ****FAC status*: FAC = non-impregnated FAC sheet module used**
FAC-TiO_2 = TiO_2 impregnated FAC sheet module used

*******UV status***: 0 = UV irradiation excluded**
UV = UV irradiation applied

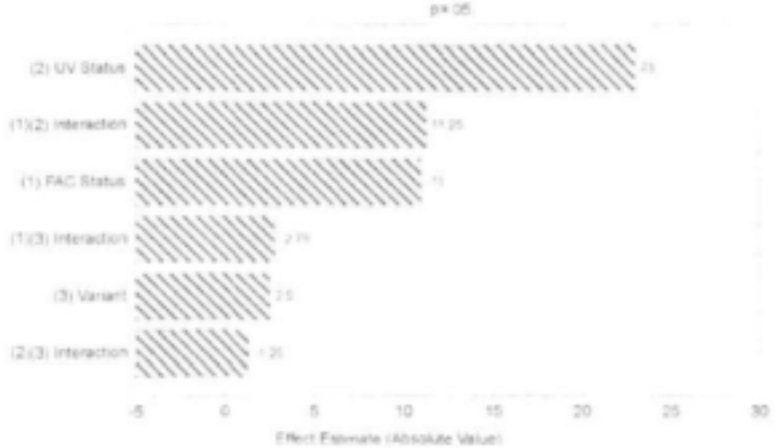

Figure 6.14: Pareto chart illustrating standardised parameter main effects for the 3 first order rate constant responses. (Grade = Type of FAC sheet, CSL = Catalyst suspension loading, L = Vertical length of TiO_2 impregnated segment, N = Number of TiO_2 segments per sheet.)

The results obtained from these experiments (Tables 6.18-19 and Figures 6.10-6.14) indicated that :

- the mean initial concentration for microcystins LR and RR is 98 ± 14 and 133 ± 20 ug/L, respectively. The corresponding RSD values amount to approximately 15% for both variants. The observed inconsistency is attributed to (1) chromatographic separation problems encountered during HPLC analysis and (2) the highly variable adsorptive nature of FAC as a function of its physical properties and general water quality parameters ;
- first order exponential decay kinetics apply only to the treatment of LR and RR in the FAC-UV-TiO_2 reactor (viz.: when applying photocatalytic conditions). The corresponding first order rate constants for the FAC, FAC-UV and FAC-TiO_2 reactors could therefore not be calculated (see Table 6.18a) ;

- concentration data for both variants are compared after 18 minutes of reaction time. This is due to one sample analysis not being completed for 20 minutes reaction time (see Table 6.18b) ;
- the FAC reactor yields a removal efficiency of 37% (for LR) and 52% (for RR) after 18 minutes of reaction. This result confirms the existence of significant mass transfer adsorption of the microcystin molecules onto non-coated (bare) FAC. The higher mass transfer of RR is attributed to a higher initial concentration ;
- the FAC-UV reactor performs better than the FAC reactor by reducing LR and RR with 65% and 71% respectively. This result confirms the positive auxiliary effect of UV photolysis in addition to mass transferred adsorption ;
- the FAC-TiO_2 reactor failed to significantly reduce the microcystin-concentration during its recirculation period. This results is possibly due to TiO_2 particles blocking most of the adsorption sites on the FAC surface and demonstrates that (1) mass transfer of relatively large organic molecules (such as microcystins) to FAC can be prevented and (2) microcystins do not significantly adsorb on impregnated TiO_2 under these conditions ;
- the FAC-UV-TiO_2 reactor yields an efficient removal efficiency after 18 minutes of reaction (reducing LR and RR with 69% and 68% respectively). The observed efficiency do not present a marked improvement on the FAC-UV reactor, however the positive auxiliary effect (with respect to the corresponding mass transfer component) is substantially greater for UV photocatalytic oxidation than UV photolysis (Table 6.18).
- For LR, the gain in efficiency (through photocatalysis) is 69%, compared to 28% achieved for UV photolysis. A similar trend exists for RR removal ;
- screening design analysis (Table 6.19 and Figure 6.14) of the relative parameter main effects and interactions (with respect to the removal efficiency response) reveals (1) the highly significant effect of UV irradiation (2) a significant positive interaction effect (null-hypothesis probability of around 0.05) when applying UV in tandem with TiO_2 (3) a significant negative effect when impregnating FAC with TiO_2 and (4) the significant effect of microcystin variant ;
- photocatalytic oxidation susceptibility for LR and RR is fairly similar in Reactor 2B. This observation is based on comparison of *first order removal rates* (as calculated from rate constants for the FAC-UV-TiO_2 reactor). (LR: 8.7 ug/L/minute; RR: 10.8 ug/L/minute).

Based on the results obtained above, it is evident that TiO_2 photocatalytic oxidation may enhance the performance of FAC reactors when relatively large organic molecules are prevented from adsorbing onto FAC. It is possible to accomplish this using TiO_2 as catalyst. Moreover, by fine-tuning of experimental conditions, organic molecules (such as microcystins) will interact favourably with impregnated TiO_2 and thus render an efficient FAC photocatalytic reactor.

6.2.2 Single Pass Modes

The application of Reactor 2B for studying the photocatalytic oxidation of microcystin toxins was limited to the recirculation mode of operation.

6.2.3 Treatment of Algal Derived Compound

Introduction and Objectives:

A blue-green algal extract (containing microcystin YR) was used in a series of experiments conducted with Reactor 2B as IMM reactor operated in recirculation mode. The objective of this study was to ascertain the effect of elevated catalyst suspension loadings used for TiO_2 impregnation onto FAC grade 15 sheet modules. Two suspension loadings were investigated, viz.: 5 g/L TiO_2 (the standard), against 20 g/L. The respective impregnation loadings amounted to 13.0 and and 35.6 g/m^2 TiO_2. The remainder of the system parameters were evaluated at their standard reference levels (Table 6.17) and the reactions were conducted in 5 L natural lake water (Zeekoevlei) spiked with 10 mL of extract. The extract, however, was thought to contain microcystin YR (based on its HPLC elution time and a match of its UV spectrum with that of a microcystin YR standard). Unfortunately subsequent analysis (using HPLC and electrospray LC-MS) showed that the algal extract did not contain the required microcystin variant and that an unknown organic pollutant (with approximately half the molecular mass of YR) was present. Hence the results obtained for this study pertains to the photocatalytic treatment of an *unknown* algal derived compound (which is significantly smaller in size than the average microcystin molecule). Results were interpreted in terms of the first order rate constants for total removal (k_T), mass transferred adsorption (k_A) and photocatalytic oxidation (k_P), as defined and calculated before (see Section 6.1.1)

Results and Discussion:

Table 6.20: Normalized concentration of unknown algal compound as a function of reaction time

Reaction Time (min)	Normalised Concentration			
	Catalyst SuspensionLoading *used for impregnation* (in g/L TiO_2)			
	5^a (dark adsorption)	20^b (dark adsorption)	5 (UV photocatalysis)	20 (UV photocatalysis)
0	100	100	100	100
2	58.8	72.3	63.0	65.4
4	35.0	54.2	26.1	43.6
6	21.3	32.5	7.6	23.1
8	11.3	25.3	ND	16.7
10	ND*	20.5		10.3
12		7.2		ND
14		ND		
10^2 k_T (min^{-1})	-	-	43.06	23.03
10^2 k_A (min^{-1})	26.94	19.94	-	-
10^2 k_P (min^{-1})	-	-	16.12	3.09
R^2	0.99	0.95	0.96	0.99

Note: *ND = Not detected (below 10 ug/L) ; Impregnation loading: a = 13.0 g/m^2 ; b = 35.6 g/m^2 TiO_2

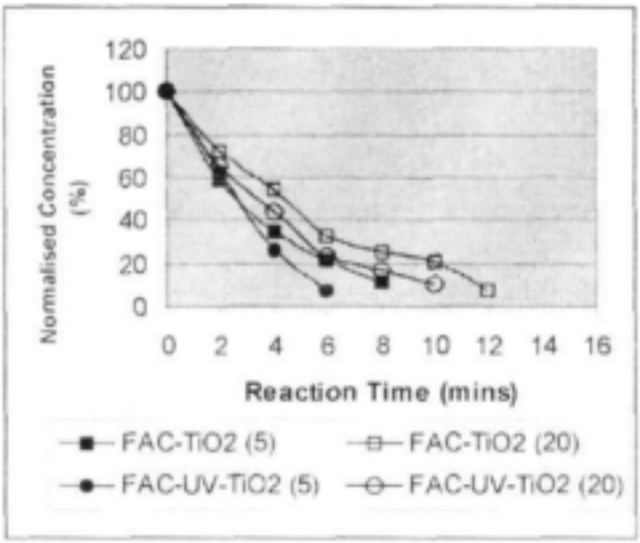

Figure 6.15: Normalised concentration **of unknown algal compound as a function of time, catalyst impregnation loading and UV irradiation. [$TiO_2(5)$ = 5 g/L Catalyst Suspension Loading used for impregnation ; $TiO_2(20)$ = 20 g/L Catalyst Suspension Loading used for impregnation]**

The results obtained from these experiments (Table 6.20 and Figure 6.15) indicated that :

- Reactor 2B is efficient in removing the unknown organic pollutant originating from the algal extract ;
- the removal rate of the compound follows first order exponential decay kinetics ;
- the lower level catalyst impregnation loading (using 5 g/L TiO_2) yields better adsorption of the unknown compound onto impregnated TiO_2. This result is attributed to a lower degree of FAC surface saturation attained through TiO_2 impregnation with 5g/L. The enhanced adsorption indicates a degree of overlapping of the molecular size of the molecule with the mean pore size volume of FAC. The equivalent microcystin experiments yielded no mass transferred adsorption ;
- using the lower catalyst loading (viz.: 5 g/L or 13 g/m^2) yields a higher (1) total removal rate constant and (2) higher gain in removal efficiency (due to UV photocatalysis). This result is in good agreement with earlier experiments conducted with p-CP (Section 6.1) and demonstrates the utility of Reactor 2A for treatment of relatively small organic compounds through a balanced FAC mass transfer and photocatalytic oxidation effects.

APPENDIX 6.1

Woven structure of FAC sheet

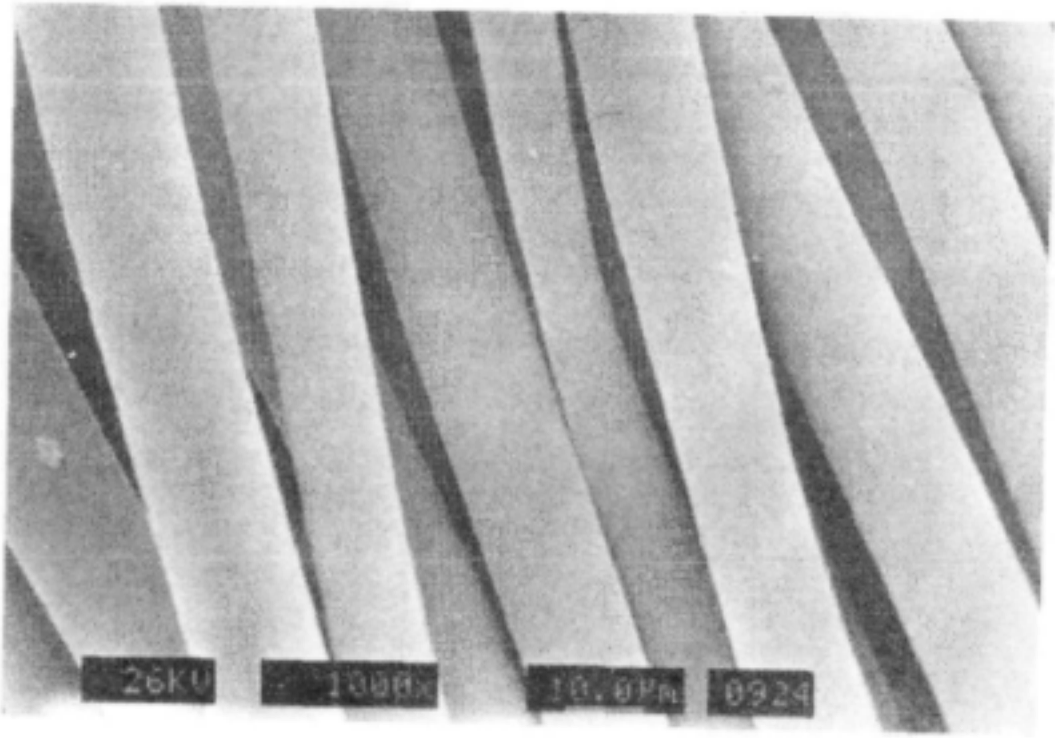

Microstructure of FAC sheet

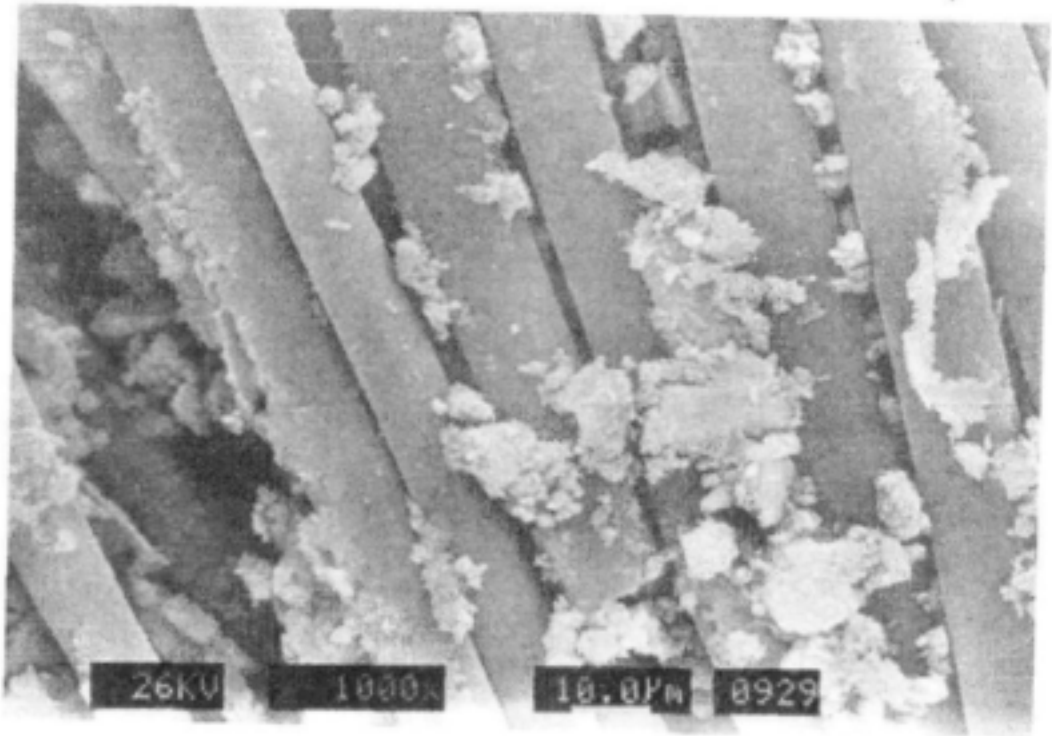

FAC sheet covered with TiO_2 particles

CHAPTER 7 : SUMMARY OF RESULTS, CONCLUSIONS AND RECOMMENDATIONS

7.1 SUMMARY OF RESULTS

1. An existing model of a falling film photocatalytic reactor (Reactor 1) based on TiO_2 catalyst (Degussa P-25), operating as a slurry phase system, has been tested and optimised for the destruction of:

   (i) *para*-chlorophenol as representative of industrial pollutants

   (ii) the microcystin toxins YA, YR, LR and RR

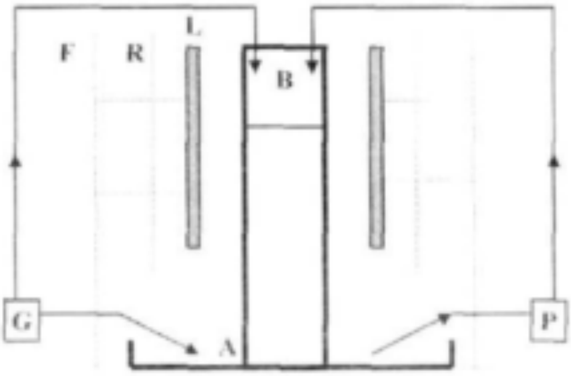

A: Glass cylinder B: Cup F: Frame R: Reflector L: Germicidal lamps
G: Gas purge P: peristaltic pump

Figure 7.1: Schematic of Reactor 1

2. It was established that the destruction of the above mentioned compounds follow first order kinetics when the reactor was operated in recirculation and flow through modes.

   This was the first ever demonstration of TiO_2 photocatalytic removal of microcystin toxins (Stockenström *et al.*, 1996).

3. Due to the difficulty of separating the TiO_2 particles from purified water, Reactor 1 was not considered as a suitable system for upscaling.

4. A novel design of a falling film photocatalytic reactor based on TiO_2 catalyst (Degussa P-25) immobilised on a fibre glass sheet and driven by commercially available UV lamps (Reactor 2A), has been developed :

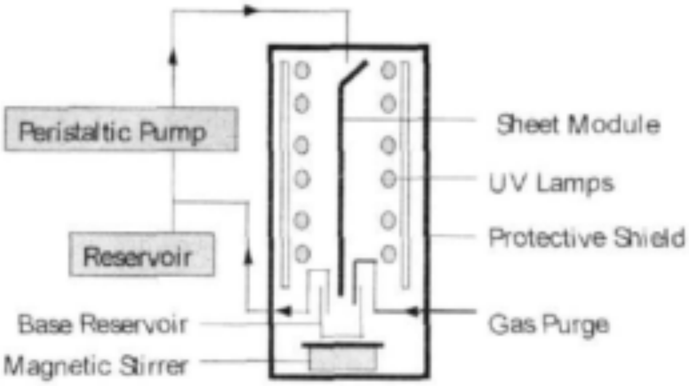

Figure 7.2: Schematic of Reactor 2A

5. Two types of fibre glass sheets were evaluated and the reactor has been operated on an immobilised (IMM) and combined slurry phase and immobilised configuration (SLIMM). This reactor has been tested and optimised in the recirculation and flow through modes of operation for the removal of *para*-chlorophenol as representative of industrial pollutants. The following curves were generated.

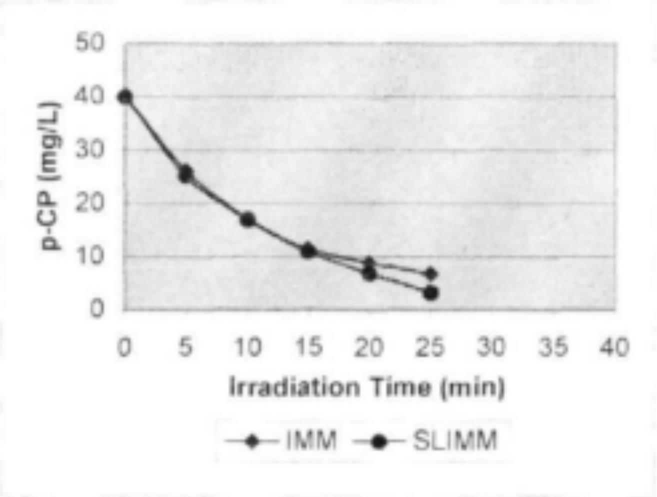

Figure 7.3: *para*-chlorophenol concentration as a function of irradiation time and reactor configuration (IMM and SLIMM) in recirculation mode and using Fibre Glass Type 1 as sheet module

Figure 7.3 shows that additional suspended catalyst (1 g/L) did not enhance *para*-chlorophenol oxidation. Therefore an immobilised configuration is preferred.

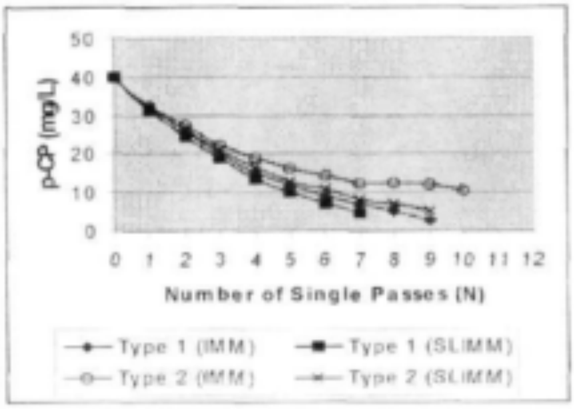

Figure 7.4: ***para*-chlorophenol concentration as a function of sheet module, reactor configuration and single pass number (N) - where each N equals 4.1 sec of UV irradiation**

The curves in Figures 7.3 and 7.4 were converted to rate constants ($10^2 k_{obs}$) and are summarised in Table 7.1.

Table 7.1: Summary of kinetic results for photocatalytic oxidation of *para* -chlorophenol

	Fibre Glass Type 1 (reinforced sheet)		Fibre Glass Type 2 (non-reinforced tissue sheet)	
Kinetic Response Function	IMM Reactor	SLIMM Reactor	IMM Reactor	SLIMM Reactor
10^2 k_{obs} (N)* (pass^{-1})	27.9	30.3	13.2	22.9
Half-life (passes)	2.5	2.3	5.3	3.0
10^2 k_{obs} (t)** (sec^{-1})	6.73	7.37	3.19	5.64
Half-life (sec)	10.3	9.4	21.7	12.3
10^2 k_{obs} (t) (*min*$^{-1}$)	403.8	442.4	191.4	338.1
Half-life (min)	0.17	0.15	0.36	0.21
R^2	0.99	0.99	0.96	0.99

k_{obs} (N)* = Observed first order rate constant as a function of single pass number (N) (each single pass is equivalent to a UV contact time of 4.1 sec)
k_{obs} (t) = Observed first order rate constant as a function of irradiation time (in sec or min)**

The results for the two types of fibre glass sheets and IMM and SLIMM configurations are compared by means of the following bar graph :

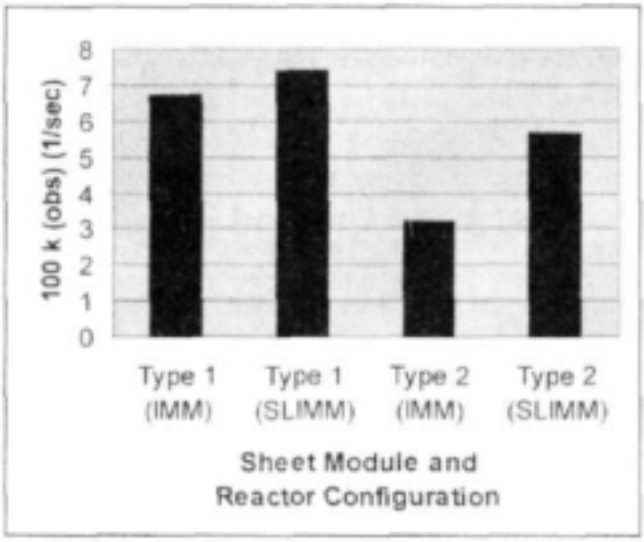

Figure 7.5: First order rate constants for photocatalytic oxidation of *para* -chlorophenol as a function of sheet module and reactor configuration

The fibre glass sheet Type 1 had been proved to be the better choice for immobilising TiO_2 for photocatalytic oxidation.

6. Reactor 2A has also been evaluated for the destruction of the microcystin toxins YA, YR, LR and RR.

   The following tables give representative examples of the results.

Table 7.2: Concentrations of microcystins as functions of single pass number (N)

Single Pass Number (N).	Microcystins (ug/L)		
	YA	YR	LR
0	21	71	49
1	17	57	18
2	20	47	14
3	9	30	10
4	ND	20	ND
5		19	
6		16	
7		15	
8		ND	
9			
10			
10^2 k(N) (pass^{-1})	28.75	24.23	50.19

Table 7.3: Concentration of microcystins as functions of cumulative time of irradiation

Cumulative Time of Irradiation (sec)	Microcystins (ug/L)		
	YA	YR	LR
0.00	21	71	49
4.1	17	57	18
8.2	NA	47	14
12.3	9	30	10
16.4	ND	20	ND
20.5		19	
24.6		16	
28.7		15	
32.8		ND	
36.9			
41.0			
10^2 k (sec^{-1})	7.10	5.98	12.40
Half-life (sec)	9.8	11.6	5.6
R^2	0.99	0.95	0.90

NA = Not analysed ; ND = Not detected

7. According to Bolton's formula for "Electrical Energy per Order" (EE/O (Bolton *et al.*, 1996)), data obtained from Reactor 2A operating in single pass mode, predicted :

    - The cost for the reduction of 40 mg/L p-chlorophenol in distilled water (conductivity 2.4 μS/m) to 4 mg/L (one order of magnitude reduction), as 11 cent/m^3 .

- The cost for the destruction (one order of magnitude) of a mixture of the microcystins YA, YR and LR (total initial concentration 141 μg /L) in lake water (See Table 3.4)) as 26 cent / m^3

These are running (operation) costs and were based on a unit cost of 11.8 cent / kWh in Stellenbosch (May 2000). Administration and labour costs and replacement cost of UV lamps were ignored.

8. It has been proved that Reactor 2A can break down NOM in highly coloured water (TOC 41.6 mg C / L), thereby reducing the total organic carbon (TOC).

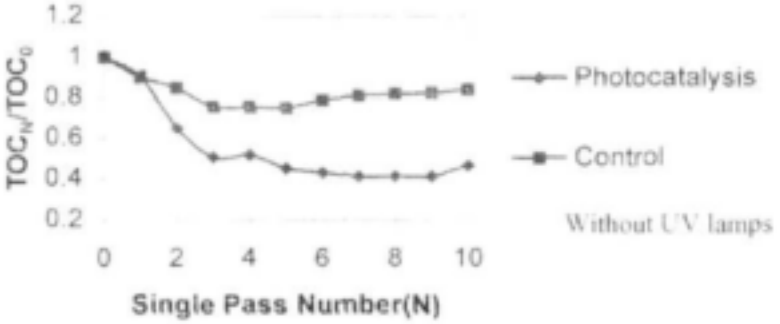

Figure 7.6 : The photocatalytic oxidation of NOM in terms of normalised TOC by Reactor 2 A

The cost for the reduction of NOM by one order of magnitude was calculated as 53 cent / m^3.

This however was regarded as too expensive. The situation can be remedied by using this reactor system in series with a conventional coagulation / flocculation plant. Those pollutants e.g. fulvic acids as part of NOM and industrial pollutants passing through the first plant will be destroyed in the reactor, thereby reducing e.g. the disinfectant byproducts on chlorination.

9. It was established that NOM adsorbs reasonably strongly on glass fibre sheets with immobilised TiO_2 . The rate of mass transfer, however, reaches a steady state.

10. It was realized that reactor 2A operating in the IMM configuration and in the recirculation mode should be an excellent system to obtain relative rate constants for the photocatalytic destruction of pollutants in various water matrixes.

11. The contact time on Reactor 2A was regarded as too short (4.1 ± 0.1 sec). Increasing the contact time should increase the rate of removal and result in a reduction of treatment cost. Efforts to increase the contact time by variations in the configuration of the glass fibre sheet, did not substantially improve the contact time.

12. In order to further improve the contact time of Reactor 2A, the glass fibre sheet has been replaced by a fibrous activated carbon (FAC) sheet. This reactor (Reactor 2B) with various percentages of immobilised TiO_2 , has been investigated for the removal of:

    (i) *para*-chlorophenol as representative of industrial pollutants

    (ii) the microcystin toxins LR and RR

The following curves were generated.

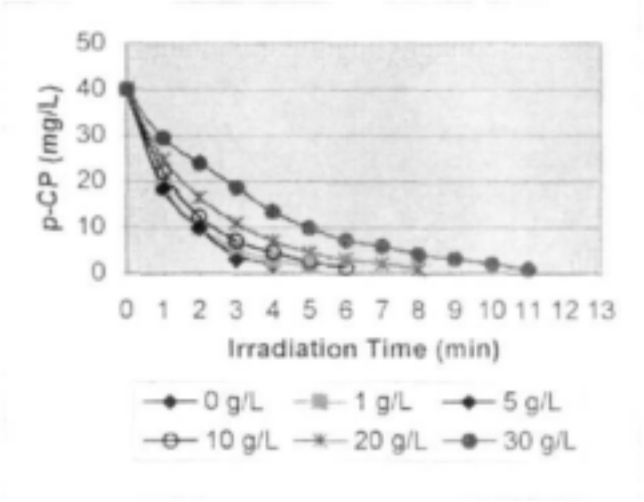

Figure 7.7: p-CP concentration as a function of UV irradiation time and catalyst impregnation loading (expressed as catalyst suspension loading used for FAC impregnation)

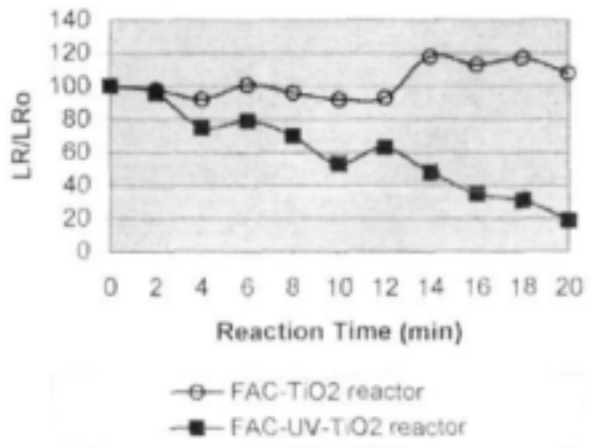

Figure 7.8: Microcystin LR concentration as a function of time in FAC-TiO_2 and FAC-UV-TiO_2 (photocatalytic) reactors. (Concentrations normalised)

The high rate of removal of p-chlorophenol (Figure 7.7) must be attributed to strong adsorption on the FAC sheet.

The microcystin toxins being larger molecules do not adsorb strongly on the FAC sheet (Figure 7.8), therefore the removal of these species must be attributed to the photocatalytic oxidation effect.

13. Efforts to achieve a balance between adsorption and the photocatalysis of p-chlorophenol, by using intermittent TiO_2 covered and uncovered sections of the FAC sheet, were not successful. Adsorption remained the predominant factor.

14. Objectives 3 to 6 (as stated in Chapter 1) were not achieved; due to the difficulty in obtaining authentic samples to produce cultures without contamination.

15. The problem of obtaining the microcystin toxins for experiments on photocatalytic oxidation, was circumvented by using extracts of the appropriate toxins from lake water, when the relevant algal blooms occurred.

7.2 CONCLUSIONS

1. Reactor 2A - being a very rugged model and easy to operate - must be retained and used to obtain relative rate constants for the destruction of pollutants in various water matrices.

   These rate constants can be converted to absolute rate constants for a particular type of commercial reactor operating with the same water matrix, once the absolute rate constant for a standard compound e.g. *para* -chlorophenol has been determined on the commercial reactor.

   The rate constants can eventually be used to predict the performance of commercial reactors for various pollutants and various raw water matrixes.

   A more sensitive analytical technique e.g. capillary electrophoresis should be employed.

2. A falling film photocatalytic reactor based on TiO_2 immobilised on a glass fibre sheet (Reactor 2A) can remove p-chlorophenol, microcystin toxins and NOM from raw water of a low alkalinity.

   Although this reactor system is based on lower cost construction material and can be scaled up, the contact time is too short, thereby placing a restriction on the volume of raw water and the level of contamination that can be treated.

   This reactor system, however, due to its small size and utilisation of lower cost components for construction, can find application in households, clinics and hospitals in urban areas where flocculated water or water with a low TOC could be purified.

   Since the reactor requires UV lamps as radiation source, it is not suited for isolated rural communities.

3. In a falling film photocatalytic reactor based on TiO_2 immobilised on a FAC sheet, adsorption of the pollutants on the FAC is too strong and competes with the photocatalytic destruction process. This type of reactor is not recommended for water treatment. Other configurations employing FAC are however recommended.

4. A substantial body of knowledge has been developed with regard to the coating behaviour of fibre glass sheets and FAC sheets with Degussa P25 TiO_2 catalyst and the photocatalytic behaviour.

5. Based on the predicted treatment cost for photocatalytic purification of polluted water with germicidal lamps and TiO_2 , the development of photocatalytic reactors should continue, especially for large reactors employing solar radiation.

7.3 RECOMMENDATIONS

Recommendations for short term application

1. The application of UV lamp-driven falling film photocatalytic reactors based on fibre glass sheets (Reactor 2A – see Appendix 7.3), should be further investigated for the small scale final purification of flocculated water and raw water with a low total organic carbon content.

2. The disinfection and potential for bacterial regrowth in water treated by Reactor 2A for the purposes described under 1 should be investigated.

3. Lamp-driven falling film photocatalytic reactors based on fibre glass and/or FAC sheets should be evaluated for the purification of polluted air in buildings and removal of volatile organic compounds (VOCs), SO_2 and NO_x from emissions of factories. The body of knowledge generated in this project must be applied in such investigations

Recommendations for long term application

1. In order to increase the contact time of UV photocatalytic oxidation, a modular type of reactor based on horizontal flow and TiO_2 catalyst immobilised on glass fibre rods should be investigated.

   The modules must be configured to operate on solar radiation in daytime, while the number of modules must be sufficient to remove pollutants to the required level.

   This reactor must be operated in series with a conventional coagulation/flocculation plant when raw water of a high TOC must be treated.

2. A modular reactor with a similar construction as under 1, but with TiO_2 catalyst immobilised on FAC should be investigated.

   This reactor must be placed parallel to the reactor under 1 and would be engaged during nighttime operations. Enough modules must be included to remove all pollutants through adsorption.

   During daytime water will be circulated in a closed loop through this reactor to clean the FAC modules by photocatalysis and restore its adsorptive properties.

Proposed configurations

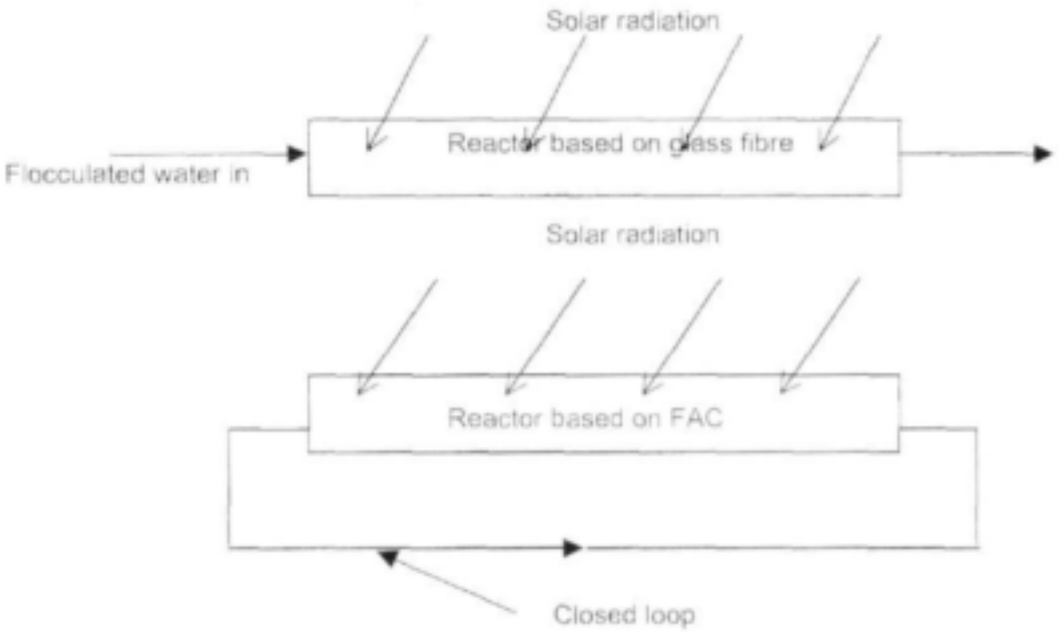

Day time operation

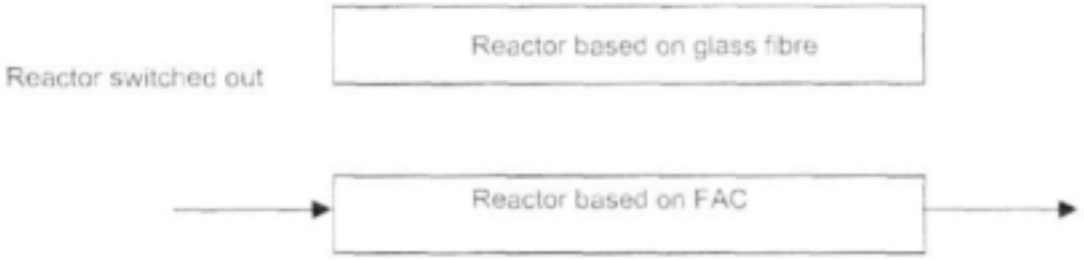

Night-time operation

FAC exhibits very strong adsorptive properties and by including a sufficient number of modules, this reactor will adsorb all the pollutants coming through from a conventional flocculation/coagulation plant during nighttime operations.

When the solar intensity is high enough after sunrise, operations will be switched back to the glass fibre reactor. A conventional pump in a closed loop then circulates water – a reversed flow direction is recommended – through the FAC based reactor under solar radiation. This can continue – for the entire day if necessary – till the FAC is cleaned by photocatalysis.

Individual modules of the FAC based reactor can periodically be removed and subjected to steamstripping to restore adsorptive properties.

The capital and operating cost of this dual reactor system should be much reduced in comparison with a system where lamps are used for nighttime operation.

This reactor system should also be applicable for the continuous wastewater treatment of industrial plants.

3. Small batch operating reactor systems based on solar radiation and TiO_2 immobilised on fibre glass should be developed for use by isolated rural communities.

4. Due to the interdisciplinary nature of the proposed investigations, a project team consisting of chemists, chemical engineers, microbiologists, specialists in microcystin toxins and community health specialists, should be established.

5. International co-operation should be established in order to develop better photocatalysts and better techniques for immobilising these catalysts.

6. A programme should be launched to determine the relative rate constants for the destruction of pollutants of various origin using Reactor 2A.

APPENDIX 7.1

Classification of microcystins

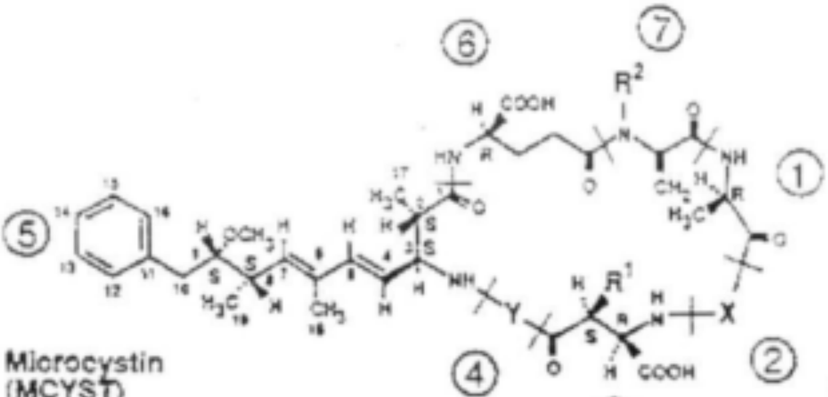

Microcystin (MCYST)

			M.W.
	MCYST - LA:	X = Leu; R^1 = CH_3; Y = Ala; R^2 = CH_3	909
	MCYST - M(O)R:	X = Met(O); R^1 = CH_3; Y = Arg; R^2 = CH_3	1028
	MCYST - YA:	X = Tyr; R^1 = CH_3; Y = Ala; R^2 = CH_3	959
	MCYST - LR:	X = Leu; R^1 = CH_3; Y = Arg; R^2 = CH_3	994
	MCYST - FR:	X = Phe; R^1 = CH_3; Y = Arg; R^2 = CH_3	1028
	MCYST - AR:	X = Ala; R^1 = CH_3; Y = Arg; R^2 = CH_3	952
	MCYST - YM:	X = Tyr; R^1 = CH_3; Y = Met; R^2 = CH_3	1018
	MCYST - RR:	X = Arg; R^1 = CH_3; Y = Arg; R^2 = CH_3	1037
[D-Asp^3]	MCYST - RR:	X = Arg; R^1 = H; Y = Arg; R^2 = CH_3	1023
[D-Asp^3,Dha^7]	MCYST - RR:	X = Arg; R^1 = H; Y = Arg; R^2 = H	1009
	MCYST - YR:	X = Tyr; R^1 = CH_3; Y = Arg; R^2 = CH_3	1044
	MCYST - HtyrR:	X = Htyr; R^1 = CH_3; Y = Arg; R^2 = CH_3	1055
[D-Asp^3]	MCYST - HtyrR:	X = Htyr; R^1 = H; Y = Arg; R^2 = CH_3	1044
	MCYST - WR:	X = Trp; R^1 = CH_3; Y = Arg; R^2 = CH_3	1067

Appendix 7.2

REACTOR 1

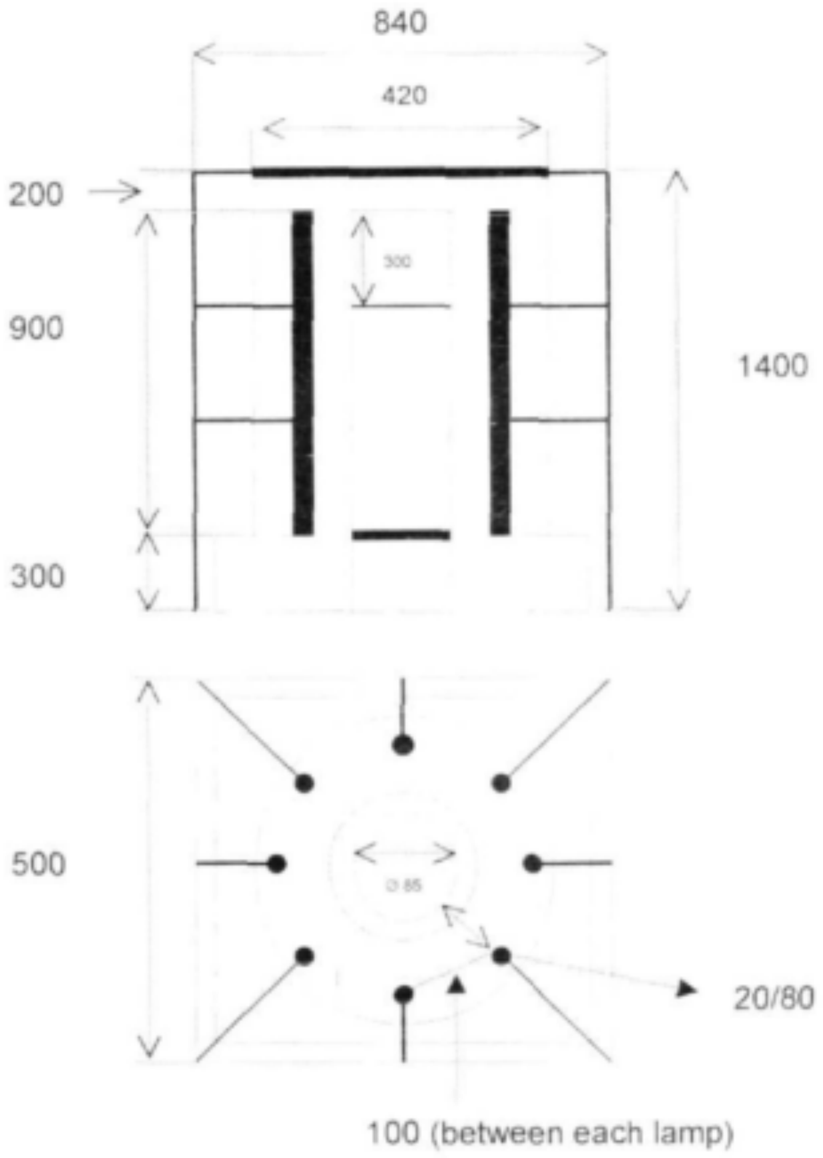

Dimensions (mm) of Reactor 1
(A) Frontal and (B) top view

APPENDIX 7.3

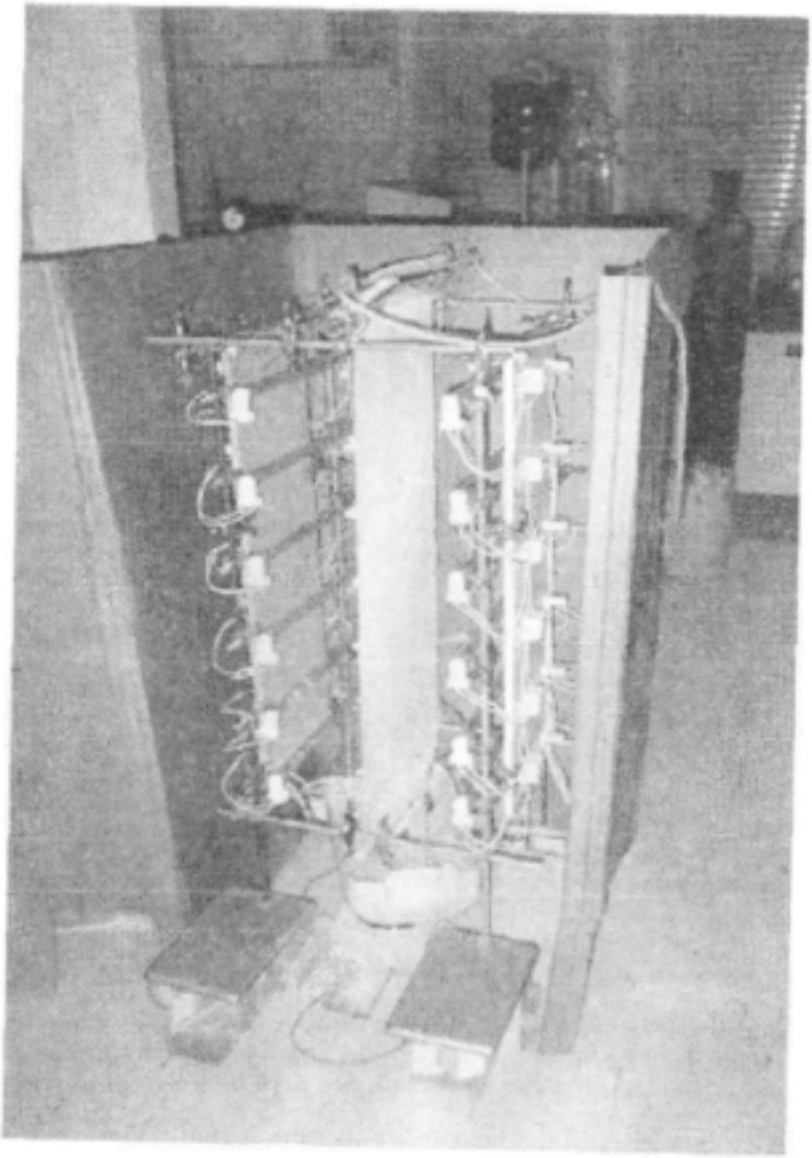

Reactor 2 A

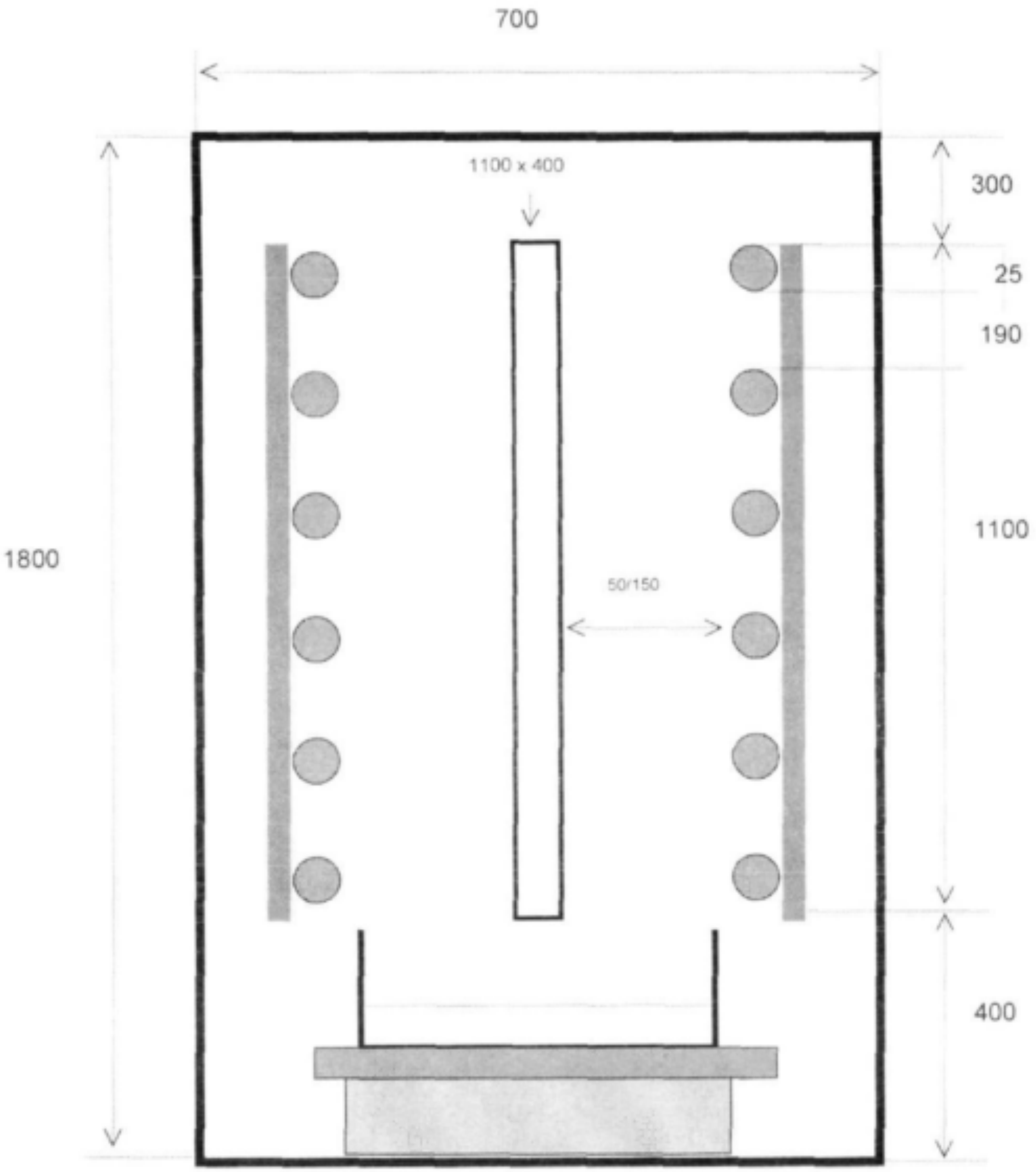

Dimensions (mm) of Reactor 2 A

Sheet module: 1100 mm x 400 mm

APPENDIX 7.4

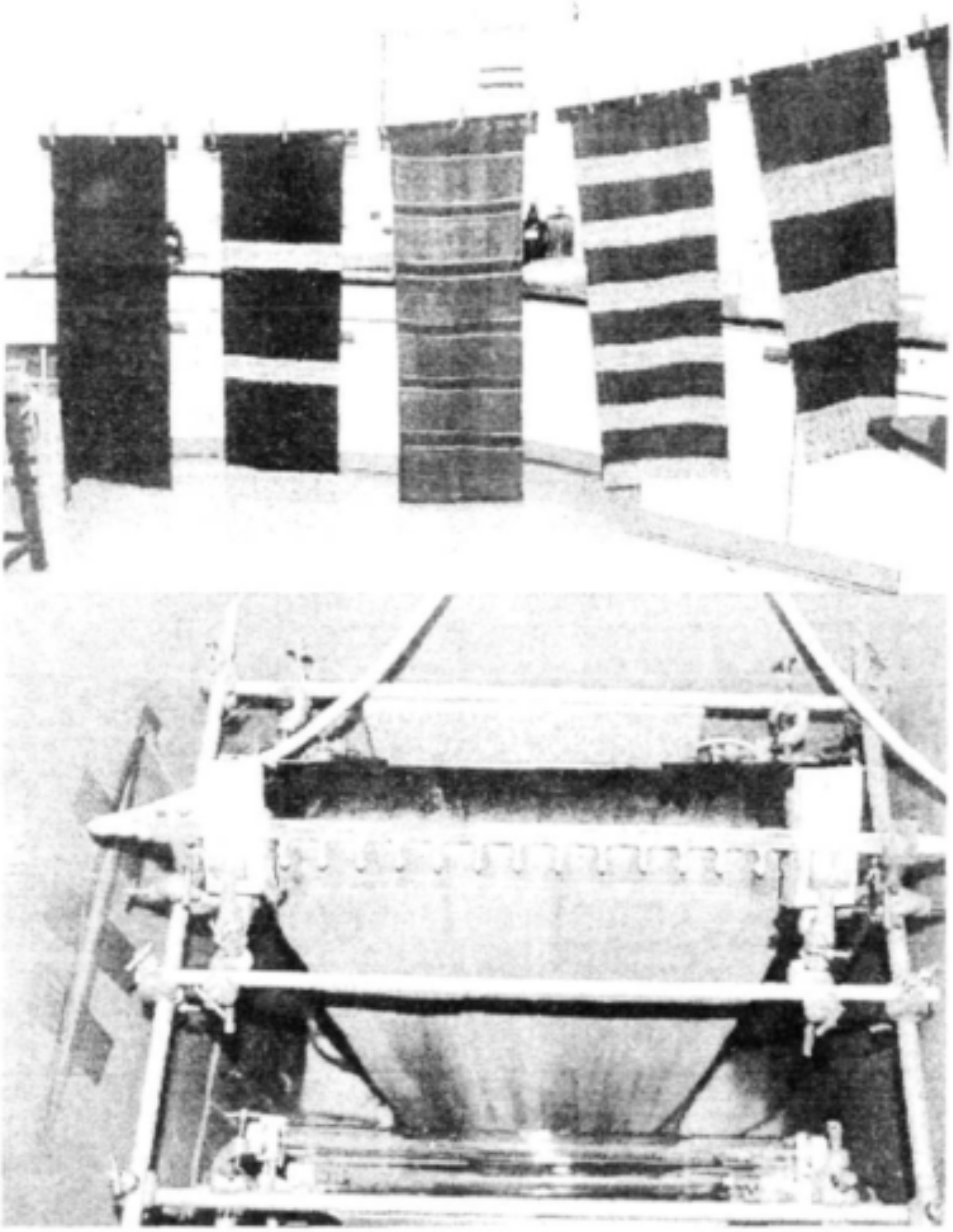

Sheet modules and top view of Reactor 2 B

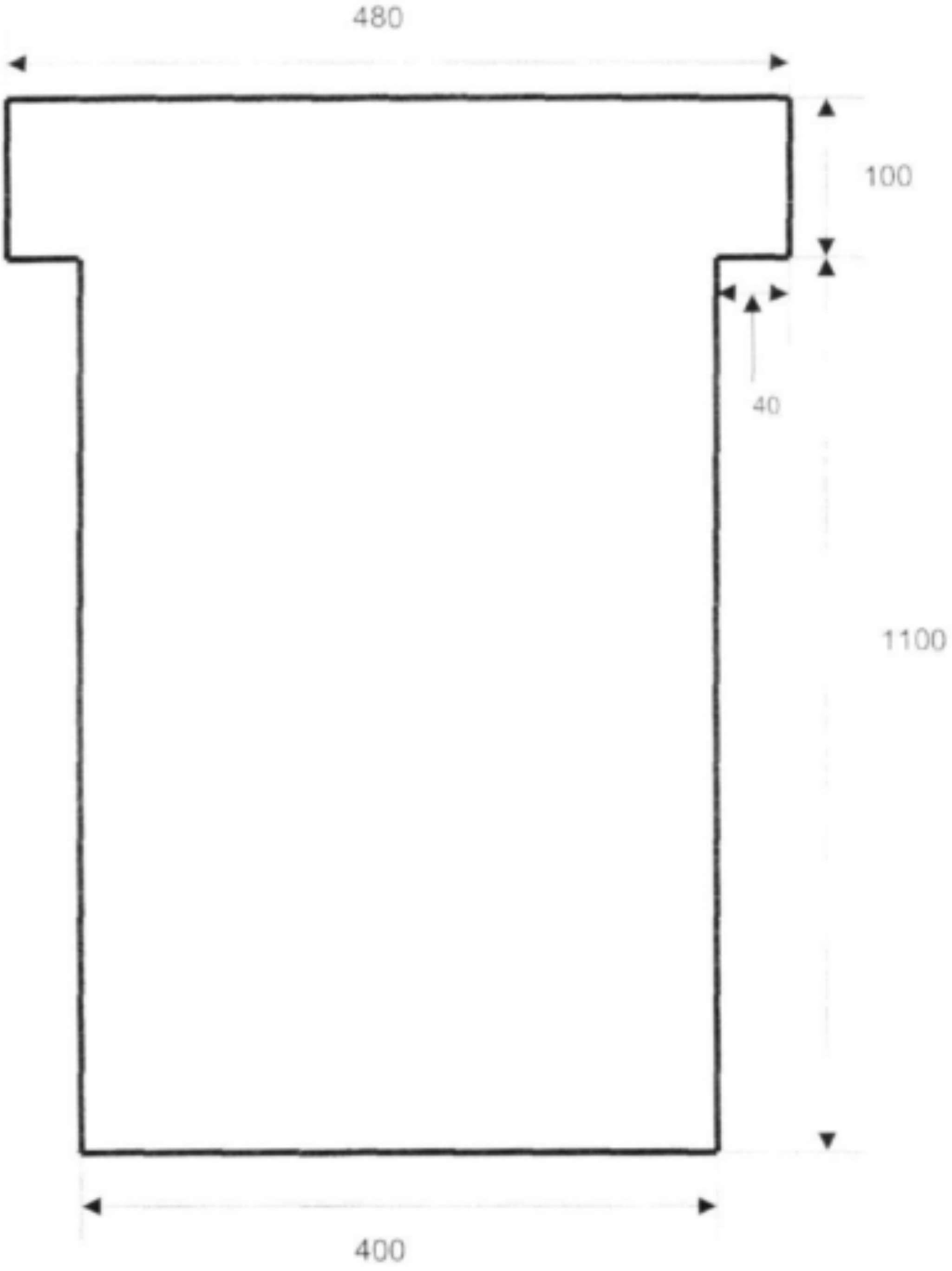

Dimensions (mm)of sheet module

REFERENCES

AGUER JP and RICHARD C (1996) Reactive species produced on irradiation at 365nm of aqueous solutions of humic acids. *J. Photochem. Photobiol. A: Chem.* **93** 193-198.

AL-EKABI H (1999) Advanced oxidation technologies: Fundamentals and environmental applications. In: *Proceedings of Workshop on Advanced Oxidation Technologies*, Albuquerque, New Mexico, USA. 1-19.

BALNOIS E, WILKINSON KJ, LEAD JR and BUFFLE J (1999) Atomic force microscopy of humic substances: Effects of pH and ionic strength. *Environ. Sci. Technol.* **33** 3911-3917.

BATEMAN KP, THIBAULT P, DOUGLAS DJ and WHITE RL (1995) Mass spectral analyses of microcystins from toxic cyanobacteria using on-line chromatographic and electrophoretic separations. *J. Chromatogr. A* **712** 253-268.

BEKBOLET M (1996) Destructive removal of humic acids in aqueous media by photocatalytic oxidation with illuminated titanium dioxide. *J. Environ. Sci. Health* **A31(4)** 845-858.

BENNETT PA and VAN DER MERWE J (1995) Photocatalytic oxidation – a safe and clean alternative in TOC analysis. *Water Sewage & Effluent* **15** 7-9.

BLAKE M (1999) *Bibliography of work on the photocatalytic removal of hazardous compounds from water and air (update number 3 to January 1999)*. NREL/TP-570-26797, National Renewable Energy Laboratory, Golden, CO, USA. Available from National Technical Information Service, Springfield, VA 22161, USA.

BLAZE WH and KANG JW (1988) Advanced oxidation processesfor treating groundwater contaminated with TCE and PCE: laboratory studies.*J.AWWA, May, 57 – 63.*

BOLTON JR (1999) *Ultraviolet Applications Handbook*. Bolton Photosciences Inc., Ayr, Ontario, Canada (ISBN 0-9685432-0-0).

BOLTON JR, BIRCHER KG, TUMAS W and TOLMAN CA (1996) Figures-of-merit for the technical development and application of advanced oxidation processes. *J. Adv. Oxid. Technol.* **1** 13-17.

BOX GEP, DRAPER NR (1986) Empirical Model-Building and Response Surfaces. John Wiley & Sons

BRASQUET C, BOURGES B and LE CLOIREC P (1999) Quantitative structure-property relationship (QSPR) for the adsorption of organic compounds onto activated carbon cloth: Comparison between multiple linear regression and neural network. *Environ. Sci. Technol.* **33** 4226-4231.

BRASQUET C, ROUSSY J, SUBRENAT E and LE CLOIREC P (1996) Adsorption and selectivity of activated carbon fibers application to organics. *Environ. Technol.* **17** 1245-1252.

BRAUN AM, JACOB L (1963) Advances in Photochemistry **18** Chapter 2

BRAUN AM, JAKOB L and OLIVEROS E (1993) Advanced oxidation processes – concepts of reactor design. *Aqua* **42** 166-173.

CARMICHAEL WW (1992) Cyanobacterial secondary metabolites-the cyanotoxins. *J. Appl. Bacteriol.* **72** 445-459.

CARMICHAEL WW (1994) The toxins of cyanobacteria. *Scientific American* **27** 64-72.

CHIN YP, AIKEN G and O'LOUGHLIN E (1994) Molecular weight, polydispersity and spectroscopic properties of aquatic humic substances. *Environ. Sci. Technol.* **28** 1853-1858.

CHORUS I and BARTRAM J (eds.) (1999) *Toxic cyancbacteria in water: A guide to their health consequences, monitoring and management.* E & FN Spon, New York, USA.

CLOETE V (1999) Methods for establishing the efficiency of the photocatalytic destruction of humic substances in drinking water. *M.Sc. (Chemistry) Thesis, University of Stellenbosch.*

CRITTENDEN JC, LIU J, HAND DW and PERRAM DL (1997) Photocatalytic oxidation of chlorinated hydrocarbons in water. *Wat. Res.* **31** 429-438.

CRITTENDEN JC, SURI RPS, PERRAM DL and HAND DW (1997) Decontamination of water using adsorption and photocatalysis. *Wat. Res.* **31** 411-418.

DEMING SN, MORGAN SL (1973) Simplex Optimisation of Variables in Analytical Chemistry. *Analytical Chemistry* **45** 278A-283A

DE VILLIERS D (2000) Design and evaluation of photocatalytic reactors for water purification. *Ph.D. (Chemistry) Thesis in preparation, University of Stellenbosch.*

DEVOR RE, CHANG TH, SUTHERLAND JW (1992) Statistical Quality Design and Control: Contemporary Concepts and Methods. Macmillan Publishing Company

DONATI C, DRIKAS M, HAYES R and NEWCOMBE G (1994) Microcystin-LR adsorption by powdered activated carbon. *Wat. Res.* **28** 1735-1742.

EGGINS BR, PALMER FL and BYRNE JA (1997) Photocatalytic treatment of humic substances in drinking water. *Wat. Res.* **31** 1223-1226.

ENGELBRECHT WJ, DE VILLIERS D, STOCKENSTROM S, SHEPHARD GS, CLOETE V and WESSELS GFS (1998) Photocatalytic purification of drinking water. *Progress Report to the Water Research Commission (Project K5/834).*

FEITZ AJ, WAITE TD, JONES GJ, BOYDEN BH and ORR PT (1999) Photocatalytic degradation of the blue-green algal toxin microcystin-LR in a natural organic aqueous matrix. *Environ. Sci. Technol.* **33** 243-249.

FOX MA and DULAY MT (1993) Heterogeneous photocatalysis. *Chem. Rev.* **93** 341-357.

FUJISHIMA A, HASHIMOTO K and WATANABE T (1999) *TiO_2 Photocatalysis: Fundamentals and Applications.* BKC Inc., Tokyo, Japan (ISBN4-939051-03-X).

FUKUSHIMA M, NAKAYASU K, TANAKA S and NAKAMURA H (1995) Chromium (III) binding abilities of humic acids. *Anal. Chim. Acta* **317** 195-206.

FUKUSHIMA M, TANAKA S, HASEBE K, TAGA M, NAKAMURA H (1995) Interpretation of the acid-base equilibrium of humic acid by a continuous pK distribution and electrostatic model. *Anal. Chim. Acta* **302** 365-373.

GHOSH S. (Editor) (1990) Statistical Design and Analysis of Industrial Experiments, Chapter 3, New York, N.Y.: Dekker

HAARSTRICK A, KUT OM and HEINZLE E (1996) TiO_2 Assisted degradation of environmentally relevant organic compounds in wastewater using a novel fluidized bed photoreactor. *Environ. Sci. Technol.* **30** 817-824.

HAND DW, PERRAM DL and CRITTENDEN JC (1995) Destruction of DBP precursors with catalytic oxidation. *J. Am. Water Works Assoc.* **87** 84-96.

HERRMANN JM (1995) Heterogeneous photocatalysis: an emerging discipline involving multiphase systems. *Catalysis Today* **24** 157-164.

HITZFELD BC, HOGER SJ and DIETRICH DR (2000) Cyanobacterial Toxins: Removal during water treatment and human risk assessment. *Environ. Health Perspect.* **108** 113-122.

HOFFMANN MR, MARTIN ST, CHOI W and BAHNEMANN DW (1995) Environmental applications of semiconductor photocatalysis. *Chem. Rev.* **95** 69-96.

IRELAND JC, KLOSTERMANN P, RICE EW and CLARK RM (1993) Inactivation of *Escherichia coli* by titanium dioxide photocatalytic oxidation. *Appl. Environ. Microbiol.* **59** 1668-1670.

JACKSON NB, WANG CM, LUO Z, SCHWITZGEBEL J, EKERDT JG, BROCK JR and HELLER A (1991) Attachment of TiO_2 powders to hollow glass microbeads. *J. Electrochem. Soc.* **138** 3660-3664.

KOPINKE FD, PORSCHMANN J and STOTTMEISTER U (1995) Sorption of Organic Pollutants on Anthropogenic Humic Matter. *Environ. Sci. Technol.* **29** 941-950.

KUNIN R (1986) The role of organic matter in water treatment – A universal theory. *Amber-hi-Lites* **179** 1-8.

LAM AKY, FEDORAK PM and PREPAS EE (1995) Biotransformation of the cyanobacterial hepatotoxins microcystin-LR, as determined by HPLC and protein phosphatase bioassay. *Environ. Sci. Technol.* **29** 242-246.

LANG K, WAGNEROVA DM, STOPKA P and DAMERAU W (1992) Reduction of dioxygen to superoxide photosensitized by anthraquinone-2-sulphonate. *J. Photochem. Photobiol. A: Chem.* **67** 187-195.

LAWTON LA, EDWARDS C and CODD GA (1994) Extraction and high-performance liquid chromatographic method for the determination of microcystins in raw and treated waters. *Analyst* **119** 1525-1530.

LAWTON LA and ROBERTSON PKJ (1999) Physico-chemical treatment methods for the removal of microcystins (cyanobacterial hepatotoxins) from potable waters. *Chem. Soc. Rev.* **28** 217-224.

LE CLOIREC P, BRASQUET C and SUBRENAT E (1997) Adsorption onto fibrous activated carbon: applications to water treatment. *Energy & Fuels* **11** 331-336.

LEGRINI O, OLIVEROS E and BRAUN AM (1993) Photochemical processes for water treatment. *Chem. Rev.* **93** 671-698.

LI XZ and ZHANG M (1996) Decolorization and biodegradability of dyeing wastewater treated by a TiO_2 sensitized photooxidation process. *Wat. Sci. Tech.* **34** 49-55.

LIANG EJ, YANG Y and KIEFER W (1999) *Surface-enhanced raman spectra of fulvic and* humic acids adsorbed on copper electrodes. *Spectrosc. Lett.* **32** 689-701.

LINSEBIGLER AL, LU G and YATES JT (1995) Photocatalysis on TiO_2 surfaces: Principles, mechanisms, and Selected Results. *Chem. Rev.* **95** 735-758.

LONG DE (1969) Simplex optimization of the response from chemical systems. *Anal.Chim.Acta* **46** 193-206.

MANSFIELD J (2000) Personal communication. Cape Water Programme, Environtek, CSIR, Stellenbosch, South Africa

MARTIN CA, ALFANO OM and CASSANO AE (1999) UV radiation + hydrogen peroxide decolorization of waters for domestic supply. In: *Proceedings of The 5th International Conference on Advanced Oxidation Technologies for Water and Air Remediation*, Albuquerque, New Mexico, USA. 3-4.

MASON RL, GUNST RF, HESS JL (1989) Statistical Design and Analysis of Experiments with Applications to Engineering and Science. New York, N.Y.: Wiley

MATTHEWS RW (1986) Photo-oxidation of organic material in aqueous suspensions of titanium dioxide. *Wat. Res.* **20** 569-578.

MATTHEWS RW (1991) Photooxidative degradation of coloured organics in water using supported catalysts: TiO_2 on sand. *Wat. Res.* **25** 1169-1176.

MATTHEWS RW (1993) Photocatalysis in water purification: Possibilities, problems and prospects. In: *Photocatalytic Purification and Treatment of Water and Air*, Ollis DF and Al-Ekabi H (eds.), Elsevier Science Publishers B.V., Amsterdam. The Netherlands. 121-138.

MILLER JC, MILLER JN (1984)Statistics for Analytical Chemistry. John Wiley & Sons

MILLS A, DAVIES RH and WORSLEY D (1993) Water purification by semiconductor photocatalysis. *Chem. Soc. Rev.* **22** 417-425.

MILLS A and MORRIS S (1993) Photomineralisation of 4-chlorophenol sensitized by titanium dioxide: a study of the initial kinetics of carbon dioxide photogeneration. *J. Photochem. Photobiol. A: Chem.* **71** 75-83.

MILLS A and LE HUNTE S (1997) An overview of semiconductor photocatalysis. *J. Photochem. Photobiol. A: Chem.* **108** 1-35.

MORGAN E (1995) Chemometrics: Experimental Design. John Wiley & Sons (Eng.)

NASKAR S, PILLAY SA and CHANDA M (1998) Photocatalytic degradation of organic dyes in aqueous solution with TiO_2 nanoparticles immobilized on foamed polyethylene sheet. *J. Photochem. Photobiol. A: Chem.* **113** 257-264.

NICHOLSON BC, ROSITANO J and BURCH MD (1994) Destruction of cyanobacterial peptide hepatotoxins by chlorine and chloramine. *Wat. Res.* **28** 1297-1303.

NISHIWAKI-MATSUSHIMA R, OHTA T, NISHIWAKI S, SUGANUMA M, KOYAMA K, ISHIKAWA T, CARMICHAEL WW and FUJIKI H (1992) Liver tumor promotion by the cyanobacterial cyclic peptide toxin microcystin LR. *J. Cancer Res. Clin. Oncol.* **118** 420-424.

OWEN DM and AMY GL (1995) NOM characterization and treatability. *J. Am. Water Works Assoc.* **87** 46-63.

PEILL NJ and HOFFMANN MR (1998) Mathematical model of a photocatalytic fiber-optic cable reactor for heterogeneous photocatalysis. *Environ. Sci. Technol.* **32** 398-404.

PIETERSE SA (1997) *Personal communication.* Scientific Services Branch, Cape Town Metropolitan Council, Cape Town.

PUMA GL and YUE PL (1999) Enhanced photocatalysis in a pilot laminar falling film slurry reactor. *Ind. Eng. Chem. Res.* **38** 3246-3254.

RAJESHWAR K (1996) Photochemical strategies for abating environmental pollution. *Chemistry & Industry* **17 June** 454-458.

RAY AK and BEENACKERS AACM (1998) Novel photocatalytic reactor for water purification. *AIChE Journal* **44** 477-483.

ROBERTSON PKJ, LAWTON LA, MUNCH B and CORNISH B (1999) The destruction of cyanobacterial toxins by titanium dioxide photocatalysis. *J. Adv. Oxid. Technol.* **4** 20-26.

SCHNITZER M and KHAN SU (Eds.) (1978) *Soil Organic Matter.* Elsevier Scientific Publishing Company, Amsterdam, The Netherlands.

SCLAFANI A, SCIASCIA A and RIZZUTI L (1999) Pollutants photocatalytic degradation in a falling film reactor. *J. Adv. Oxid. Technol.* **4** 91-96.

STOCKENSTROM S, DE VILLIERS D, ENGELBRECHT WJ, SHEPHARD GS, SYDENHAM EW, THIEL PG and WESSELS GFS (1996) Photocatalytic decomposition of microcystins in water. *Proceedings of IX^th^ IUPAC International Symposium on Mycotoxins and Phycotoxins*, Rome, Italy.

TSUJI K, WATANUKI T, KONDO F, WATANABE MF, SUZUKI S, NAKAZAWA H, SUZUKI M, UCHIDA H and HARADA K (1995) Stability of microcystins from cyanobacteria – Effect of UV light decomposition and isomerization. *Toxicon* **33** 1619-1631.

VAN HALDEREN A, HARDING WR, WESSELS JC, SCHNEIDER DJ, HEINE EWP, VAN DER MERWE J and FOURIE JM (1995) Cyanobacterial (blue-green algae) poisoning of livestock in the Western Cape province of South Africa. *J. S.Afr. Vet. Ass.* **66** 260-264.

VILGE-RITTER A, MASION A, BOULANGE T, RYBACKI D and BOTTERO J (1999) Removal of natural organic matter by coagulation-flocculation: A pyrolysis-GC-MS study. *Environ. Sci. Technol.* **33** 3027-3032.

WARWICK P, HALL A and READ D (1994) A comparative study employing three different models to investigate the complexation properties of humic and fulvic Acids. *Radiochim. Acta* **66** 133-140.

WICKS RJ and THIEL PG (1990) Environmental factors affecting the production of peptide toxins in floating scums of the cyanobacterium *Microcystis aeruginosa* in a hypertrophic African reservoir. *Environ. Sci. Technol.* **24** 1413-1418.

YARBO LA, DEMING SN (1974) Selection and Preprocessing of Factors for Simplex Optimisation. *Analytica Chimica Acta* **73** 391-398

ZHANG Y, CRITTENDEN JC and HAND DW (1994) The solar photocatalytic decontamination of water. *Chemistry & Industry* **19 September** 714-717.

RESEARCH OUTPUTS BY PROJECT TEAM

SCIENTIFIC PUBLICATIONS

- **Publications in scientific journals (refereed)**

1. GS Shephard, S Stockenström, D de Villiers, WJ Engelbrecht, EW Sydenham, GFS Wessels, *Photocatalytic degradation of cyanobacterial microcystin toxins in water*, Toxicon Vol.36 (12) p.1895-1901 (1998).

- **Published conference proceedings (refereed)**

1. S Stockenström, D de Villiers, WJ Engelbrecht, GS Shephard, EW Sydenham, PG Thiel, GFS Wessels, *Photocatalytic Decomposition of Microcystins in Water*, Mycotoxins and Phycotoxins - Developments in Chemistry, Toxicology and Food Safety, p.517, M Miraglia, H van Egmond, C Brera, J Gilbert (ed.), Fort Collins, Colorado, USA, 1998.

- **Published conference proceedings (not refereed)**

1. D de Villiers, S Stockenström, WJ Engelbrecht, GS Shephard, EW Sydenham, GFS Wessels, PG Thiel, L van Niekerk, *Novel photocatalytic reactors for water treatment*, Biennial Conference and Exhibition of the Water Institute of South Africa (WISA), May 1998, Cape Town, South Africa, Volume 3, p.3G-1, ISBN: 0-620-22424-3.

2. GS Shephard, S Stockenström, D de Villiers, WJ Engelbrecht, EW Sydenham, PG Thiel, GFS Wessels, *Photocatalytic degradation of cyanobacterial microcystin toxins in water*, Biennial Conference and Exhibition of the Water Institute of South Africa (WISA), May 1998, Cape Town, South Africa, Volume 1, p. P53, ISBN: 0-620-22424-1.

PARTICIPATION AT CONFERENCES AND SYMPOSIA

INTERNATIONAL

- **Poster papers**

1. GS Shephard,S Stockenström, D de Villiers*, WJ Engelbrecht, EW Sydenham, PG Thiel and GFS Wessels *Photocatalytic Degradation of Cyanobacterial Microcystin Toxins in Water*. Fourth International Conference on TiO_2 Photocatalytic Purification and Treatment of Water and Air, Albuquerque, New Mexico, USA, May 1999.

2. V Cloete, JJ Cruywagen, D de Villiers*, WJ Engelbrecht, TW Nieuwoudt, *Application of the Photocatalytic Process to the Treatment of Tannery Waste*, Fourth International Conference on TiO_2 Photocatalytic Purification and Treatment of Water and Air, Albuquerque, New Mexico, USA, May 1999.

- **Oral papers**

1. S Stockenström, D de Villiers, WJ Engelbrecht, GS Shephard*, EW Sydenham, PG Thiel, GFS Wessels, *Photocatalytic Decomposition of Microcystins in Water*, IXth IUPAC International Symposium on Mycotoxins and Phycotoxins, Rome, Italy, May 1996.

2. D de Villiers*, S Stockenström, WJ Engelbrecht, GS Shephard, EW Sydenham, GFS Wessels, *Novel reactor designs for the photocatalytic destruction of cyanobacterial microcystins in water*, International Conference on Environmental Management in South Africa (CEMSA), East London, South Africa, February 1998.

3. V Cloete, D de Villiers*, WJ Engelbrecht, GFS Wessels, *Photocatalytic breakdown of humic substances in drinking water - An analytical method for the determination of chloroform*, International Conference on Environmental Management in South Africa (CEMSA), East London, South Africa, February 1998.

4. D de Villiers*, WJ. Engelbrecht, GS Shephard, S Stockenström and GFS Wessels, *TiO_2 Immobilization on Fibrous Activated Carbon Sheet Modules in a Falling Film Photocatalytic Reactor*, Fourth International Conference on TiO_2 Photocatalytic Purification and Treatment of Water and Air, Albuquerque, New Mexico, USA, May 1999.

5. V Cloete, D de Villiers*, WJ Engelbrecht and GFS.Wessels, *Photocatalytic Treatment of Humic Substances in Raw Natural Water Destined for Drinking Purposes*, Fourth International Conference on TiO_2 Photocatalytic Purification and Treatment of Water and Air, Albuquerque, New Mexico, USA, May 1999.

6. D de Villiers, *Research in TiO_2 Photocatalysis at Stellenbosch University*, Seminar presented at the National Renewable Energy Laboratory (NREL), Golden, Colorado, USA, June 1999.

7. WJ Engelbrecht, V Cloete, D de Villiers*, TW Nieuwoudt, GFS Wessels, *Novel Photocatalytic Reactors for Water Treatment*, CNRS-CSIR-WRC-French-South African Workshop on Water Issues, Pretoria, South Africa, July 1999.

NATIONAL (South Africa)

- **Poster papers**

1. D de Villiers*, WJ Engelbrecht en GFS Wessels, *Designing a Photocatalytic Reactor for Water Treatment Applications*, 33rd Convention of the South African Chemical Institute, Cape Town, January 1996.

2. S Stockenström, D de Villiers*, WJ Engelbrecht, GS Shephard, EW Sydenham, PG Thiel en GFS Wessels, *Photocatalytic Decomposition of Microcystins in Water*, Workshop on "Treatment of Coloured Surface Waters for Potable Use", Mossel Bay, October 1996.

3. GS Shephard, S Stockenström*, D de Villiers, WJ Engelbrecht, EW Sydenham, PG Thiel, GFS Wessels, *Photocatalytic degradation of cyanobacterial microcystin toxins in water*, Biennial Conference and Exhibition of the Water Institute of South Africa (WISA), Cape Town, May 1998.

4. GS Shephard*, S Stockenström, D de Villiers, WJ Engelbrecht, EW Sydenham, PG Thiel, GFS Wessels, *Photocatalytic degradation of cyanobacterial microcystin toxins in water*, Analitika '98, Midrand, October 1998.

- **Oral papers**

1. D de Villiers, *Ontwikkeling van 'n fotokatalitiese reaktor vir watersuiwering*, South African Academy for Science and Arts – Young Chemists' Symposium, Pretoria, November 1995.

2. D de Villiers*, S Stockenström, WJ Engelbrecht, GS Shephard, EW Sydenham, GFS Wessels, PG Thiel, L Van Niekerk, *Novel photocatalytic reactors for water treatment*, Biennial Conference and Exhibition of the Water Institute of South Africa (WISA), Cape Town, May 1998.

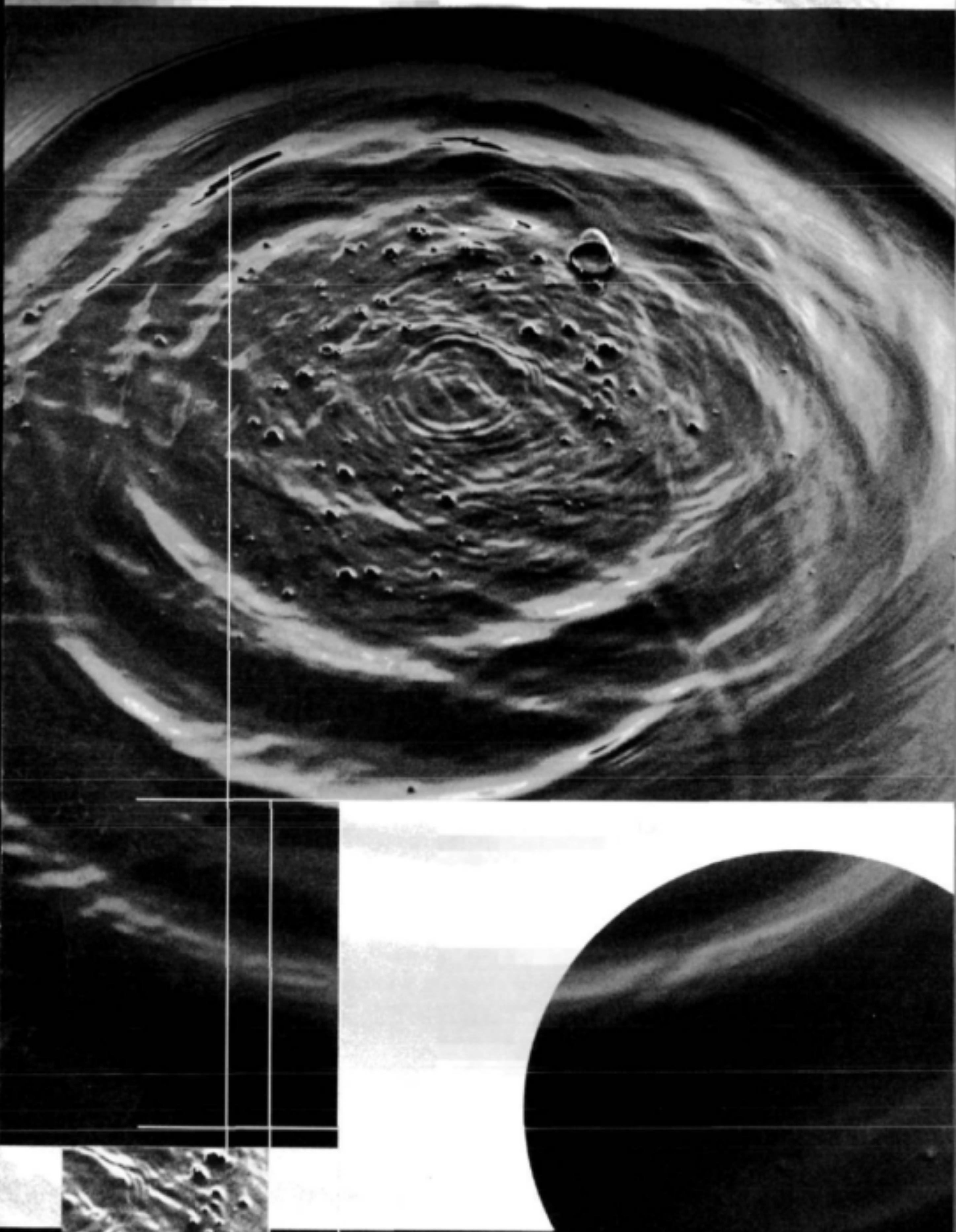

Water Research Commission

PO Box 824, Pretoria, 0001, South Africa

Tel: +27 12 330 0340, Fax: +27 12 331 2565

Web: http://www:wrc.org.za

1868456986